Synthesis and supramolecular properties of molecular tweezers and clips substituted by dendrimer and sulphate groups

Dissertation

zur Erlangung des Doktorgrades der Naturwissenschaften
dem Fachbereich Chemie
der Universität Duisburg-Essen

vorgelegt von
Marçal Casas Cartagena
aus Badalona

Essen 2007

Referent	Prof. Dr. Frank-Gerrit Klärner
Korreferent:	Prof. Dr. Dr. h.c. Reiner Sustmann
Prüfungsvorsitzender:	Prof. Dr. Matthias Epple
Tag der Disputation:	08.06.2007

„Hiermit bestätige ich, diese Arbeit nur mit den angegebenen Hilfsmitteln ohne fremde Hilfe angefertigt zu haben“.

The present work was performed from April 2003 until April 2007 in the Institut für Organische Chemie of the University of Duisburg-Essen, campus Essen, under the supervision of Prof. Dr. Frank-Gerrit Klärner

I would like to express my deep and sincere gratitude to my supervisor, Prof. Dr. Frank-Gerrit Klärner for giving me the opportunity to work in such interesting topic of research. His wide knowledge and his logical way of thinking have been of great value for me.

I am deeply grateful to Prof. Dr. Dr. h.c. Reiner Sustmann for taking over the co referee.

I am also deeply grateful to Prof. Dr. Matthias Ulbricht for chairing the disputation.

I am also deeply grateful to Prof. Roland Boese and Herrn Dipl.-Ing. Dieter Bläser for the elucidation of the crystal structure of clip **104**.

Herr Dipl.-Ing Heinz Bandmann and Herr Dr. Torsten Schaller have done many NMR measurements for this work. Additionally they have been really helpful in many other matters, most of the times far beyond their actual duties. For all that I own them my sincere gratitude.

I also want to thank Herrn Klaus Kowski and Herrn Rainer Poppek, not only for their assistance in the measurement of IR and GC but also for helping me in any (and I really mean any) kind of situation. For the same reason Frau Ingeborg Reiter and Frau Heike Wöll have also my deeply gratitude.

During the period I spent doing this work I have been given the opportunity to work with the best group of colleagues one can ever imagine, which makes me feel very lucky. For that I sincerely thank: Frank Wurche, Matthias Lobert, Björn Kahlert, Anke Nellesen, Jolanta Polkowska, Frank Bastkowski, Marc Blecking and Caroline Breitkreuz.

At last, but most important, I wish to thank my parents and my partner Mireia. This work could not have been done without their emotional support. I could never have gone so far all alone.

A la Mireia i als meus pares

Index of contents

List of abbreviations

In the present work the following abbreviations have been used.

AcOEt	Ethyl acetate
ACN	Acetonitrile
COSY	Correlation spectroscopy
Cp	Dicyclopentadiene
CT	Charge transfer
DDQ	2,3-dicyano-5,6-dichloro-parabenzoquinone
DHNA	1,3-dihydroxynaphthalene-2-carboxylic acid
DMF	*N,N*-dimethylformamide
EDA	Electron-donor-acceptor
EPS	Electrostatic potential surface
ESI	Electrospray ionization
et al.	and others (Latin: et alia)
HMBC	Heteronuclear multiple bond connectivity
HMQC	Heteronuclear multiple quantum coherence
HPLC	High pressure liquid chromatography
HR-MS	High resolution mass spectrometry
^{i}PrOH	Isopropanol
IR	Infra red
ITC	Isothermal titration calorimetry
MALDI	Matrix-assisted laser desorption/ionization
MeOH	Methanol
MPLC	Medium pressure liquid chromatography
MS	Mass spectrometry
NAD^+	Nicotinamide adenine dinucleotide
NEt_3	Triethylmanine
NMO	*N*-methylmorpholine-*N*-oxide
NMP	1-methylpyrrolidin-2-one
NMR	Nuclear magnetic resonance
OAc	Acetoxy (group)

OMe	Methoxy (group)
Ph	Phenyl (group)
^{t}BuOH	*tert*-butanol
TEG	Triethyleneglycol monomethylether (group)
TOF	Time-of-flight
UV	Ultraviolet

According to the standard DIN 1301 the units of pressure and energy should have been given in [Pa] and [J] respectively. In order to compare the obtained values with previously done works, in the present work the units of energy are given in [cal] and the units of pressure are given in [bar].

1 Introduction

1.1 Supramolecular chemistry

The concept of supramolecular chemistry was first introduced in 1978 by Lehn as the chemistry of non covalent interactions.[1] While molecular chemistry is built up by means of covalent synthesis, supramolecular chemistry has its basis in intermolecular interactions responsible for the association of discrete molecules to a superstructure named supramolecule.[2] Despite the formation of a supramolecule, the starting molecules keep their individuality. Since no covalent bond is broken or formed, the formation of the supramolecules does not involve chemical reactions. However, the supramolecule can show new characteristics, which differ from those of its individual components.

Biological systems are, probably, the most interesting fields where supramolecular chemistry plays a crucial role. In this area one finds supramolecules between proteins and ligands, enzymatic catalysis and inhibition, genetic information storage and retrieval, immunological response and ion transport. Both components of the supramolecule differ from each other on basis of their topology. Cram *et al*. described the host or receptor in a supramolecule as the component whose binding sites converge in the complex. Analogously the guest or substrate is described as the component whose binding sites diverge in the complex.[3] The formation process of a supramolecule from its individual components is known as molecular recognition and it comprises both selection and bonding of guest molecules by the host.

Basic courses in biochemistry teach us two intuitive models of molecular recognition between enzymes and substrates. There is, in a first instance, the key-lock model described by Fischer.[4] In this model the receptor has a pre-organized active site where only a substrate molecule with a complementary topology and bonding properties can be accommodated (Figure 1.1).[4]

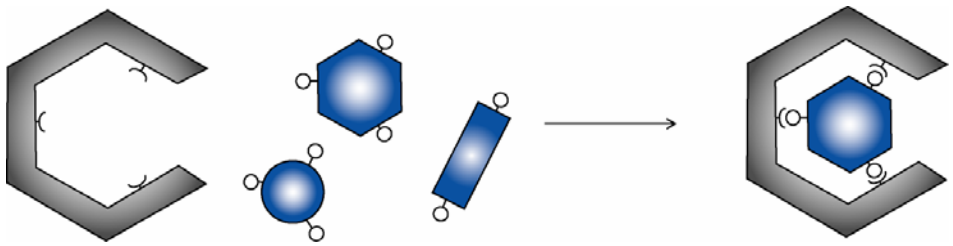

Figure 1.1: Schematic representation of Fischer's key-lock model.

The extended induced-fit model described by Koshland considers a non-static active site of the receptor. This active site can be reshaped by interactions with the substrate adapting its topology and leading to the receptor-substrate complementary state (Figure 1.2).[5]

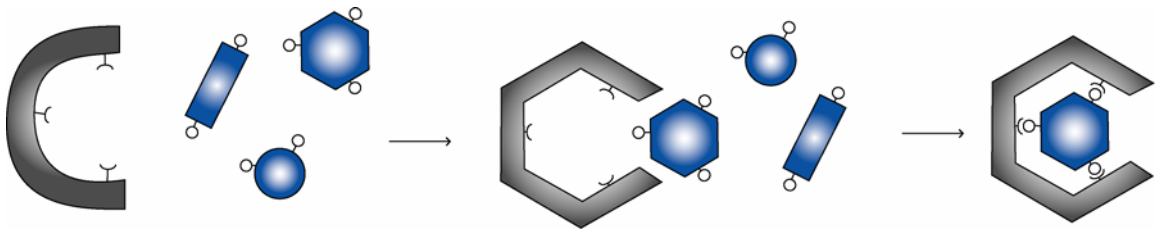

Figure 1.2: Schematic representation of Koshland's induced-fit model.

Beside the molecular recognition, self-organization, the spontaneous formation of superstructures due to intermolecular forces, is the second basic concept in supramolecular chemistry. Once again biological systems give an impressive example for supramolecular concepts. It is by means of self-association that polypeptides are able to link to each other, leading to the secondary, tertiary and quaternary structures and finally to a protein.

The structure of DNA shows a perfect example of efficient combination of both notions of supramolecular chemistry.[6] The supramolecular recognition of adenine and thymine as well as guanine and cytosine is based on the selective formation of hydrogen bonds, and controls the formation of DNA double strands which, by means of self-organization, induced by series of π-π interactions between the aromatic systems of the bases, is finally responsible for the helical structure.[7]

The objective of supramolecular chemistry is to design, synthesize and study simple models, which are able to undergo both molecular recognition and self-organization, in order to provide an insight into these relatively complex processes and to allow us to design new materials and new active agents.

1.2 Non covalent interactions of organic molecules

Supramolecular processes are based on weak, but highly specific, intermolecular forces such as hydrogen bonds,[8-11] ion pairing[12-15] and arene-arene interactions[16-19] as well as less specific van-der-Waals or dispersion forces. Arene-arene interactions are of particular importance in both chemical and biological recognition processes, for example the protein ligand recognition.[20]

Attractive interactions between aromatic molecules were first observed in the crystal structure of benzene, where it is possible to see that benzene units prefer an Edge-to-Face arrangement (Figure 1.3).[21] By use of molecular beam spectroscopy[22, 23] and ^{1}H NMR studies[24] it was possible to characterize the Edge-to-Face benzene dimer both in gas and liquid phases. With the analysis of crystal structures of proteins, Burley and Petsko found that 60 % of the interactions between the aromatic substituents of the amino acids are, in fact, Edge-to-Face arrangements.[25-27]

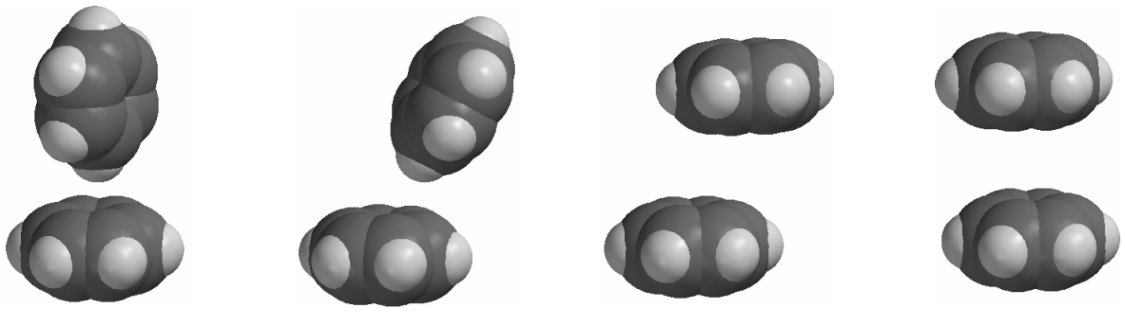

Edge-to Face | Tilted-T | slipped Face-to-Face | Face-to-Face

Figure 1.3: Representation of the possible geometries of a benzene dimer.

Quantum chemical calculations identify the Edge-to-Face arrangement of the non covalent benzene dimer as global minimum, although there is only a slightly energetical difference between the Edge-to-Face, Tilted-T, and slipped-Face-to-Face arrangements.[16, 17, 28-32] Only the Face-to-Face arrangement is substantially energetically unfavourable (Figure 1.3).

One descriptive interpretation for the formation of those energetically favoured geometries is delivered by the idealized model of π atoms developed by Hunter and Sanders in 1990.[33] This is a merely electrostatic model in which π atoms of aromatic residues are represented as point charges. In that model, regions with high electron density correspond to a formal negative charge. Analogously regions with low electron density correspond to a formal positive charge. In any case the total of all the charges must be in accordance with the atom's netto charge. Figure 1.4 shows the Hunter and Sanders' representation for one idealized π atom of benzene.

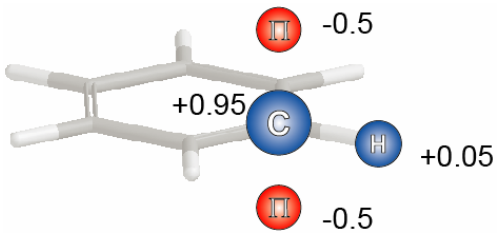

Figure 1.4: Representation of an ideal carbon atom of benzene according to Hunter and Sanders' model. Regions with positive electron density are depicted in blue while regions with negative electron density are shown in red.

The application of this model to the possible orientations of the benzene dimer, shows that in all the energetically favourable orientations there is an attractive electrostatic interaction, while in the less energetically favourable orientation the electrostatic interaction is repulsive (Figure 1.5).

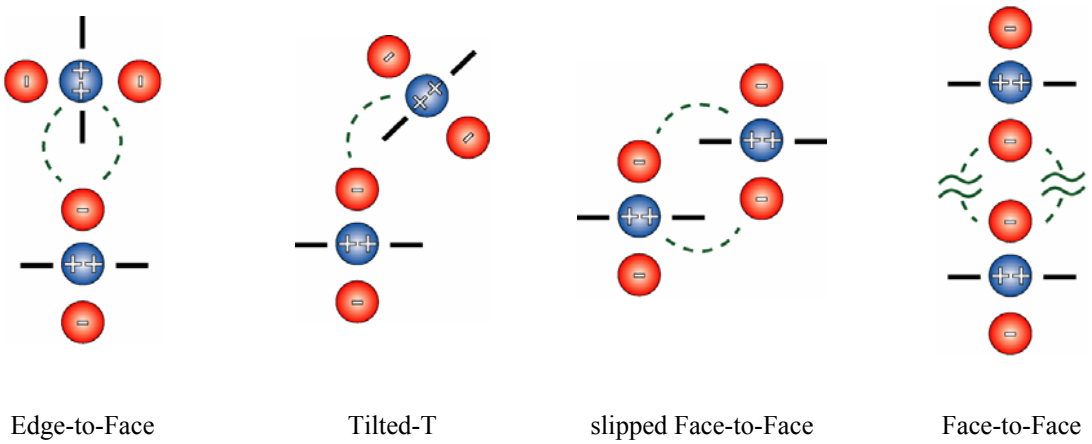

Figure 1.5: Hunter and Sanders' model representation of the possible geometries of the benzene dimer. Electrostatic interactions (both positive and negative) are highlighted with dashed green lines.

Even though Hunter's and Sanders'[33] model describes the benzene dimer quite accurately, more recent ab-initio calculations demonstrate that the electrostatic effect has been overestimated.[34] Although the electrostatic component, based on the quadrupole moment of benzene (Figure 1.6), has a considerable influence on the interaction geometry[20] in its dimer, today is generally accepted that the London dispersion interactions are the principal component in the stabilization energy in the dimer geometry.

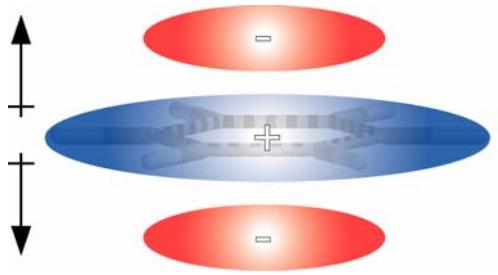

Figure 1.6: Schematic representation of the quadrupole moment of benzene.

In a later study[18, 35] Wilcox *et al.* investigated the stabilizing effect of the Edge-to-Face arrangement by means of a molecular torsion balance and showed that the substituent at the benzene ring do not have a large effect on the equilibrium between the open and the folded conformation, which is favoured (Figure 1.7), in solution as well as in the solid state. This finding leads to the conclusion that the electrostatics are less important for the stabilization of the arene-arene interaction. Hunter *et al.* came to different conclusion with their study of arene-arene interactions.[36] Additionally the effect of the substituent X in the conformational equilibrium is not fully explained by electrostatic interactions and it points out to a substantial contribution of dispersive interactions.

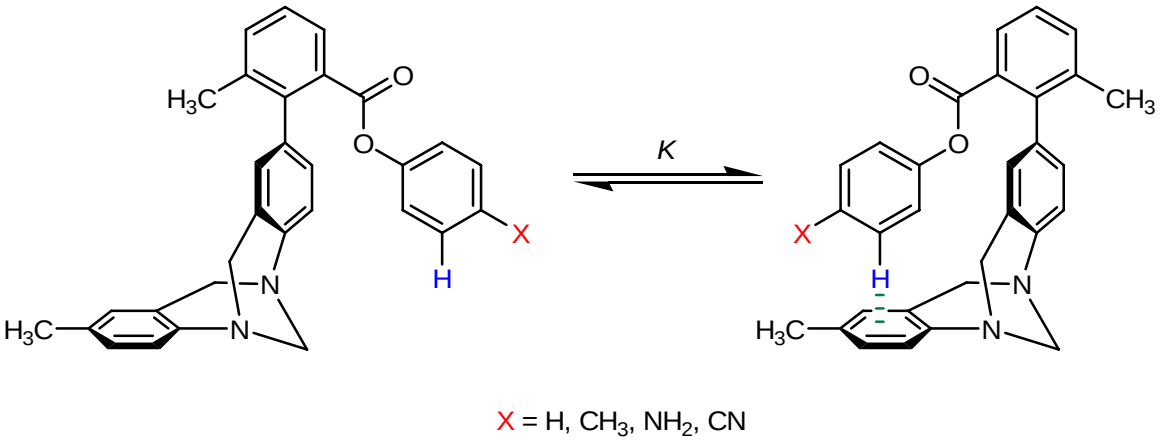

Figure 1.7: Molecular torsion balance studied by Wilcox *et al*. [18, 35] The equilibrium is shifted to the right hand side (folded conformation).

Siegel *et al*. were able to analyze the Face-to-Face interactions studying the rotation barrier in substituted 1,8-diarylnaphthalenes (Figure 1.8).[37] That experiment confirmed the model from Hunter and Sanders[33] in which the electrostatic interactions between two parallel oriented aromatic rings are of repulsive nature and sensitive to the variations of the ring substituents. With electron-withdrawing substituents, the electrostatic repulsion is reduced, the unfavoured Face-to-Face geometry is stabilized and the rotational barrier increases. Electron-donating substituents have the opposite effect. They increase the electrostatic repulsion, destabilize the Face-to-Face arrangement and lead to a decrease of the rotational barrier.

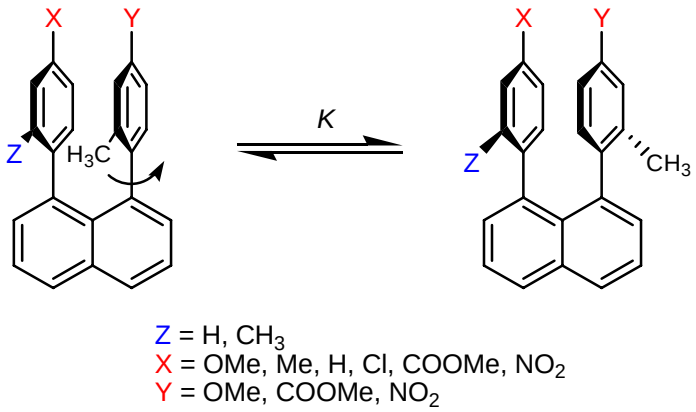

Figure 1.8: Conformational equilibrium used by Siegel *et al*. to study Face-to-Face interactions in 1,8-diarylnaphthalenes.

When an arene-arene interaction between two different aromatic units with different electronic demand is established, it is designated as electron-donor-acceptor (EDA) interaction. The resulting EDA-complexes are often called charge-transfer (CT) complexes,[38] even though the actual CT-interaction effect has only a minor influence on the stability of those complexes.[39]

In addition to arene-arene interactions, cation-π interactions are also of a great importance in supramolecular chemistry.[20, 40] According to the findings of Kerbarle *et al.*, the benzene is able to bind alkaline metals in gas the phase.[41] Further experiments in the gas phase have demonstrated that aromatic compounds can form a complex with a wide sequence of organic an inorganic cations.[40] According to quantum-chemical calculations the metal cation matches with the quadrupole of benzene and takes always a position along the C_6 axis above the ring plane (Figure 1.9)

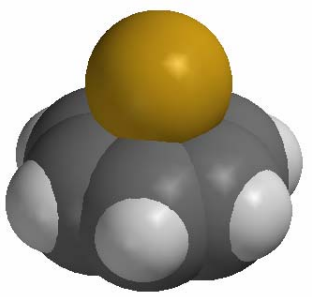

Figure 1.9: Schematic representation of the π-cation interaction, in this example the complex between benzene and potassium is shown.

1.3 Synthetic receptors

For the investigation of molecular interactions and supramolecular processes, different synthetic receptors have been developed. Although these synthetic receptors are relatively simple systems, they provide a basis for the understanding of more complicated biological systems.[36] The success of an artificial new receptor will be subject to several factors. Breslow[42] recognized that a very good pre-organized host avoids an entropically unfavourable conformational change resulting in a favourable complexation with a suitable guest molecule. The second characteristics for a good host molecule, beside the good pre-organization, is the number[43] and size[44] of the contact surfaces which are available for an intense host-guest interaction. According to this premise, the more and the larger the contact surfaces between host and guest are, the enhanced the binding process becomes.

Pedersen[45-47] and Lehn[48] developed very well known receptors for the complexation of alkaline and alkaline earth cations. Pedersen's coronands (crown ethers) have a macrocyclic structure and are widely used as phase transfer catalysts.[49-52] Lehn's cryptands, feature cage-like structures (Figure 1.10).

Figure 1.10: Structures of the receptors for alkaline and alkaline earth cations: a) crown ether synthesized by Petersen[45-47] and b) cryptand developed by Lehn.[48]

Macrocycles such as cyclophanes,[40, 53-55] cyclodextrines,[56-58] cryptophanes[59, 60] and carcerands[61, 62] (Figure 1.11) have been extensively investigated as host molecules for aromatic guests since all of them accomplish the principle of pre-organization explained before.

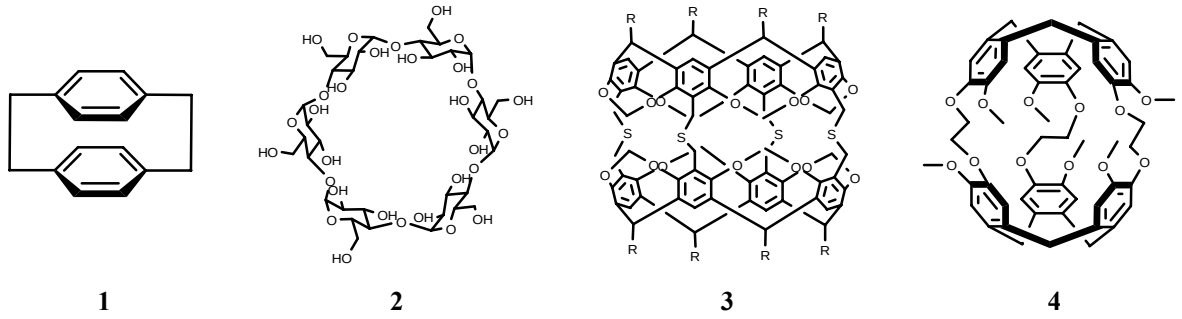

Figure 1.11: Schematic examples of cyclophanes (**1**), cyclodextrines (**2**), cryptophanes (**3**) and carcerands (**4**).

Furthermore non cyclic compounds, with more open structures, are suitable as synthetic receptors. These open-structure molecules have a certain degree of flexibility, provided that the cavity is large enough and the geometry is optimal to accommodate the desired guest molecule. The cavity of this new kind of receptors is made up of two so-called sidewalls connected to each other by a central spacer unit, which can be either flexible or rigid. Chen and Whitlock[63] described this type of receptor for the first time and, due to the binding mechanism (Figure 1.12), refer to them as molecular tweezers.

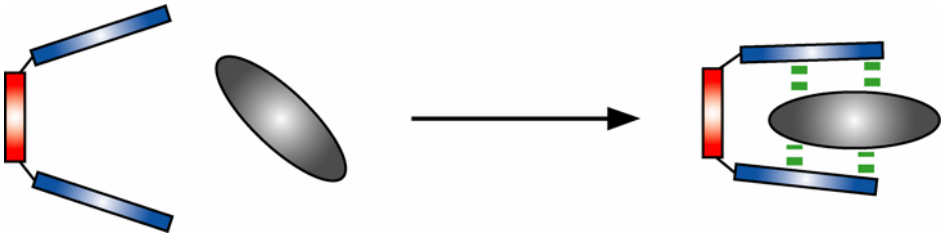

Figure 1.12: Representation of the operation mode of a molecular tweezer, formed by the sidewalls (blue) connected through a central spacer unit (red). Thanks to the pre-organized cavity, the tweezer is able to bind substrate molecules of an adequate size.

The first molecular tweezers developed by Chen and Whitlock consisted of caffeine sidewalls and different kinds of spacer units, a flexible (**5**, Figure 1.13) or a rigid one (**6**, Figure 1.13). Both receptors form complexes with aromatic substrates such as 1,3-dihydroxynaphthalene-2-carboxylic acid (DHNA, **7**) due to π-π interactions between host and guest.[63]

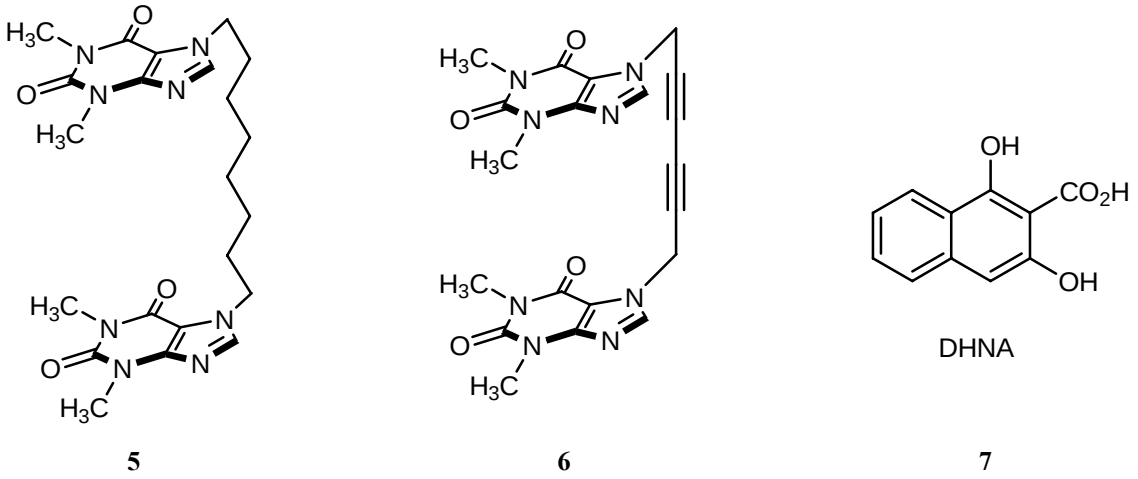

Figure 1.13: First molecular tweezers prepared by Chen and Withlock and 1,3-dihydroxynaphthalene-2-carboxylic acid used as a guest molecule.

The receptor **5**, with a flexible spacer unit, binds DHNA, in water solution at room temperature with an association constant of $K_a=10^3$ M^{-1}, whereas receptor **6**, with a rigid spacer unit, shows an association constant of $K_a=10^4$ M^{-1} under the same experimental conditions. This example shows how a good pre-organization of the host cavity affects the binding properties. The cavity of the receptor **6** has an optimal pre-organization because of the rigid spacer resulting in an increase of the association constant.

Zimmerman *et al*. investigated molecular tweezers such as **8**, which have aciridine, anthracene or phenanthrene sidewalls (Figure 1.14). These tweezers bind nitro aromatic polycycles like 2,4,5,7-tetranitro-9*H*-fluoren-9-one, **9**, forming strong EDA-complexes, which are stabilized by π-π interactions.[37, 64-66] With this type of receptor it is possible to investigate

the effect of the polarizability of the contact surface on the association constant. Accordingly it was found that the association constant between the clip **8** and 2,4,5,7-tetranitro-9 *H*-fluoren-9-one increases with the better polarizability when changing the sidewalls from aciridine to anthracene.[64]

Nolte *et al*. described the molecular clips of the type **10**, with a glycouril spacer unit where both benzene and anthracene sidewalls can be annulated.[67] This way it is possible to study the effect of the size and electrostatic nature of the sidewalls on the binding properties of aromatic molecules.

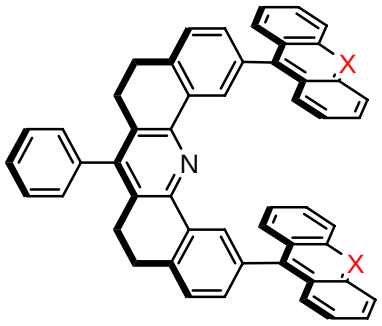

8

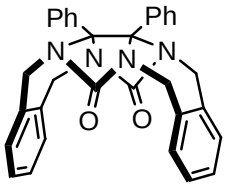

10

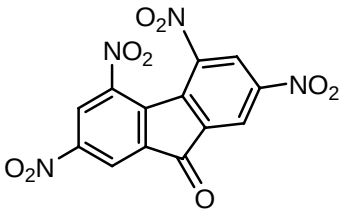

9

Figure 1.14: Molecular tweezers developed by Zimmerman (**8**) and Nolte (**10**) and the 2,4,5,7-tetranitro-9*H*-fluoren-9-one (**9**) used as a guest molecule on Zimmerman's tweezers.

Klärner's research group succeeded in the synthesis of molecular tweezers **11** and **12**,[68, 69] with ester groups at the end of the sidewall. These molecular tweezers are synthesized via repetitive Diels-Alder reactions between norbornadiene, benzene and naphthalene building blocks. This method was first developed by Stoddart *et al*. and it can be considered as a molecular LEGO.[70, 71] These first tweezers synthesized in our group show only relatively low binding properties with benzoaromatic and aliphatic molecules. Afterwards the unsubstituted benzene and naphthalene spaced tweezers **13a-d** and **14a,b,d** were synthesized.[72-74] These new tweezers form more stable complexes with electron-withdrawing, neutral and cationic guest molecules. Due to the size of its cavity, receptor **13** forms more stable complexes with aliphatic guests, while receptors **14** can better stabilize both aromatic and quinoid substrates. Quantum-chemical calculations[75, 76] show that the cavity of tweezers **13** and **14** has a highly negative electrostatic potential, which explains why the binding with electron-withdrawing substrates is a favourable process. Due to the effect of the electron pulling ester groups, the electrostatic potential on the cavity of tweezers **11** and **12** appears to be less negative than that of the unsubstituted tweezers **13a-d** and **14a,b,d**. This fact, explains why tweezers **11** and **12** form weaker complexes with electron-withdrawing substrates than tweezers **13** and **14**. Even so, the electron pulling strength of the ester groups is not large enough to make tweezers appropriate receptors for electron rich guests.

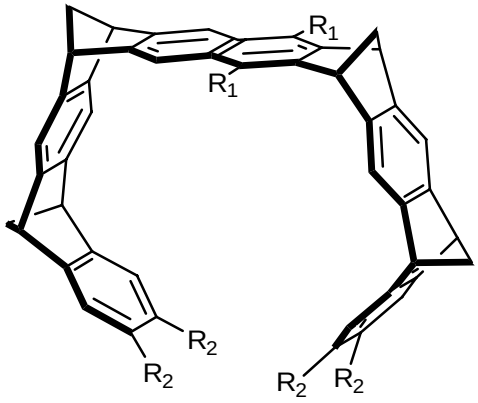

12: R_1= OMe; R_2= CO_2Me

14: R_1= R_2= H

15: R_1= OAc; R_2= H

16: R_1= OMe; R_2= H

17: R_1= O-P(O)(CH_3)OLi; R_2= H

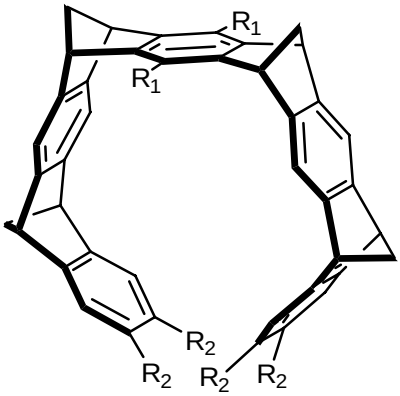

11: R_1= OMe; R_2= CO_2Me

13: R_2= H

a: R_1= H; **b**: R_1= OAc

c: R_1= OH; **d**: R_1= OMe

e: R_1= OP(O)($OLi)_2$

Figure 1.15: Molecular tweezers synthesized on Klärner's research group.

In order to study the impact of the receptor topology on the stability of the complexes, the dimethylene bridged clips **18**, **19** and **20** were prepared.[77-79] Binding experiments with these clips evidence that, although the clips are able to bind aromatic electron-withdrawing and quinoid substrates, the association constant of the complexes formed with these clips are significantly smaller than those observed for the tweezer **14**. Due to their open topology, clips **18a-d** are less selective (in reference to the size of the guest molecules) than the tweezers **13** and **14**. For that same reason they have the ability to bind more bulky substrate molecules, such as 2,4-dinitrofluorobenzene, which shows no association with tweezer **14**.

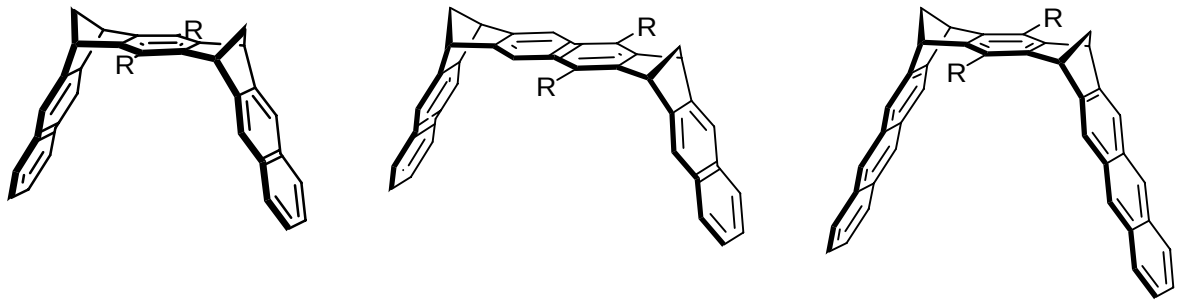

18 **19** **20**

a: R= H; **b**: R= OAc; **c**: R= OH; **d**: R= OMe; **e**: R= O-P(O)(CH_3)OH

f: R= O-P(O)(CH_3)O^-·N^+(nBu)$_4$: **g**: R= O-P(O)(CH_3)O^-·Li^+, **h**: R= OP(O)(OLi)$_2$, **i:** R= -OP(OH)O^-·Li^+

Figure 1.16: Dimethylene bridged clips synthesized in Klärner's research group.[77-79]

The different receptor properties between clips **18** and the tweezers **13** or **14** result in the number of contact surfaces (three in the clip **18** and five in the tweezer **13**) as well as their topology. In the formation of π-π attractive interactions between receptor and substrate, the naphthalene sidewalls of clip **18** have to be contracted as shown in the crystal structure,[77, 78] which increases the potential energy of the receptor cavity. This observation has its most dramatic example in the anthracene clips recently synthesized. The comparison between the crystal structures of the empty clip **20d** and the complex of clip **20c** with 1,2,4,5-tetracyanobenzene (TCNB) shows a contraction of the distance between the end of both sidewalls of 8 Å, being 14.5 Å in the empty clip **20d** and 6.5 Å in the complex **TCNB@20c**.[79] In contrast, as a result of their topology, tweezers **11-14** do not require such a deformation for the formation of arene-arene interactions in the complexes. Furthermore, the quantum chemical calculated EPS[75] inside the clip cavities of **18** is significantly less negative than those calculated for the tweezers' cavities (**14**). For that reason, the arene-arene interactions depending on both electrostatic and dispersive forces make the clip **18** a worse receptor than the tweezer **14**.

For the study of the properties of **18** as a receptor in water, the phosphonate substituted clip **18f**[80] has been most recently synthesized. This clip binds selectively *N*-alkylpyridinium salts such as *N*-methylnicotinamide iodide (NMNA) and NAD^+ in protic solvents. Further studies showed that **18f** is able to form complexes with an extensive collection of biological relevant molecules both in water and in methanol. These results point to a significant contribution of the hydrophobic effect to the host-guest interaction in aqueous solution.[81]

In order to achieve a receptor which combines an open cavity and an optimal distance for the binding of aromatic guest molecules which does not need contraction of the sidewalls, the trimethylene-bridged clips **21** and **22** were also synthesized.[82, 83] Binding experiments with this clip show that this new receptor forms more stable complexes with aromatic guests than the dimethylene clips and, in some cases, more stable complexes than the molecular tweezers. An example of these intermediate properties is the complex formation of **22** with

TCNB: the association constant for this (1:1)-complex was determined to be K_a= 1.4·10^7 M^{-1}[82, 83] and is much higher than those found for the tweezer **14b** (K_a= 7.3·10^5 M^{-1})[84] and the clip **18b** (K_a= 1.4·10^2 M^{-1}).[77, 78]

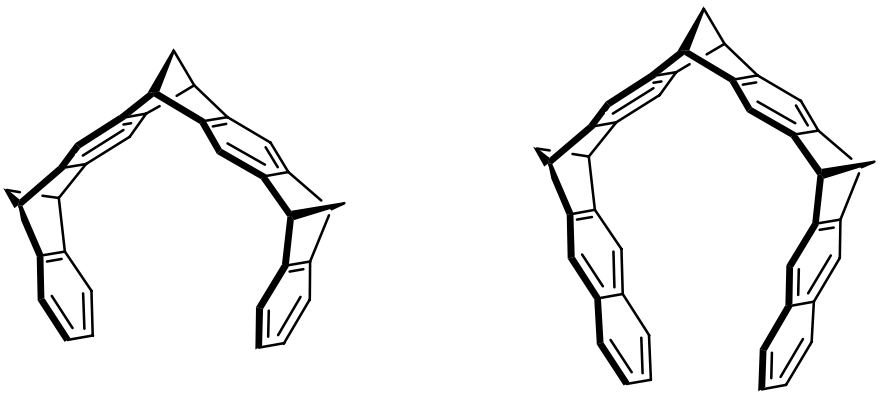

21 **22**

Figure 1.17: Trimethylene-bridged clip synthesized by Lobert.

1.4 Target of the work

All three water-soluble molecular clips **18f-h** have anionic substituents at the spacer unit, therefore it is to be expected that in the binding processes with these clips, the attractive ionic interaction of the positively charged guest molecule (like NMNA and NAD$^+$) plays an important role for the host-guest complex stability. Therefore, water-soluble receptors (molecular tweezers and clips) with neutral hydrophilic substituents were the first targets of this work.

The use of hydrophilic substituents such as dendrimer units in order to tailor the properties of supramolecular receptors is a well known methodology with increasing perspectives. For instance, Diederich *et al*. have successfully incorporated dendrimer substituents to porphyrin units in order to alter the polarity of the environment of the electrophore and modify the electrochemical behaviour.[85] Moreover, the use of hydrophilic substituents to obtain water-solubility of hydrophobic groups is an effective method observed in the nature itself: in most of the α-helices of many proteins it is possible to observe how the hydrophobic residues of the amino acids are predominantly in one side of the axis while the hydrophilic ones are on the other side. The result is a tertiary structure where these amphipathic helices are well adapted to the formation of interfaces between polar and non polar regions such as the hydrophobic interior of the protein and its aqueous environment.[86]

Hence, our target was to synthesize molecular tweezers with hydrophilic dendritic substituents of first and second generation of building block **23** and **24** respectively (Figure

1.18) in order to analyze the importance of salt bridges for the complex stability in water solution.

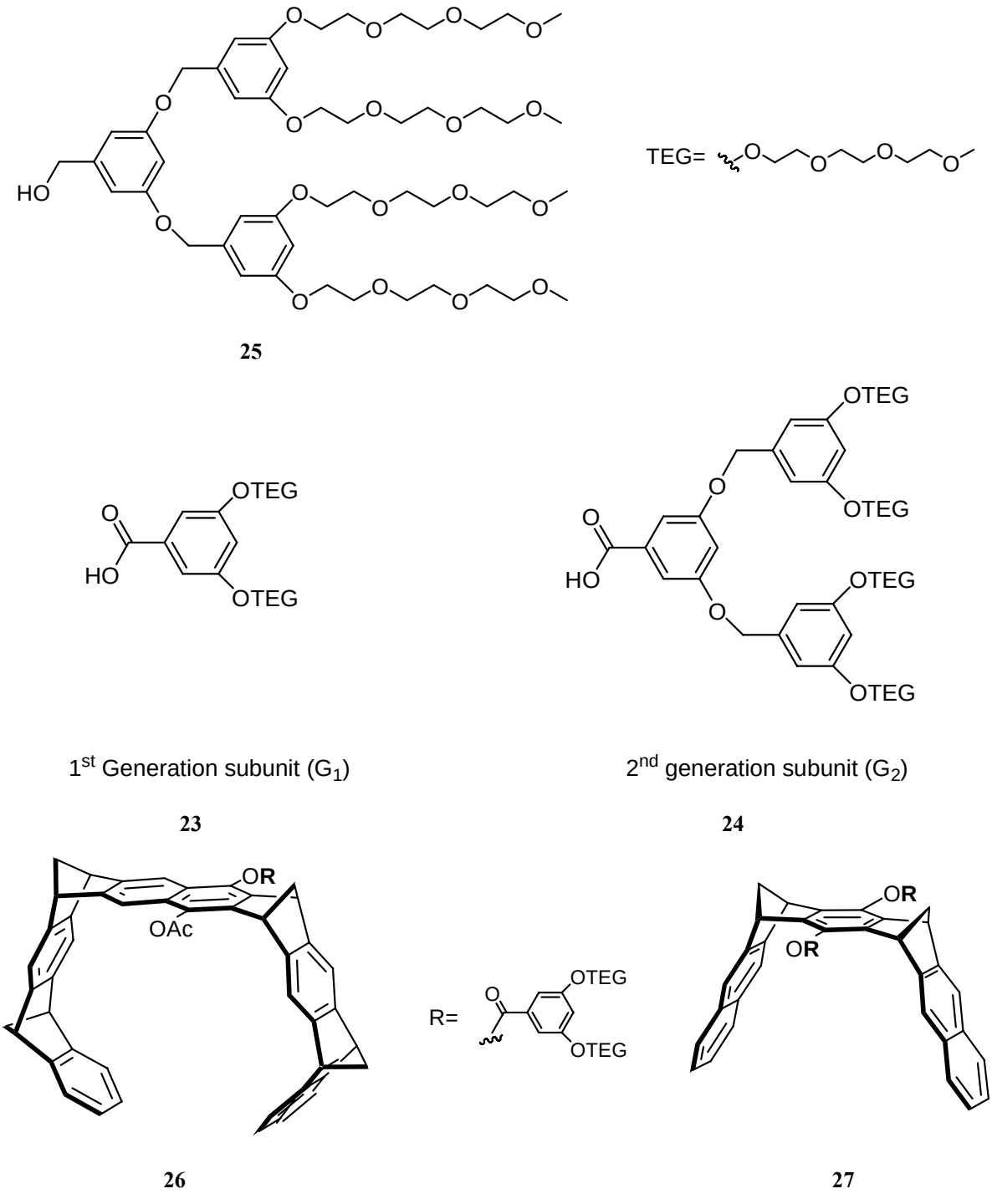

Figure 1.18: Top: triethyleneglycol dendritic structures developed by Hannon *et al.* (**25**),[87] starting point of this work Middle: dendritic substituents with acyl groups which shall be used (**23** and **24**). Bottom: Molecular tweezer, **26** and clip **27** with dendritic substituents planned as a first target.

The dendrimer skeleton requested for the synthesis of the substituted tweezers and clips (**25**, Figure 1.18) has already been prepared by Hannon *et al.* in multistep synthetic

procedures.[87] Since the diacetoxy substituted tweezers **15** and clip **18a** are usually better receptors in organic media than the corresponding dimethoxy substituted systems (**16** and **18d** respectively), we planned to link the dendrimer with acyl groups to the tweezers and clips instead of the original dendrimers from Hannon *et al.* (**25**, Figure 1.18) [87] as shown in Figure 1.18 (**26** and **27**).

Another possibility to obtain water-soluble clips on a less conventional synthetic route, less elaborate than the stepwise synthesis of the dendrimers of first, second and third generation, is the one-pot synthesis of the molecular clips with hyperbranched polyglycerol substituents (**28**, Figure 1.19) developed by Prof. Haag *et al*.[88] These hyperbranched polyglycerol substituted clips shall provide the possibility to study the effect of the hydroxyl groups in the substituents on the host-guest complex formation in comparison to the clip **27**. A significant difference in the complex stability is to be expected with guest molecules having hydrogen-bond acceptors. In the case of the hyperbranched polyglycerol substituted clips, the presence of many hydroxyl groups can increase the stabilization of the complex, due to the formation of intermolecular hydrogen bonds between host and guest.

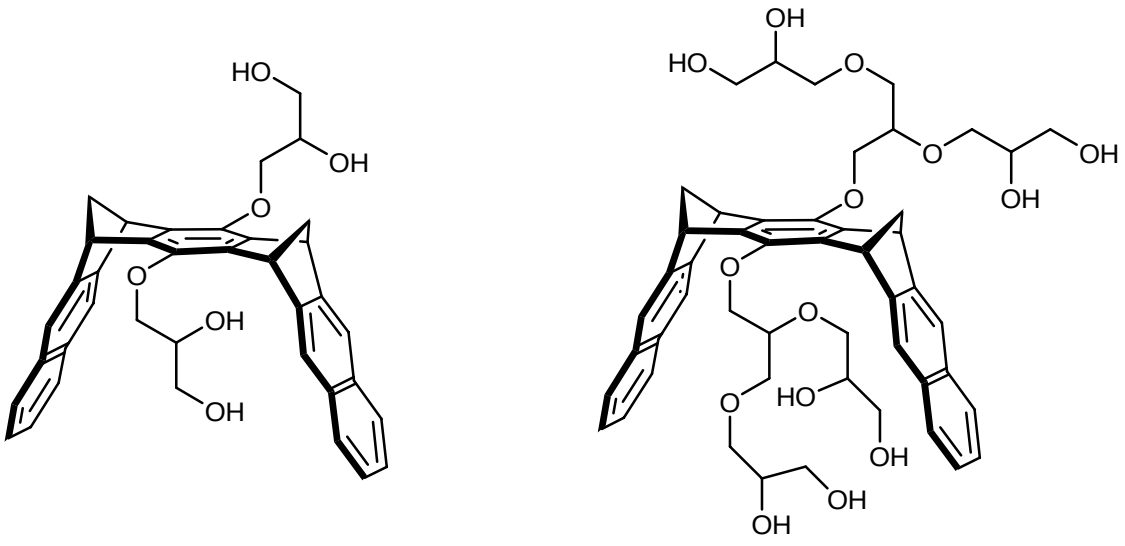

1st Generation

28

2nd Generation

29

Figure 1.19: Hyperbranched molecular clips **28** and **29**.

Water-soluble molecular clips substituted with both phosphonate (**18e**) and phosphate groups (**18h**) have been a topic of research in the past few years. Despite the similarity between the phosphonate and phosphate functional groups, the supramolecular properties of both clips appear to be significantly different from each other. For instance, the phosphate clip tetralithium salt **18h** shows self-aggregation in water solution while there is not evidence of this phenomenon for the phosphonate clip dilithium salt **18e**.[89] Additionally, the binding

properties of these clips in phosphate buffer solution (pH= 7.2), change dramatically from one clip to another as well as with the pH values of the solution.[90] A representative example of these binding properties is shown in Table 1.1, where the association constants in buffer solution for the guest molecules shown on Figure 1.20 are compared.

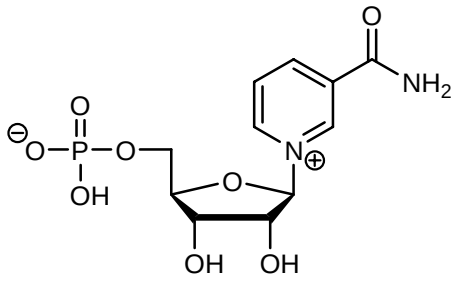

Nicotinamide mononucleotide

(NMN) **30**

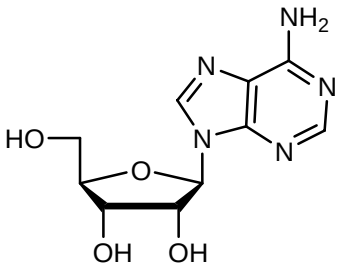

Adenosine

31

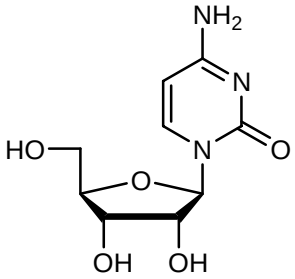

Cytidine

32

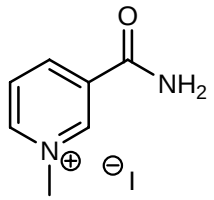

N-methylnicotineamide iodide

(NMNA) **33**

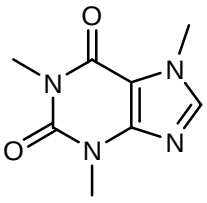

Caffeine

34

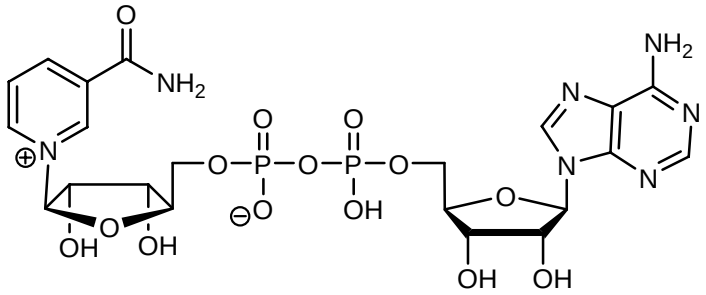

Nicotinamide adenine dinucleotide

(NAD^+) **35**

Figure 1.20: Biological relevant molecules used to compare the binding properties of the phosphonate and the phosphate clips.

Guest	Phosphonate clip 18e K_a [M^{-1}]	Phosphate clip 18h K_a [M^{-1}]
Nicotinamide mononucleotide **30**	550	1120
Adenosine **31**	1115	1400
Cytidine **32**	1070	9685
N-methylnicotinamide iodide **33**	11270	35000
Caffeine **34**	9550	42700
NAD^+ **35**	4200	5630

Table 1.1: Comparison of association constants (M^{-1}) among some biological relevant molecules with the phosphonate and phosphate clips in phosphate buffer solution (pH= 7.2).

As summarized on Table 1.1 above, the binding properties of adenosine (**31**) and nicotinamide adenine dinucleotide (**35**) with the receptors **18e** and **18h** are not significantly different. However, for the other guest molecules in Table 1.1, the phosphate clip **18h** shows association constants between 2 and 10 times larger than those of the phosphonate clip **18e**.

The study of supramolecular properties of ionic water-soluble clips, such as **18f-h**, with biological relevant substrate molecules shall be expanded in this work. We propose sulphate substituents to be appropriate functional groups for the molecular clips.

Since sulphuric acid is one of the strong acids in contrast to the phosphoric acid, the sulphate group is expected to be pH neutral and hence an appropriate substituent for the preparation of another water-soluble clip. Furthermore the negative charge of the sulphate group ($R\text{-}O\text{-}SO_3^-$) is delocalized in three S---O bonds whereas in the phosphonate group ($R\text{-}O\text{-}P(CH_3)O_2^-$) the negative charge is only delocalized in two P---O bonds and in phosphate group ($R\text{-}O\text{-}PO_3^{2-}$) the two negative charges are delocalized in three P---O bonds. Because the $R\text{-}O\text{-}PO_3^{2-}$ groups reacts as base in aqueous solution, this group is certainly partially protonated in buffer solution at pH= 7.2.

Sulphur-arene interactions are also of special importance in molecular recognition[20] and additional sulphate groups are widely present in nature and are also of interest for the finding of new substances with pharmacological relevance.[91-97] Thus, in order to study the substituent effect on anionic water-soluble clips, the sulphate substituted clips **36**, **37** and **38** (Figure 1.21) are planned to be synthesized and their supramolecular properties shall be compared to those of the clips substituted with phosphate and phosphonate groups (**18f-h** and **20f**).

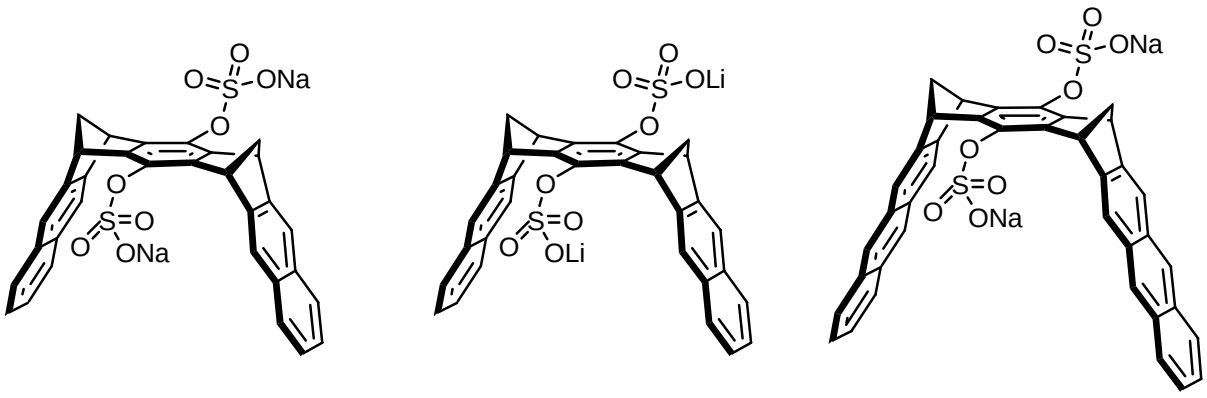

36 **37** **38**

Figure 1.21: Sulphate substituted clips planned for the study of the substituent effect of anionic groups on complexation processes in water solution.

2 Results and discussion

2.1 Synthesis of molecular tweezers and clips substituted by triethyleneglycol-based groups

2.1.1 Synthesis of molecular tweezers

The starting molecular tweezer for this work is the diacetoxy substituted tweezer **15**, which was synthesized by Burkert[74, 98] (Scheme 2.1 below).

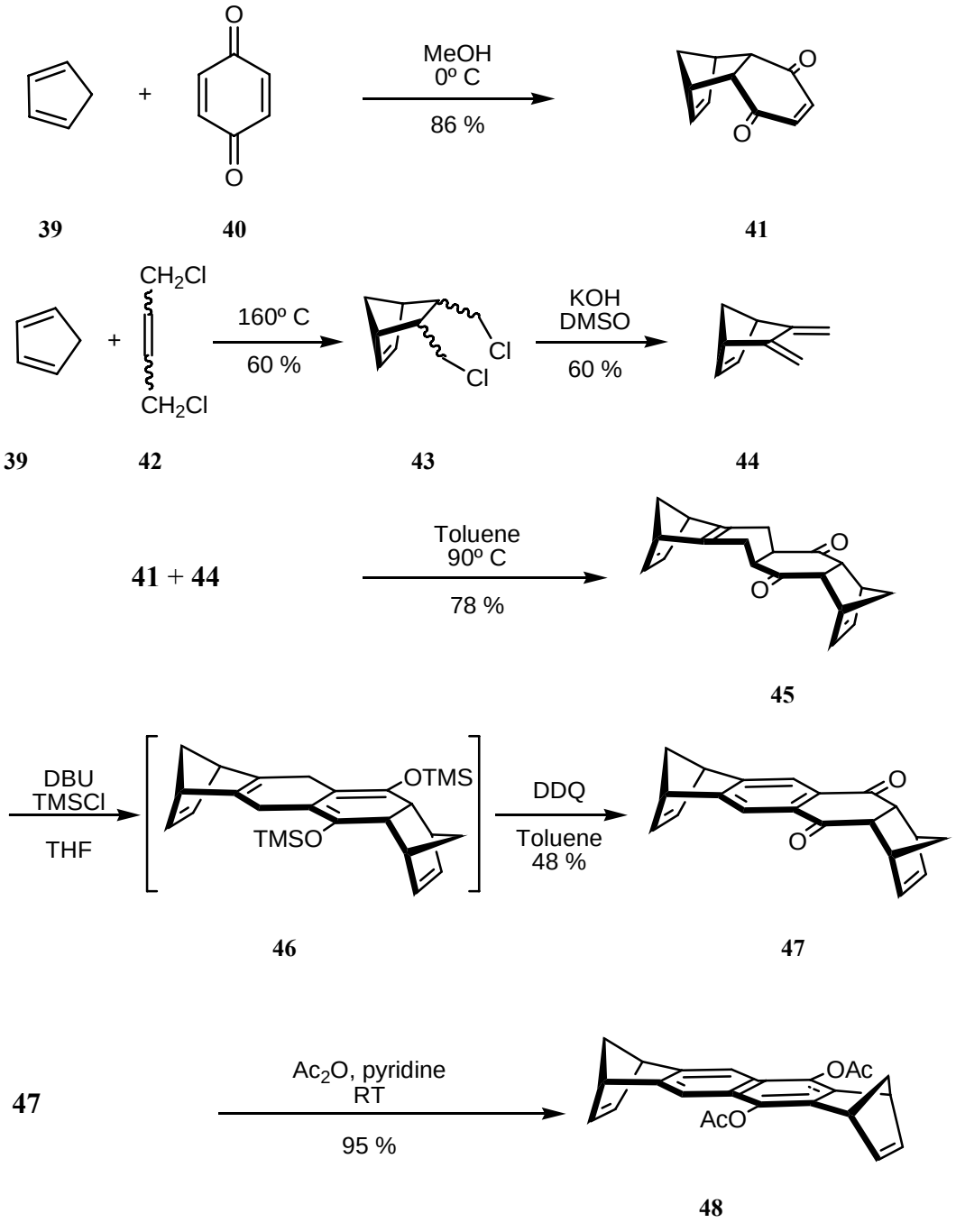

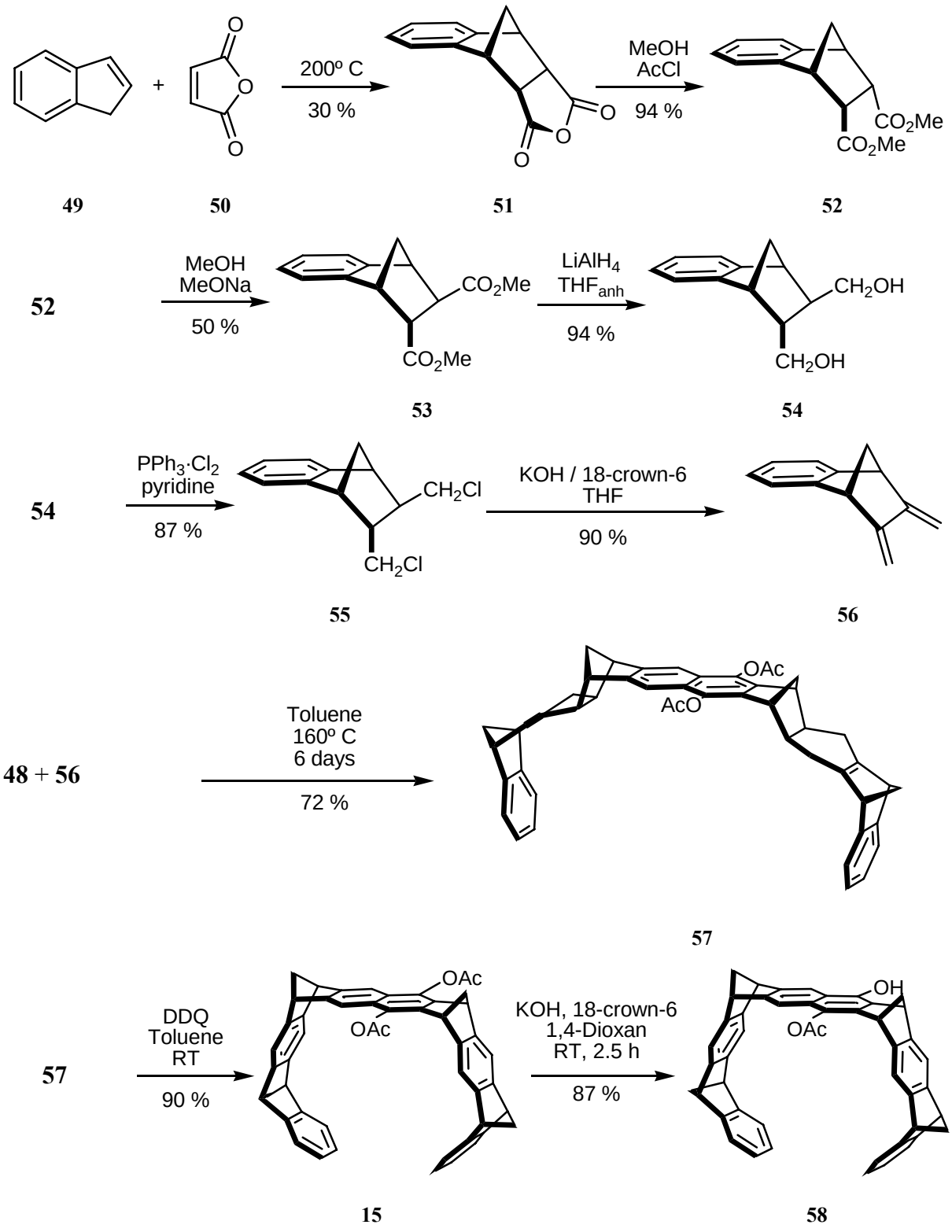

Scheme 2.1: Synthetic pathway to the acetoxy tweezer **15** and hydroxy-acetoxy tweezer **58** developed in Klärner's research group.

The overall reaction can be considered as a molecular LEGO[70, 71] consisting of Diels-Alder reactions of the two building blocks: the bisdienophile **48** and diene **56**. The high stereoselectivity of the Diels-Alder reaction, which occurs exclusively on the *exo* face of the

dienophile and the *endo* face of the diene leading to the (2:1) adduct **57** and in the subsequent step leads to the concave-convex topology of the tweezer **15** after oxidative dehydrogenation of the cyclohexene rings with 2,3-dicyano-5,6-dichloro-parabenzoquinone (DDQ).

2.1.2 Synthesis of triethyleneglycol-based dendrimers

Molecular tweezers of type **26**, substituted by dendrimers, can be formally obtained by the reaction between the corresponding hydroxyl substituted tweezer **58** and the acyl chloride of the dendrimer substituent (Scheme 2.2). In order to obtain tweezer **58** one of the two acetoxy groups of **15** has to be selectively hydrolyzed by potassium hydroxide in the presence of crown-ether (18-crown-6), leading to the monohydroxy-acetoxynaphthalene tweezer **58**.

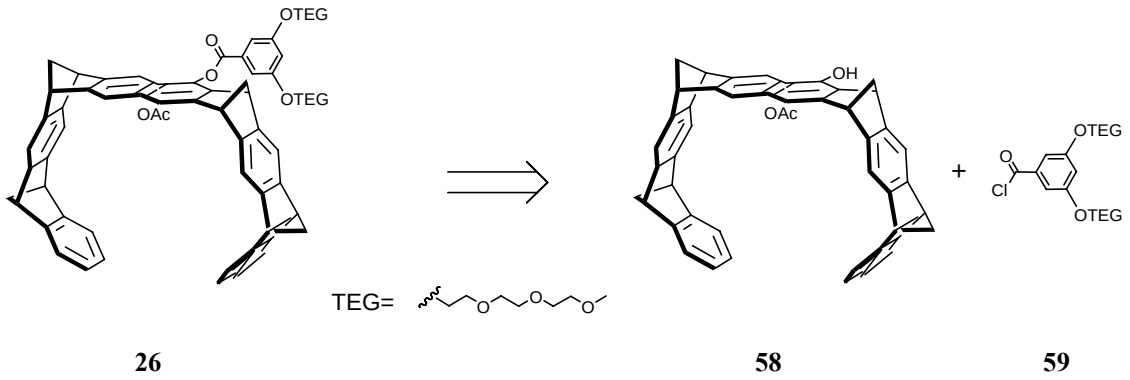

26 **58** **59**

Scheme 2.2: Retrosynthetic analysis of the dendrimer substituted receptors.

For an easier handling and better understanding, these compounds are classified by generations, **59** being the *first generation* of the dendrimer (G_1) with one benzene ring and two triethyleneglycol monomethyl ether (TEG) branches and the **60** *second generation* (G_2) with three benzene rings and fours TEG branches (Figure 2.1).

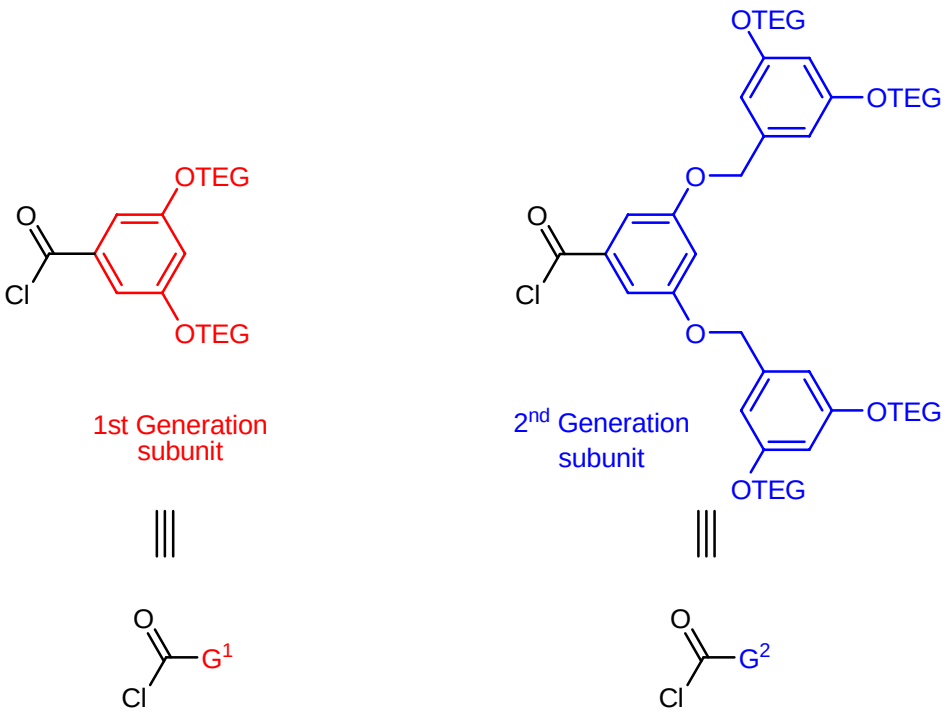

59 **60**

Figure 2.1: Classification of the dendrimer substituents according to their generation.

Although the methyl carboxylate of the dendrimer of first generation (G_1) **61** (Scheme 2.3) has been already described by Hannon *et al.*,[87] the synthesis has been modified and improved in this work. Hannon's further generations of dendrimer (**25**, Figure 1.18) are significantly different from those required for this work. However, the synthetic pathway developed by Hannon was easily adapted and optimized in order to obtain the acyl chloride of the G_2 dendrimer, **60**. The complete retrosynthesis of the G_2 acyl chloride **60** is shown in Scheme 2.3. The G_1 acyl chloride **59** can be easily obtained from the G_1 methyl carboxylate **61** by hydrolysis of the ester functions and conversion of the resulting carboxylic acid into the acyl chloride **60**.

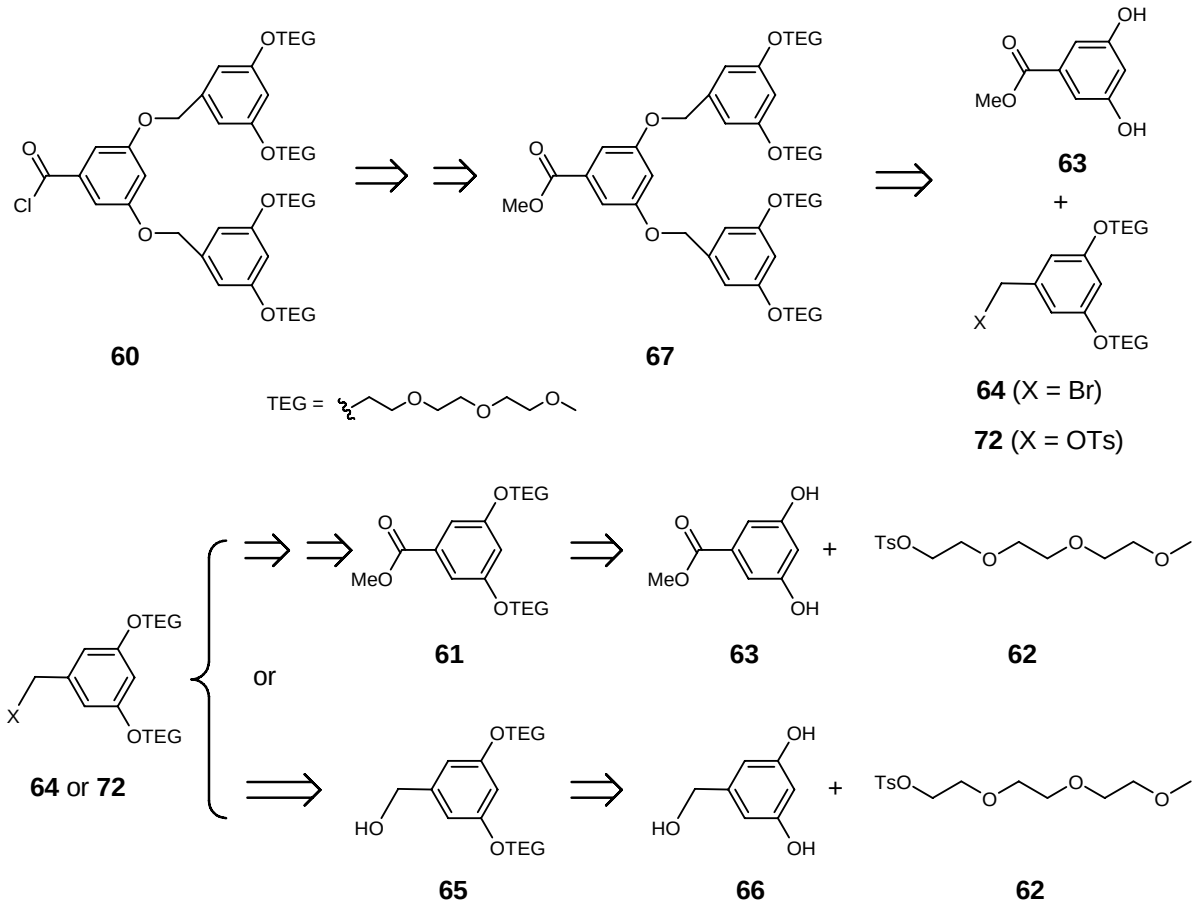

Scheme 2.3: Retrosynthesis of the triethylene glycol (TEG) substituted dendrimers **61** (G_1) and **60** (G_2).

The synthesis of the G_1 substituted benzoyl chloride **59** starts with the triethyleneglycol monomethyl ether (TEG) tosylate **62**, which was prepared according to the procedure reported by Hannon *et al*.[99]

Nucleophilic S_N2 substitution of tosylate **62** with methyl 3,5-dihydroxy-benzoate **63** leads to the TEG substituted methyl benzoate **61** (Scheme 2.4). Following the literature procedure **62** was reacted with **63** and sodium hydride at 60 ºC for 22 hours using dry DMF as a solvent. Unfortunately we could not obtain the literature[99] yield 76 %, achieving just 51 %. Therefore we decided to use another coupling method for phenol derivatives and alkyl tosylates.[100] This method uses potassium carbonate as a base and a shorter reaction time (three hours) at a higher temperature (80 ºC) also in dry DMF as a solvent. Using this method, not only a higher yield of 96 % was obtained compared to the maximum yield of 75 % found in the literature but it also allowed us to run the reaction under less rigorous conditions than those required for the reaction with NaH.

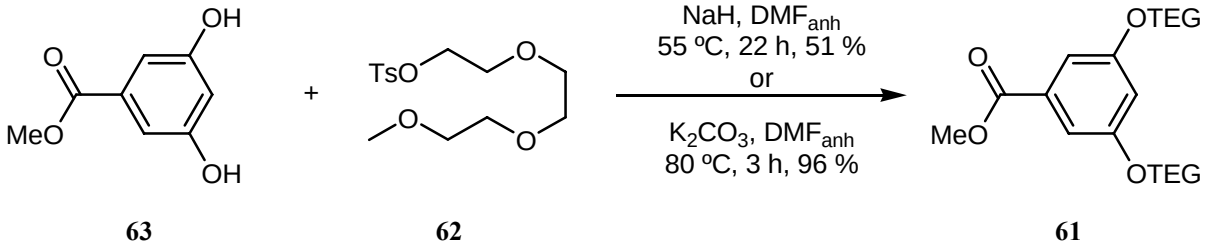

63 **62** **61**

Scheme 2.4: Reaction conditions for the first to steps to the first generation dendrimer substituent.

The hydrolysis of the methyl ester **61** with potassium hydroxide was carried out at reflux in a mixture of water-ethanol (1:1) as solvent for 18 hours. The free acid **23** was obtained after an acidic work-up in 91 % yield, which is slightly lower than that reported in the literature (98 %).[99]

The acyl chloride **59** was first obtained from the reaction of the benzoic acid **23** and thionyl chloride in toluene at 90 ºC for 18 hours. This method gave the desired benzoyl chloride **59** as a dark oil with the same yield as that obtained in the literature[101] (99 %). Because of the dark colour of **59**, another chlorination procedure was tried.[102] The reaction of the benzoic acid **23** with oxallyl chloride in toluene as a solvent at room temperature for two and a half hours, gave the benzoyl chloride **59** as a pale yellow oil. The yield of 79 % was, however, lower than that obtained by us and in the original reference[102] (99 %) using thionyl chloride for the chlorination.

Despite the colour, benzoyl chlorides **59** obtained in both ways showed identical NMR (^{1}H and ^{13}C), IR, UV spectra and HR-MS (ESI-TOF) spectrum. However, since the benzoic acid **23** can be easily prepared in gram-scale amounts, the oxallyl chloride method was used for the preparation of the benzoyl chloride **59** in this work.

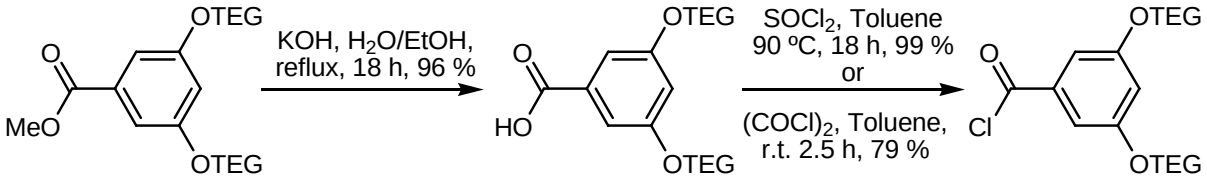

61 **23** **59**

Scheme 2.5: Reaction conditions to obtain the final G_1 dendrimer substituent (G_1-TEG).

The synthesis of **64**, the G_2 dendrimer subunit, reported in the literature[87] started with the reduction of the G_1 methyl ester **61** to the G_1 benzyl alcohol **65** by means of $LiAlH_4$ in dry THF. However, taking advantage of the higher reactivity of the two aromatic hydroxyl groups in the 5-(hydroxymethyl)benzene-1,3-diol **66** (Scheme 2.6) we chose a more straight-forward synthetic path.

The benzyl alcohol **66** reacts with two equivalents of the tosylate **62** in dry acetone for 14 hours at reflux in presence of potassium carbonate and 18-crown-6. Acidic working-up leads to the desired TEG benzyl alcohol **65** in quantitative yield.

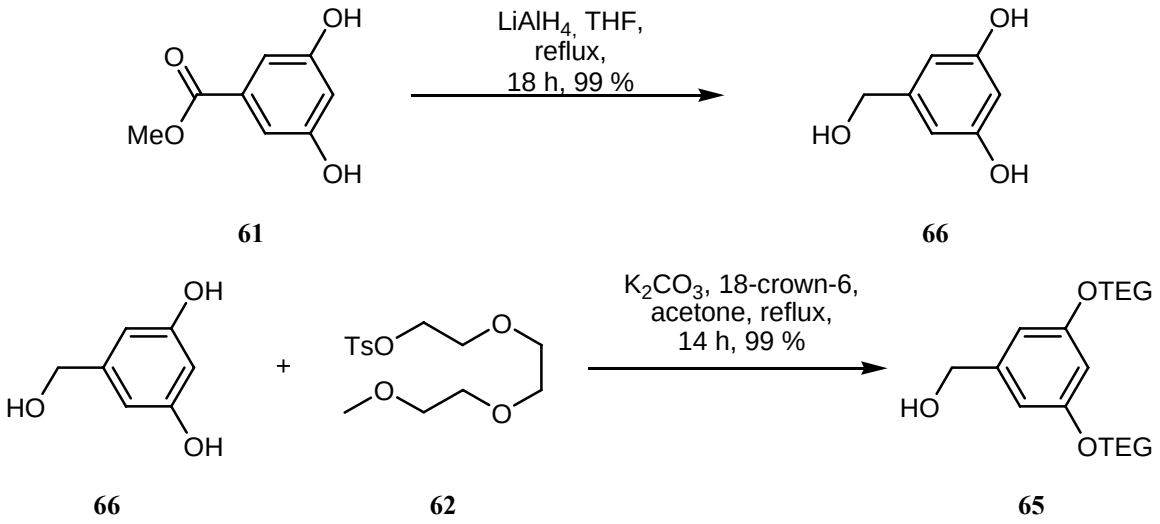

Scheme 2.6: First step for the synthesis of G_2 subunit dendrimer substituent.

The coupling of the subunits **65** with the methyl 3,5-dihydroxy benzoate **63** leading to the G_2 substituted methyl benzoate **67** requires a good leaving group in the methylene position. In the original work,[87] Hannon *et al*. prepared the G_1 benzyl bromide **64**. In this work the G_1 benzyl alcohol **65** was reacted with tetrabromomethane (CBr_4) and 1,2-bis(diphenylphosphoryl)ethane **68** in dry THF at 0 ºC for 15 minutes leading to the benzyl bromide derivative **64** in 79 % yield after purification by column chromatography. Although this procedure exceeded the literature[87] yield of 60 %, the difficult isolation of **64** from by-products and the excess of unreacted 1,2-bis(diphenylphosphoryl)ethane **68**, made us look for an alternative synthetic method that allows an easier purification of the product. Since the tosylation of triethyleneglycol monomethylether **62** proceeds without the need of additional purification, the reaction of benzyl alcohol **65** with tosyl chloride **70** was carried out under the same conditions leading to the TEG-benzyl tosylate **72** in 85 % yield (Scheme 2.7).

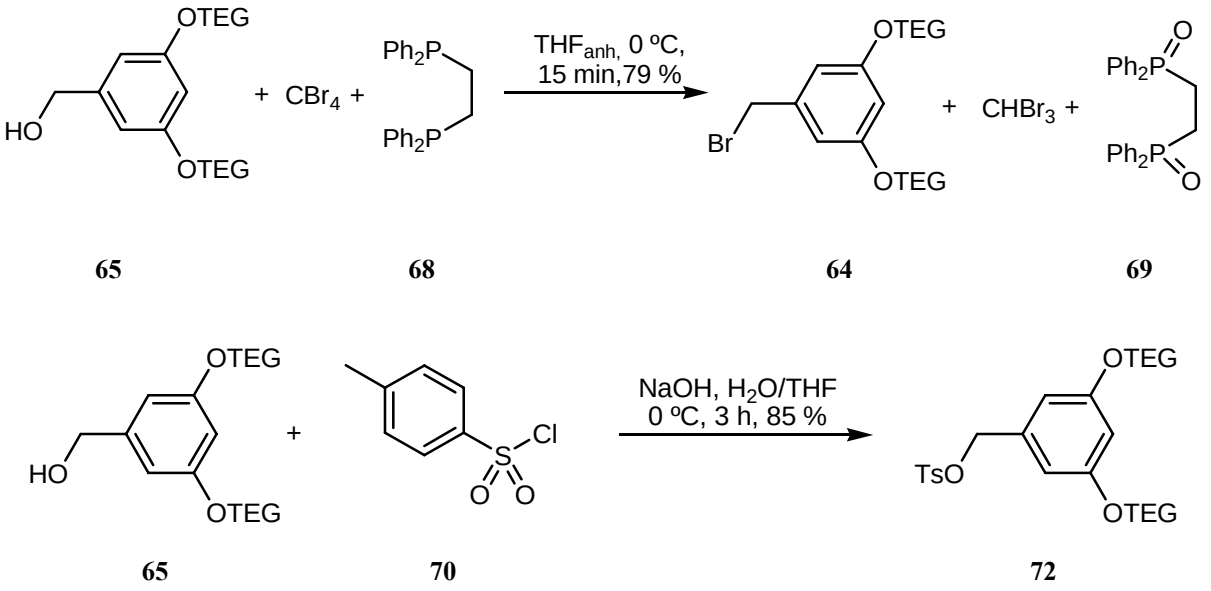

Scheme 2.7: Conversion of the hydroxyl into a good leaving group.

The G_2 methyl ester **67** was obtained by the S_N2 reaction of the methyl 3,5-dihydroxy benzoate **63** with the G_1-benzyl bromide **64** or the tosylate **72**. In both cases, the ester **63** reacts with two equivalents of bromide **64** or tosylate **72** under similar conditions to those used for the preparation of G_1 benzyl alcohol **65** (Scheme 2.6), changing only the reaction time from 3 to 18 hours. The yield varies from 37 % for the reaction of the bromide **64**, to 91 % for the reaction of the tosylate **72**. The obtained G_2 methyl benzoate **67** was saponified and then chlorinated under the same conditions than those used for the reaction of the corresponding G_1 methyl benzoate giving, finally, benzyl chloride **60** in 99 % yield (using $SOCl_2$ for the chlorination) or 76 % yield (using $(COCl)_2$ for the chlorination) (Scheme 2.8).

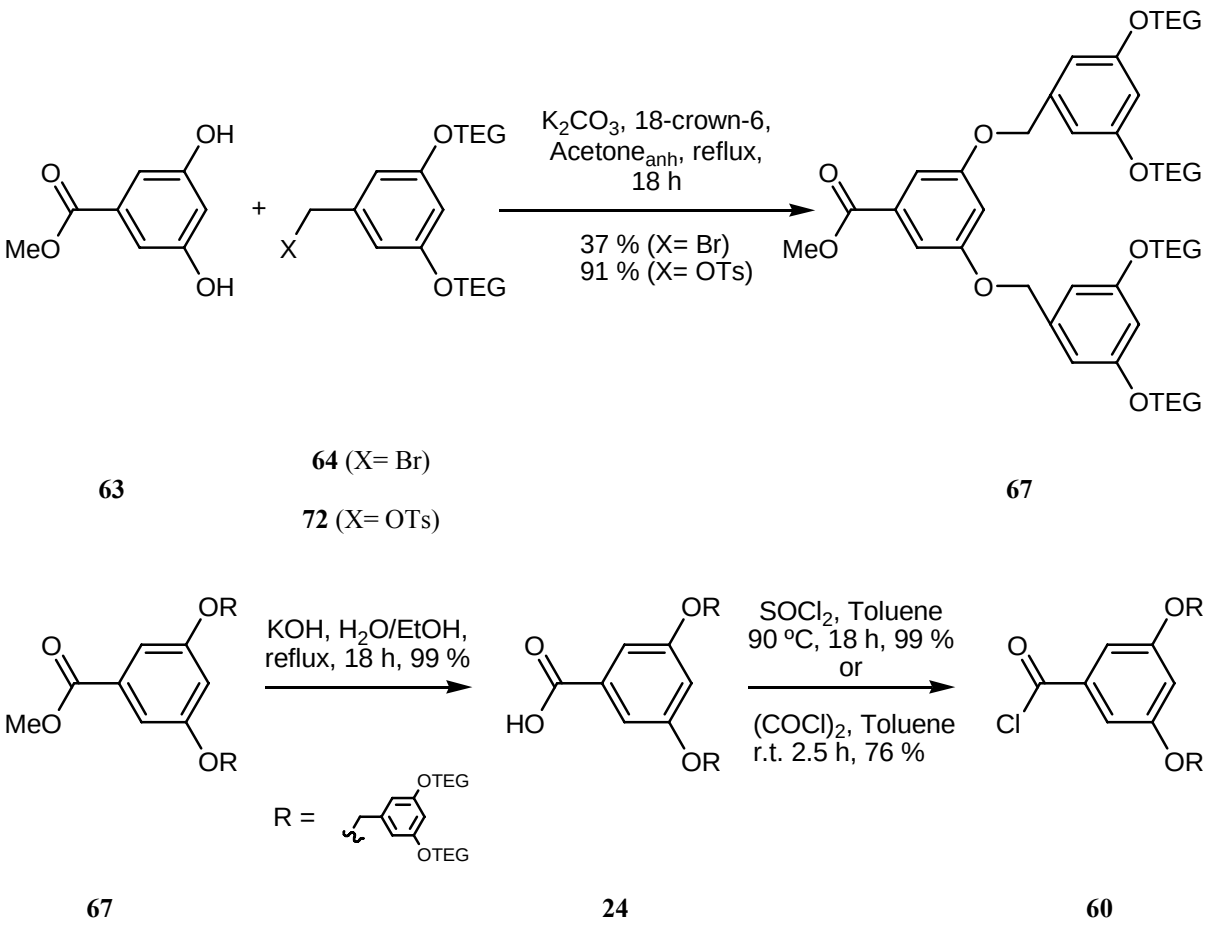

Scheme 2.8: Synthesis of the G_2 benzoyl chloride **60**.

2.1.3 Synthesis of the molecular tweezer 26

2.1.3.1 Functionalization of molecular tweezers

As explained in chapter 1.4, the dendrimers **59** and **60** shall be coupled to the tweezer and clip molecules in order to achieve solubility of these compounds in water without the use of an anionic substituent such as phosphonate or phosphate. In principle, the hydrophilic dendrimer groups should compensate the highly hydrophobic nature of the multiple aromatic rings of the tweezers and clips (Figure 2.2). The oligoether functions of the TEG branches are expected to serve as hydrogen-bond acceptors for the surrounding water molecules and hence to contribute to water solubility of the tweezer and clip molecules.

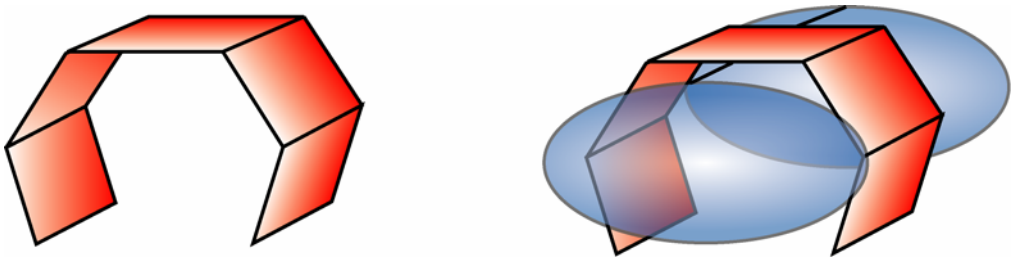

Figure 2.2: Schematic representation of a hydrophobic tweezer (left). The multi-aromatic ring system creates highly repulsive interactions with water molecules. The dendrimer groups attached to the central spacer unit of the tweezer (right), will compensate these hydrophobic interactions, creating hydrogen-bond interactions with the solvent.

First we planned to couple two G_1 and G_2 substituted benzoyl chlorides **59** and **60** to the naphthalene tweezer. This requires the preparation of the hydroquinone tweezer **73** which was unknown as all attempts to prepare the hydroquinone tweezer **73** failed. Basic hydrolysis or $LiAlH_4$ reductions of the diacetoxynaphthalene tweezer **15** did not allow the isolation of **73**. Only secondary oxidation products such as naphthoquinone tweezer **74** or the epoxyquinone **75** could be isolated in low yield from these reactions[74] (Scheme 2.9).

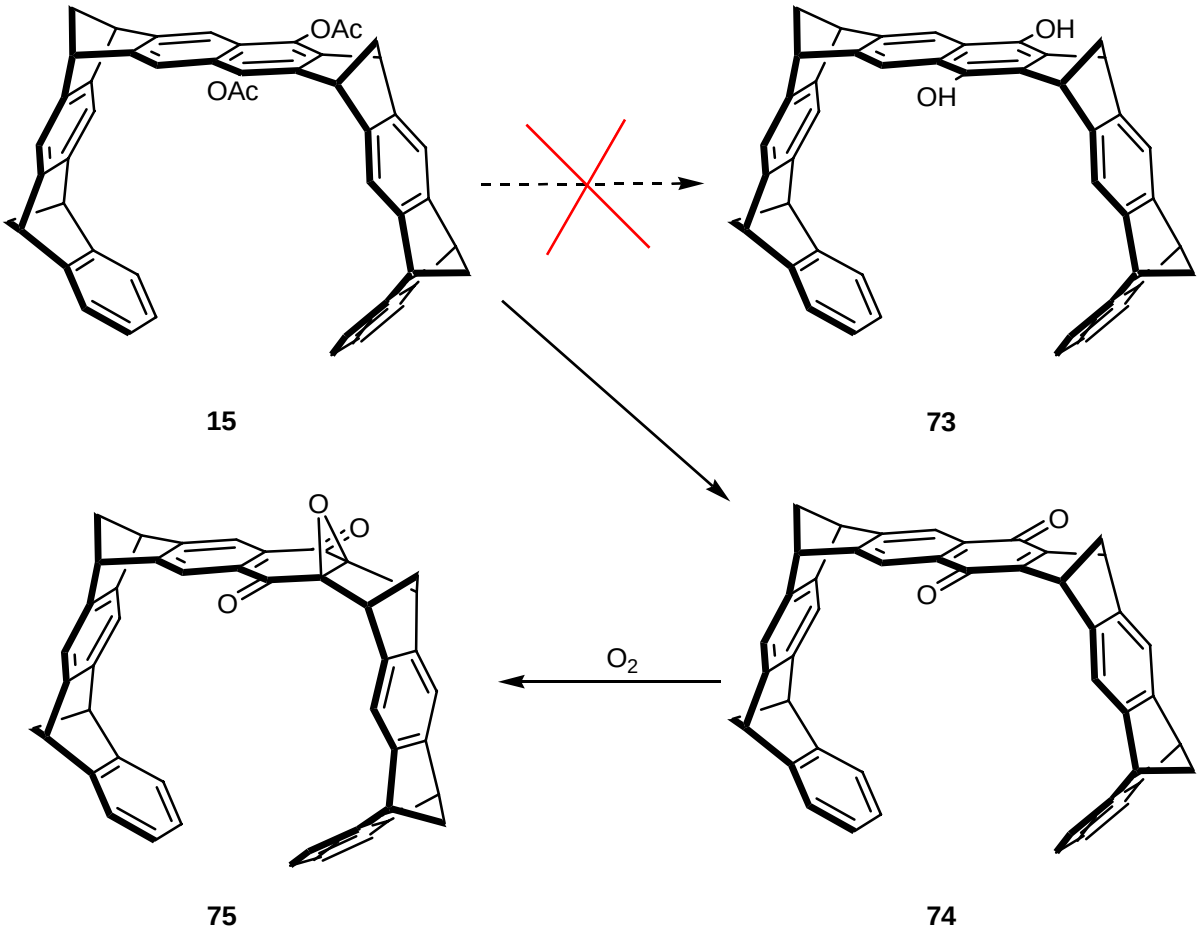

Scheme 2.9: Postulated mechanism of decomposition of the dihydroxy tweezer **73** to the epoxy side product **75**.

In contrast to the dihydroxy tweezer **73**, the dihydroxy naphthalene spacer **76** is stable.[74] However the dihydroxy tweezer **73** can not be prepared from it because after the Diels-Alder reaction which couples the spacer with the sidewalls, an aromatization with DDQ is required. We assumed that under these conditions the hydroquinone **77** is also oxidized (Scheme 2.10) making this procedure inapplicable.

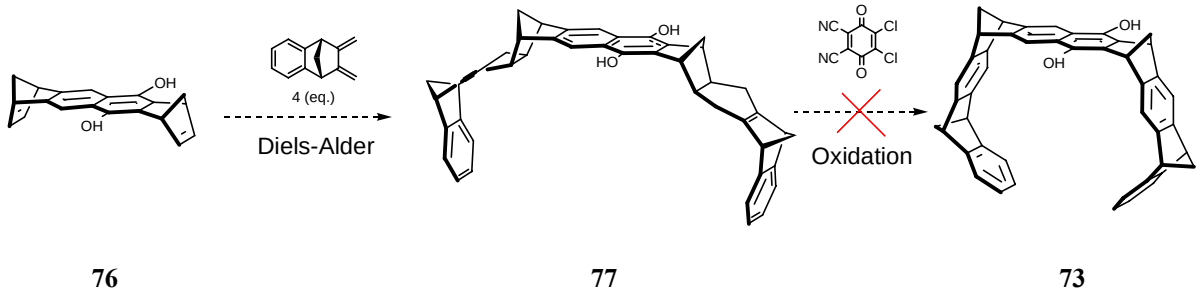

76 **77** **73**

Scheme 2.10: The last step of the synthesis, the oxidation with DDQ, does certainly not allow to isolate the dihydroxynaphthalene tweezer **73**

2.1.3.2 Coupling reactions between the spacer 78 and the tweezer 58 with the first generation dendrimer unit 59

Because the dihydroxytweezer **73** was not available up to date, the stable asymmetrical hydroxy-acetoxynaphthalene tweezer **58** was chosen for the coupling reaction with the G_1 dendrimer **59**. Since the tweezer **58** is only obtained after a multi-step synthesis in mg-scale, the better accessible hydroxy-acetoxynaphthalene spacer **78** was used as a model for the coupling reaction between the hydroxy-acetoxynaphthalene moiety and the G_1 benzoyl chloride **59**.

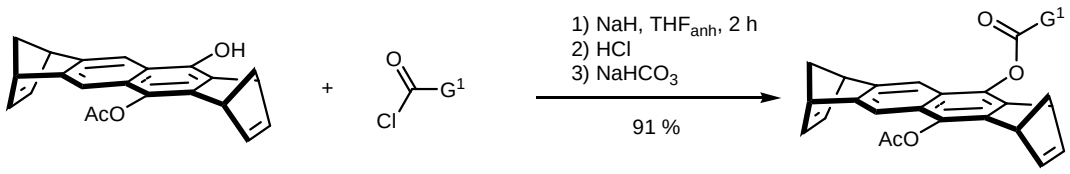

78 **59** **79**

Scheme 2.11: Reaction carried out with the hydroxy-acetoxynaphthalene spacer unit **78**.

The hydroxy-acetoxynaphthalene spacer **78** reacted with pure sodium hydride (obtained from the commercially available parafine suspension by filtrating and washing with dry *n*-hexane) in dry THF, followed by the addition of **59**. After two hours at room temperature, the desired dendrimer substituted bisdienophile **79** was obtained after column chromatography of the crude product in 91 % yield. The structure of **79** was characterized by the usual spectroscopic methods. The ESI-TOF high resolution mass spectrum, with a detected mass for $[M+Na]^+ = 781.3247$ (calculated for $[C_{43}H_{50}NaO_{12}]^+ = 781.3200$) proves

that the bond between spacer and dendrimer unit was formed. Molecules with TEG dendrimers show clear ESI-TOF mass spectra, being the molecular peak plus sodium very sensitive and easy to detect. Additionally the ^{1}H and ^{13}C NMR spectra, discussed in the experimental section, are in accord with the proposed structure of **79**.

Under the same conditions as those used for the spacer **79**, the tweezer **26**, substituted with one G_1 dendrimer unit, was successfully synthesized in 70 % yield by the reaction between the hydroxy-acetoxynaphthalene tweezer **58** and the G_1 benzoyl chloride **59** (Scheme 2.12). The purification by column chromatography under the conditions used for the spacer **79** did not succeed and for this reason, the tweezer **26** was purified by means of medium pressure liquid chromatography, MPLC (SiO_2, AcOEt, 50 bar, 10 mL·min^{-1}).

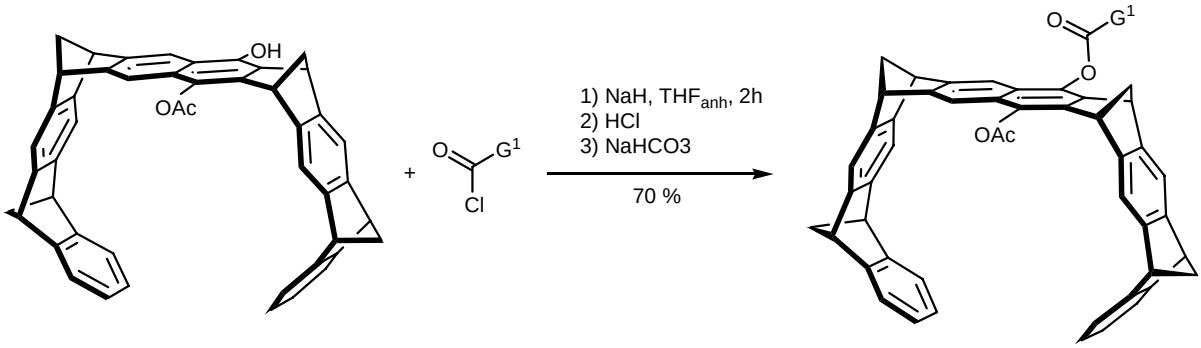

58 **59** **26**

Scheme 2.12: Coupling reaction between the tweezer **58** and the G_1 benzoyl chloride **59**.

2.1.3.3 Structural assignment of tweezer 26

Analogously to the bisdienophile **79**, the ESI-TOF mass spectrometry confirmed the formation of the bond between the tweezer and the dendrimer substituent. The characteristic peak for the tweezer **26** is found to be $[M+Na]^+ = 1109.4398$ (calculated for $[C_{69}H_{66}NaO_{12}]^+ = 1109.4452$). Especially, the structural assignment of tweezer **26** by ^{1}H NMR is worth to be mentioned here. The structural asymmetry of **26** makes the ^{1}H NMR spectrum significantly more complicated than that of the diacetoxy tweezer **15**. The comparison of the ^{1}H NMR spectra of diacetoxy naphthalene tweezer **15**, hydroxy-acetoxynaphthalene tweezer **58** and G_1 substituted naphthalene tweezer **26** is shown in Figure 2.3. In this figure it is interesting to note how the asymmetry of the receptor increases along with the substitution. Two dimensional NMR techniques such as ^{1}H, ^{1}H correlation (COSY), ^{1}H, ^{13}C correlation (HMQC) and ^{1}H, ^{13}C long range correlation (HMBC) were necessary in order to determine the chemical shift value of each nucleus. The final assignment of the ^{1}H NMR spectrum of the tweezer **26** is shown in Figure 2.4.

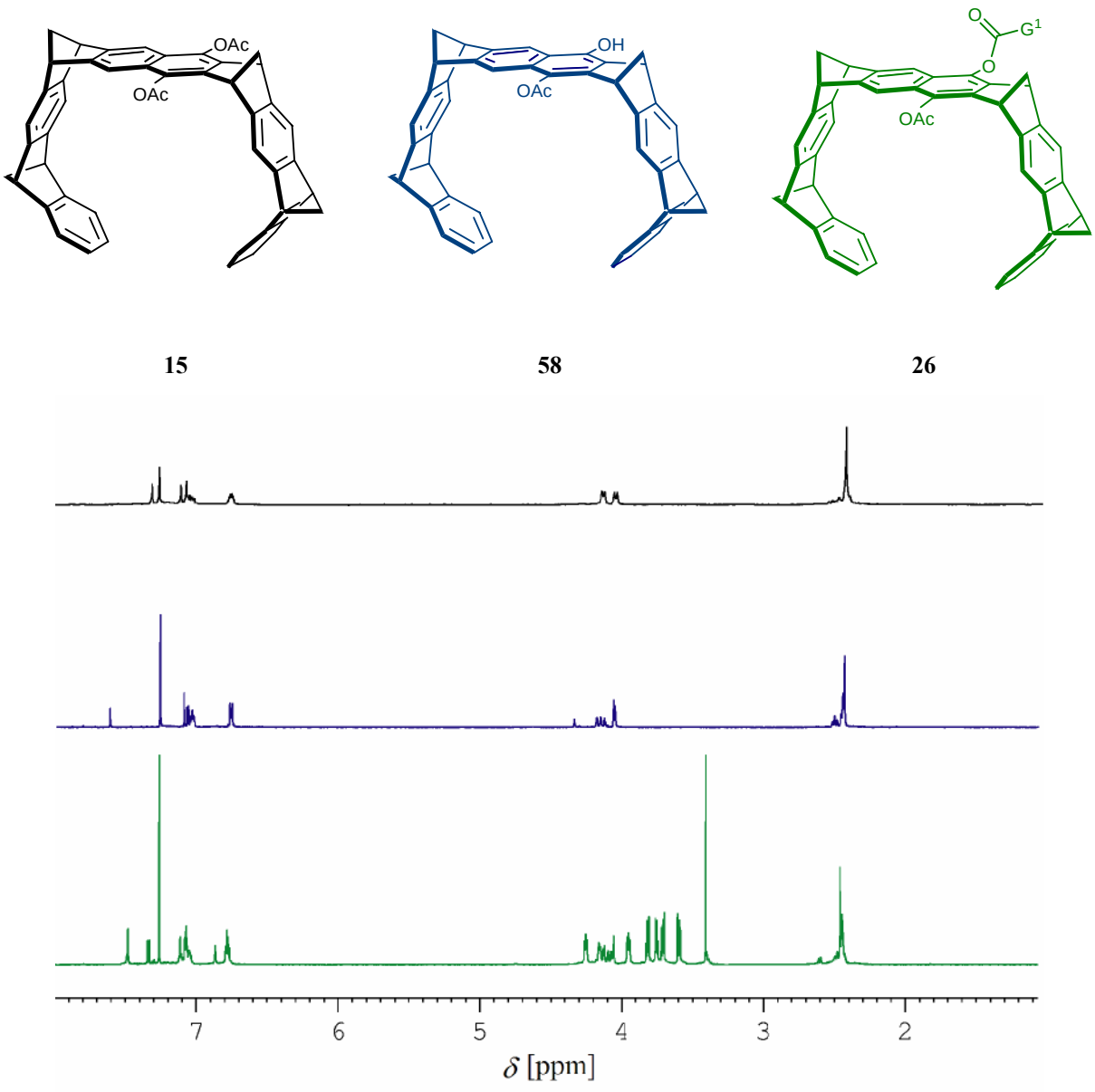

Figure 2.3: Comparison of the ^{1}H NMR spectra of the diacetoxy naphthalene tweezer **15** (top), the hydroxy-acetoxynaphthalene tweezer **58** (middle) and the G_1 substituted naphthalene tweezer **26** (bottom).

Two dimensional NMR techniques such as ^{1}H, ^{1}H correlation (COSY), ^{1}H, ^{13}C correlation (HMQC) and ^{1}H, ^{13}C long range correlation (HMBC) were necessary in order to determine the chemical shift value of each nucleus. The final assignment of the ^{1}H NMR spectrum of **26** is shown in Figure 2.4.

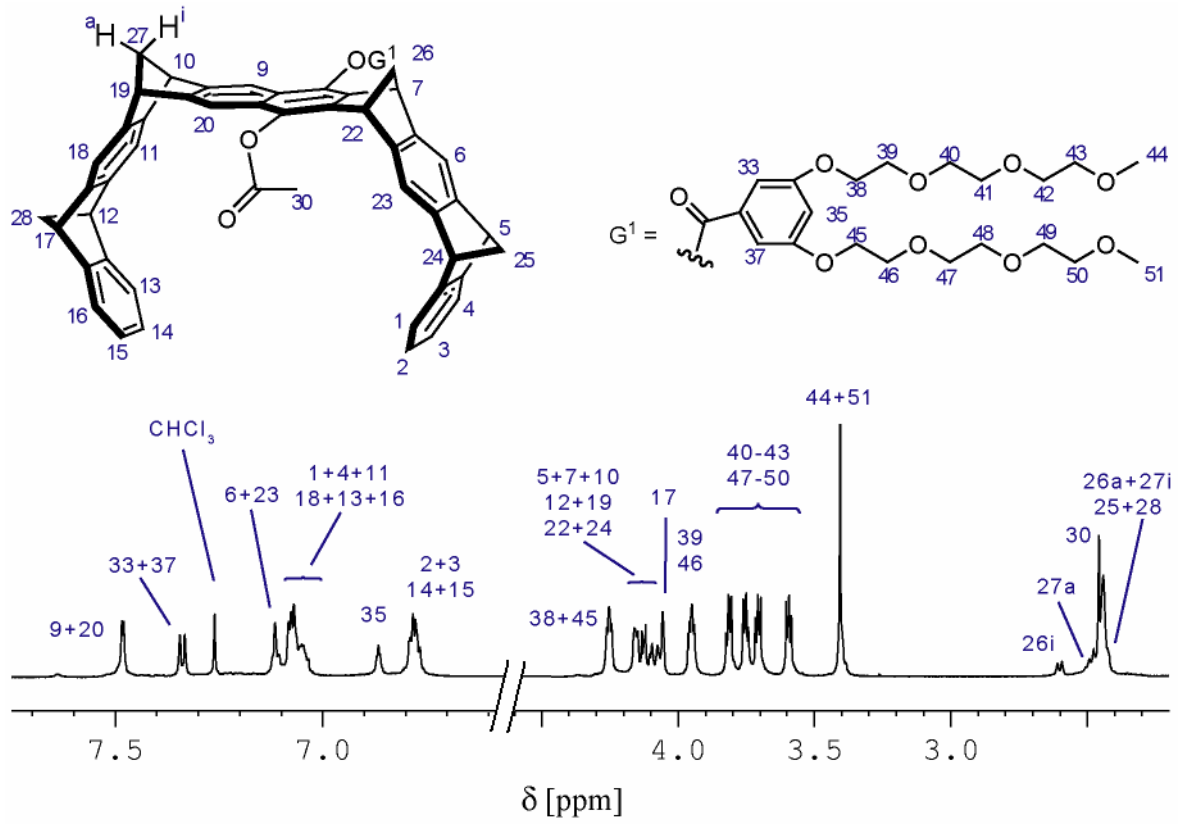

Figure 2.4: Assignment of the ^{1}H NMR spectrum of **26** (500 MHz, $CDCl_3$).

2.1.3.4 Alternative path to tweezer 26

An alternative path to obtain the tweezer **26** could consist in the Diels-Alder reaction between the dendrimer substituted spacer **79** and the diene **80** followed by the DDQ oxidation. This synthetic way is similar to that used for the synthesis of the diacetoxy tweezer **15** (Scheme 2.1). If successful, this procedure could be adapted in order to obtain the disubstituted dendrimer tweezer **81** since the dihydroxy naphthalene spacer **76**, in contrast to the analogous tweezer **73**, is stable (Scheme 2.13).

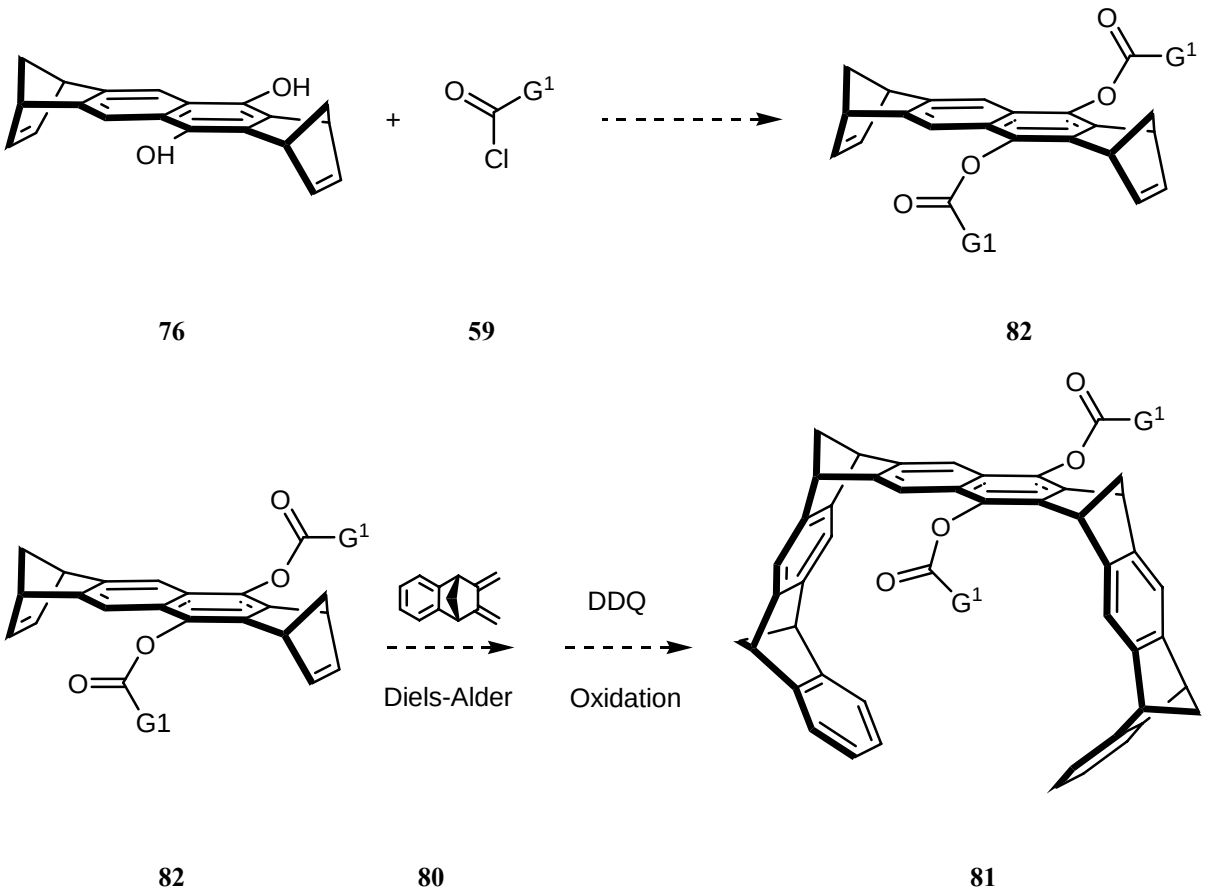

Scheme 2.13: Hypothetical synthetic route to the disubstituted dendrimer tweezer **81**.

The repetitive Diels-Alder reactions between the monosubstituted spacer **79** and the diene **80** (Table 2.1) were carried out under the same conditions as those used for the reactions of the diacetoxy spacer **48**. Both components, **79** and **80**, were dissolved in toluene in a sealed ampoule and heated up to 160 ºC for 6 days. Purification of the crude product by column chromatography (SiO_2, AcOEt:MeOH in different ratios) and MPLC (different pressures, AcOEt:MeOH in different ratios) only led to an unidentifiable mixture of products and 45 % of the starting spacer **79**.

Many Diels-Alder reactions show a strong pressure-induced acceleration which is often turned to good synthetic purposes.[103] Thus, the Diels-Alder reaction of the bisdienophile **79** with the diene **80** was also carried out at 9 kbar and 40 ºC (Table 2.1). The outcome of this experiment, conducted in a sealed tube at 160 ºC, was similar to that of the previous experiment. After the purification by column chromatography and MPLC, the only product was the starting bisdienophile **79** with a recovery of 55 %.

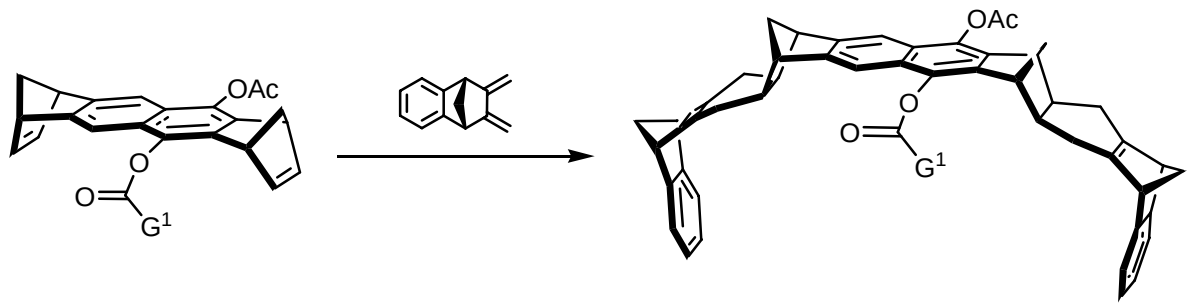

79 **80** **83**

Entry	Solvent/s	Conditions	Reaction time [h]	Temperature [ºC]	Results
1	Toluene	Sealed ampoule + traces NEt_3	144	160	45 % **79** + undefined products
2	Toluene + ACN	9 kbar + traces NEt_3	24	40	55 % **79** + undefined products

Table 2.1: Experimental conditions carried out for the Diels-Alder reaction between the substituted spacer **79** and the diene **80**.

According to these results it is unlikely that the repetitive Diels-Alder reactions of the bisdienophile **82**, substituted with two G_1 dendrimers, with the diene **80** proceed to the desired (2:1) adducts which is needed for the synthesis of the G_1 disubstituted tweezer **81**. For that reason we focussed our efforts on the properties of the monosubstituted G_1 tweezer **26**.

2.1.3.5 Supramolecular properties of the receptor 26

2.1.3.5.1 Solubility of the tweezer 26

In order to quantify the solubility of **26** in different solvents, we designed a solubility evaluation by ^1H NMR (refer to chapter 4.4 for detailed explanation of the method). The result of this experiment in D_2O, CD_3OD and $CDCl_3$ are shown in Table 2.2.

Solvent	mg Tweezer 26	Internal standard	Solubility [mg/mL]
$CDCl_3$	4.1	CH_2Cl_2	Complete
CD_3OD	3.5	CH_2Cl_2	2.8
D_2O	5.3	1,4-dioxane	Not detected

Table 2.2: Solubility experiments for the tweezer **26** in solvents used for tweezers and clips complexation experiments.

For non-ionic organic molecules it is proven that the smaller the C/O ratio is, the more soluble the molecule becomes in water. Table 2.3[104] shows that compounds with a C/O ratio < 4 are completely miscible or highly soluble in water. With an increasing of C/O ratio the solubility in water decreases. For example camphor, with a C/O ratio of 10 is completely insoluble in water.

Structure	Formula	C/O Ratio	Solubility in Water at 20 ºC [g/L]
	CH_4O	1	Total miscibility
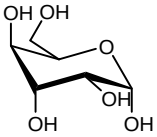	$C_6H_{12}O_6$	1	900
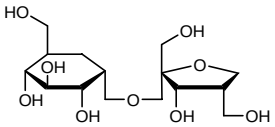	$C_{15}H_{28}O_9$	1.7	1970
	C_2H_6O	2	Total miscibility
	$C_4H_8O_2$	2	Total miscibility
	C_3H_8O	3	Total miscibility
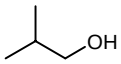	$C_4H_{10}O$	4	95
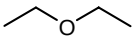	$C_4H_{10}O$	4	69
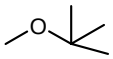	$C_5H_{12}O$	5	51
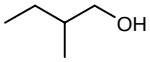	$C_5H_{12}O$	5	36
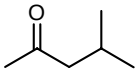	$C_6H_{12}O$	6	19
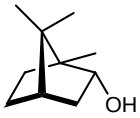	$C_{10}H_{18}O$	10	Insoluble

Table 2.3: Comparison between the C/O ratio of different organic molecules and their solubility in water at 20 ºC.

For the tweezer **26**, the molecular formula is $C_{69}H_{66}O_{12}$, and it leads to a C/O ratio = 5.75 which belongs to the *low-solubility* range. It is important to take into account that the data in Table 2.3 do not reflect the effect of the aromatic rings. In case of tweezer **26**, four benzene rings and one naphthalene unit are present. These rings which represent apolar moieties create highly repulsive interactions with polar molecules such as water.

With this respect, it only seems possible to achieve water solubility of the tweezer by either the substitution of the naphthalene spacer unit by two G_1 dendrimers or a substitution with a single G_2 dendrimer. Both assumptions are based on the increasing number of oxygen atoms in the molecule, so that the larger hydrophilic area compensates the hydrophobic area created by the five aromatic rings and the two methylene bridges of the hydrocarbon frame of the tweezer.

2.1.3.5.2 Chirality of the tweezer 26

A very important property of tweezer **26** is its chirality resulting from the two different substituents at the central naphthalene spacer unit, which make the eight bridge head carbon atoms stereogenic centers (Figure 2.5). As in any asymmetrical molecule, the chirality in the tweezer **26** can be confirmed by trying to overlap the two mirror images, as schematically shown in Figure 2.5.

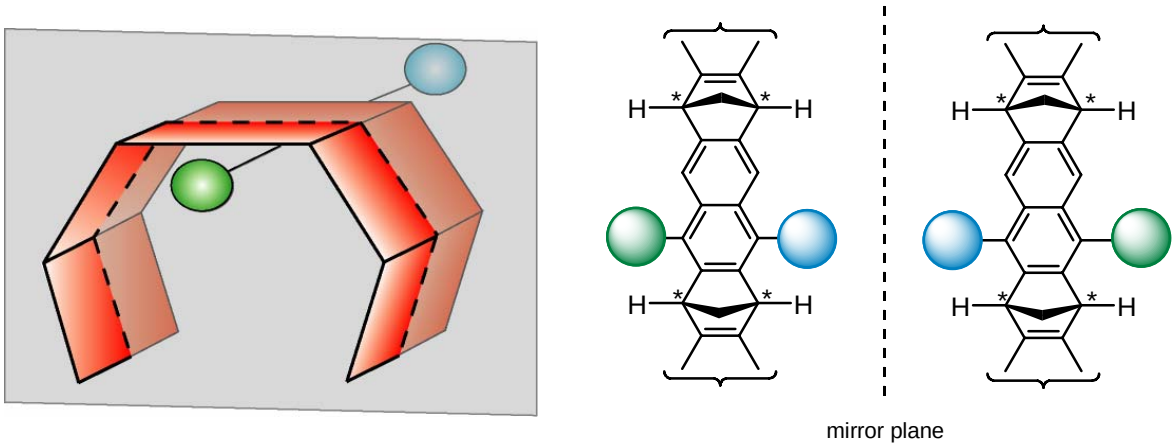

Figure 2.5: Schematic representation of the chirality of an asymmetrically substituted tweezer. Right: two mirror images of the top view of the tweezer. Note that when trying to overlap the two structures the substituents are interchanged which is, actually, the definition of chirality in molecules. Left: the plane which crosses the complete aliphatic and aromatic system of an asymmetrically substituted naphthalene-spaced tweezer.

The hydrolysis of the diacetoxy substituted tweezer **15** with potassium hydroxide is a *non-stereoselective* process in which each acetoxy group present in the tweezer **15** reacts at the same rate (Scheme 2.1). Thus the subsequent coupling with the G_1 substituted benzoyl chloride **59** produces the tweezer **26** in its racemic form. The enanantiomers of **26** could be analytically separated on a chiral HPLC column as shown in Figure 2.6.

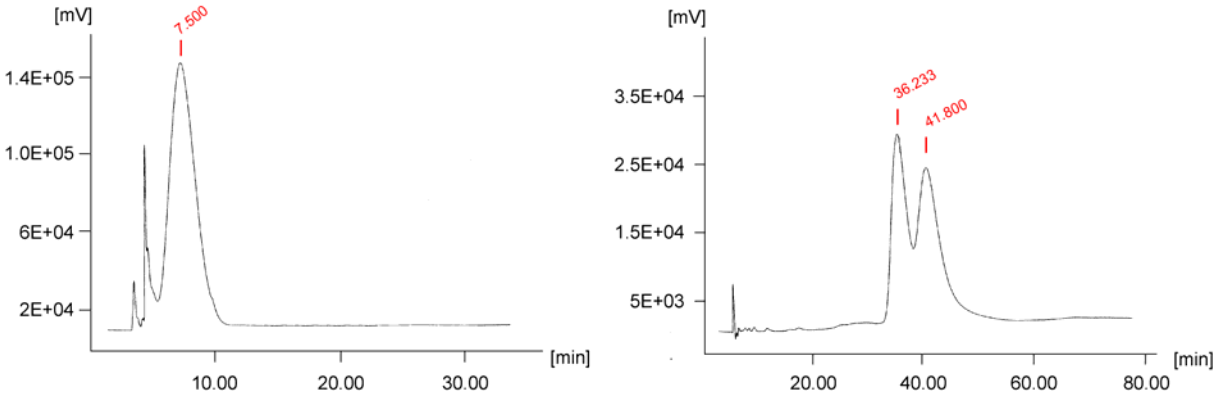

- Eluant: Heptan :AcOEt (30:70)
- Detector: UV-vis 254 nm
- Column: Nucleosil 100-5:

- Eluant: Heptan :^{i}PrOH (60:40)
- Detector: UV-vis 250 nm
- Column: Chiracel®-OD analytical column (cellulose derivative)

Figure 2.6: Comparison between the two HPLC analyses carried out with the receptor **26**. Left: HPLC chromatogram with an achiral column, there is only one peak. Right: HPLC chromatogram with a chiral column. Two peaks are observed, each one corresponding to one of the enantiomers.

2.1.3.5.3 Complexation of the receptor 26 with Kosower salt 84

2.1.3.5.4 ^{1}H NMR titration as a method to evaluate association constants (K_a), maximum-induced chemical shifts ($\Delta\delta_{max}$) and Gibbs energy (ΔG)

The magnetic anisotropy[105] of the tweezer arene units makes ^{1}H NMR spectroscopy a very sensitive probe for uncovering the complexation of electron-withdrawing substrate molecules inside the receptor cavity. The complex formation can be easily detected by pronounced up-field shifts of the substrate signals in the ^{1}H NMR spectrum of a mixture consisting of the receptor molecule and a substrate molecule. The maximum complexation-induced NMR shifts, $\Delta\delta_{max}$, of the substrate protons, the association constant, K_a, and, hence, the Gibbs energy of association, ΔG, can be determined by ^{1}H NMR titration. [36, 98, 106]

In a standard NMR titration the complexation-induced ^{1}H NMR shifts of the guest protons, $\Delta\delta_{obs}$, are measured in dependence of the host concentration at constant guest concentration. An alternative method is to measure the dependence of the complexation-induced ^{1}H NMR shifts of the guest protons in a 1:1 mixture with the host molecule at different overall concentrations, which is known as titration by dilution. In both cases the evaluation of the data is based on the following equations and performed by the use of the program TableCurve.[107]

$$\Delta\delta_{obs} = \frac{\Delta\delta_{max}}{[G]_0}\left(\frac{1}{2}\left([H]_0 + [G]_0 + \frac{1}{K_a}\right) - \sqrt{\frac{1}{4}\cdot\left([H]_0 + [G]_0 + \frac{1}{K_a}\right)^2 - [H]_0\cdot[G]_0}\right)$$ Equation 2.1

$$\Delta G = -RT \ln K_a$$ Equation 2.2

Where:

- $\Delta\delta_{obs}$: Observed $\Delta\delta$ for the protons of the guest.
- $\Delta\delta_{max}$: Maximum complexation-induced chemical shifts for the protons of the guest.
- $[G]_0$: Total concentration of the guest.
- $[H]_0$: Total concentration of the host
- K_a : Association constant
- ΔG : Gibbs energy
- T : Temperature given in Kelvin
- R : 1.987 cal·K^{-1}·mol^{-1}

2.1.3.5.5 ^{1}H NMR titration with Kosower salt 84

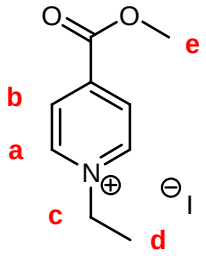

84 (KS)

Figure 2.7: Structure of the 4-methoxycarbonyl-1-ethyl-pyridinium iodide, commonly named Kosower salt.

The ^{1}H NMR signals assigned to the protons of Kosower salt ([**84**]$_0$ = 2.38·10^{-3} M in $CDCl_3$) are shifted in the presence of tweezer ([**26**]$_0$ = 6.51·10^{-3} M). In order to assign the signals of the protons of **84** and to distinguish them from the signals of the host **26**, two-dimensional NMR experiment were carried out.

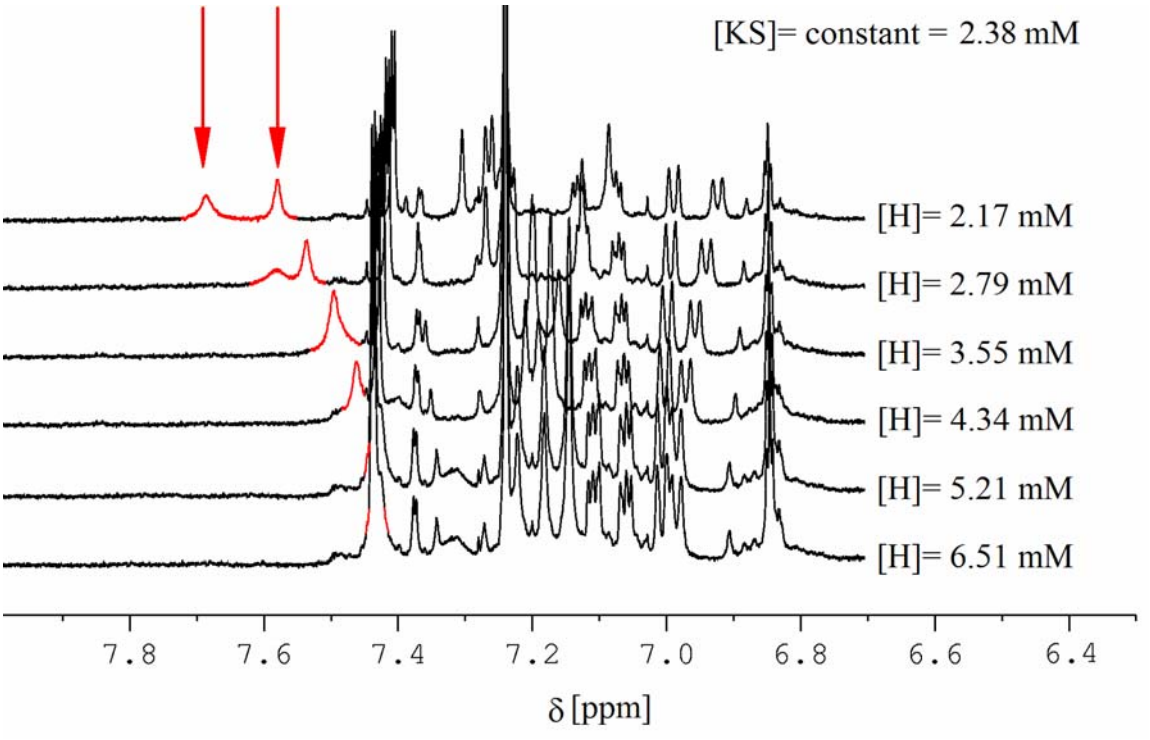

Figure 2.8: Aromatic region expansions of some of the spectra of the titration of **26** with Kosower salt in CDCl3. Highlighted in red colour are the aromatic protons that show an up-field shift in the first titration point.

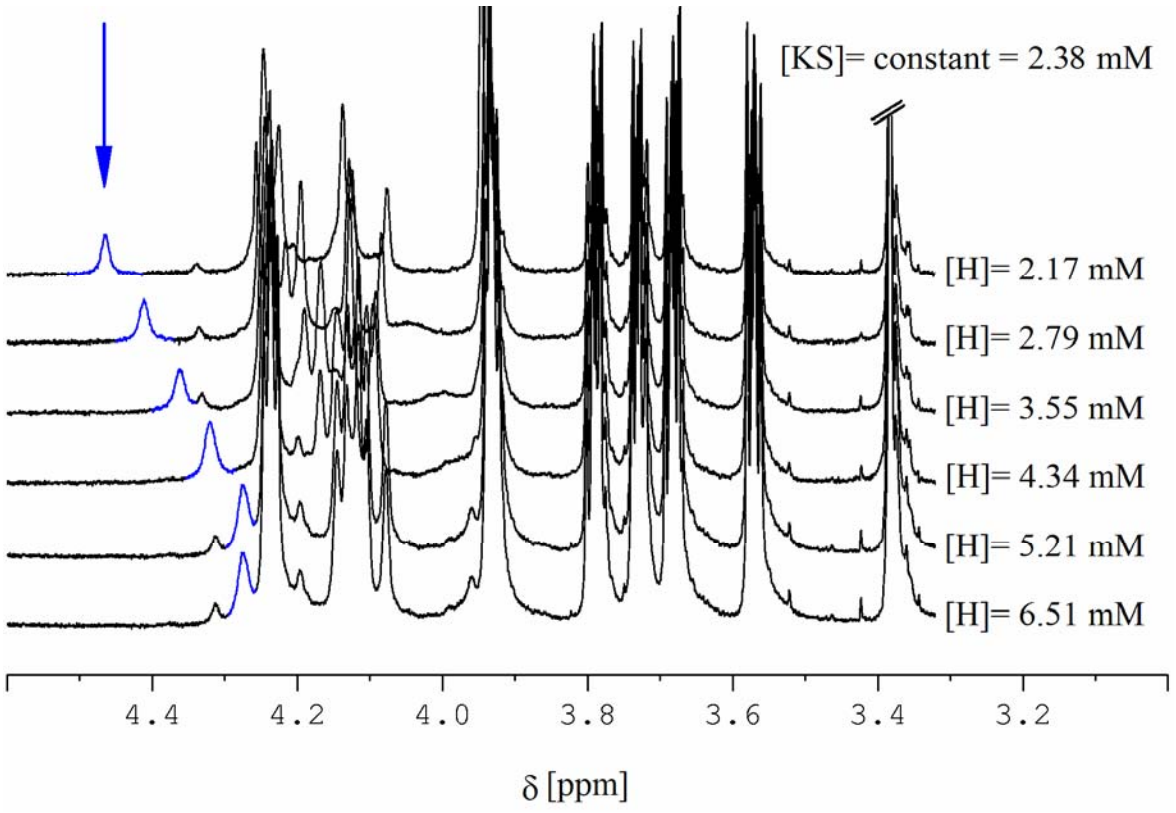

Figure 2.9: Aliphatic region expansion of some of the spectra of the titration of **26** with Kosower salt in $CDCl_3$. Highlighted in blue colour is the proton that shows an up-field shift in the first titration point.

In a host-guest mixture, scalar coupling constants, ^3J, are usually not visible in the ^{1}H NMR due to the dynamic effect of the binding process between the two molecules. However this coupling can be observed on ^{1}H, ^{1}H-COSY spectra. The ^{1}H, ^{1}H-COSY spectrum of a (1:1)-mixture of tweezer **26** and Kosower salt (Figure 2.10) reveals that the two aromatic signals (indicated with red arrows in the Figure 2.8) have no correlation with each other, which is a first indication that they do not belong to the guest molecule.

Although the carbon atoms are also inside the cavity of the tweezer, the magnetic anisotropy of the aromatic system of the tweezer has a smaller influence on the ^{13}C chemical shifts and therefore the complexation-induced ^{1}H NMR shifts, $\Delta\delta_{obs}$, are significantly lower in the ^{13}C NMR spectra in comparison with those of the ^{1}H NMR spectra. Thus the ^{13}C, ^{1}H-correlation has been proven to be a useful method to find the chemical shifts of protons whose signals are overlapped by other signals and estimate the $\Delta\delta_{obs}$ values.

In addition to the absence of ^{1}H, ^{1}H-correlation, the two aromatic signals show heteronuclear correlation with carbon atoms at 114 ppm and 118 ppm (Figure 2.). These chemical shifts do not match with the values for the C_a and C_b of the Kosower salt in $CDCl_3$ (127 ppm for C_b and 146 ppm for C_a).

We finally proved that these signals do not belong to the Kosower salt, but to the tweezer **26**, by means of the relative integration. The integrals of those signals remain rather constant in relation to the signals corresponding to the G_1 dendrimers along with the titration, which could not be possible if the signals corresponded to the Kosower salt, since the host-guest ratio remains not constant.

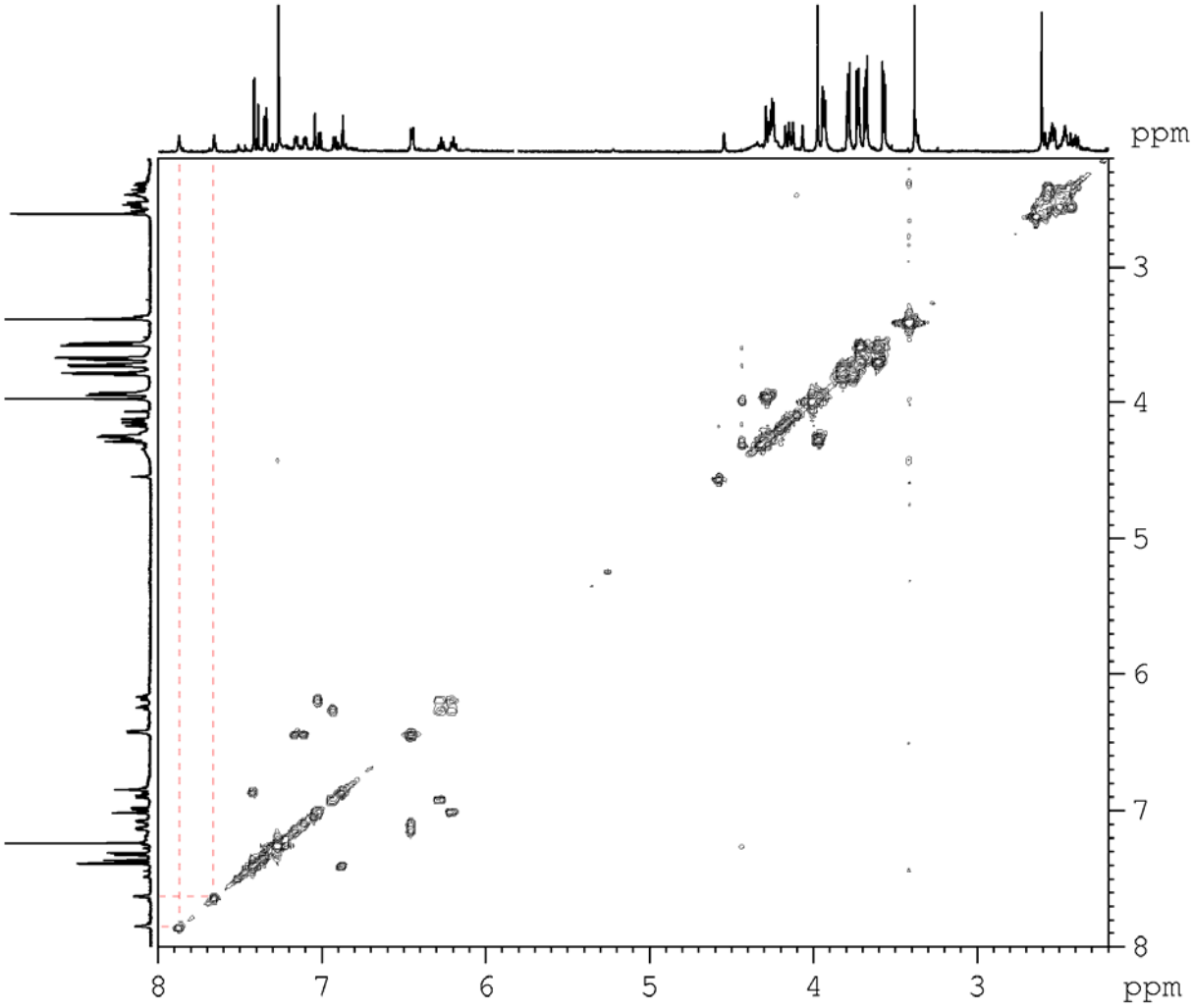

Figure 2.10: ^{1}H, ^{1}H-COSY NMR spectrum of the mixture of Kosower salt **84** ([**KS**]= 2.38 mM) and the tweezer **26** ([**26**]= 2.17 mM).

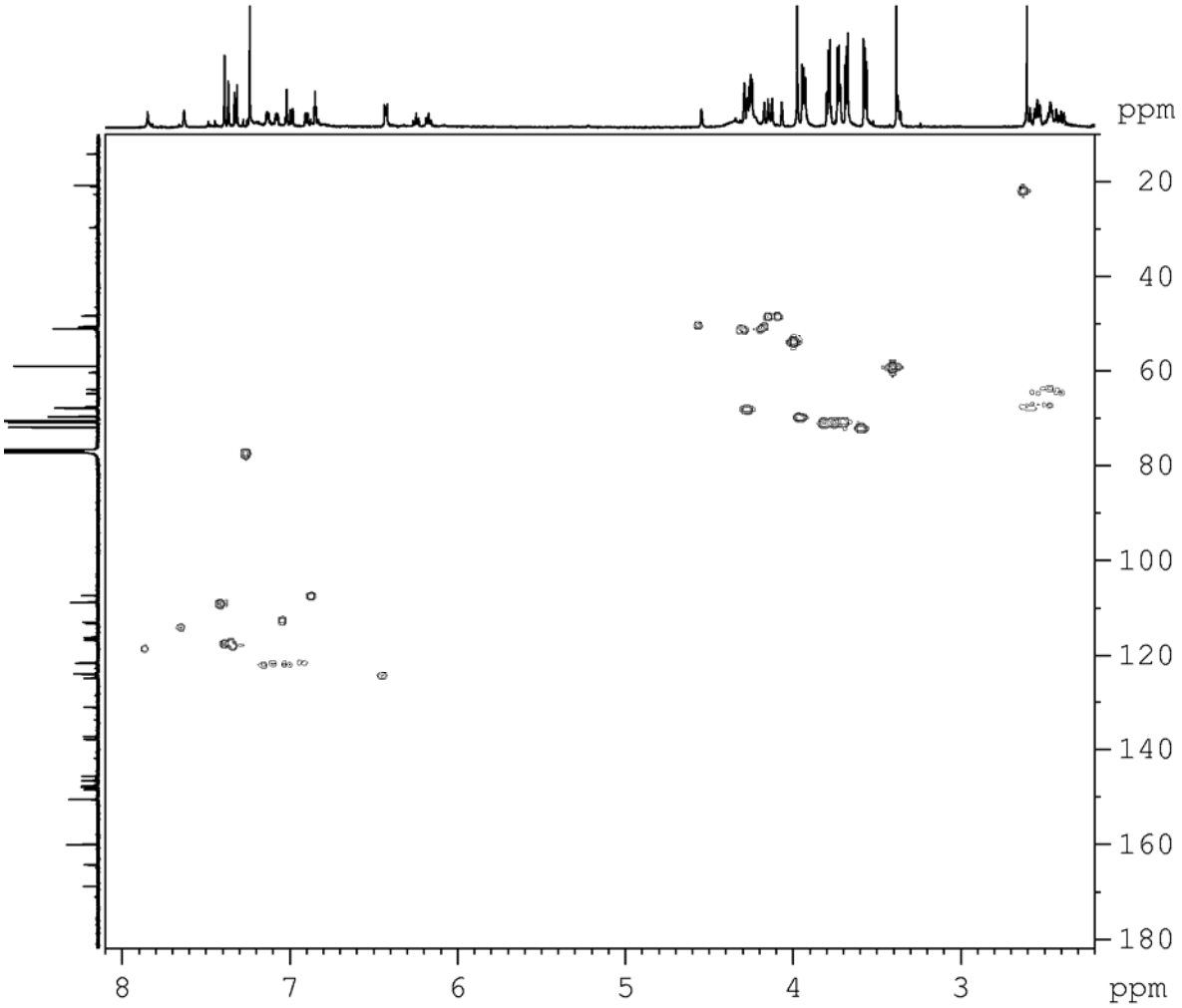

Figure 2.11: ^{13}C, ^{1}H-correlation spectrum of the mixture of Kosower salt **84** ([**KS**]= 2.38 mM) and the tweezer **26** ([**26**]= 2.17 mM).

The formation of host-guest complexes may cause not only up-field shifts but also a broadening of the ^{1}H NMR guest signals resulting from the dynamic exchange between the signals of the complexed and free guest provided that the exchange rate is comparable to the so-called NMR time scale. This signal broadening makes the detection and assignment difficult, especially in the case of the dendritic substituted tweezer **26** with the strong overlap of the host and guest signals. In Table 2.4 the maximum ^{1}H NMR shifts ($\Delta\delta_{max}$ and δ_{com}) of the signals of various guest molecules in the complexes with the diacetoxy naphthalene tweezer **15** are shown.[108] The up-field shifts found for aromatic guests protons are all in the range of about $\Delta\delta_{max} \approx 4$ ppm. In the bulk of signals between $\delta = 6.8$ ppm and $\delta = 7.7$ ppm or between $\delta = 3.3$ ppm and $\delta = 4.5$ ppm, observed in the ^{1}H NMR spectrum of the mixture of Kosower salt **84** ([**KS**]= 2.38 mM) and tweezer **26** ([**26**]= 2.17 mM), only the signal corresponding to the proton H_c of the Kosower salt can be observed (highlighted in blue in Figure 2.9). None of the aromatic signals (highlighted in red in Figure 2.8) can be assigned to one of the guest aromatic protons of Kosower salt **84** neither by application of the two-dimensional ^{1}H, ^{1}H COSY nor ^{1}H, ^{13}C COSY methods. However, the ^{1}H NMR chemical shifts of these signals of the mixtures of tweezer **26** are dependent of the tweezer

concentration. The comparison of the ^{1}H NMR spectra of the tweezer **26** and the mixture of **26** and Kosower salt **84** suggests the assignment of these signals to the tweezer protons H-9, H-20, H-33, H-37.

Entry	Guest	Solvent	δ_0 [ppm]	$\Delta\delta_{max}$ [ppm]	δ_{com} [ppm]
1	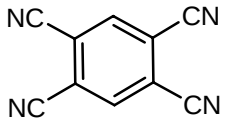	$CDCl_3$	8.3	5.9	2.4
2	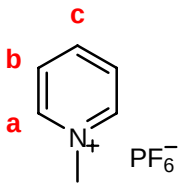	$CDCl_3$: Acetone-d_6 (1:1)	H_a 9.0 H_b 8.6 H_c 8.2	5.0 4.5 4.1	4.0 4.1 4.1
3	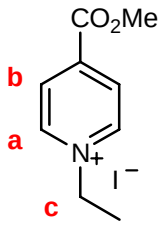	$CDCl_3$	H_a 9.6 H_b 8.6 H_c 4.1	4.0 4.1 --[a]	5.6 4.4 --[a]

[a] The signal of H_c was too broad to be detectable and no evaluation of $\Delta\delta_{max}$ was possible.

Table 2.4: Values of chemical shifts of the free guest molecules, δ_0, maximum induced chemical shift, $\Delta\delta_{max}$, and the chemical shifts of the guest molecules in the complex, δ_{com}, of some guests with the diacetoxy tweezer **15**.[108]

The evaluation of the signal on the aliphatic region (highlighted in blue in Figure 2.9) with Equation 2.1 by means of the Table Curve software does not lead to a reasonable result, as the representation values of $\Delta\delta_{obs}$ against the tweezer concentration do not fit with the predicted slope for that equation, having a linear tendency instead (Table 2.5).

$\Delta\delta_{obs}$ [ppm]	[26] [mM]
0.8385	6.51
0.8265	6.01
0.8108	5.58
0.7928	5.21
0.7820	4.89
0.7659	4.60
0.7523	4.34
0.7379	4.11
0.7266	3.91
0.7034	3.55
0.6821	3.26
0.6689	3.01
0.6500	2.79
0.6360	2.61
0.6268	2.44
0.6172	2.17
0.6063	1.95

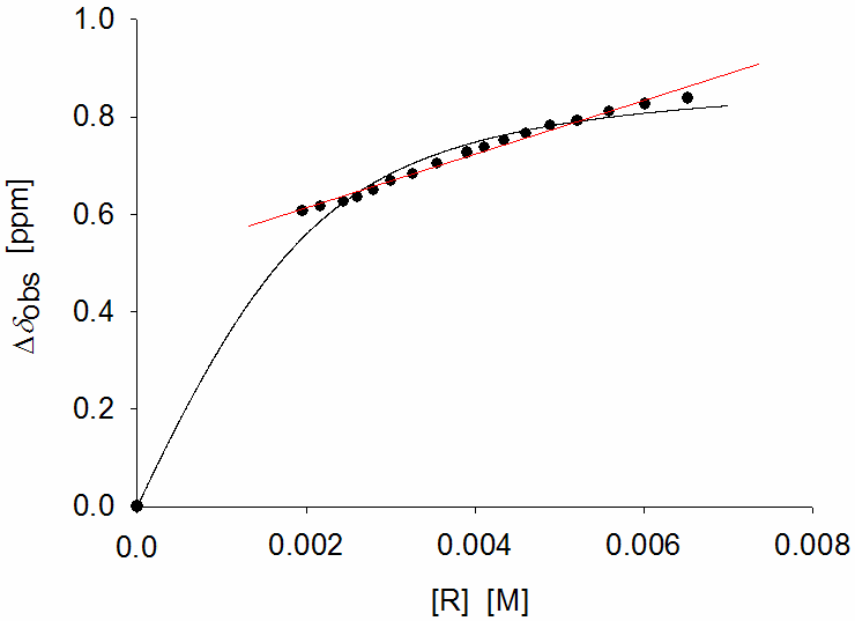

K_a= 2100±210 M^{-1}

ΔG= -4.5±0.5 kcal·mol^{-1}

$\Delta\delta_{max}$= 0.90 ppm

Table 2.5: Representation of the values of $\Delta\delta_{obs}$ of the signal assigned to the H_c of Kosower salt **84** against the concentration of the tweezer **26** and the values of K_a and $\Delta\delta_{max}$ obtained from their evaluation. While the predicted behaviour of the titration is represented with the black slope curve, the actual tendency of this signal is represented with a red straight line.

The evaluation of the data shown on Table 2.5 leads to an association constant for the complex **84@26** of K_a= 2100 M^{-1} and a value of maximum complexation-induced chemical shift for H_c of $\Delta\delta_{max}$= 0.90 ppm. Although these results are not fully reliable due to the non-optimum fitting with the binding isotherm (Equation 2.1), the obtained value of association constant is comparable to that of the complex of Kosower salt **84** with the diacetoxy naphthalene-spaced tweezer **15**, K_a(**84@15**)= 3800±380 M^{-1}[108], which gave us a first indication that the substitution of one acetoxy group by one G_1-TEG dendrimer groups does not have a strong influence on the binding properties of the naphthalene tweezer.

2.1.3.5.6 ^{1}H NMR titration with 1,2,4,5-tetracyanobenzene 85

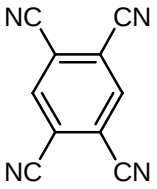

Figure 2.12: Structure of 1,2,4,5-tetracyanobenzene (**85**).

Tetracyanobenzene, TCNB (**85**) has been the reference guest molecule for the potential host-guest complex formation with tweezers. Since TCNB has only two protons which are chemically equivalent to each other and, usually, not difficult to assign, we decided to perform a ^{1}H NMR titration in $CDCl_3$ with the aim to determine the association constant, K_a, and maximum induced chemical shift, $\Delta\delta_{max}$, of the host-guest complex between tweezer **26** and TCNB, **85**. The comparison of the K_a and $\Delta\delta_{max}$ values determined for the complex formation between **26** and **85** with those corresponding to the diacetoxynaphthalene tweezer **15** should provide insight into the effect of the dendritic substituent on the stabilization and structure of this complex.

As observed before in the case of the Kosower salt, the ^{1}H NMR signal of TCNB ($[TCNB]_0 = 3.82 \cdot 10^{-3}$ M in $CDCl_3$) was shifted in the presence the tweezer **26** ($[\mathbf{26}]_0 = 12.68 \cdot 10^{-3}$ M in $CDCl_3$), probably to the area where the signals of the dendrimer substituents are, since the signal of TCNB could not be found. In order to at least locate the signal and estimate the $\Delta\delta_{max}$, the ^{1}H, ^{13}C-correlation spectrum was measured (Figure 2.13).

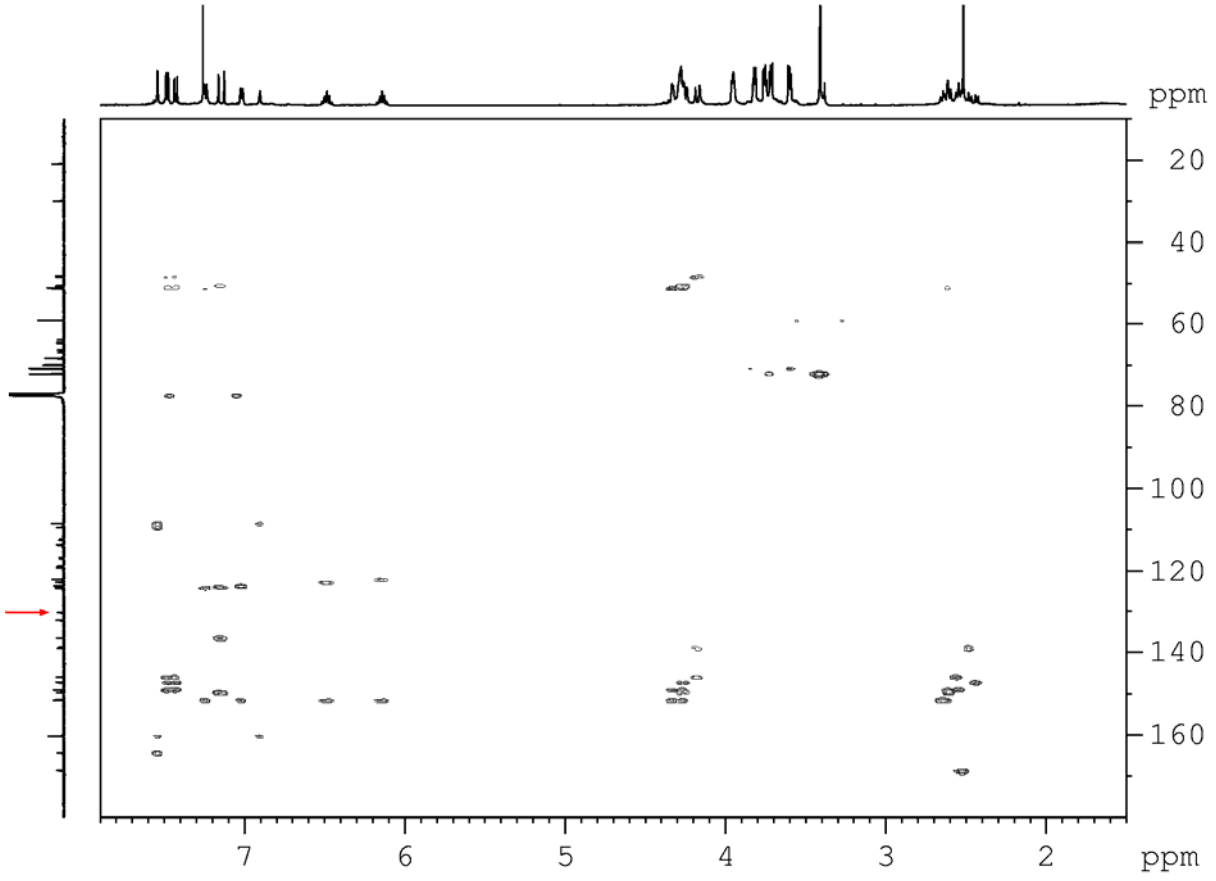

Figure 2.13: ^{1}H, ^{13}C-correlation spectrum of the mixture of **TCNB** ($[TCNB]_0$= 3.82 mM in $CDCl_3$) and **26** ($[\mathbf{26}]_0$= 3.80 mM in $CDCl_3$).

The ^{13}C NMR signal of the methine carbon of the TCNB is located at 135.25 ppm (indicated with a red arrow in Figure 2.13) but it shows no correlation with the corresponding proton in the ^{13}C, ^{1}H-correlation spectrum since the ^{1}H NMR signal of this proton seems to be too broad for that technique to be effective.

2.1.3.5.7 Isothermal microcalorimetric titration as a method to evaluate supramolecular properties

Isothermal titration microcalorimetry (ITC) has proved to be a very effective method to determine the thermodynamic data of the formation of host-guest complexes.[109-111] In addition to the K_a value, from the slope of the titration curve it is also possible to obtain the ΔH and hence ΔG and ΔS in a single measurement, which is a great advantage for the complexation studies of large supramolecular systems.[112-114] When the measurement is carried out under isothermal conditions, the heat, Q, and the difference of enthalpy, ΔH, are the directly measured parameters. By the measurement of Q in dependence of the concentration of host and guest, it is possible to determine the value of the association constant, K_a, by means of a non-linear regression for a given stoichiometry. The thermodynamic parameters ΔH, ΔG and ΔS are calculated by the use of Equation 2.2 and Equation 2.3.

$$\Delta G = -RT \ln K_a \qquad \text{Equation 2.2}$$

$$-RT\ln K_a = \Delta H - T\Delta S \qquad \text{Equation 2.3}$$

Where:

- R : Gas constant in the adequate units
- T : Temperature in Kelvin
- K_a : Association constant
- ΔG : Gibbs energy of complexation
- ΔH : Enthalpy of complexation
- ΔS : Entropy of complexation

Experimentally, the titration is carried out with the stepwise addition of a concentrated solution of guest to a diluted solution of host using a computer-controlled syringe. For the tweezer and clip systems it is proven that an optimal final host-guest ratio should be approximately one to four.

2.1.3.5.8 ITC titration with Kosower salt, 84 and 1,2,4,5-tetracyanobenzene, 85

Due to the impossibility to analyze the data obtained by the ^{1}H NMR titrations with the tweezer **26** as host and Kosower salt **84** or 1,2,4,5-tetracyanobenzene **85** as guest molecules, several ITC titrations were performed as shown in Table 2.6.

Entry	Guest	Solvent	[Host]/ [μM]	V_0 [mL]	[Guest]/ [mM]	Addition Method
1	TCNB	$CHCl_3$	246.16	1	2.45	40 x 10
2	KS	$CHCl_3$	984.63	1	9.08	48 x 5
3	KS	$CHCl_3$	984.63	1	9.08	48 x 8
4	KS	$CHCl_3$	984.63	0.8	4.54	48 x 10
5	KS	$CHCl_3$	984.63	1	15.35	30 x 7
6	KS	$CHCl_3$	984.63	1	9.08	40 x 10
7	KS	$CHCl_3$	668.03	1	2.51	40 x 10

Where:

- [Host]: is the concentration of the tweezer **26**, which is in the vessel.
- V_0: is the volume of host solution in the vessel.
- [Guest]: is the concentration of the guest, which is in the computer controlled syringe
- Addition method: is the number of titration steps and the added volume in each step expressed in μL

Table 2.6: The ITC titration experiments performed with the tweezer **26** as a host and KS **84** and TCNB **85** as guest molecules.

The experiments listed in Table 2.6 above were performed after the successful calibration of the microcalorimeter with the 18-crown-6/$CaCl_2$ standard system and did not lead to any successful result, for any stoichiometry, showing all of them highly scattered dispersion of the corrected points.

In all experiments listed in Table 2.6 a heat development was observed and did not show the characteristic sigmoidal time-dependence. Thus the analysis of these data was difficult. In Figure 2.14 the analysis of the experiment on entry 3 is shown.

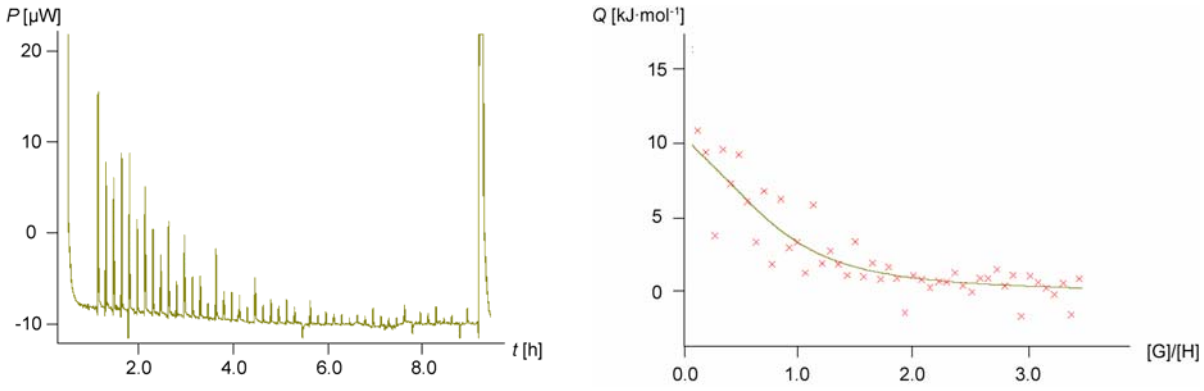

Conditions:

- [**26**]: 985 µM
- [**84**]: 9.08 mM
- Method: 48 injections x 8 µL

Results:

- Stoichiometry: 0.880
- K_a= 1490 M^{-1}
- ΔH= -2.62 kcal·mol^{-1}

Figure 2.14: Experimental data obtained from the experiment 3 in Table 2.6. Left: Raw data. Right: Data corrected with the values of concentrations and volumes.

From these data one can estimate that a stable host-guest complex between tweezer **26** and KS **84** in chloroform is formed showing a binding constant of $K_a \approx$ 1500 M^{-1} and a negative enthalpy of binding (ΔH= -2.6 kcal·mol^{-1}). These values are comparable to those found for the host-guest complex formation between the tweezer **26** and KS **84** by the use of ^{1}H NMR titration experiments (K_a= 2100±210 M^{-1}, ΔG= -4.5±0.5 kcal·mol^{-1}).

Evidently, the dendritic substituent in tweezer **26** does not have a substantial effect on the complex stability compared to the acetoxy functions in tweezer **15**. Since the dendrimer function in tweezer **26** complicates the ^{1}H NMR investigation of the host-guest complex formation, tweezer **26** is not yet water-soluble and tweezer **81**, substituted with two dendrimer in central naphthalene spacer unit could not be synthesized up to now, we gave up the study of the molecular tweezers substituted by dendrimer and focussed our interest on molecular clips substituted by dendrimers. These systems are smaller, they have a better C/O ratio than the tweezers and therefore an increase of water solubility can be expected. Additionally the molecular naphthalene-sidewalled clip **18c**, with a hydroquinone central spacer unit can be more easily synthesized and is already available in gram-scale.

2.1.4 Synthesis of the disubstituted clip 27

Since the hydroquinone clip **18c** is stable and can be prepared in a gram-scale, we decided to synthesize the dendrimer disubstituted molecular clip **27** by coupling the G_1 benzoyl chloride **59** to the hydroquinone clip **18c**. Additionally the large family of water soluble host molecules are the phosphonate and phosphate substituted clips. This will allow us to compare the substituent effect on the supramolecular properties of these clips.

The hydroquinone clip **18c** was prepared by the use of the literature procedure,[77, 78] shown in Scheme 2.14.

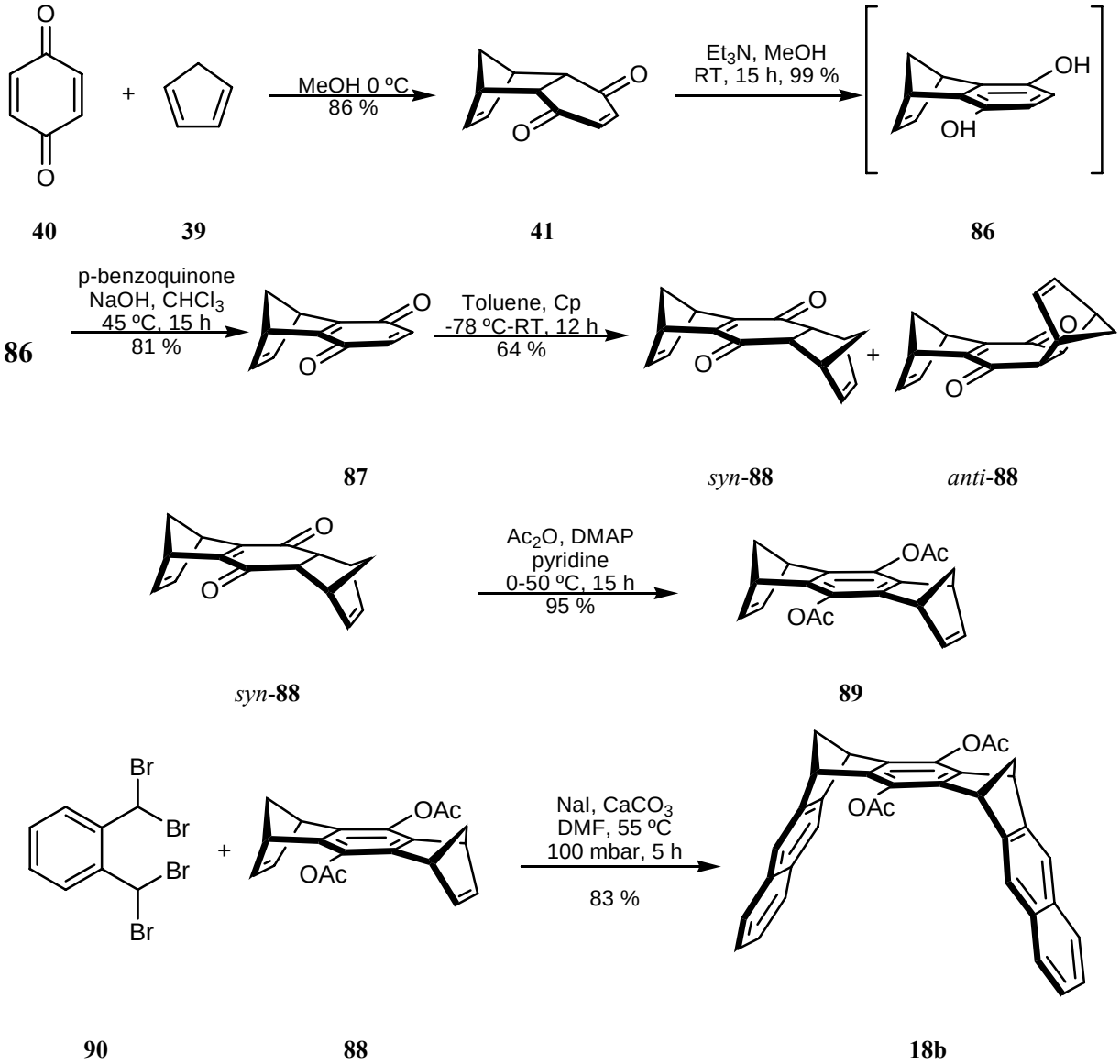

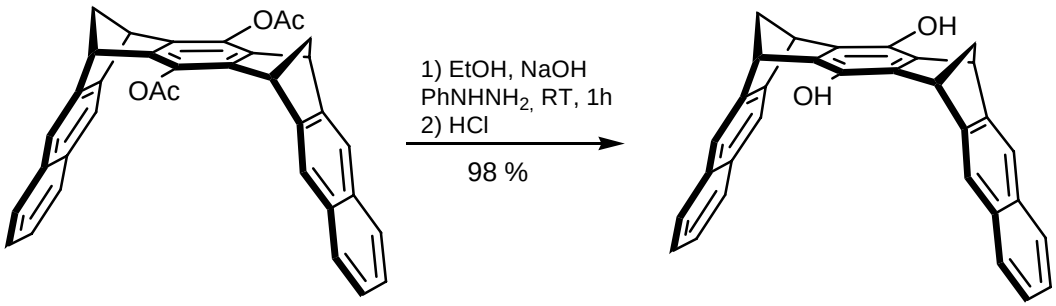

18b **18c**

Scheme 2.14: Synthesis of the hydroquinone clip **18c**.[77, 78]

The first attempt to couple the G_1 benzoyl chloride **59** to the hydroquinone clip **18c** in THF at room temperature and in presence of NEt_3 did not lead to the desired product **27**. For that reason we tested several conditions for the coupling of benzoyl chloride **91** to the hydroquinone **92** (Table 2.7).

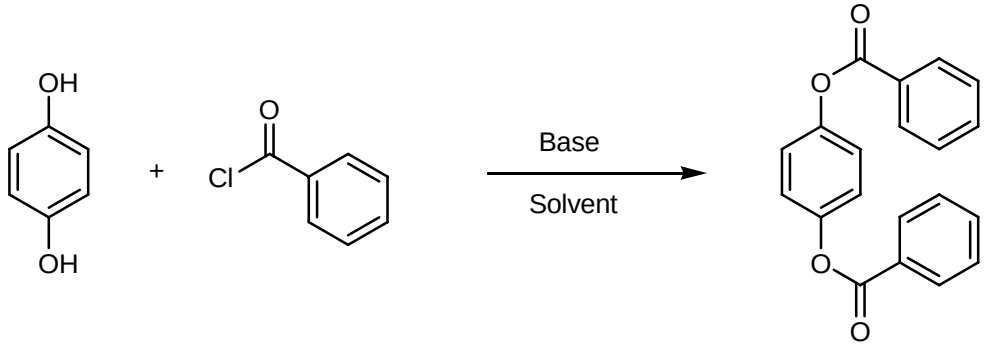

92 **91** **93**

Entry	Solvent	Base	Reaction time [h]	Temperature [ºC]	Results
1	THF_{anh}	NEt_3	33.5	0 to RT	35 % **92** + undefined products
2	THF_{anh}	NaH	18	0 to RT	41 % **92** + benzoquinone
3	Pyridine	Pyridine	24	RT	Desired product **93** (69 %)

Table 2.7: Experiments carried out in order to obtain the initial reaction conditions for the coupling of clip **18c** and the first generation dendrimer substituent **59**.

With the use of pyridine as base and solvent, the coupling between **92** and **91** was successful, leading to the desired product **93** in 69 % yield. Applying the conditions of entry 3 (Table 2.7), the reaction of hydroquinone clip **18c** with the G_1 benzoyl chloride **59** did not

lead directly to the desired dendrimer disubstituted clip **27**. Only a mixture of the starting materials and the product of monosubstitution were observed. Thus, in order to increase the reaction rate, the temperature was increased up to 90 ºC. Under these conditions (Scheme 2.15), the target clip **27** was obtained in 37 % yield after purification by column chromatography (SiO_2, AcOEt : MeOH 1:1).

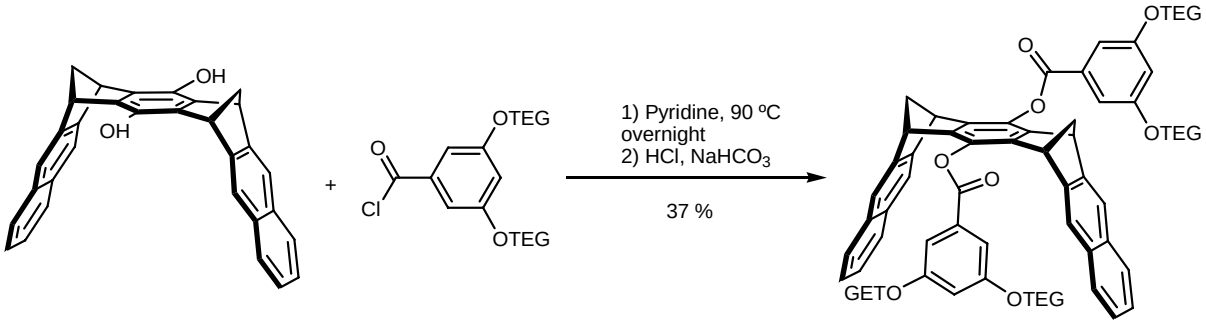

18c **59** **27**

Scheme 2.15: Optimized reaction conditions for the coupling reaction between the dihydroxy clip **18c** and the dendrimer substituent **59**.

Since the clip **27** is not chiral, its ^{1}H NMR spectrum appears to be much simpler than that of the tweezer **26**. Two dimensional NMR techniques were also used to obtain the complete assignment of the ^{1}H NMR signals of **27**, which is shown in Figure 2.15.

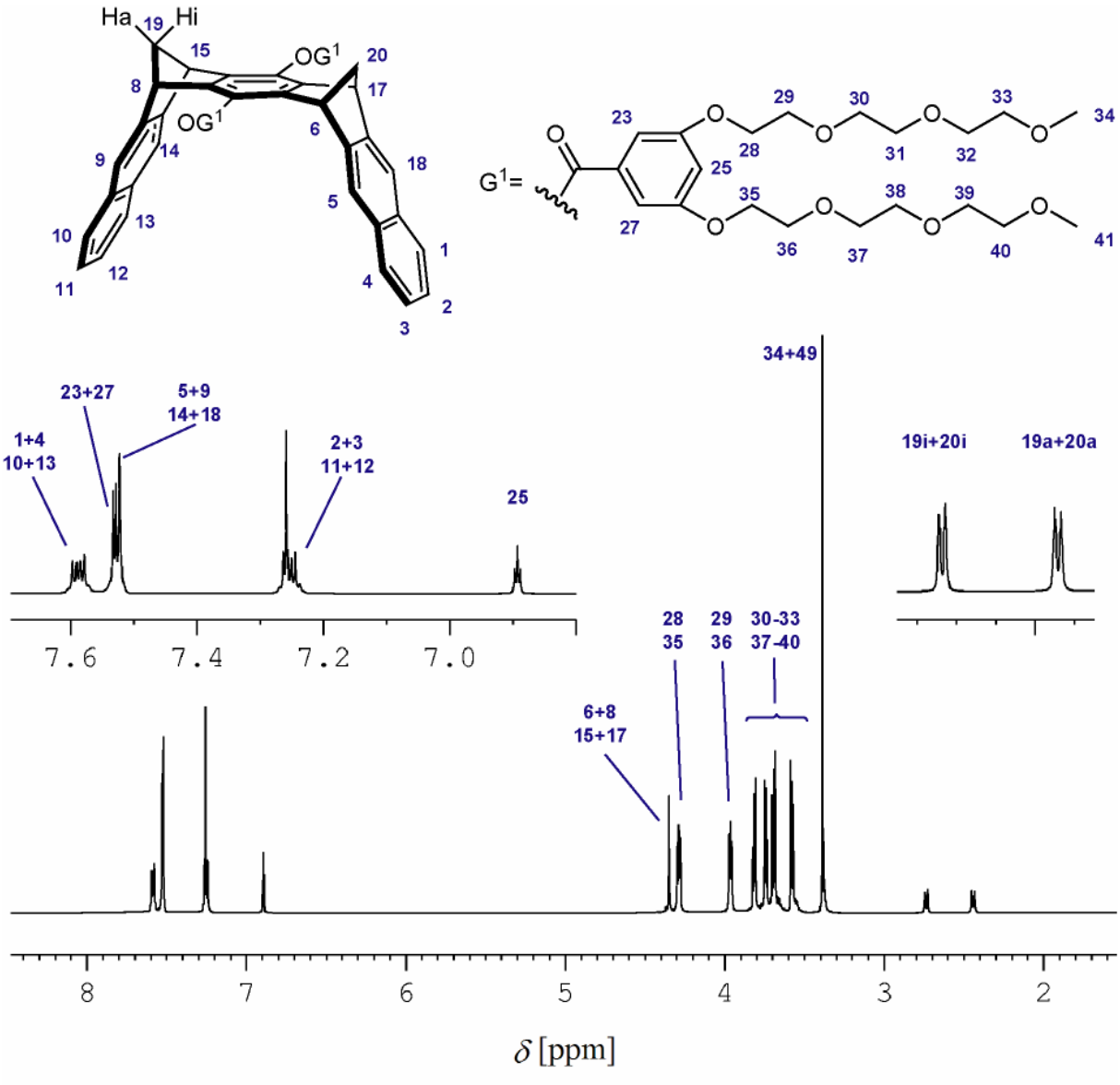

Figure 2.15: Assignment of the ^{1}H NMR spectrum of **27** (500 MHz, $CDCl_3$).

2.1.4.1 Attempt to the synthesis of the G_2-TEG disubstituted clip 94

Right after the characterization of the clip **27**, and before we started the study of its properties, we tried to prepare the next target molecule, clip **94** disubstituted by two G_2-TEG dendrimers, **60**.

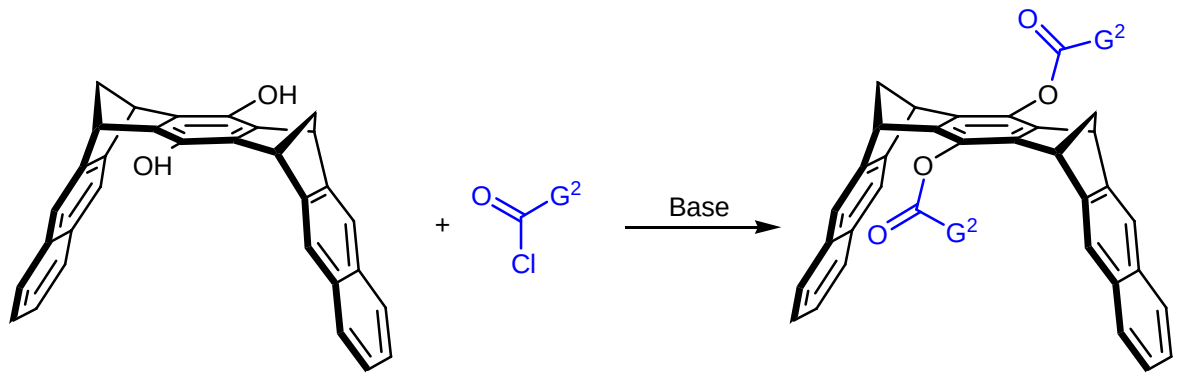

18c **60** **94**

Scheme 2.16: Reaction scheme of the synthesis of the clip substituted by second generation dendrimer groups **94**.

Surprisingly, applying the conditions successfully used for the synthesis of the G_1 dendrimer substituted clip **27** (Scheme 2.16) did not lead to the desired product **94** but only to a mixture of the starting compounds. The increase of reaction time and temperature and pressure, did not lead to the formation of the desired product **94**. In all the coupling experiments between the clip **18c** and the dendrimer **60** (summarized in Table 2.8) only starting materials were recovered in conversion between 40 and 92 %.

Entry	Solvent	Base	Reaction time [h]	Temperature [°C]	Conditions	Results[a]
1	Pyridine	Pyridine	20	RT	Argon	Starting Compounds
2	Pyridine	Pyridine	24	RT	Argon	Starting Compounds
4[b]	Pyridine	Pyridine	18	90	Argon	Starting Compounds
5	Pyridine	Pyridine	24	Reflux	Argon	Starting Compounds
6	Toluene + ACN	NEt_3	24	RT	9 kbar	Starting Compounds

[a] The starting compounds were found in different ratios (between 40 % and 92 %) and were identified by TLC (comparison with both starting compounds) and ^{1}H NMR.

[b] Standard conditions for the coupling reaction of the first generation substituent **59**

Table 2.8: Coupling reactions carried out between the clip **18c** and the dendrimer substituent **60**.

An additional method to conduct the coupling reaction is based upon of the use of the corresponding dendrimer substituted carboxylic acid and the dihydroxy clip **18c** in the presence of N^1-((ethylimino) methylene)-N^2,N^2-dimethylethane-1,2-diamine hydrochloride. The reaction is essentially a catalyzed esterification reaction (Scheme 2.17). Similar reactions using the dihydroxy clip **18c** have already been successfully performed.[115]

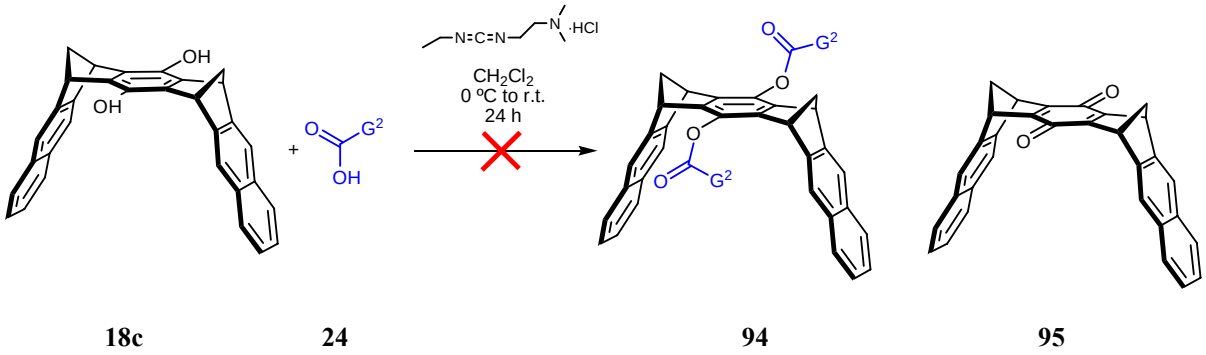

18c **24** **94** **95**

Scheme 2.17: Esterification reaction between the clip **18c** and the acid **24**.

This method did not lead to the desired clip substituted by two G_2 dendrimer groups **94** either. After the work-up, the resulting products were a mixture of the hydroquinone clip **18c** and the corresponding quinone clip **95**.

Surprisingly, although the benzoyl chloride family of molecules are usually very reactive, it was not possible to obtain the clip **94**. Consequently, the study of the TEG dendrimer-based molecular clips will be restricted to the G_1 dendrimer substituted clip **27**.

2.1.4.2 Solubility of the clip 27

Analogously as it was done for the tweezer **26** (chapter 2.1.3.5.1, page 33), the solubility of the clip, by means of the ^{1}H NMR method, was the first test carried out with the clip **27**. The solubility in methanol has been significantly enhanced (Table 2.9) whereas the solubility in water is still not detectable by this method.

Entry	Solvent	mg clip 27	Internal Standard	Solubility [mg/mL]
1	$CDCl_3$	6.2	CH_2Cl_2	Complete
2	CD_3OD	5.2	CH_2Cl_2	Complete
3	D_2O	5.7	1,4-dioxane	Not detected

Table 2.9: ^{1}H NMR solubility experiments for the clip **27** in the most usual solvents for tweezers and clips binding experiments.

Since the solubility of the clip **27** in deuterated methanol is much higher than that of the tweezer **26**, we assumed that the solubility in water should have been increased as well. In order to quantify the solubility of **27** in water, we chose another method which uses the UV-vis properties of this compound (refer to chapter 4.4.2 (page 192) for the complete experimental details of the UV-vis method). Thus, using 4.73 mg of **27** and 1.60 mL of water, we found the solubility of **27** in water to be $5.11 \cdot 10^{-5}$ mM/mL ($6.62 \cdot 10^{-3}$ mg/mL).

Despite the clip **27** appears to be slightly water-soluble, it is not high enough to perform neither ^{1}H NMR nor microcalorimetric binding studies. The increased solubility in methanol, however, will allow the study of binding properties in this solvent and, therefore and most important, the comparison of the obtained results with other methanol-soluble clips such as **18e-h**.

2.1.4.3 ESI-TOF spectrum of clip 27

The naphthalene clip **27** happens to have a very characteristic ESI-TOF mass spectrum, shown in the Figure 2.16.

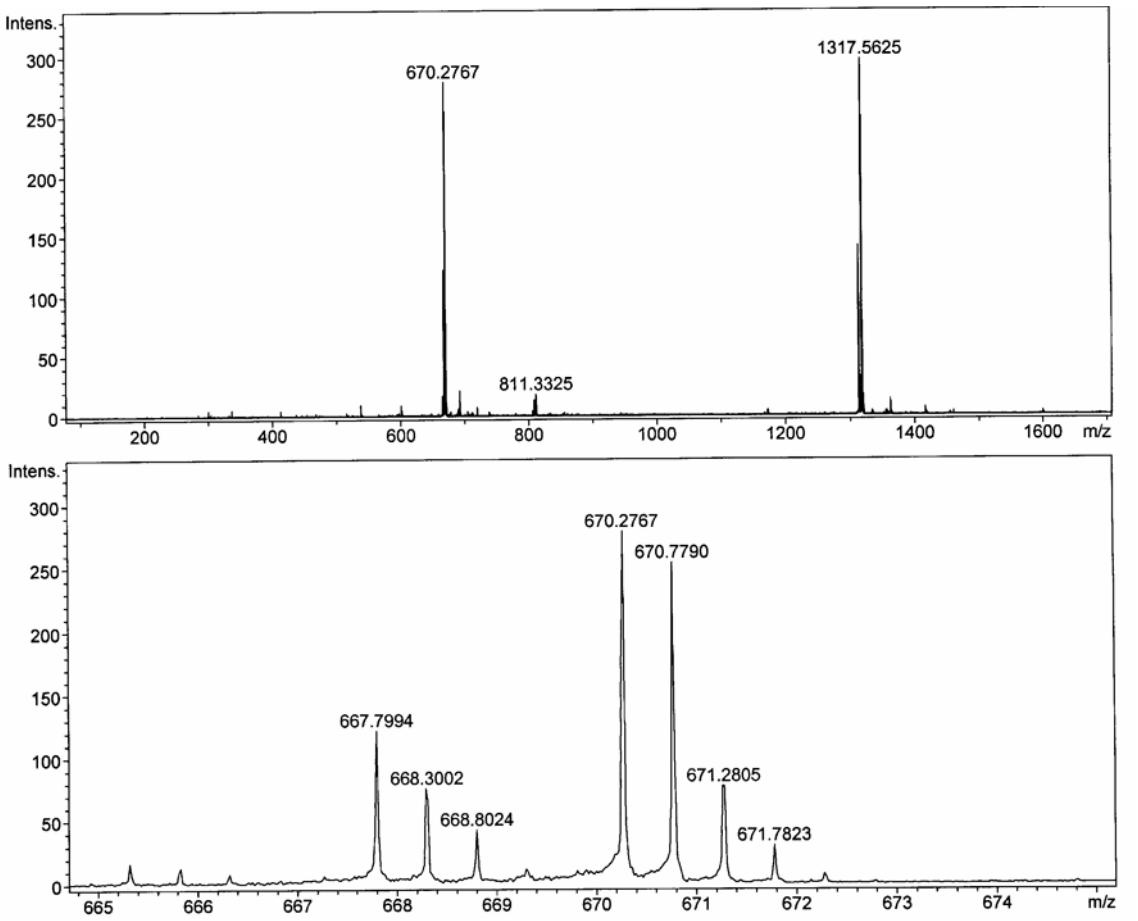

Figure 2.16: ESI-TOF spectrum (positive ionization). The main molecular peak at 1317.5625 [M+Na^{+}] shows the usual isotopic peaks due to the presence of different isotopes, whereas the doubly charged molecular peak at m/z = 670.2767 [M+2·Na^{+}] displays isotopic peaks separated by approximately 0.5 m/z units.

Besides the molecular peak plus one sodium atom at m/z= 1317.5625 (calculated for $[C_{74}H_{86}NaO_{20}]^+$ = 1317.5610) there is also an intense peak at m/z= 670.2767. It corresponds to the molecular peak with two attached sodium atoms and doubly charged $[M+2\cdot Na]^{2+}$ (calculated for $[C_{74}H_{86}Na_2O_{20}]^+$ = 1340.5508/2= 670.2754). Doubly charged ions are shown in the ESI-TOF spectra with isotopic peaks separated from each other by approximately 0.5 m/z units as it is possible to be seen in the expansion of the area around m/z= 670. On the other hand the peak at m/z= 667.7994 corresponds to the molecular peak plus one sodium atom and one water molecule (calculated for $[C_{74}H_{86}NaO_{20}+H_2O]^{2+}$= 1335.5716/2= 667.7858)

The presence of the triethyleneglycol branches in the receptor **27** reminds intuitively to the structure of a crown ether (with an open end), which are known to create supramolecules with alkali cations (chapter 1.3, page 6). Analogously to crown ethers, the sodium cation could be accommodated in the middle of the triethyleneglycol branches. Since the clip **27** is doubly substituted, each substituent can hold one sodium cation (Figure 2.17) leading finally to a doubly charged peak in the ESI-TOF mass spectrum. This is not an unexpected effect, since ESI mass spectrometry has been proven to be an effective method to assess complexation phenomena in ether crown type of receptors.[116]

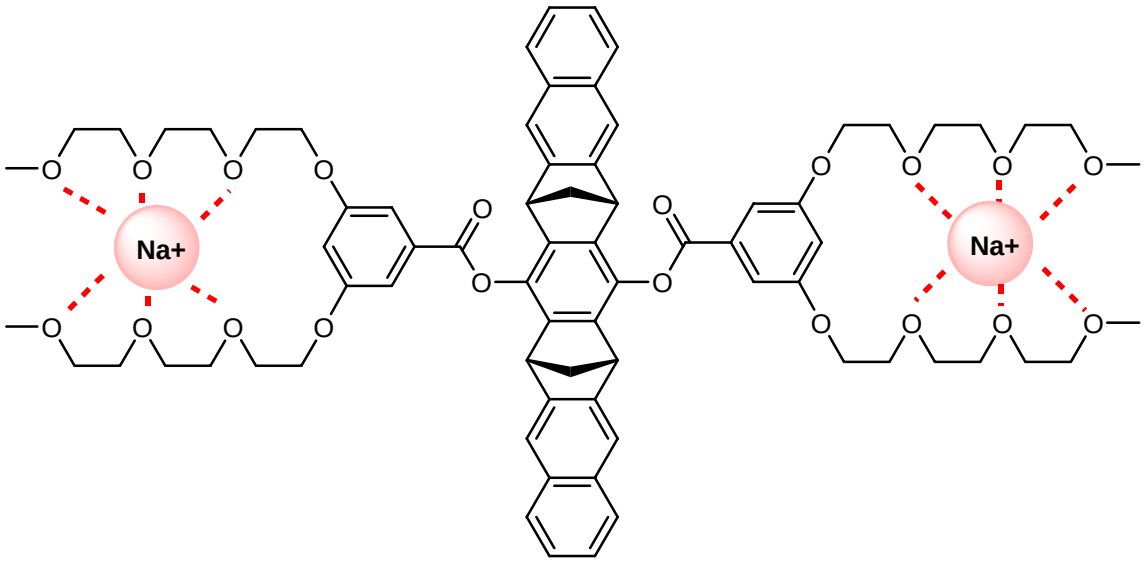

Figure 2.17: Supramolecule suggested for the complex **2·Na$^+$@27**.

This hypothesis is supported by the conformational search in gas phase calculated for the supramolecule **2·Na$^+$@27** (MacroModel 9.0, Monte-Carlo simulation, AMBER*, gas phase, 5000 structures). The conformer of minimum energy (Figure 2.18) shows how the sodium cations (represented in violet) are completely surrounded by the triethyleneglycol branches. The interaction of the oxygen lone-pairs with the sodium cation stabilizes the complex in gas phase and consequently it is detected in the ESI-TOF spectrum.

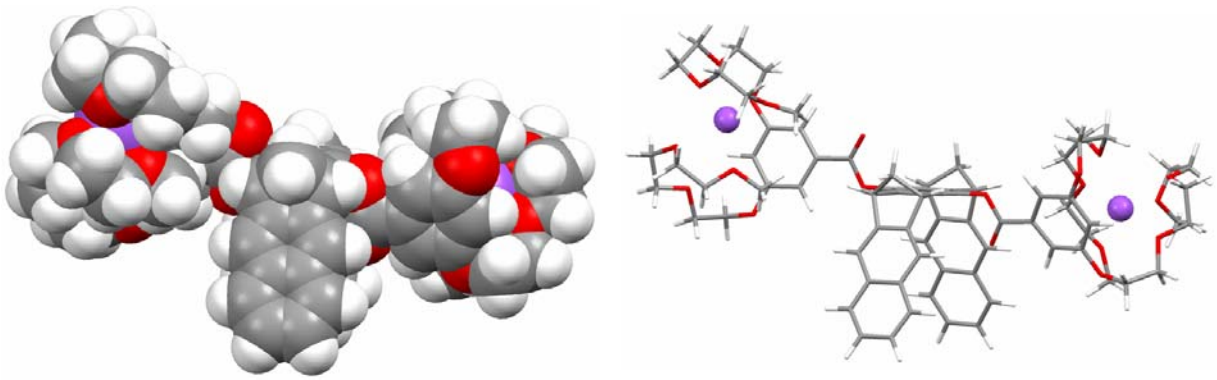

Figure 2.18: Conformer of minimum energy resulting from the Monte-Carlo conformational search (MacroModel, AMBER*, gas phase, 5000 structures) calculated for the clip **27** and two sodium cations.

Following the original work of Pedersen and Frensdorff on macrocyclic polyethers,[46] we were able to confirm the formation of this macromolecule even in solution of chloroform. We carried out the variation to the *solvent exchange* technique developed by Pedersen and Frensdorff.[46]

When 0.60 mL of chloroform were added to a mixture of one equivalent of clip **27** (15.18 mg) and 2 equivalents of NaI (3.23 mg), the clip was dissolved instantly whereas the NaI remained not dissolved. To the resulting heterogeneous mixture, 15 µL of methanol were added and the NaI crystals were dissolved instantaneously leading to a clear solution of sodium iodide in $CHCl_3$ (and traces of methanol).

According to Pedersen and Frensdorff, the little amount of methanol is vital for the solution of alkali metal salts in organic solvents because it is held by the complex becoming a part of the solvation sphere.[46] Furthermore, once the methanol is incorporated to the supramolecular system, it cannot be removed completely.

2.2 Synthesis of molecular clips substituted by hyperbranched polyglycerol groups

2.2.1 General synthetic pathway to the hyperbranched polyglycerols

The previously described tweezer **26** and clip **27** were functionalized by a triethyleneglycol-based substituent. This substituent is only a hydrogen-bond acceptor, which restricts the interaction with water molecules. In order synthesize a molecular clip with substituents having both hydrogen-bond acceptor and donor properties, a project was initiated in cooperation with Prof. Dr. Rainer Haag (Freie Universität Berlin). The research group of Prof. Haag has a wide experience in the field of polymer chemistry. The hyperbranched polyglycerols are the sort of polymers which are of particular interest in this work.

Hyperbranched polymers are also interesting in the fields of biochemistry and biomedicine, where these molecules can be used, for example, as host compartments for

controlled drug-release. The application of these compounds as host molecules is related to the goal in this work, the synthesis and study of water-soluble molecular tweezers and clips as host molecules.

Usually, the perfectly structured dendrimers must be synthesized in tedious multi-step routes, which is an important limitation for most of the applications. But the less perfectly structured hyperbranched polymers can be synthesized via one-pot reaction and considered to be an alternative to the multistep preparation, since structural perfection appears not to be a key factor for many applications.

In the present work a relatively new technique of hyperbranched polymerization was used. This is the use of a latent AB_m monomer, where the groups B are set free only by the reaction of the A group. This method also allows the control of the molecular weights of the final polymer.[117, 118] Glycidol, (oxiran-2-yl) methanol (Scheme 2.18), was one of the first AB_2 latent monomers studied as it has highly reactive epoxy and hydroxy groups and its polymerization is known for a long time.[119, 120] This monomer is going to be also used for the synthesis of the polyglycerol substituted clips. The problem of such a monomer is that, in addition to the chain-growth polymerization mechanism leading to the desired polymer, it is also able to start a polymerization by its free hydroxyl groups resulting in an uncontrolled oligomer formation.[88] This side-reaction can be avoided by a common technique in the synthesis of polymers which is the very slow addition of monomer to the initiating compound, ensuring a low concentration of monomer in the reaction mixture.[121] This technique was used by Sunder *et al*., who developed a path to a well-defined hyperbranched polyglycerol which is based on the anionic polymerization of an AB_2 latent monomer.[122, 123] Under this conditions the reaction mechanism for such a hyperbranched polymerization reaction is postulated to be as shown in Scheme 2.18.[88] The key feature here is that in the case of pseudo-chain growth conditions, the latent monomer (glycidol) reacts solely with the growing branches of the polymer, which allows a controlled growth of the molecule.

One of the problems reported of using glycidol as a latent monomer is that the resulting homopolymer is extremely polar and therefore is becomes problematical to use it for further reactions. This problem can be avoided by the use of a certain ratio of propylene oxide as an additional monomer, obtaining so a less polar copolymer. The high polarity of this sort of polymers was of our particular interest as the final target is to obtain water-soluble molecular clips.

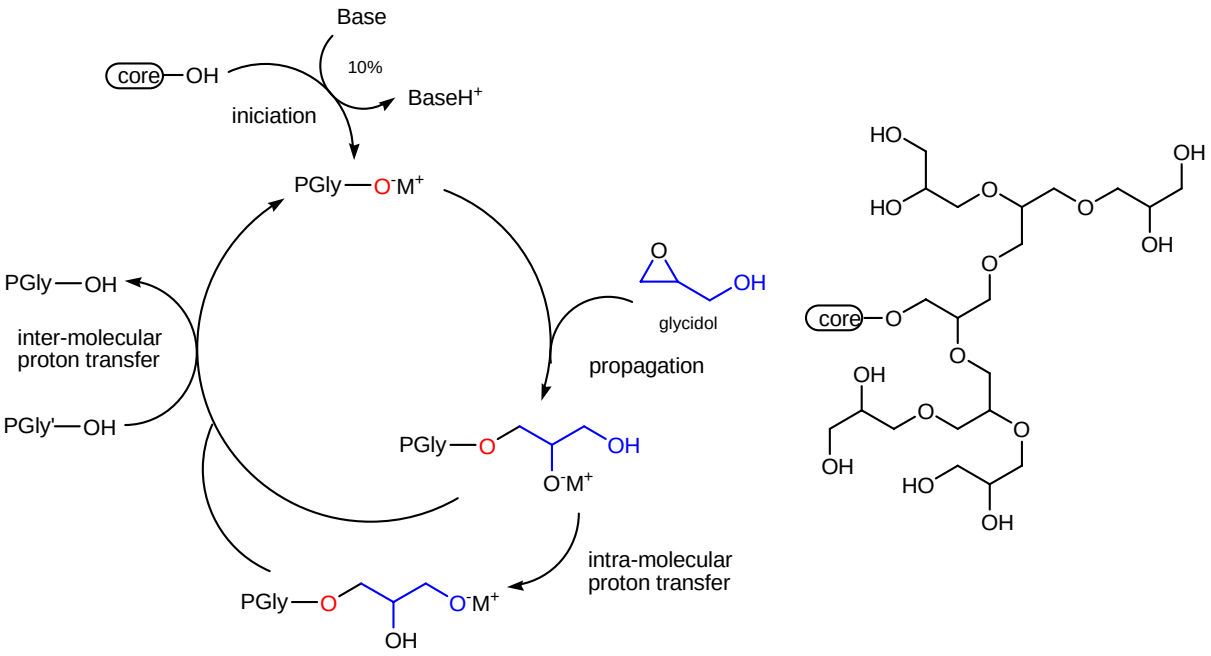

Scheme 2.18: Left: postulated reaction mechanism of the base-catalyzed hyperbranched polymerization of glycidol. [88] Right: Schematic structure of the resulting hyperbranched polyglycerol.[88]

There are many possible combinations of initiator molecules (core-OH in the Scheme 2.18) and monomers (glycidol in the Scheme 2.18). The resulting polymer of the reaction can be further modified in order to obtain a broad collection of polymers with different properties which make them suitable in fields like nanoscale reaction compartments, templates for nanoporous materials, fabrication of hybrid particles as well as the biochemical and biomedical fields mentioned before. Some of the different initiator molecules, monomers and possible further modifications are summarized in Table 2.10.

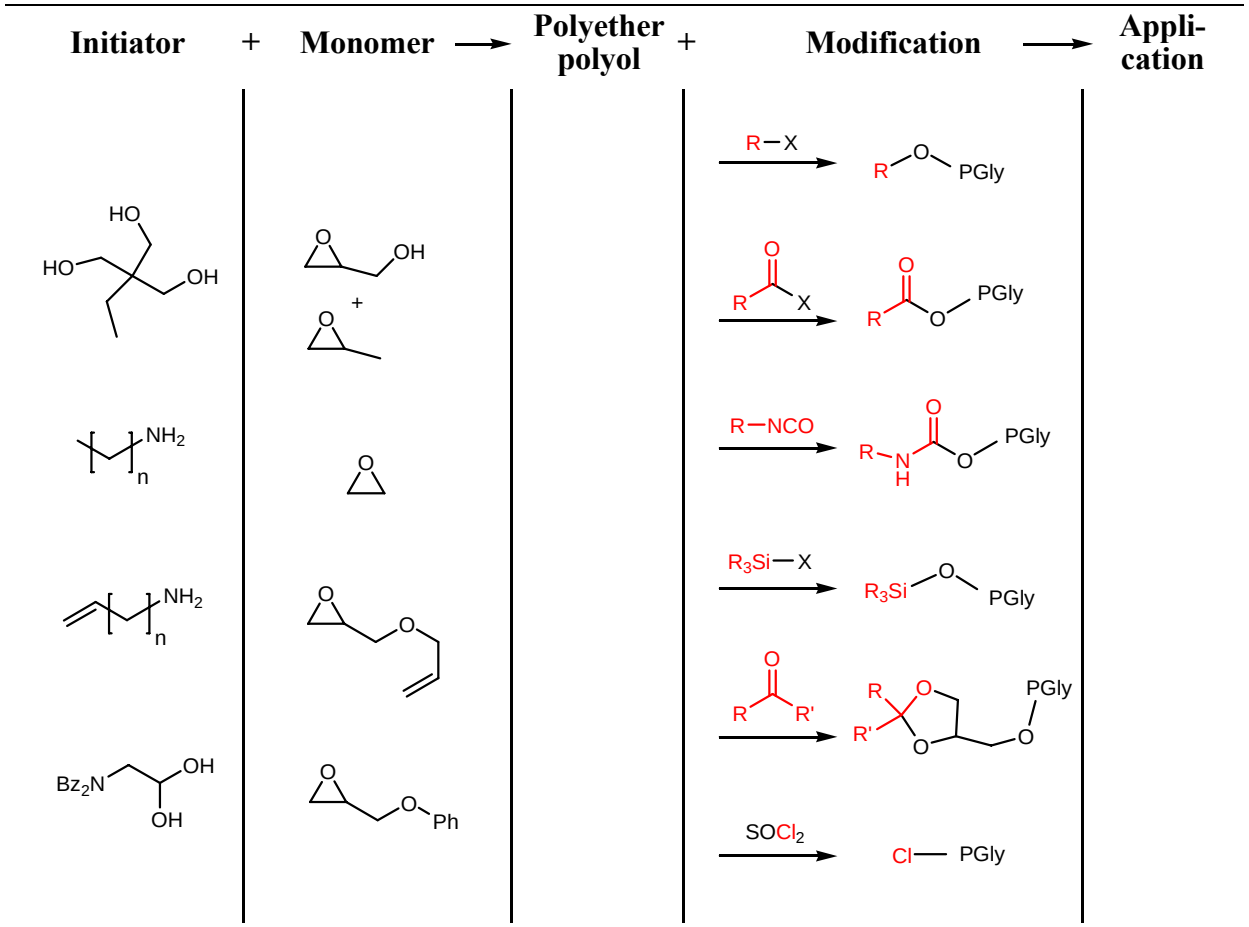

Table 2.10: Comparison of some initiator molecules, monomers and possible transformations. The properties and possible applications of the final functionalized polymer are in dependence of the functionalization.[88]

2.2.2 Synthesis of hyperbranched polyglycerol substituted molecular clip

Starting material of the synthesis of hyperbranched polyglycerol substituted clip of type **96** are the hydroquinone clip **18c** (initiator molecule) and glycidol **97** (monomer unit). Hyperbranched polyglycerol substituted clips were prepared by Ewelina Burakowska in Professor Haag's group.

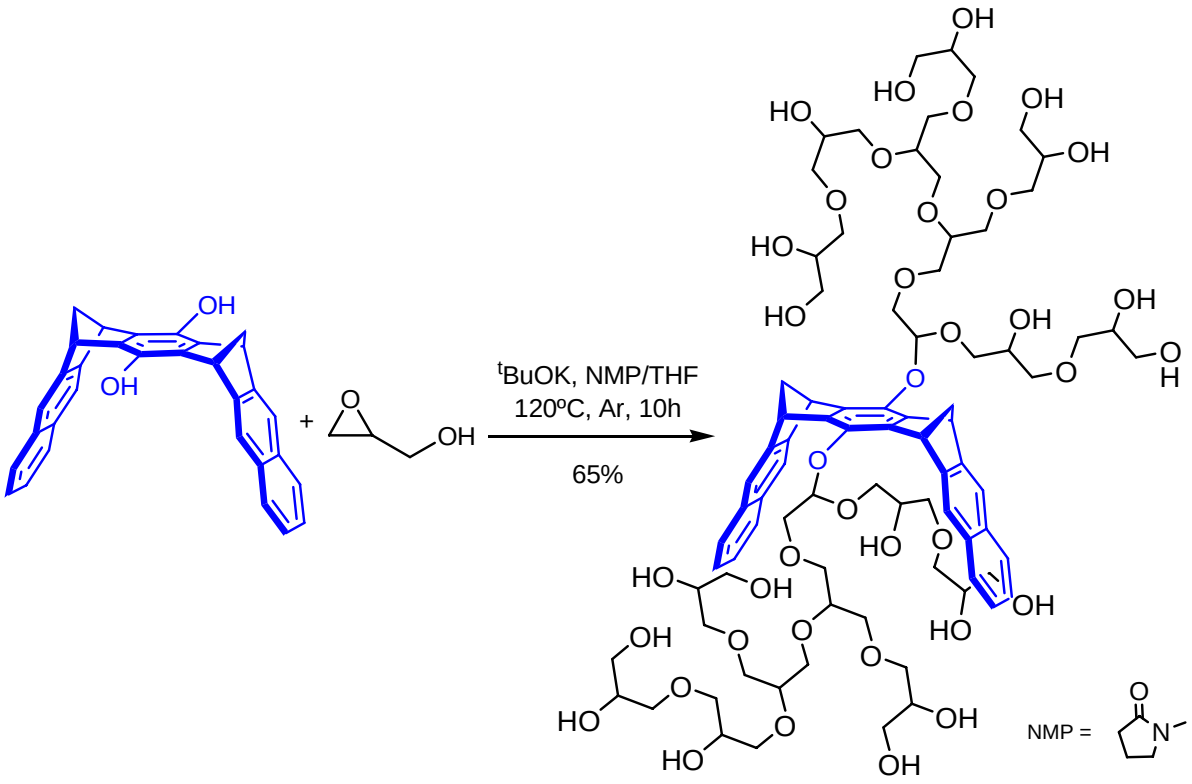

18c **97** **96**

Scheme 2.19: Synthesis of the polyglycerol substituted molecular clips. The clip **96** is one structural example of the hyperbranched polyglycerol substituted clip.

The reaction takes place at the relative high temperature of 120 ºC. Therefore a high boiling solvent such as NMP (1-methylpyrrolidin-2-one) is required. The high polarity of this solvent is also of importance for this reaction to take place. Dry THF is only necessary to dissolve the glycidol **97**, which is added very slowly by dropwise addition to the solution of clip **18c**. THF is removed from the reaction mixture by condensation after the addition is completed. The addition at very slow rate of glycidol is usually done by the use of a flow regulator dropping device in order to obtain a very constant addition rate. The final product is purified by *precipitation* from acetone, obtaining a dark oil. Using this purification method some of the solvent (NMP) remains in the oil. This solvent can only be completely removed by means of dialysis. The disadvantage of this purification method is that it needs relatively large amount of compound.

Two clips of the type of **96** substituted by hyperbranched polyglycerol units of different size were synthesized with this method. In the first place the objective was to introduce 1 kD of glycidol units at each side of the central benzene spacer unit of the clip **18c**, which means to carry out the reaction with 27 equivalents of glycidol. The reaction took place successfully and the clip **98** was obtained with 65 % yield as dark oil. Starting with 1 g of the hydroquinone clip **18c**, 3.5 g of the hyperbranched polyglycerol clip **98** were obtained. This

amount was, however, not sufficient for the purification by the use of dialysis (membrane filtration). Therefore traces of NMP were still present in this sample.

In a second experiment, the objective was to introduce up to 3 kD of glycidol units at each side of the spacer unit, which means to use 81 equivalents of glycidol. The reaction was successful and, starting with 1 g of the hydroquinone clip **18c**, 9.2 g of the hyperbranched polyglycerol substituted clip **99** were obtained in 63 % yield. Since the amount of obtained clip was significantly larger, the dialysis purification in methanol using benzylated cellulose membrane (MWCO 1000, Sigma) was possible leading finally to the NMP-free clip **99** as dark oil.

2.2.2.1 Characterization of the hyperbranched polyglycerol substituted clips

The structural assignment of clips **98** and **99** were performed by the use of NMR and MS techniques, carried out in Essen. The characterization of clips **98** and **99** was not as straight forward as that of clip **27**. The main difference among those clips is that clips **98** and **99** have not a specific well-defined structure and the aliphatic substituents in ^{1}H NMR spectrum can be only be assigned as one not-well-solved group. Additionally, the signals assigned to the aromatic and aliphatic clip protons are broad and do not show a fine structure and, hence, do not allow determining the coupling constants. The ^{1}H NMR spectrum of clip **99** and its assignment are shown in Figure 2.19.

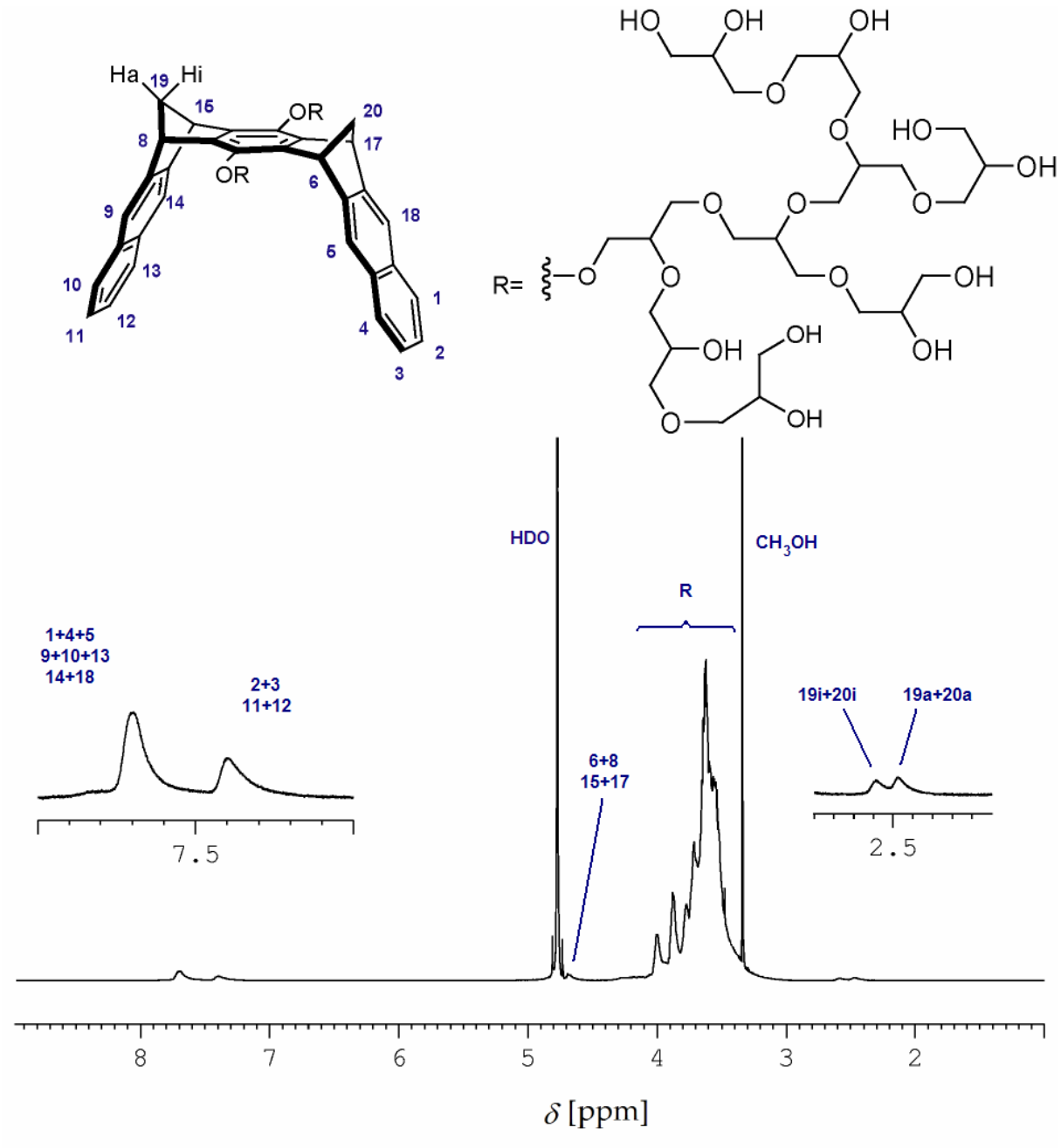

Figure 2.19: Assignment of the ^{1}H NMR spectrum of **99** (500 MHz, D_2O).

An applicable method commonly used for polymer characterization is the MALDI-TOF mass spectrometry technique.[124] With this method it is possible to reveal whether the polymerization reaction has been successful or not. If the reaction has taken place it is also possible to evaluate how many monomer units have been attached to the initiator molecule.

The MALDI-TOF mass spectrum from the clip **98** is shown in Figure 2.20.

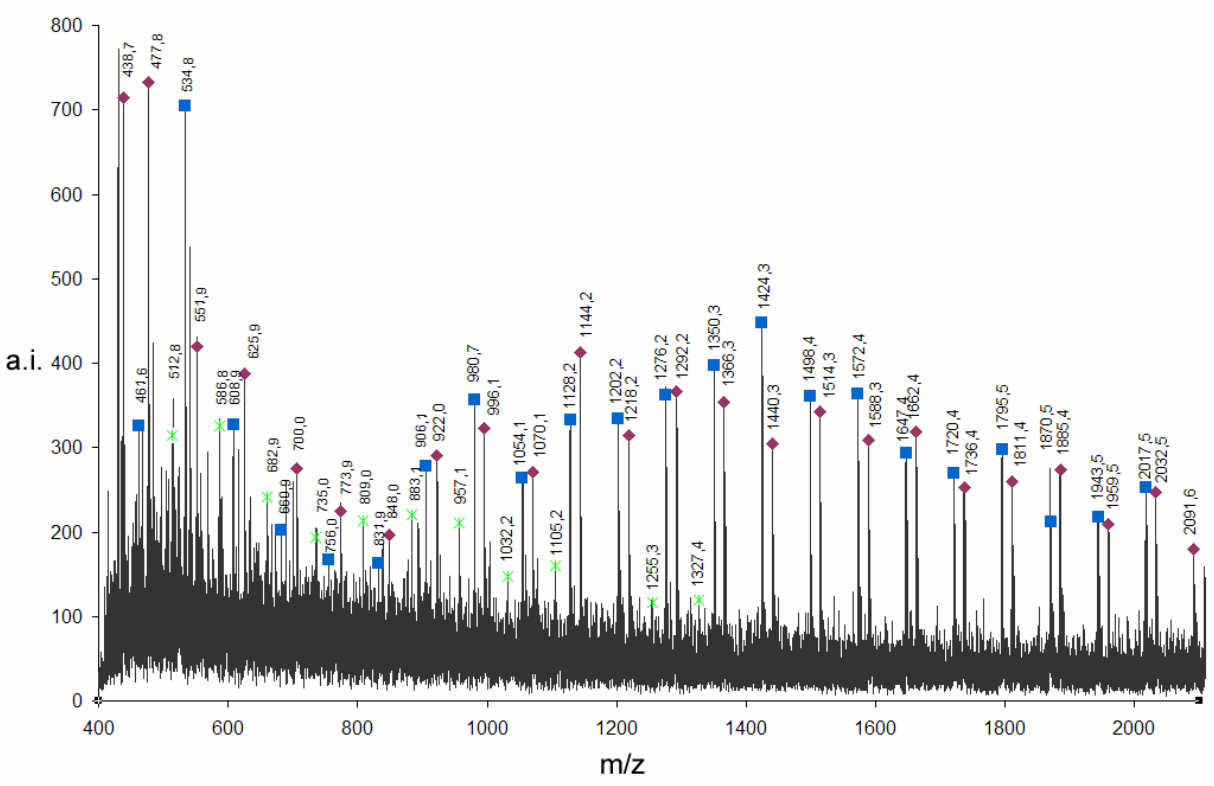

Legend:

- ♦ : clip + K + n·glycidol units
- ■ : clip + Na + n·glycidol units
- x : clip + n·glycidol units

Figure 2.20: MALDI-TOF mass spectrum of the clip **98**.

The analysis of this MALDI-TOF spectrum leads to two main conclusions. First of all the polymerization reaction was successful and the glycidol units have been attached to the initiator molecule, the clip **18c**. Secondly no oligomerization of the obtained clip is observed and therefore the glycidol units are attached to the previously attached glycidol molecules and there is no cross-coupling attachment between a glycidol of one clip to a neighbour clip. The observed mass oscillates between m/z= 534.8 which corresponds to a clip molecule plus one glycidol equivalent and one sodium cation, and m/z= 2091.6 which corresponds to a clip molecule plus 22 glycidol equivalents and one potassium cation which is significantly close to the theoretical 27 glycidol equivalents we planned to obtain. The most abundant peaks are m/z= 438.7 and m/z= 477.8 and correspond to the starting clip **18c** and **18c**+K^+ respectively.

Conclusively, and according to the MS shown in Figure 2.20, the reaction of hydroquinone clip **18c** and glycidol **97** gives a complex mixture of substituted clips of type **96** containing 1 to 22 glycidol units.

2.2.3 Stepwise synthesis of polyglycerol substituted clip

The proportion between the size of the polyglycerol substituents and the binding properties of the molecular clips is of great importance for the understanding of the mechanism of complexation and the intermolecular forces that are implied. Fortunately, there is also a synthetic route to produce perfectly structured glycerol dendrimers.[125]

The synthetic path to the perfect dendrimers starts with the S_N2 substitution of the initiator alcohol with allyl chloride followed by the dihydroxylation of new double bonds in the allyl ether with OsO_4 leading directly to the first generation of glycerol dendrimer (Scheme 2.20).

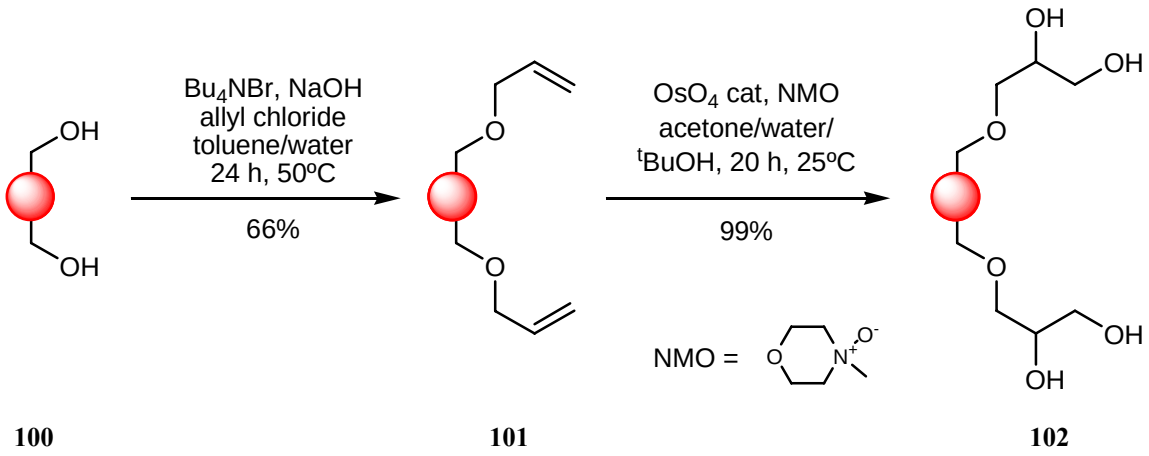

Scheme 2.20: Initial synthetic route of the perfect glycerol dendrimers.[125]

In this work the allylation of hydroquinone **92** and of the hydroquinone clip **18c** were carried out in our research group while the dihydroxylation reactions were performed in Professor Haag's research group. The dihydroxylation with OsO_4 is a well known reaction for the functionalization of double bonds. The NMO (*N*-methylmorpholine-*N*-oxide) is used as a co-oxidant and OsO_4 only in a catalytic amount. The reaction usually proceeds in almost quantitative yield.

2.2.3.1 Preparation of the 1,4-diallyloxy benzene 103 and diallyloxy clip 104

Since the initiator molecules are usually aliphatic compounds (Table 2.10), the use of an aromatic template was found appropriate in order to find the correct experimental conditions for this particular system. The easiest template compound for the dihydroxy clip **18c** is the hydroquinone **92**. Thus in a first instance the 1,4-diallyloxy benzene **103** was synthesized according to the literature[126] starting from the hydroquinone **92** (Scheme 2.21).

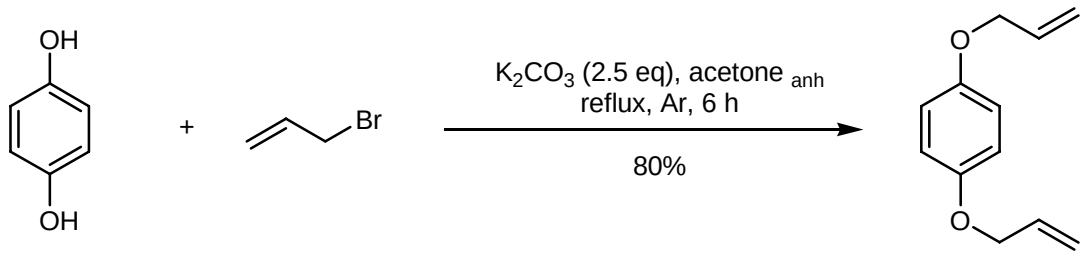

92 **105** **103**

Scheme 2.21: Synthesis of the 1,4-diallyloxybenzene.[126]

A stirred (1:2.5) mixture of hydroquinone **92** and allyl bromide **105** dissolved in acetone was heated under reflux for 6 hours in the presence of potassium carbonate instead of Bu_4NBr/NaOH used in the literature.[126] The removal of the solvent, filtration and recrystallization of the remaining solid in *n*-hexane led to the desired diallyloxybenzene in 80 % yield, significantly higher than that obtained with the original method using the Bu_4NBr/NaOH mixture (66 %).[125]

Since the experiment with the model compound 1,4-hydroquinone **92** did not lead to any unexpected complications, the same conditions were used for the synthesis of the diallyloxy substituted clip **104** (Scheme 2.22)

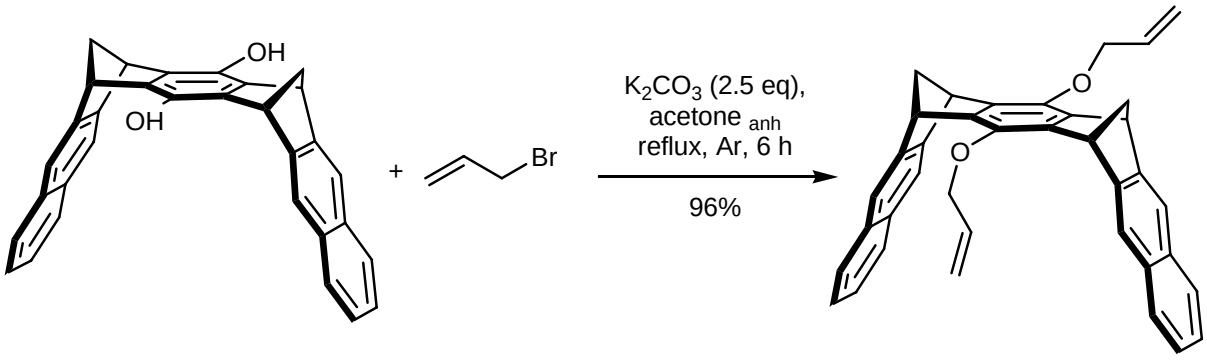

18c **105** **104**

Scheme 2.22: The same conditions used for the 1,4-hydroquinone applied to the dihydroxy clip **18c** successfully lead to the diallyloxy clip **104**.

The synthesis of the diallyloxy clip **104** was even more successful, with 96 % yield, than that of the model compound **103**.

2.2.3.1.1 Single-crystal structure of clip 104

Clip **104** was obtained as a colourless solid. The slow evaporation of an acetone solution of the diallyloxy clip **104** led to needle-like crystals which were suitable for a single crystal X-ray analysis. The details for the X-ray analysis of the clip **104** are shown in chapter 4.6 (page 236).

The crystal packing of the structure of **104** does not show much intuitive information about the clip-clip interactions (Figure 2.21). However, by using the Mercury[127] software for a carefully analysis of the crystal structure, it is possible to obtain more information about these interactions in the crystal cell.

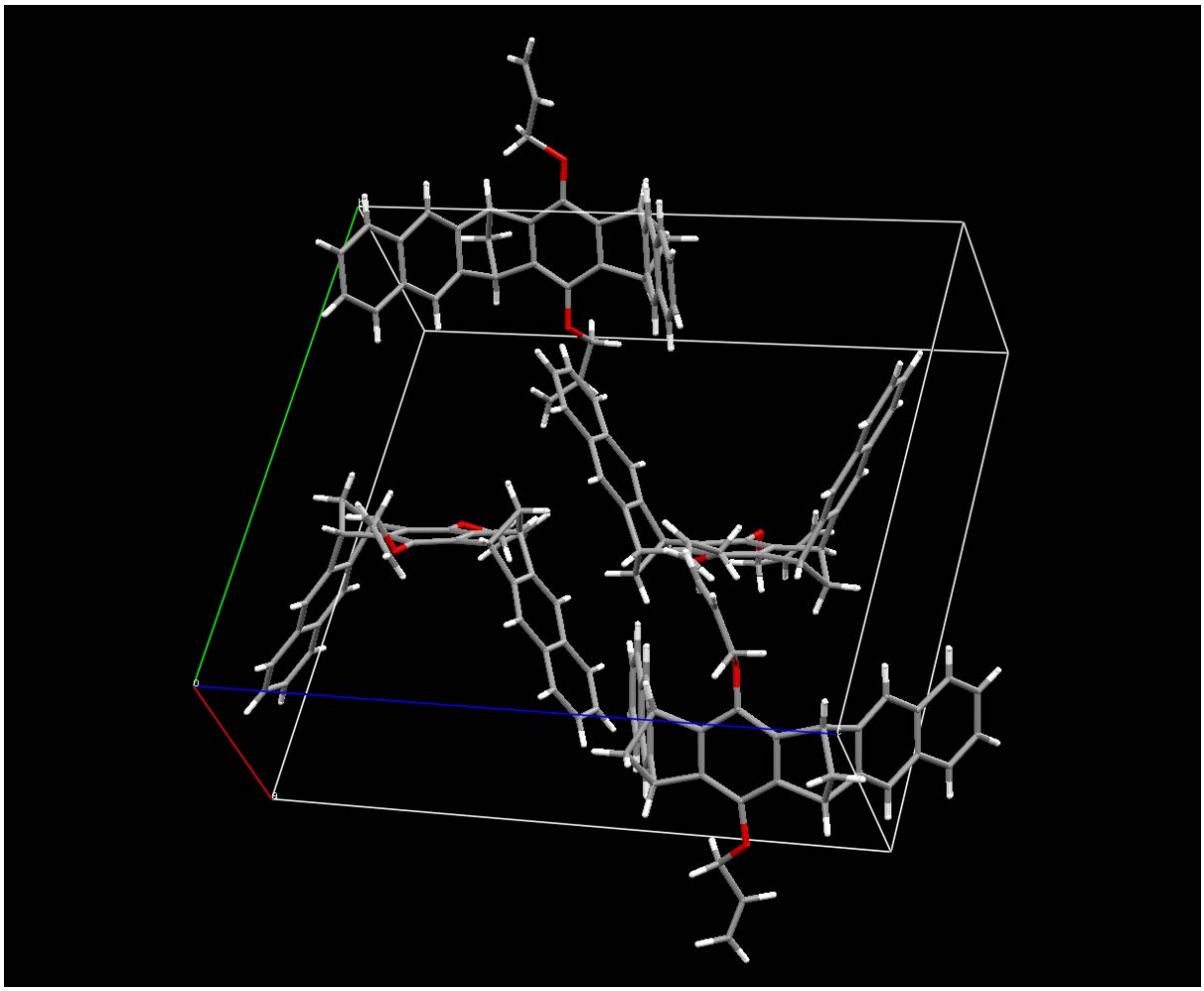

Figure 2.21: Unit cell packing view of the crystal structure of the clip **104**.

The single-crystal of **104** was obtained free of solvent, which is not often found in the case of clip and tweezer structures because the size of the cavity, generated by their convex-concave geometries, is big enough to accommodate solvent molecules.[36] With the use of the

mentioned software, it is possible to select a single molecule and show all its intermolecular close contacts with contiguous molecules (Figure 2.22).

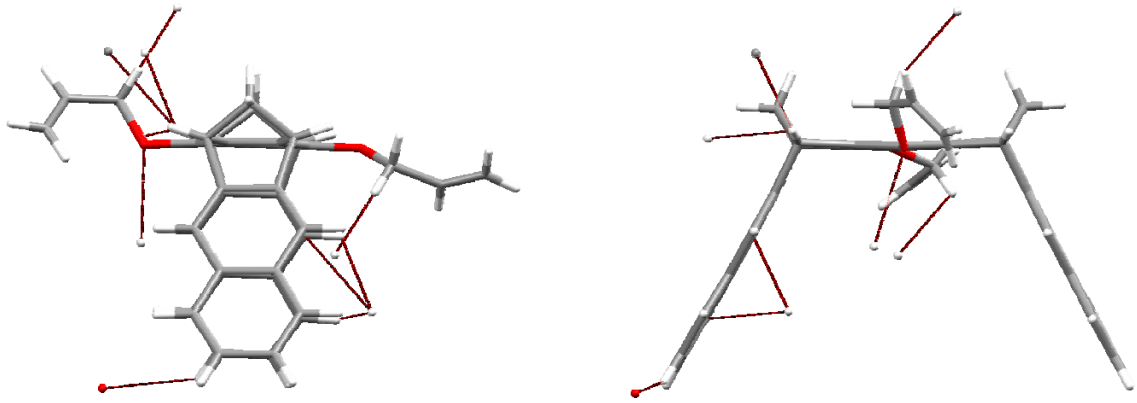

Figure 2.22: Front and lateral views of a single molecule from the crystal structure analysis with the intermolecular close contacts indicated with dashed lines.

Studying one by one the intermolecular interactions it is possible to analyze how the molecules are accommodated in the crystal. Figure 2.23 shows the C_{arom}-H – O interaction between a hydrogen atom at the end of the naphthalene sidewall and the oxygen of the allyloxy group of another clip oriented perpendicular to this hydrogen atom.

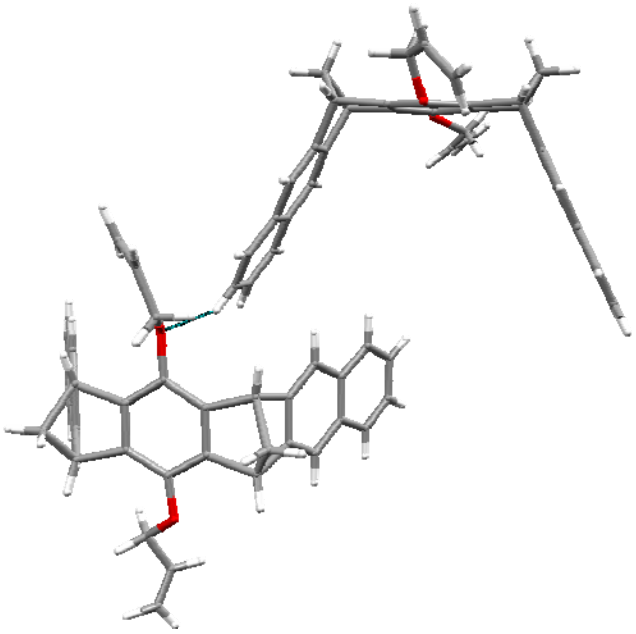

Figure 2.23: Relative orientation of one clip with a neighbour one. The C_{arom}-H – O interaction is highlighted with a dashed blue line. The relative orientation appears to be nearly perpendicular.

All the other intermolecular interactions shown in the Figure 2.22 are H – H and C – H interactions between a clip and a completely parallel located contiguous clip (Figure 2.24).

Figure 2.24 shows that the allyloxy group of one clip is positioned inside the cavity of another clip nearby.

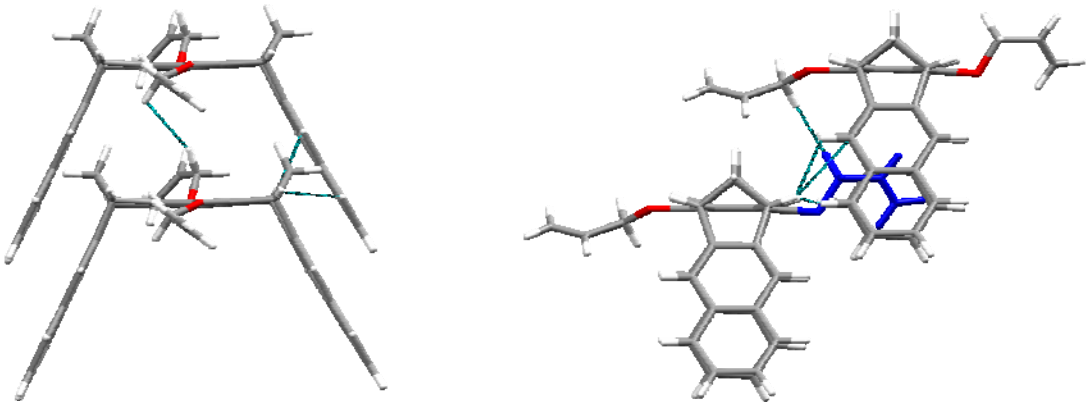

Figure 2.24: Frontal (left) and lateral (right) view of two clips one parallel to the next in the crystal structure. The intermolecular interactions are highlighted in blue dashed lines whereas the allyloxy group located inside the cavity of another clip is highlighted in dark blue (right side).

2.2.3.2 Synthesis of the glycerol substituted clip 28

The oxidation of the allyl ethers **103** and **104** were performed in Professor Haag's research group. The reaction with 1,4 diallyloxy benzene **103** with NMO and catalytic amounts of OsO_4 in a mixture of acetone, water and ^{t}BuOH produced the desired 3,3'-(1,4-phenylene(oxy))dipropane-1,2-diol **106** in 85 % yield (Scheme 2.23).

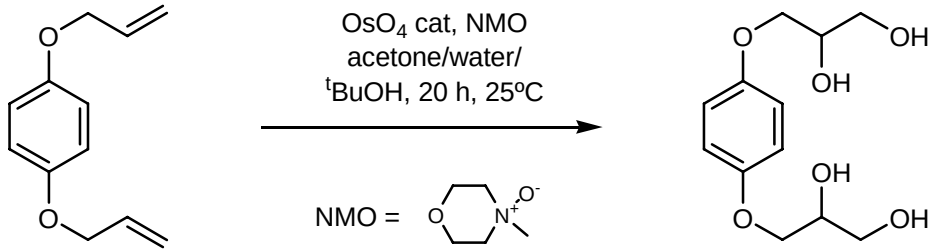

103 **106**

Scheme 2.23: Dihydroxylation reaction and final glycerol substituted benzene.

Under similar conditions the diallyloxy substituted clip **104** was oxidized leading to the bis(dihydroxypropyl) naphthalene clip **28**. This clip is the first generation polyglycerol dendrimer clip with a perfectly known structure (Scheme 2.24), which is the main difference with the other polyglycerol dendrimer clips **98** and **99** discussed in the previous section.

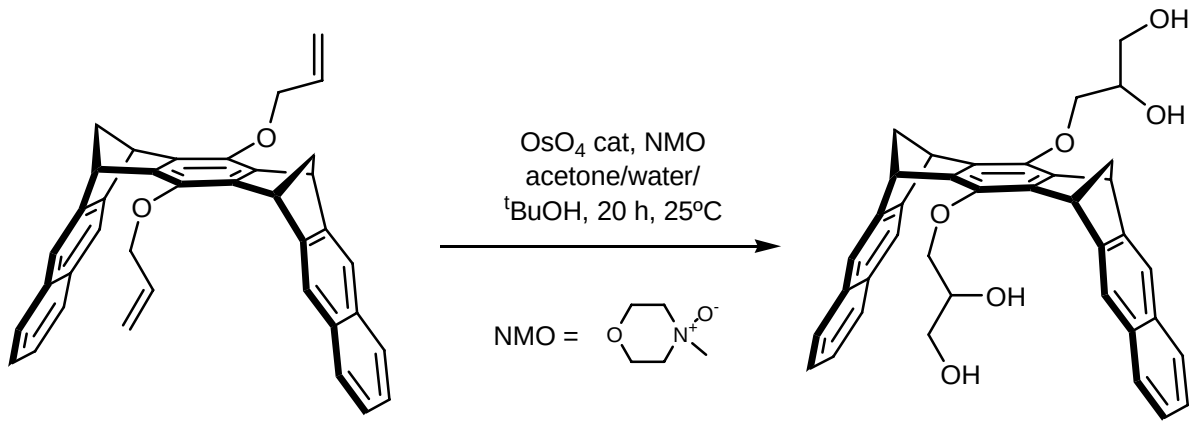

104 **28**

Scheme 2.24: Dihydroxylation reaction of the diallyloxy clip **104** and final clip **28**.

The characterization of the clip **28** was carried out with the usual spectroscopic methods. As already observed for the tweezer **26** and the clip **27**, the ESI HR-MS has proven to be a successful method of characterization. Clip **28** especially shows a very clear ESI HR-MS in both the negative and the positive ionization modes, the peak with one sodium is easily detectable at m/z = 609.2264 (calculated for $[C_{38}H_{34}NaO_6]^+$ = 609.2253). The ^{1}H NMR assignment of the clip **28** is shown in Figure 2.25.

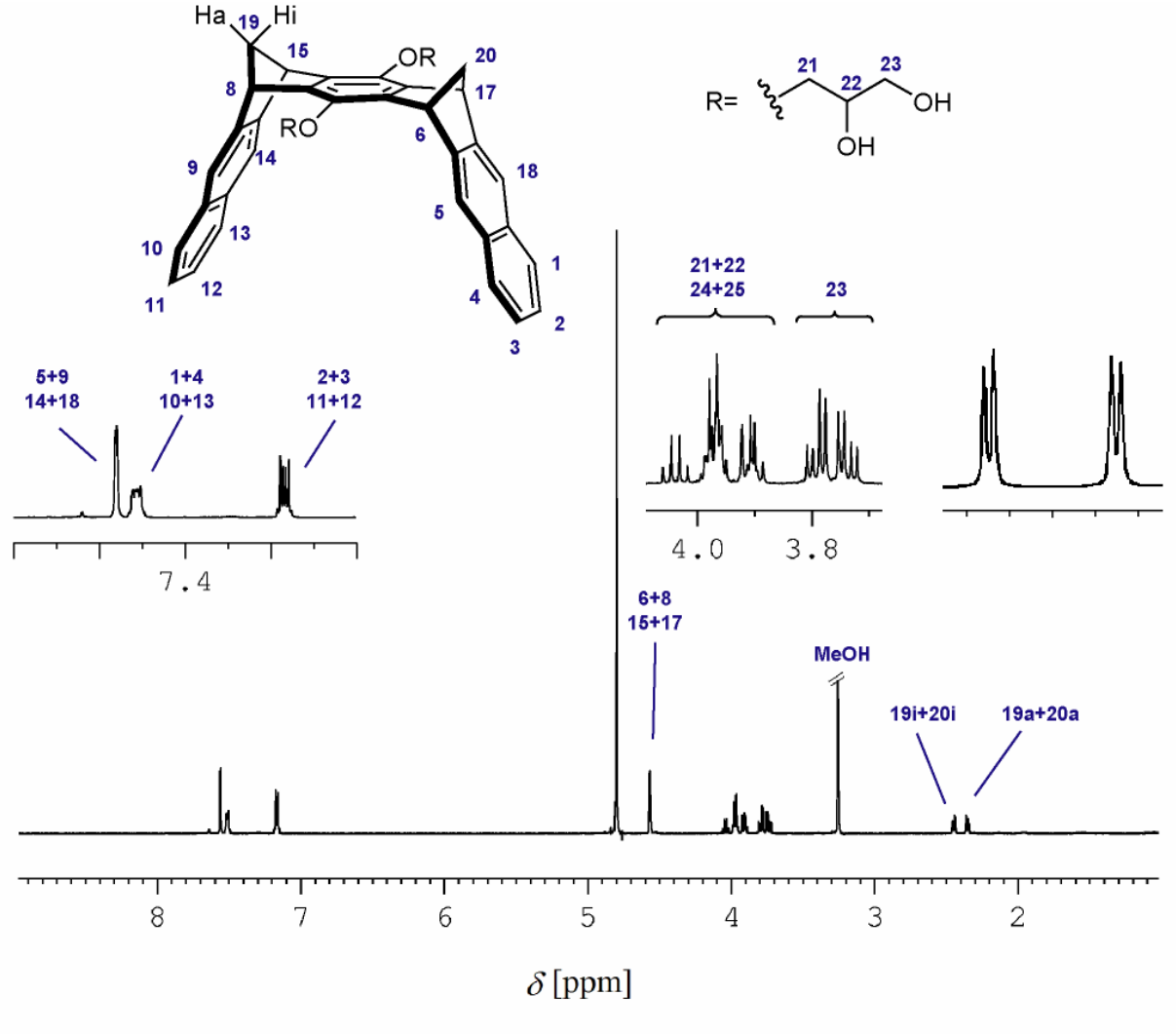

Figure 2.25: Assignment of the ^{1}H NMR spectrum of **28** (500 MHz, methanol-d_4).

2.2.3.3 Solubility of the clips 28, 98 and 99

The main problem of the clips and tweezers prepared so far, in reference to the topic of this work, is their solubility in water and other protic and aprotic solvents. Thus, the property of polyglycerol clips **98**, **99** and **28** studied first was their qualitative solubility in different solvents, which are shown in Table 2.11. Few milligrams of clips **98** or **99** are completely soluble in 0.6 mL of water, producing a clear solution. Accordingly, clip **28** seems to be insoluble in water, comparable to the G_1-TEG substituted clip **27**. All four clips, **27**, **28**, **98** and **99** are well soluble in methanol but only **27** in chloroform.

Clip	H_2O	MeOH	$CHCl_3$
98	✓	✓	-
99	✓	✓	-
28	-	✓	-
27	-	✓	✓

Table 2.11: Qualitative solubility chart of the different polyglycerol clips and the triethyleneglycol clip **27**.

In order to find out if clip **28** is at least a little soluble in water and quantify this solubility, we carried out the same UV-vis experiment as we did previously for the clip **27** (refer to chapter 4.4.2 (page 192) for the complete experimental details of the UV-vis method). Table 2.12 shows the amount of **28** used for this test as well as the resulting solubility and its comparison with that obtained for the G_1-TEG substituted clip **27**.

Clip	Solvent	mg of clip	mL of Solvent	Solubility [mg/mL]	Solubility [mmol/mL]
28	H_2O	2.12	0.80	$6.16 \cdot 10^{-3}$	$1.05 \cdot 10^{-5}$
27	H_2O	4.73	1.60	$6.62 \cdot 10^{-3}$	$5.11 \cdot 10^{-6}$

Table 2.12: UV-vis solubility experiments for the clips **28** and **27** in water.

From the data in Table 2.11 and Table 2.12 the conclusion that can be drawn is that the introduction of a large amount of hydroxyl groups in the dendrimer substituents (clips **98** and **99**) is an important factor for the solubility of the molecular clips in water whereas a smaller amount of hydroxyl groups (clip **28**) is insufficient to accomplish solubility in this solvent. We assume that the hypothetical clip **94**, substituted by two G_2-TEG dendrimer units, would be water-soluble due to the larger amount of oxygen atoms. Unfortunately, the experimental verification of this assumption has not been possible up to now.

In conclusion, the water solubility of naphthalene molecular clips cannot be achieved by means of first generation triethyleneglycol dendrimers. Evidently the hydrophilic interactions between the eight ether oxygen atoms in the case of **27**, or the four hydroxyl groups in the case of **28**, and the solvent is not yet enough to compensate the high hydrophobic nature of two naphthalene and three benzene rings. The introduction of numerous ether and hydroxyl groups by means of the polyglycerol dendrimers (**98** and **99**) results the achievement of the water solubility, however the number of ether and hydroxyl groups must be large enough in order to compensate the mentioned hydrophobicity of the molecule. This observation is in good agreement with the results shown in Table 2.3 (page 34) where the solubility of organic compounds is related to the C/O ratio. In this table it is shown

that compounds with a C/O ratio < 4 are, usually, soluble in water whereas the larger this ratio becomes, the less soluble the compound is in water. The clip **28** (first generation polyglycerol clip, $C_{38}H_{34}O_6$) has a C/O ratio = 6.66 whereas the clip **98** (approximately fourth generation polyglycerol clip, $C_{122}H_{202}O_{62}$) has a C/O ratio = 1.96. Hence while the receptor **28** belongs clearly to the *non water-soluble* group of compounds, the receptor **98** fits perfectly to the *water-soluble* group of compounds.

2.3 Synthesis of molecular clips substituted by sulphate groups

Phosphonate and phosphate disubstituted clips and tweezers of type **17** and **18e-h** have been synthesized previously.[89, 128, 129] These compounds are water soluble and show promising receptor properties in aqueous solution. With the aim to further study the effect of the substituents on the properties of the clips, molecular clips substituted by sulphate groups shall be synthesized.

Again 1,4-hydroquinone **92** was used as a model molecule to test the sulphonation reaction of phenolic OH groups. The procedures found in literature[130, 131] were adapted to our particular system; hydroquinone **92** reacted with sulphur trioxide-pyridine complex **107** (4 equivalents) in pyridine for 18 hours at 50 ºC followed by the quenching of the reaction solution by an aqueous solution of sodium hydrogen carbonate. Under these conditions the sodium disulphate benzene derivative **108** was isolated in 99 % yield (Scheme 2.25).

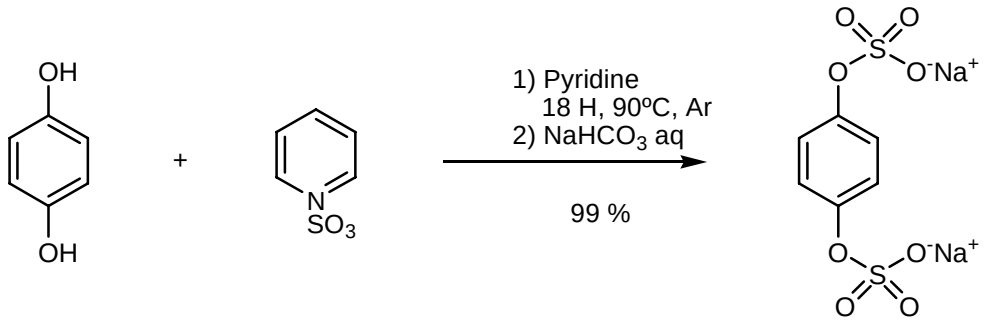

92 **107** **108**

Scheme 2.25: General sulphonation reaction and its conditions.

Analogous conditions applied to clip **18c** led to a mixture of mono and disubstituted sulphate clips which are both water-soluble. Therefore, the sulphonation reaction had to be optimized in order to obtain the desired sulphate clip **36** as a pure and single product. The reaction scheme and tested conditions are shown in the Table 2.13.

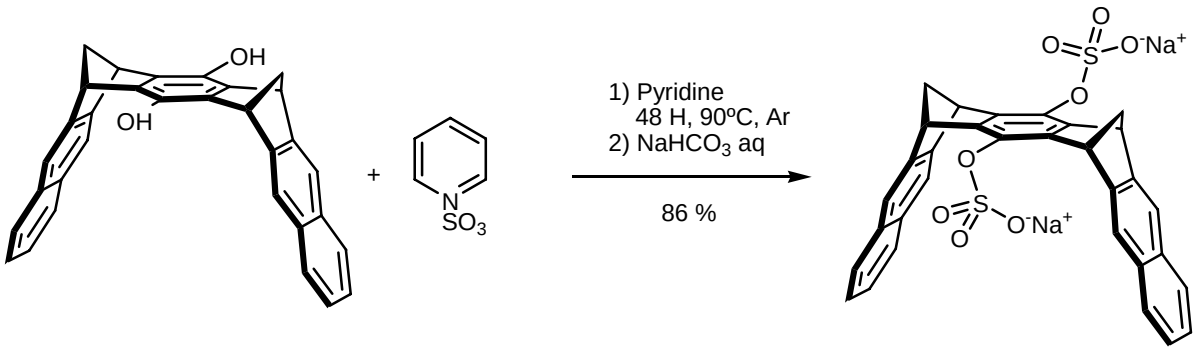

18c **107** **36**

Entry[a]	Equivalents of 107	Reaction time [h]	Temperature [ºC]	Results[b]
1	4	18	50	Starting materials
2	4	18	90	Mixture of mono-and-disubstituted sulphate clips
3	4	24	90	Mixture of mono-and-disubstituted sulphate clips
4	4+3	48	90	Disubstituted sulphate clip in 86 % yield

[a] All reactions were carried out in pyridine as solvent/base and under argon atmosphere.

[b] The identification of products was carried out by ESI-TOF mass spectrometry with negative ionization.

Table 2.13: Conditions of sulphonation reaction carried out with the clip **18c**.

Under the reaction conditions described in entry 2 and 3 of Table 2.13 only mixtures of mono and disubstituted sulphate clips are formed. The reaction described on entry 4 was again monitored by means of ESI-TOF mass spectrometry. After 24 hours of reaction of 4 equivalents of **107** with clip **18c**, monosubstituted sulphate clip was still present in the reaction mixture so that 3 additional equivalents of **107** were added to the mixture allowing 24 additional hours of reaction time. Clip **36** was obtained as the only product in 86 % yield. Further assays under these reactions conditions led to similar results showing no traces of the monosubstituted sulphate clip.

By the use of lithium carbonate instead of sodium hydrogen carbonate for the quenching of the reaction mixture, the lithium sulphate clip **37** was obtained in 91 % yield, similar to that of **36**. Furthermore, the use of the dihydroxy anthracene clip **20c** as starting material led to the corresponding sodium sulphate anthracene clip **38** in 96 % yield.

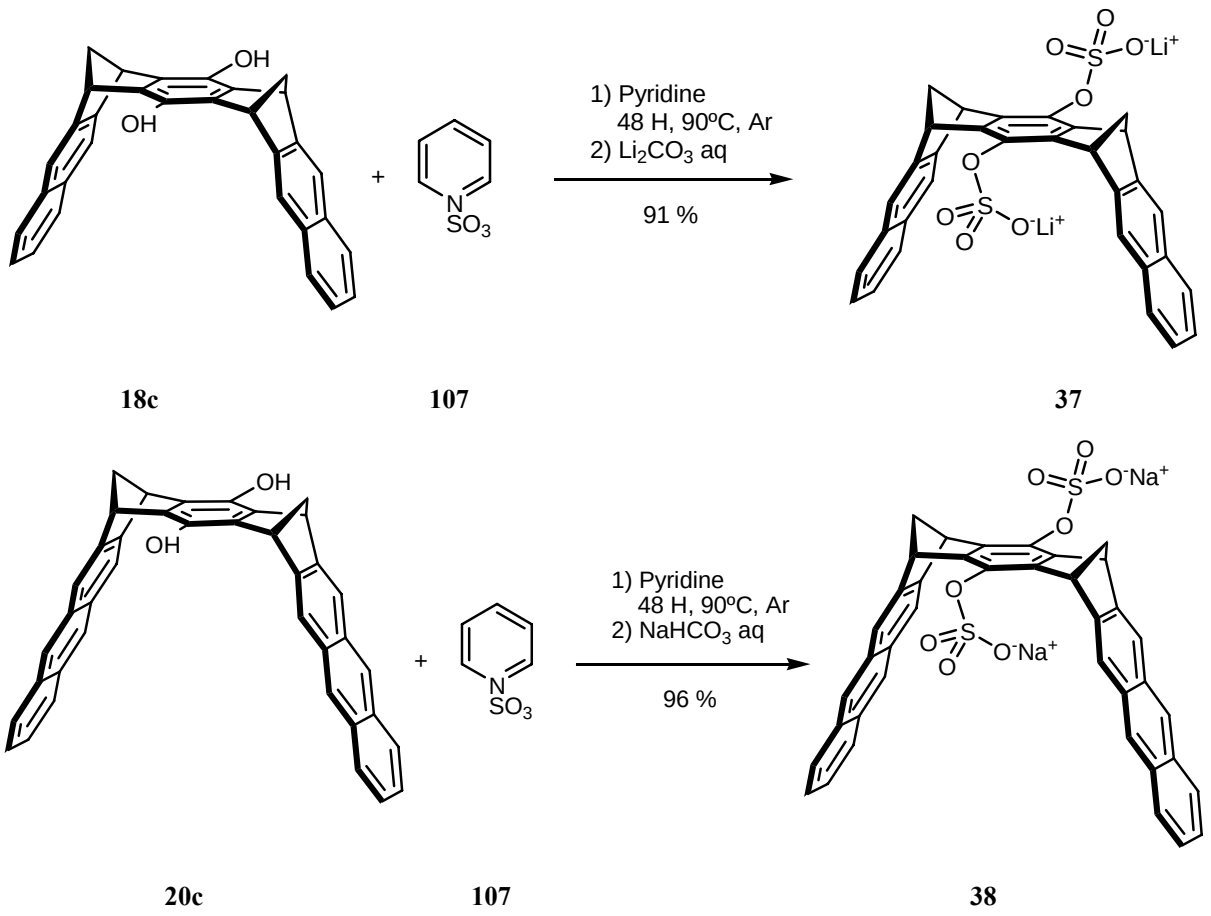

Scheme 2.26: General sulphonation reaction and its conditions.

ESI-TOF mass spectrometry characterization of the sulphate substituted clips was of special interest. Since the sulphate substituted clips are negatively charged, the negative ionization was particularly helpful giving, in all the cases, clear molecular peaks for both mono and dianionic forms. Since the sulphate groups have little effect on the NMR spectra, the ^{1}H NMR spectra of the sulphate clips are similar to those of the analogous phosphonate and phosphate clips, **18g** and **18h** respectively. The complete assignments of **36** and **38** in methanol-d_4 are shown in Figure 2.26 and Figure 2.27 respectively.

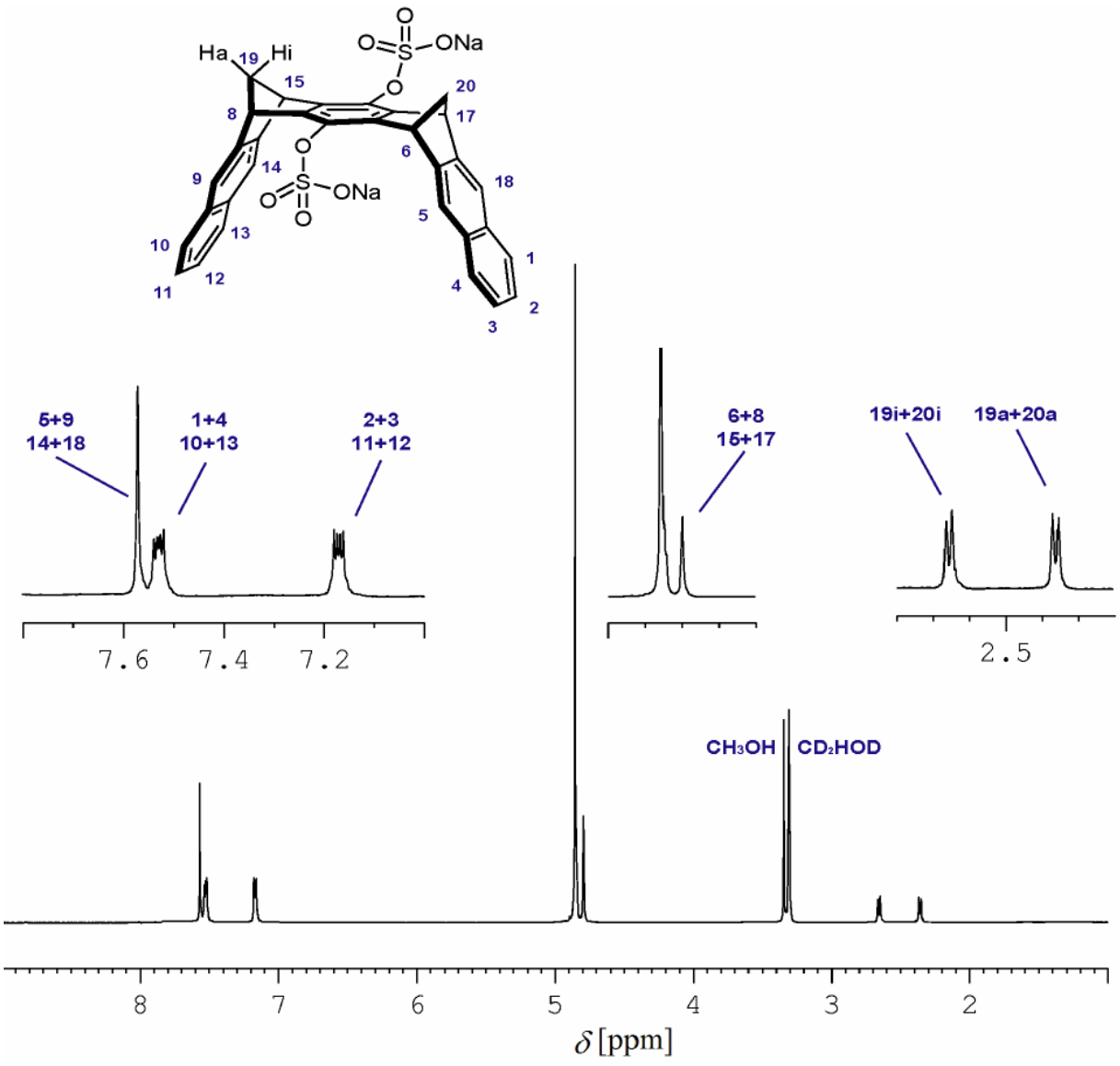

Figure 2.26: ^{1}H NMR spectrum and assignment of the naphthalene sulphate substituted clip **36** (500 MHz, methanol-d_4.).

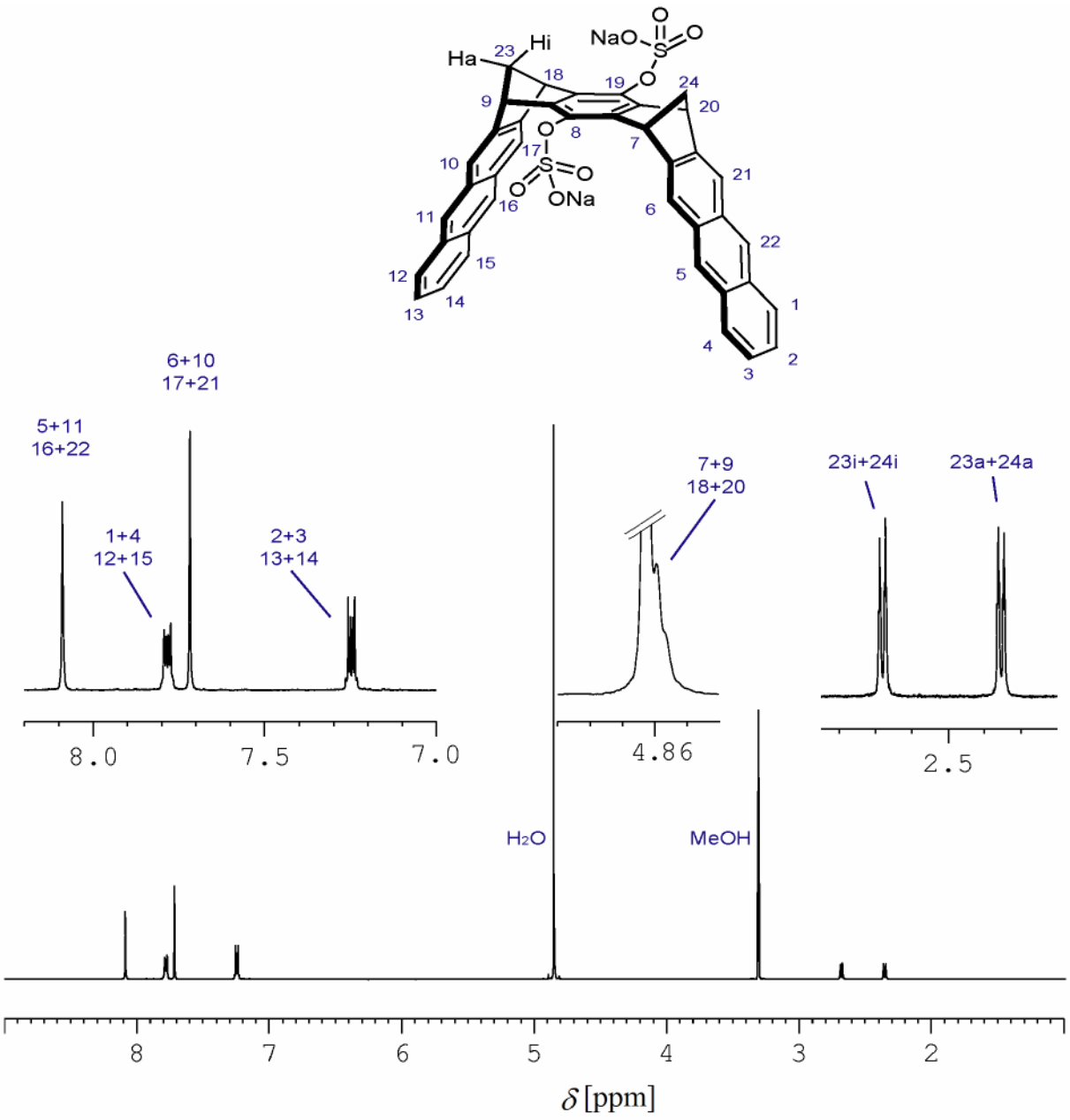

Figure 2.27: ^{1}H NMR spectrum and assignment of the anthracene sulphate substituted clip **38** (500 MHz, methanol-d_4.).

2.4 Host-guest complex formation with clip G_1-TEG substituted clip 27

For the evaluation of the receptor properties of the molecular clip **27**, the association constants with the guests shown in Figure 2.28 (both neutral and cationic aromatic molecules) were investigated by means of ^{1}H NMR titrations. The guest molecules chosen for the evaluation of supramolecular properties are, due to their substitution by electron-withdrawing substituents or a positive charge inside the aromatic ring, electron-withdrawing and therefore show a complementary electrostatic potential surface (EPS)[36, 77] to that of the clip **27**. All the titration experiments data are described in detail in chapter 4.5.

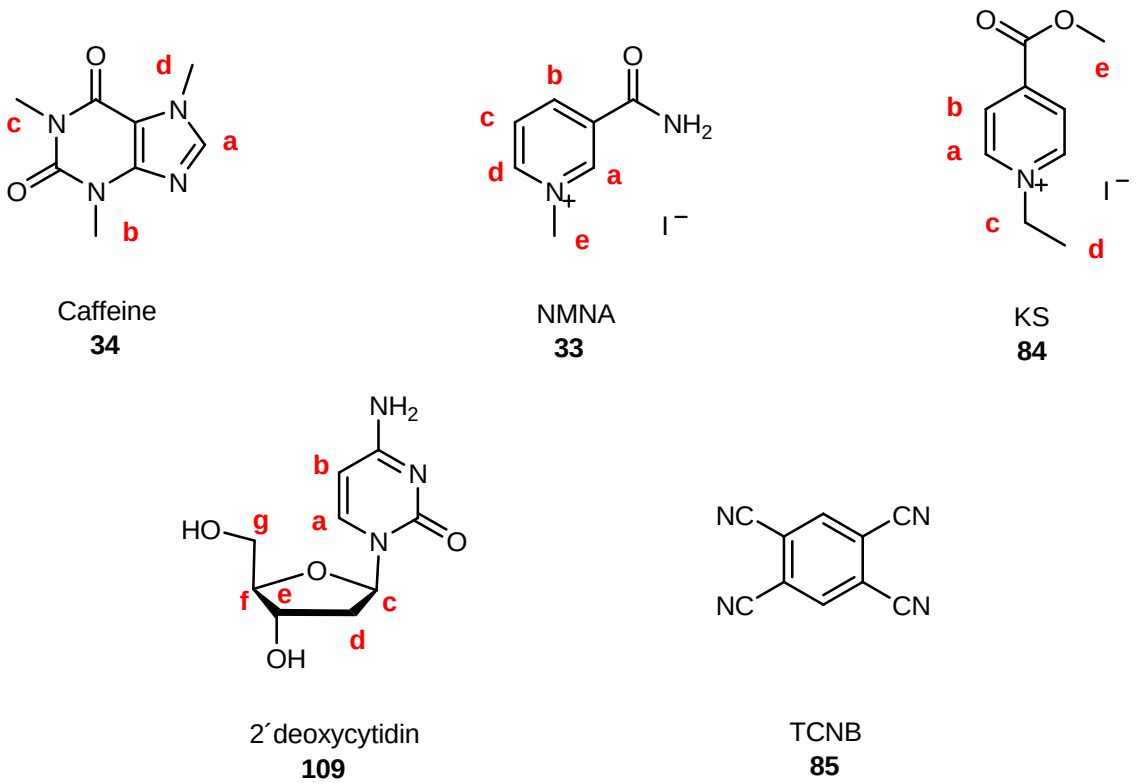

Figure 2.28: Structures of the guest molecules used for the study of supramolecular properties of the naphthalene clip **27** in methanol. Kosower salt **84** was examined in both methanol and chloroform as solvents whereas the tetracyanobenzene **85** was tested only in chloroform.

The values of association constant, K_a, maximum induced chemical shift, $\Delta\delta_{max}$, and Gibbs energy, ΔG, obtained for all guest molecules shown in Figure 2.28 in methanol-d_4 and chloroform-*d* are summarized in Table 2.14.

Guest	Solvent	K_a [M^{-1}]	ΔG [kcal·mol^{-1}]	$\Delta\delta_{max}$ [ppm]
caffeine **34**	CD_3OD	415 ± 45	-3.57	0.22 (H_a)
NMNA **33**	CD_3OD	65 ± 7	-2.47	2.50 (H_a) 2.75 (H_b) 3.12 (H_c) 2.04 (H_d) 2.93 (H_e)
2´deoxycytidin **109**	CD_3OD	n.a.o.	-	-
Kosower salt **84**	CD_3OD	235 ± 25	-3.23	1.50 (H_a) 1.28 (H_b) 0.87 (H_c) 0.60 (H_d)
Kosower salt **84**	$CDCl_3$	135 ± 15	-2.91	2.33 (H_a) 1.96 (H_b) 0.82 (H_e)
Tetracyanobenzene **85**	$CDCl_3$	315 ± 35	-3.41	3.61

n.a.o.= no association observed

Table 2.14: Association constants, K_a [M^{-1}], Gibbs energy, ΔG [kcal·mol^{-1}], and maximum induced chemical shifts of the guest protons, $\Delta\delta_{max}$ [ppm], of the host-guest complexes of **27** in methanol-d_4 and chloroform-*d* at 25 ºC.

2.4.1 Special structural features of 27

An extraordinary property of the clip **27** must be taken into account in order to comprehend its binding properties. The structure of any clip in solution is not rigid, but dynamic. The carbonyl groups attached to the central spacer unit are in continuous rotation along the C_{arom}-O bond and, consequently, there are three main possible conformers: *syn, syn*, *syn, anti* and *anti, anti* (Table 2.15). By means of conformational search (Monte-Carlo simulation, AMBER*), it is found that the relative position of the carbonyl groups (*syn, syn*; *syn, anti* and/or *anti, anti*) of the substituents at the central spacer unit is dependent on the solvent. In aprotic solvents, such as chloroform, the difference of energy between *syn, syn* and *anti, anti* is calculated to be 0.5 kcal·mol^{-1} whereas in protic solvents such as *n*-octanol this gap is 34.5 kcal·mol^{-1}. Table 2.15 shows the values of the conformational analysis for the clip **27** in different solvents.

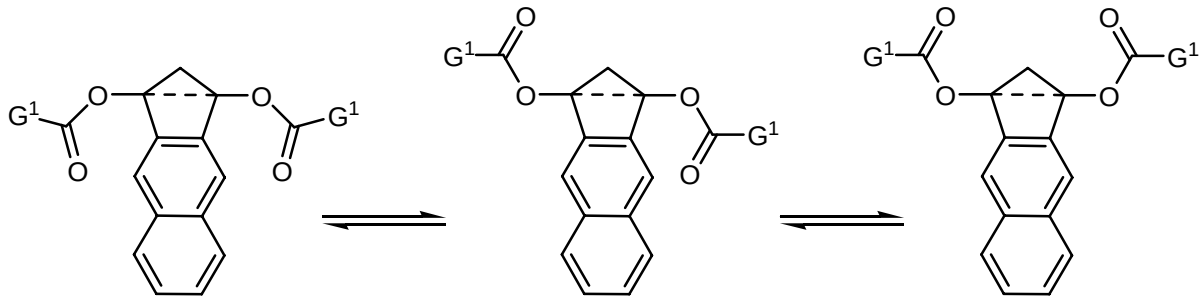

syn, syn *syn, anti* *anti, anti*

	ΔE_{rel} (AMBER*) [kcal·mol^{-1}]		
Solvent	***syn, syn***	***syn, anti***	***anti, anti***
Chloroform	3.5	0.0[a]	4.0[b]
n-Octanol	0.0[a, b]	14.4[b]	34.5
Gas phase	6.4[b]	0.0[a, b]	21.8

[a] The values of ΔE_{rel}= 0.0 indicate the structure of minimum energy resulting from the conformational search.

[b] The conformer shows a TEG branch included in the cavity of the clip.

Table 2.15: Relative energy of the different conformers of the clip **27** in different solvents obtained by conformational search (Monte-Carlo simulation, AMBER*, 5000 structures to search).

The TEG branches on clip **27** are very long and flexible and therefore they can create steric interactions with guest molecules. Additionally, these TEG branches are long enough to accommodate themselves inside the cavity of the clip creating a sort of self-inhibition. Evidently, due to this self-inclusion process, the guest binding mechanism of **27** is slightly more complicated than that of the receptors with small substituents at the central spacer unit. During the complexation process of a guest molecule by a receptor with small substituents at the central spacer unit the inclusion of the guest molecule into the cavity of the receptor will occur without any intermediate step. However, for clip **27** the guest molecule can only enter into the cavity if the clip adopts a favourable conformation, with the TEG branches outside the cavity. The self-inclusion process of the TEG branches inside the clip cavity is found to be also solvent-dependent. The energy of this process in different solvents can be also quantified by means of Monte-Carlo conformational search and are shown in the Table 2.16. It turns out to be a favourable process in both *n*-octanol and gas phase while it is a faintly unfavourable process in chloroform, where the TEG branches are preferentially located outside the cavity of the clip.

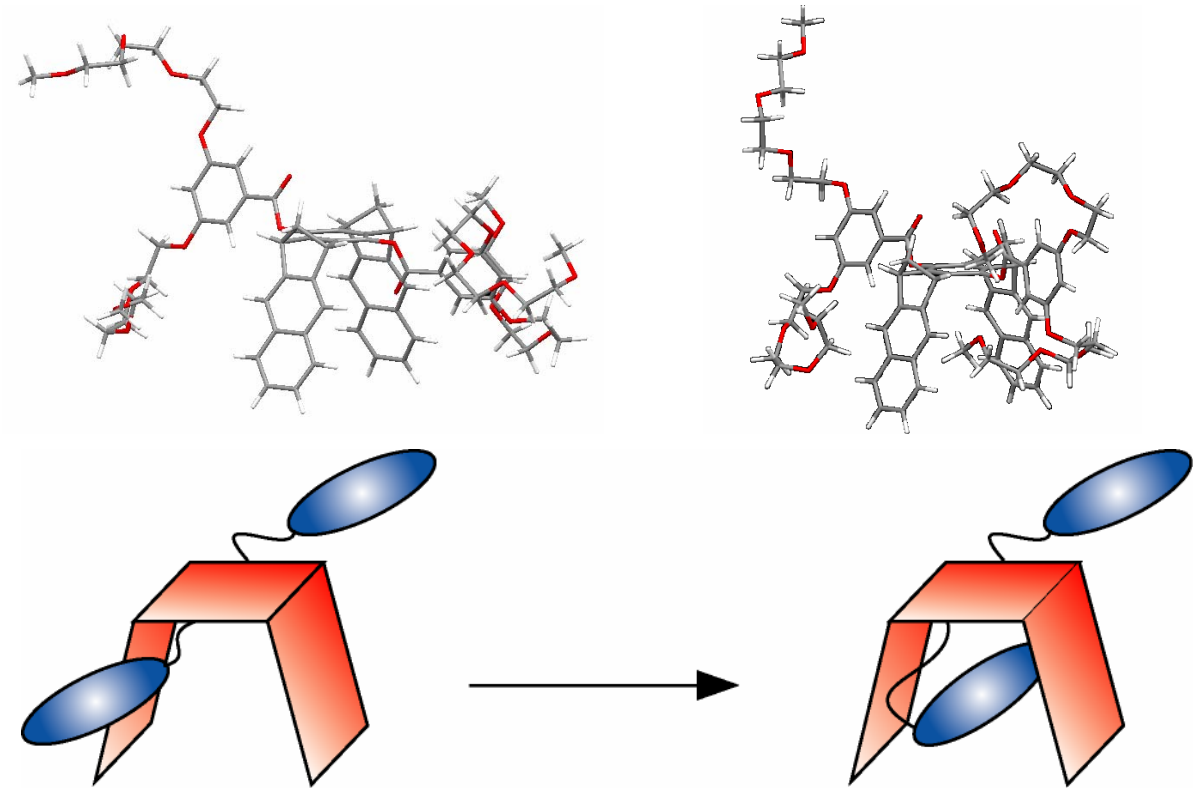

Solvent	$\Delta E = E_{in} - E_{out}$ [kcal·mol^{-1}]
$CHCl_3$	+ 6.2
n-Octanol	- 0.6
Gas phase	+ 8.6

Table 2.16: Relative energy (Monte-Carlo conformational search, AMBER*, 5000 structures to search) of the process of self-inclusion of the TEG branches inside the cavity of the clip **27**. The calculated structures on the top correspond to the calculation in chloroform.

2.4.2 Comparison of the thermodynamic data of the complexes of 27 with those of other receptors

The association constant of complex **KS@27** could be determined in $CDCl_3$ as well as in CD_3OD. It turned out to be larger in CD_3OD (K_a= 235 M^{-1}) than in $CDCl_3$ (K_a= 135 M^{-1}) (Table 2.14). This finding indicates a stabilization of this host-guest complex in CD_3OD by a solvophobic effect. Evidently the π-cation interaction is in CD_3OD as strong as in$CDCl_3$ in agreement with the calculations performed by Dougherty and Gallivan.[12]

The receptor properties of the clip **27** in an aprotic solvent, such as chloroform-*d*, are comparable to those of the diacetoxy clip **18b** (Table 2.17). The similar association constants found for both clips refer to a comparable conformation of the clip molecules. As discussed

before, the TEG self-inclusion process of clip **27** plays only a minor role in chloroform. In consideration of clip **18b**, the small acetoxy substituents are not able to perform self-inclusion in their cavity. Therefore in both cases a similar, not hindered cavity leads to similar values of association constants.

Guest	Clip 27		Clip 18b	
	K_a [M^{-1}]	$\Delta\delta_{max}$ [ppm]	K_a [M^{-1}]	$\Delta\delta_{max}$ [ppm]
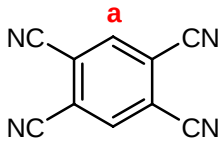 TCNB **85**	315	3.61	230	3.40
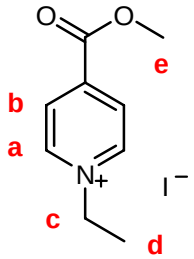 Kosower salt **84**	135	2.33 (H_a) 1.96 (H_b) 0.87 (H_c)	140	2.40 (H_a) 1.82 (H_b) 1.59 (H_c)

Table 2.17: Comparison between the association constants of the TEG-dendrimer substituted clip **27**, and the diacetoxy clip **18b** in $CDCl_3$ at 25 ºC.

Table 2.18 shows the comparison of association constants, K_a, for the guests shown in Figure 2.28 with the dendrimer substituted clip **27**, the tetralithium phosphate clip **18h** and the dilithium phosphonate clip **18g**. At first sight it is obvious that the receptor **27** features much weaker binding properties with both neutral and cationic guest molecules due to the fact that both **18h** and **18g** are able to stabilize the complexes by electrostatic interactions while **27** cannot. For instance the association constant of the complex **NMNA@18h** in methanol-d_4 (K_a= 34000 M^{-1}) is 523 times larger than the association constant for the complex **NMNA@27** (K_a= 65 M^{-1}), which is in the threshold of no-association. The difference is not so dramatically large for the complex with phosphonate clip, **NMNA@18g** (K_a= 1660 M^{-1}), which is only 25 times larger than the one for the complex **NMNA@27**. From these results it becomes evident that the electrostatic interactions between a negatively charged host (**18h** and **18g**) and a positively charged guest play a significant role in the stabilization of the corresponding complex. An analogous situation is observed for the complexes with Kosower salt, **84**. The association constant for the complex with tetralithium phosphate clip **KS@18h**

(K_a= 19000 M^{-1}) is 81 times larger than that for the complex **KS@27** (K_a= 235 M^{-1}), whereas for the complex **KS@18g** it is only 14 times larger.

With neutral guest molecules such as caffeine, **34**, and 2'-deoxycytidin, **109**, the same tendency is observed. The association constants for the clips **18h** and **18g** with caffeine are much larger than that of the clip **27**. This observation manifests that the negatively charged substituents of the phosphate and phosphonate clips, **18h** and **18g** respectively, not only stabilize the interaction with cationic guest molecules but also stabilize the complexes with neutral, electron-deficient, aromatic guests.

The complexes of **18h** and **18g** show, generally, much larger association constants in water solution than the corresponding complexes of **27** in methanol. This finding allows us to conclude that with water as a solvent, the complex is highly stabilized due to hydrophobic effect and, consequently, the thermodynamic parameters (K_a and ΔG) of the complexes are much higher than those in methanol solution confirming the importance of the solvent on binding assays.[129]

Guest	Clip 27 K_a [a] [M^{-1}]	Clip 18h K_a [129] [M^{-1}]	Clip 18g K_a [81, 90, 115] [M^{-1}]
Caffeine **34**	415	42700 [b]	9550 [b]
NMNA **33**	65	29400 [b] 34000 [a]	1660 [a]
Kosower salt **84**	235	19000 [b]	4800 [c] 3200 [a]
2′-deoxycytidin **109**	n.a.o.	2600 [b]	3000 [b]

[a] Measured at 25 ºC in methanol-d_4

[b] Measured at 25 ºC in D_2O-Buffer (pH= 7.2)[132]

[c] Measured at 25 ºC in pure D_2O

n.a.o.= no association observed.

Table 2.18: Comparison of the association constants between the TEG-dendrimer substituted clip **27** and the tetralithium phosphate clip (**18h**), the dilithium phosphonate clip (**18g**) in protic solvents such as methanol-d_4 and water (both pure and buffer).

2.4.3 Structures of the complexes of 27

While the association constant is an indicator for the complex stability, the maximum complexation induced ^{1}H NMR shifts, $\Delta\delta_{max}$, of the guest protons provide insight into the complex geometry. For instance those protons positioned outside the receptor cavity usually show lower $\Delta\delta_{max}$ values due to the fact that they are less affected by the magnetic anisotropy of the arene system of the clip.

2.4.3.1 Comparison of $\Delta\delta_{max}$ values of the G_1-TEG clip 27 and the diacetoxy clip 18b

In order to find out the effect of the TEG branches on the structure of the complexes of **27** we considered appropriate the comparison of $\Delta\delta_{max}$ values of the complexes of **27** and those of the complexes of diacetoxy clip **18b** (Table 2.19) since the latter has also ester functions as substituents at the central benzene spacer unit.

KS and TCNB show similar values of $\Delta\delta_{max}$ in chloroform with both G_1-TEG substituted clip **27** and diacetoxy clip **18b** as receptors, which could be an indication that the guest molecules are not significantly different positioned inside the cavity of both clips.

Guest	G_1-TEG clip 27 $\Delta\delta_{max}$ [ppm]	Diacetoxy clip 18b $\Delta\delta_{max}$ [ppm]
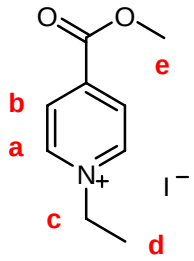 Kosower salt **84**	2.33 (H_a) 1.96 (H_b) 0.87 (H_c)	2.40 (H_a) 1.82 (H_b) 1.59 (H_c)
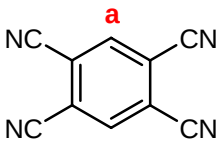 Tetracyanobenzene **85**	3.61	3.40

Table 2.19: Comparison of $\Delta\delta_{max}$ values (ppm) of the complexes with Kosower salt **84** and tetracyanobenzene **85** between the G_1-TEG substituted clip **27** and the diacetoxy clip **18b** in $CDCl_3$ at 25 ºC.

It has been proven that the single-crystal structures obtained from the clips complexes are usually in good agreement with the corresponding calculated structures obtained from the conformational search (Monte Carlo simulation, AMBER*). For instance, the crystal structures of the complexes **KS@18b**[77, 78] and the **TCNB@18c** (both obtained from chloroform) are concordant with the corresponding calculated structures of the complexes (Figure 2.29)**.**

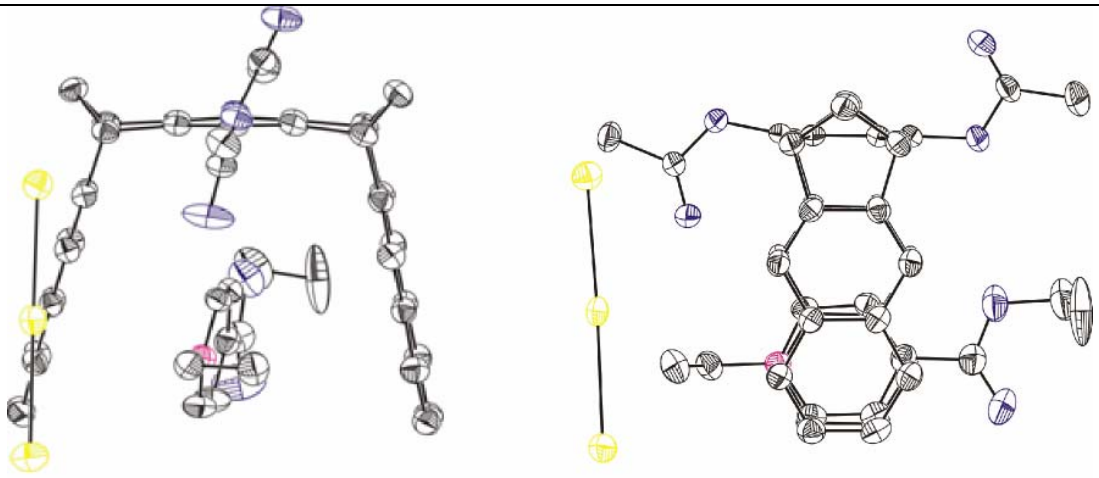

KS@18b, single-crystal structure

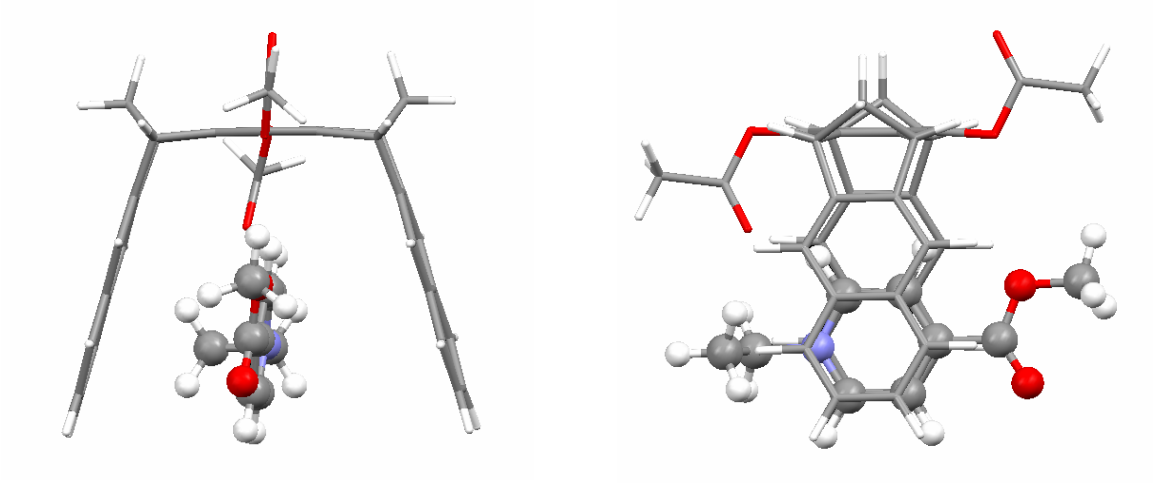

KS@18b, calculated structure

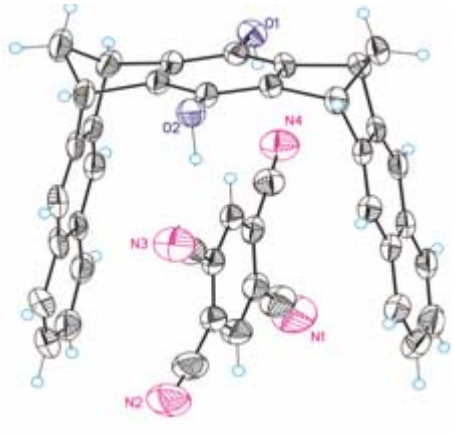

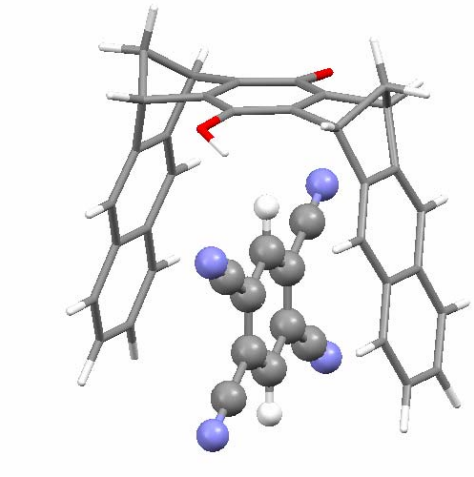

TCNB@18c, single-crystal structure

TCNB@18c, calculated structure

Figure 2.29: Single-crystal structure of the complex **KS@18b** (up) and **TCNB@18c** (down left)[77, 78] and the corresponding calculated structures (Monte Carlo simulation, AMBER*, 5000 structures to search) (middle and down right).

Thus, since no single-crystal structure of the host-guest complexes of clip **27** were obtained, most likely due to the oily nature of clip **27**, we considered it to be appropriate to correlate the experimental $\Delta\delta_{max}$ values with complex structures calculated by Monte Carlo conformer searches using the AMBER* force field in *n*-octanol, which is implemented in MacroModel 9.0.[133] MacroModel 9.0 features corrections of the force fields in order to simulate different environments around the molecules, such as chloroform, *n*-octanol, water and gas phase and thus have a better approximation to the molecular geometry. Since methanol is not included into the force field corrections, *n*-octanol was chosen instead, if methanol-d_4 was the solvent used in the titration experiment. Figure 2.30 shows the calculated structures, in *n*-octanol, of the host-guest complexes **34@27**, **NMNA@27** and **KS@27**. The structures are depicted in two different views - perpendicular to each other - for a better visualization

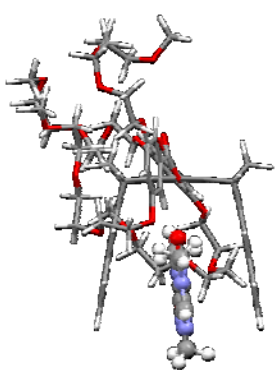

34@27, front view

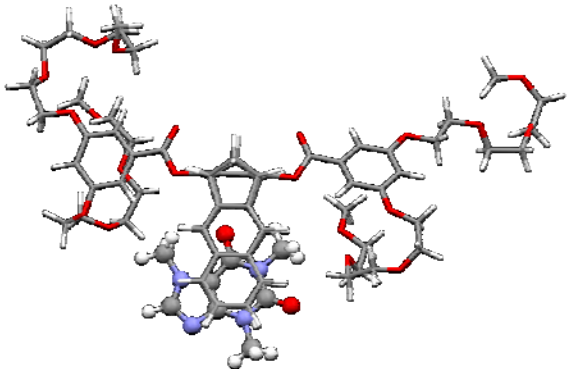

34@27, side view

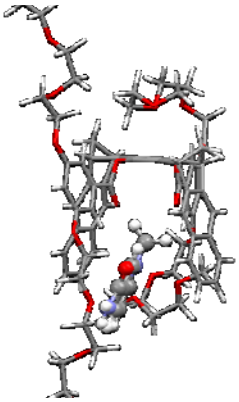

NMNA@27, front view

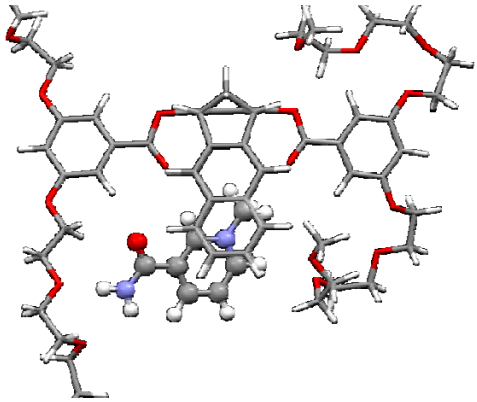

NMNA@27, side view

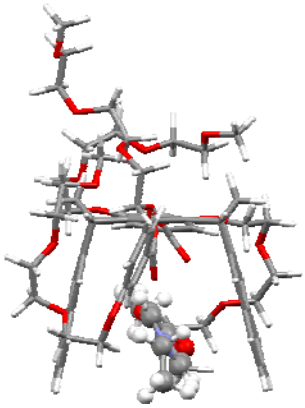

KS@27, front view

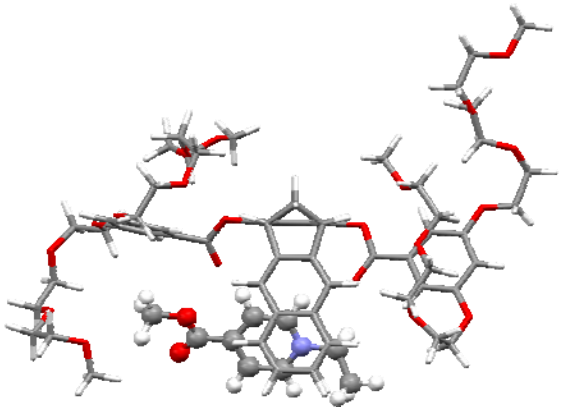

KS@27, side view

Figure 2.30: Calculated structures (MacroModel 9.0, Monte-Carlo simulation, AMBER*, *n*-octanol, 5000 structures) of the complexes **34@27**, **NMNA@27** and **KS@27**.

The proton H_a of the caffeine in the complex **34@27** in methanol-d_4 shows the lowest maximum complexation-induced chemical shift, $\Delta\delta_{max}$, in comparison with other complexes in methanol-d_4 (Table 2.14). This observation is in agreement with the calculated structure of the complex, where this proton is located completely outside the cavity of clip **27**, being only little affected by the magnetic anisotropy of the arene-units of it.

The protons H_b and H_c of the *N*-methylnicotinamide iodide, **33**, are outside the cavity in the calculated structure of the complex **NMNA@27** but they show large $\Delta\delta_{max}$ values (H_a= 2.50 ppm, H_b= 2.75 ppm, H_c= 3.12 ppm and H_d= 2.04 ppm) comparable to those determined for protons which are calculated to be positioned inside the receptor cavity (Table 2.14). These large values of $\Delta\delta_{max}$ determined for the protons H_b and H_c of **33** can be explained in the following way: the structures shown in Figure 2.30 are those of minimum energy calculated by a conformational search and do not reflect the large number of conformations which are possible. For each one of these possible conformations, the protons of the guest molecules are differently affected by the magnetic anisotropy of the arene-units of the clip. The values of $\Delta\delta_{max}$ obtained by ^{1}H NMR titration are, actually, average values of all the possible conformations. F. Koziol and C. Ochsenfeld corroborated this hypothesis by the study of the host-guest system consisting of the phosphonate substituted naphthalene clip **18g** and *N*-methylnicotinamide iodide **33** (host and guest respectively). ^{1}H NMR chemical shifts of the guest molecule were calculated by quantum chemical methods (HF/6-31G**) for two different conformations of the complex[81] (Figure 2.31).

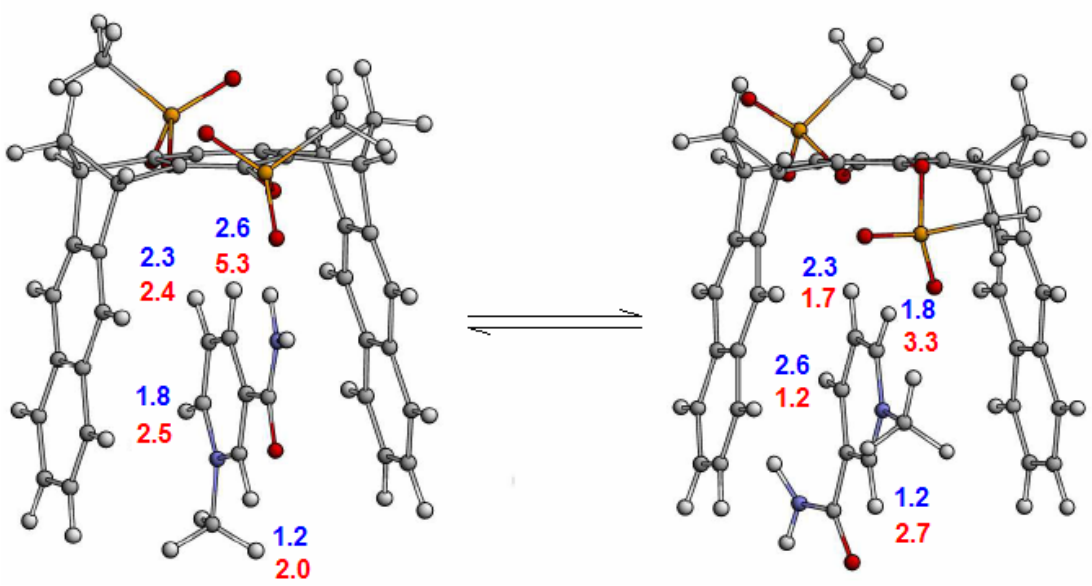

Figure 2.31: Comparison between the $\Delta\delta_{max}$ values obtained by quantum chemical calculations and ^{1}H NMR titrations experiments for two conformations of the complex **NMNA@18g**. The calculated complexation-induced chemical shifts are shown in blue whereas the experimental complexation-induced chemical shifts values are shown in blue.[81]

Figure 2.31 shows that the $\Delta\delta_{max}$ values calculated for a single conformer (either the one on the left-hand side or the one on the right-hand side in Figure 2.31) are not in agreement with the values determined by ^{1}H NMR titration. Only if a fast exchange between both conformers is assumed, so that an average of the values calculated for both structures has to be formed, the calculated and observed values are in good accord to each other.

In comparison to the x-ray structure and the calculated structure of complex **KS@18b**, the positively charged nitrogen atom of the pyridinium ring in complex **KS@27** is calculated

to be further pushed into the cavity of clip **27**. This structure is different to the experimental and calculated structure of the complex **KS@18b**. The shifted position between the positively charged nitrogen is probably caused by steric interactions of the guest molecule with the TEG branches of clip **27**.

The aromatic protons of the Kosower salt **84** show values of $\Delta\delta_{max}$= 1.50 ppm for H_a and $\Delta\delta_{max}$= 1.28 ppm for H_b. This finding is in good agreement with the calculated structure of the complex, in which proton H_a is completely positioned inside the cavity whereas proton H_b is slightly shifted outside. In the calculated structure of complex **KS@27** (Figure 2.30) the protons H_a and H_b attached to the pyridinium ring of **KS** –the protons pointing toward the central spacer unit and toward the tips of clip **27**- are no longer chemically equivalent. In the ^{1}H NMR spectrum of **KS@27** four signals for these protons are expected, but only two signals are observed. This finding is again good evidence for various dynamic processes occurring rapidly with respect to the so-called NMR time scale. One process is the mutual complex association-dissociation and the other one the rotation of the guest molecule inside the clip cavity. Both processes have already been observed by variable temperature ^{1}H NMR spectroscopy for host-guest complexes of the tetramethylene-bridged tweezers **14** and **15** and trimethylene-bridged clips **21** and **22**. According to force-field calculations, the topology of the dimethylene-bridged clips **18** is more open than that of **14**, **15**, **21** and **22**, so that smaller activation barriers are expected for these dynamic processes which require ^{1}H NMR measurements at very low temperature, T< 150 K, which are not accessible with the ordinary ^{1}H NMR spectrometer used in Essen.

Figure 2.32 shows the calculated structures for the complexes **TCNB@27** and **KS@27** in chloroform, which are in good agreement with the values of $\Delta\delta_{max}$ observed for the aromatic protons of the guest molecules in this solvent, as they are located between the sidewalls of the clip.

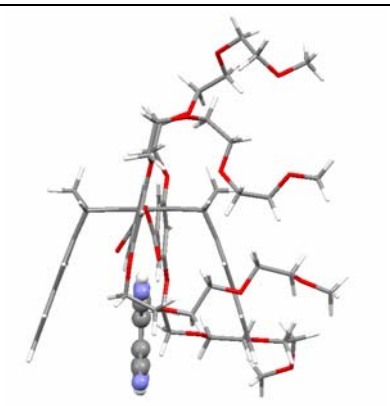

TCNB@27, front view

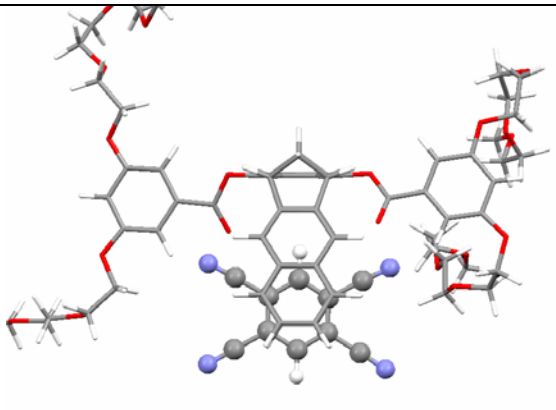

TCNB@27, side view

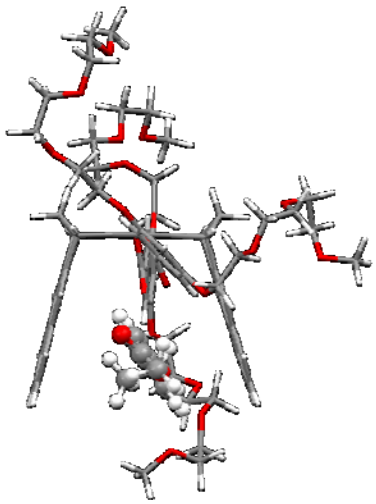

KS@27, front view

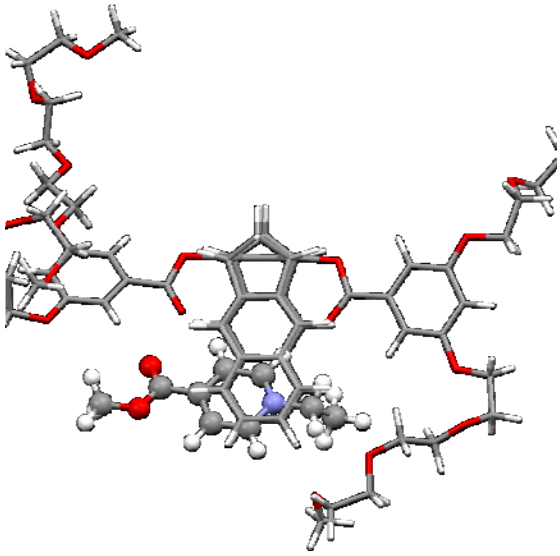

KS@27, side view

Figure 2.32: Calculated structures (MacroModel 9.0, Monte-Carlo simulation, AMBER*, $CHCl_3$, 5000 structures) of the complexes **TCNB@27** and **KS@27**.

2.4.4 Comparison of the structures of the complexes of 27 with those of the diacetoxy naphthalene clip 18b

As indicated before, the large TEG branches of the substituents of the clip **27** have certainly an effect on the structures of the supramolecular complexes. For instance the oxygens of those branches are hydrogen-bond acceptors and can interact with hydrogen-bond donors of guest molecules, such as the amide group of the *N*-methylnicotinamide iodide **33**

and therefore influence the guest orientation. In order to find out whether the TEG branches have a strong outcome on the supramolecule or not, we performed conformational searches for the complexes **NMNA@18b**, **KS@18b**, **TCNB@18b** and **34@18b** under the same conditions as those used for the complexes with clip **27** (Figure 2.33 and Figure 2.34).

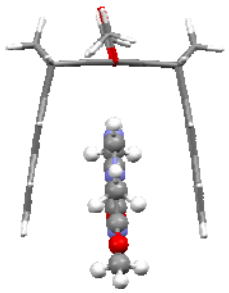

34@18b, front view

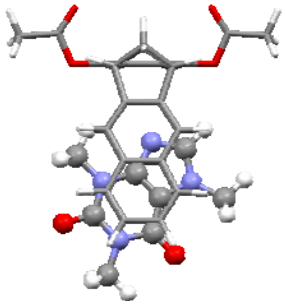

34@18b, side view

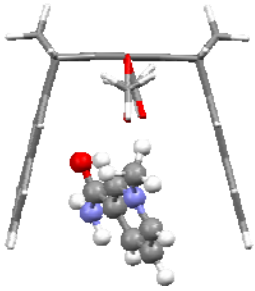

NMNA@18b, front view

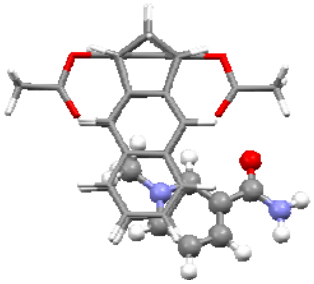

NMNA@18b, side view

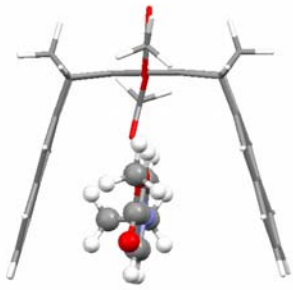

KS@18b, front view

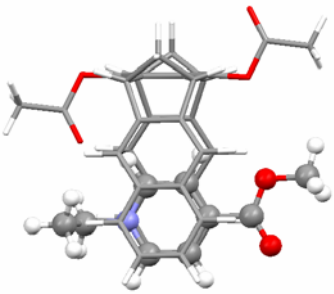

KS@18b, side view

Figure 2.33: Calculated structures (MacroModel 9.0, Monte-Carlo simulation, AMBER*, *n*-octanol, 5000 structures) of the complexes **34@18b**, **NMNA@18b** and **KS@18b**.

The calculated complex **34@18b** in *n*-octanol shows the caffeine with both rings inside the cavity of the receptor whereas in the complex **34@27** in *n*-octanol only the aromatic ring was located inside the cavity.

While the calculated structure of the complex **NMNA@27** in *n*-octanol (Figure 2.30) does not show any significant change in its geometry in comparison to the complex with the

diacetoxy clip **18b**, **NMNA@18b** (Figure 2.33), the calculated complex **KS@27** in *n*-octanol (Figure 2.30) shows a slight shift in the position of the pyridinium ring in comparison to the structure of the complex with the diacetoxy clip **KS@18b** in the same solvent (Figure 2.33), which is in good agreement with the single-crystal structure found for this complex (Figure 2.29).

The minimum-energy structures found for the complexes **TCNB@18b** and **KS@18b** in chloroform (Figure 2.34) appear to be quite similar to those found for the complexes with the G_1-TEG substituted clip **27** (**TCNB@18b** and **KS@18b**, Figure 2.32).

While all the other guest molecules consist of a single six-member aromatic ring, caffeine is a fused system of a five- and a six-member ring. During the complexation process of **27** and caffeine, a steric interaction takes place between the TEG branches of the receptor and the guest molecules. Consequently, the caffeine molecule can not be fully incorporated into the receptor cavity in the complex **34@27** as it occurs when the receptor is the diacetoxy clip **18b**. This steric interaction is accentuated by the presence of atoms with lone electron pairs in both the TEG branches (oxygen) and caffeine (oxygen and nitrogen). A similar phenomenon can be observed during the complexation process of Kosower salt and **27**. In this case the steric hindrance could be caused by the two relatively large substituents (in comparison to the clip cavity) at the pyridinium ring.

This finding allows us to conclude that while the TEG branches on clip **27** do not have an influence on the supramolecular structures of its complexes with relatively small guest molecules, they appear to have a certain effect on them when the size of the guest molecules is increased either by polycyclic systems (caffeine) or by their substituents (Kosower salt).

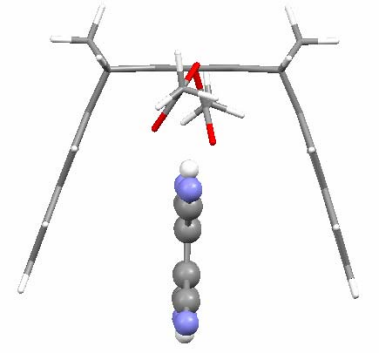

TCNB@18b, front view

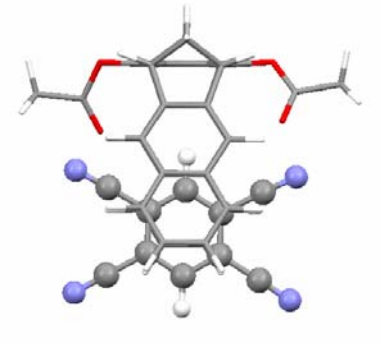

TCNB@18b, side view[a)]

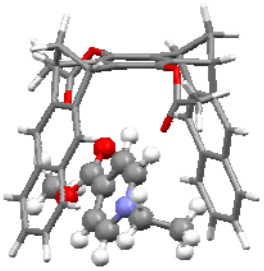

KS@18b, front view

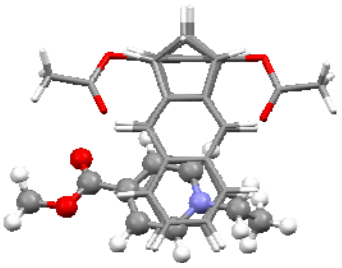

KS@18b, side view [a)]

Figure 2.34: Calculated structures of minimum energy (MacroModel 9.0, Monte-Carlo simulation, AMBER*, $CHCl_3$, 5000 structures) of the complexes **TCNB@18b** and **KS@18b**.

2.5 Host-guest complex formation with the hyperbranched polyglycerol substituted clips 98, 99 and 28

With the intention of comparing the binding properties of the polyglycerol clips **28**, **98** and **99**, we used the same guest molecules as we used for the clip **27** (Figure 2.35).

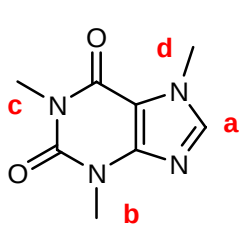

34

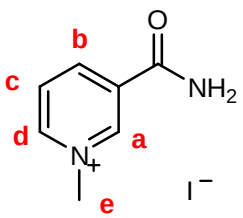

33

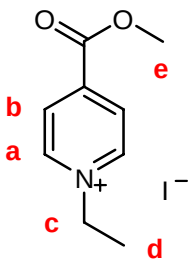

84

Figure 2.35: Guest molecules used for the study of complexation properties of the polyglycerol clips **28**, **98** and **99**.

The results of the ^{1}H NMR titration experiments of the guests pictured in Figure 2.35 and the clips **28**, **98** and **99** are shown in the Table 2.20, Table 2.21 and Table 2.22 respectively. While the binding properties of the clips **28** and **98** were measured in methanol-d_4 to facilitate the comparison with the association constants with the clip **27**, the properties of the clip **99** were studied in deuterated water.

Since the dimethoxy substituted clip **18d** only shows a small tendency to form host-guest complexes with TCNB **85** and Kosower salt **84** differently to the diacetoxy substituted clip **18b**, we expected the same tendency for polyglycerol substituted clips **28**, **98** and **99**. Evidently, the substitution of the central benzene spacer unit by –OCH-R groups hinders the host-guest complex formation contrary to –OCOR substituents leading to complex stabilization in most cases. So it was interesting to study the properties of the polyglycerol substituted clips **28**, **98** and **99** in order to find out the effect of the additional binding sites of the polyglycerol side chains on the host-guest complex stabilities.

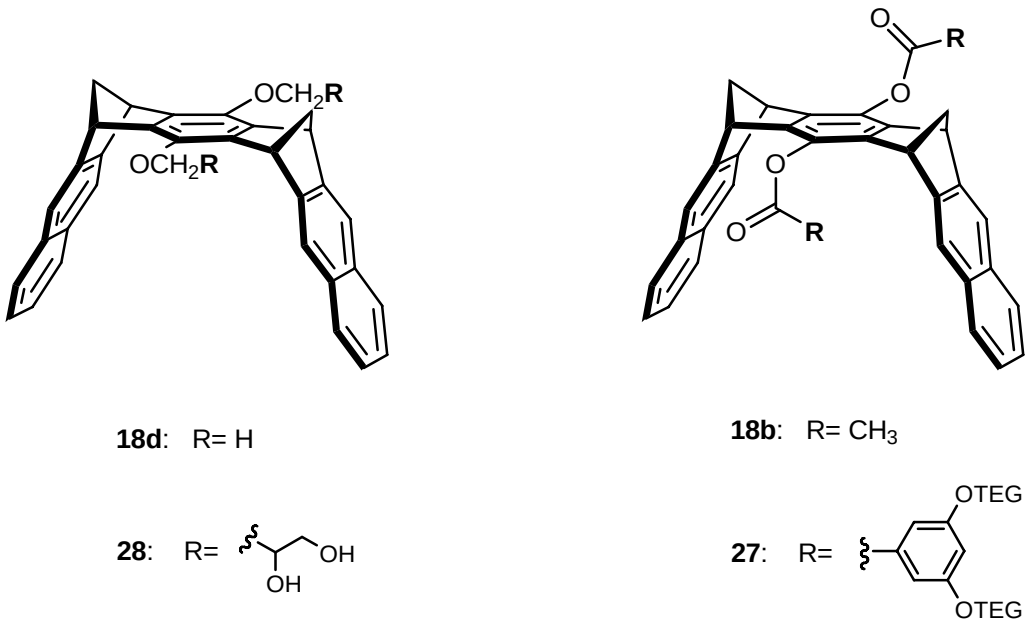

Figure 2.36: Structural similarities between **18d** and **28** and between **18b** and **27**.

Guest	K_a [M^{-1}]	ΔG [kcal·mol^{-1}]	$\Delta\delta_{max}$ [ppm]
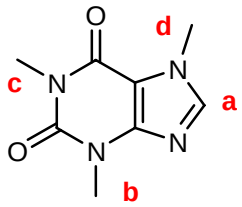 Caffeine **34**	41 ± 4	-2.20	1.60 (H_a) 0.64 (H_b) 0.53 (H_c) 1.14 (H_d)
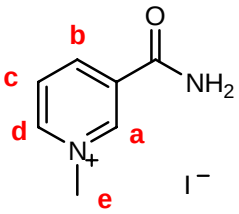 NMNA **33**	60 ± 6	-2.43	0.75 (H_a) 0.64 (H_b) 0.53 (H_c) 1.14 (H_d) 1.14 (H_e)
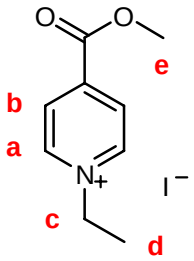 Kosower salt **84**	45 ± 5	-2.26	1.24 (H_a) 1.45 (H_b) 0.52 (H_c) 0.33 (H_d)

Table 2.20: Association constants, K_a [M^{-1}], Gibbs energy, ΔG [kcal·mol^{-1}], and maximum complexation-induced chemical shifts of the guest protons, $\Delta\delta_{max}$ [ppm], of the host-guest complexes of **28** in methanol-d_4 at 25 °C.

Guest	Solvent	K_a [M^{-1}]	ΔG [kcal·mol^{-1}]	$\Delta\delta_{max}$ [ppm]
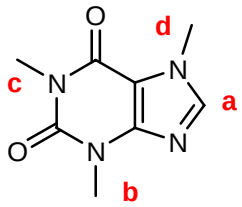 Caffeine **34**	CD_3OD	1035 ± 110	-4.110	2.02 (H_a)
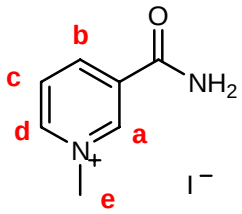 NMNA **33**	CD_3OD	230 ± 23	-3.22	0.36 (H_a) 0.68 (H_b) 0.65 (H_c) 0.30 (H_d)
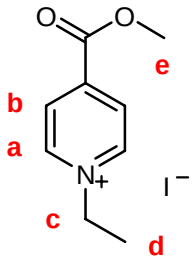 Kosower salt **84**	CD_3OD	85 ± 9	-2.63	0.90 (H_a) 0.91 (H_b)
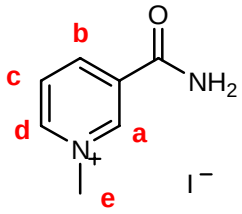 NMNA **33**	D_2O	210 ± 21	-3.17	0.23 (H_a) 0.33 (H_b) 0.47 (H_c) 0.40 (H_d)

Table 2.21: Association constants, K_a, Gibbs energy, ΔG [kcal·mol^{-1}], and maximum complexation-induced chemical shifts of the guest protons, $\Delta\delta_{max}$, of the host-guest complexes of **98** in methanol-d_4 and D_2O at 25 ºC.

Guest	K_a [M^{-1}]	ΔG [kcal·mol^{-1}]	$\Delta\delta_{max}$ [ppm]
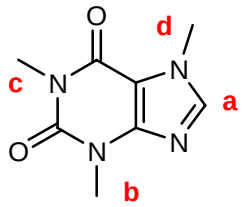 Caffeine **34**	175 ± 20	-3.10	2.33 (H_a) 0.80 (H_d)
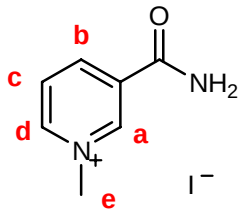 NMNA **33**	40 ± 4	-2.19	0.60 (H_a) 0.45 (H_b) 0.77 (H_c) 0.64 (H_d)
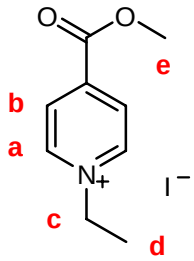 Kosower salt **84**	50 ± 5	-2.32	0.73 (H_a) 0.56 (H_b)

Table 2.22: Association constants, K_a [M^{-1}], Gibbs energy, ΔG [kcal·mol^{-1}], and maximum complexation-induced chemical shifts of the guest protons, Δδmax [ppm], of the host-guest complexes of **99** in D_2O at 25 °C.

2.5.1 Special structural features of 98, 99 and 28

In order to gain further insight into the structural properties of molecular clips substituted by polyglycerol dendrimers, we performed a Monte-Carlo conformer search, using AMBER* force-field under various conditions, on a model clip system substituted in the central benzene spacer unit with one methoxy group on one side and one polyglycerol dendrimer of third generation on the other side (Table 2.23). In water and in the gas phase only conformers with a dendritic side chain folded into the clip cavity were found. In chloroform a conformer having an extended side chain was calculated to be energetically similar to that having the side chain folded into the clip cavity. Evidently, in the gas phase

calculation the attractive dispersion interactions between the clip and the dendritic side chain lead to its folding into the cavity. In water the folding certainly results largely from the hydrophobic effect that the clip cavity cannot be well solvated by water molecules. Chloroform is able to solvate the clip cavity as well as the dendritic side chains. This is indicated by the fact that the conformer with the extended side chain is now favoured.

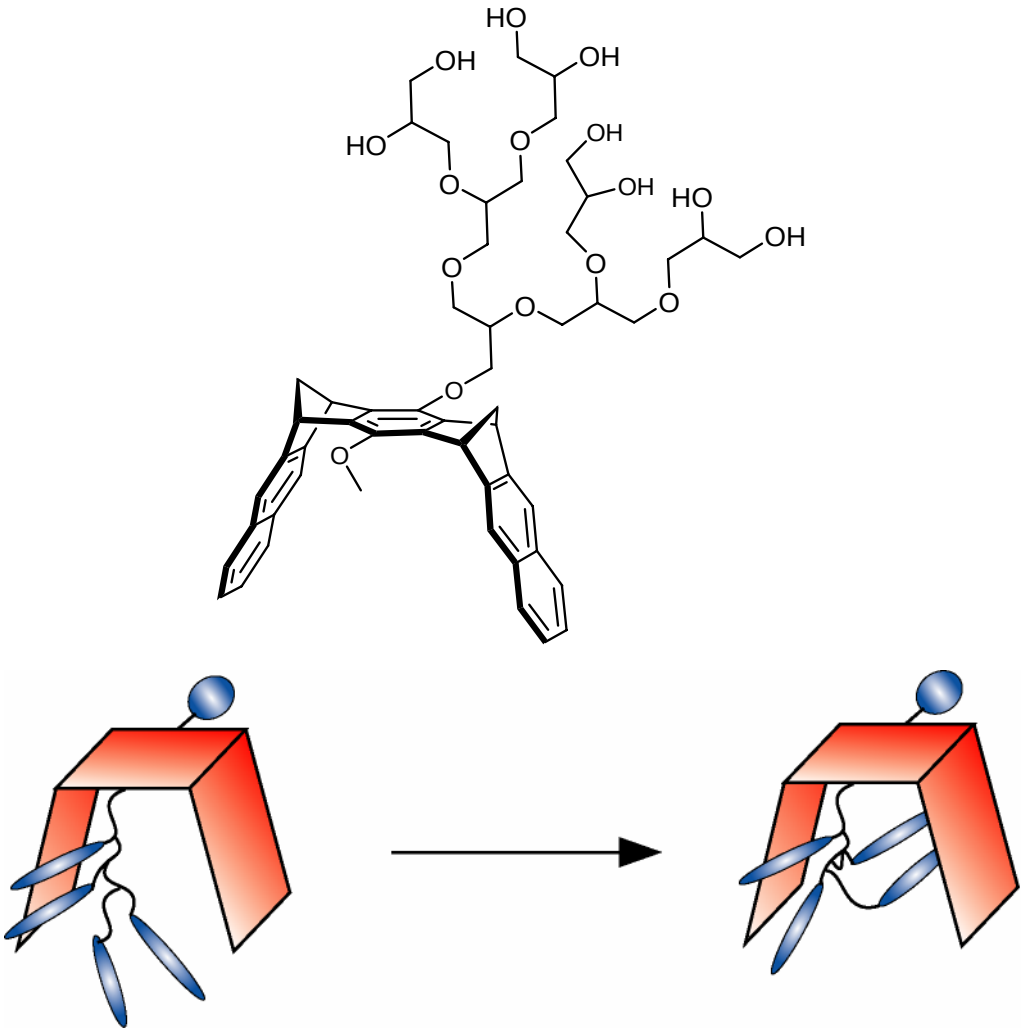

out **in**

Solvent	$\Delta E = E_{in} - E_{out}$ [kcal·mol^{-1}]
H_2O	--
$CHCl_3$	+1.3
Gas phase	--

Table 2.23: Stabilization energy (Monte-Carlo conformational search, AMBER*, 5000 structures) of the process of self-inclusion of the polyglycerol branches inside the cavity of the asymmetric polyglycerol-methoxy clip.

Figure 2.37 shows the structure of minimum energy obtained from the conformational search in water of the model clip used for the structural study of polyglycerol substituted clips.

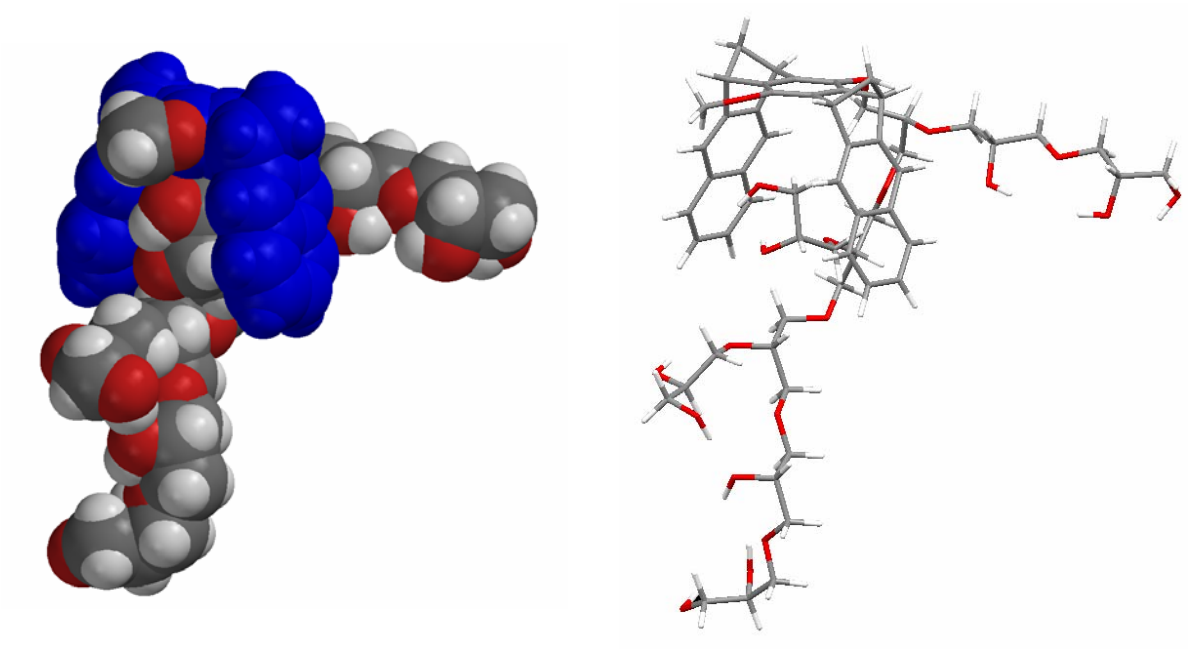

Figure 2.37: Structure of minimum energy obtained from the conformational search (Monte-Carlo, AMBER*, water, 5000 structures). Left: space-filling model. The model clip (hydrophobic, highlighted in blue) is embraced by the hyperbranched polyglycerol substituent (hydrophilic) achieving thusly water solubility. Right: stick-model.

The ^{1}H NMR spectrum of **99** (page 63) in D_2O gives no indication of the preference of a folded conformer. Compound **99** (and **98**) consists of a mixture of oligomers, so that the signals assigned to the dendritic side chains are broad, ranging from δ= 3.0 ppm to δ= 4.3 ppm. These broad signals do not allow us to detect a potential folded conformer. In order to gain information on this potential side chains folding, a structural defined clip has to be investigated. For that reason we compared the ^{1}H NMR spectra of the clip **28**, substituted by the polyglycerol dendrimer of first generation and the correspondingly substituted benzene derivative **106** (Figure 2.38).

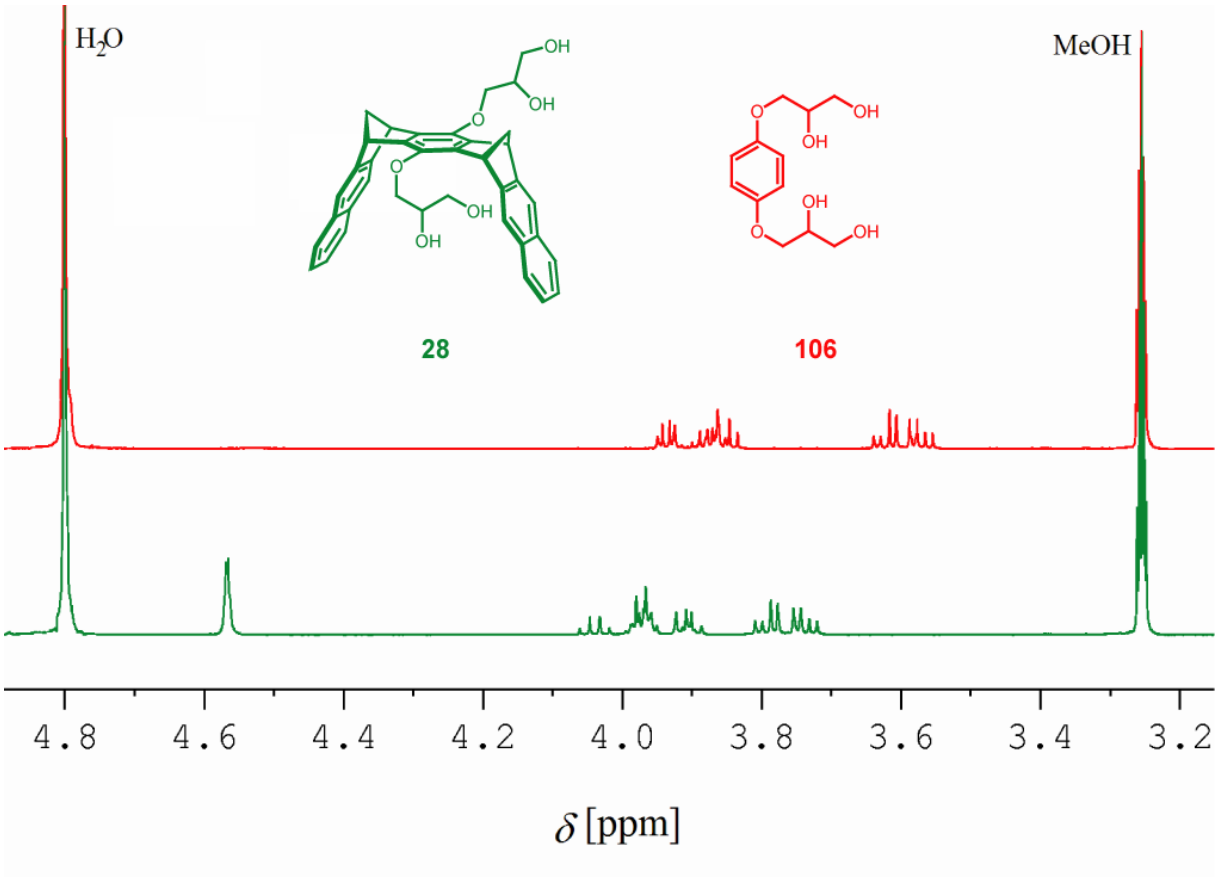

Figure 2.38: Comparison of the aliphatic regions of the clip **28** and the benzene derivative**106**. Spectra measured in methanol-d_4 (500 MHz).

According to Figure 2.38 there is no evidence for the folding of the side chain in clip **28**. Compared to the signals of the CH_2 groups of the benzene derivative **106**, δ= 3.58 ppm, the signals of the substituent of the clip **28**, δ= 3.75 ppm, are even down-field shifted, that is contrary to the expectations for the folded structure. In this case an up-field shift at least of the terminal CH_2 groups of the side chains of **28** compared to the corresponding signals of **106** is expected. The multiplicity of the signals of **28** is perfectly defined and no broadening effect on the substituent signals is observed. That is in agreement with the hypothesis of an extended conformation of the side chains of **28**. A conformational search (MacroModel, Monte-Carlo, AMBER*, water, 5000 structures) confirmed this finding that the glycerol side chains attached to the central benzene spacer unit of **28** are not long enough to be included into the cavity of the clip (Figure 2.39).

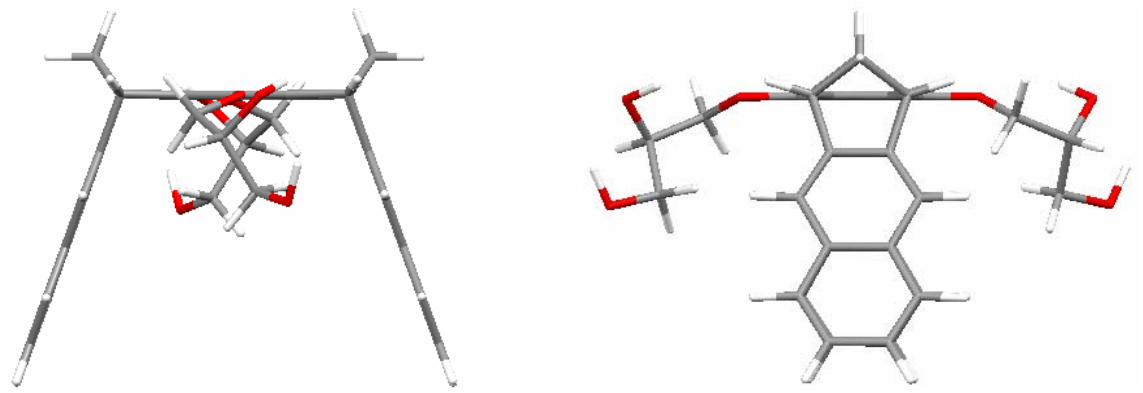

Figure 2.39: .Calculated structure of minimum energy (MacroModel 9.0, Monte-Carlo simulation, AMBER*, water, 5000 structures) of clip **28**.

As for these lines were written, we received a few mg of clip **29**, substituted with the second generation of the polyglycerol dendrimer. A preliminary study, comparing ^{1}H NMR spectra of **28** and **29**, shows no indication of the folding of the side chains into the clip cavity.

Thus, the question remains open: are the polyglycerol side chains of higher generation dendrimers folded into the clip cavity as it is predicted by force-field calculations?

2.5.2 Comparison of the binding properties of 98, 99 and 28 with those of the dimethoxy naphthalene clip 18d

The comparison of the hyperbranched polyglycerol substituted clips with the dimethoxy substituted clip **18d** is of special interest, as both kinds of clips have –OCH_2R groups as a common structural feature in the substituent at the central benzene spacer unit (Figure 2.40). The comparison of the binding properties of both kinds of clips is certainly a good approach to evaluate the effect of the polyglycerol branches on the binding properties.

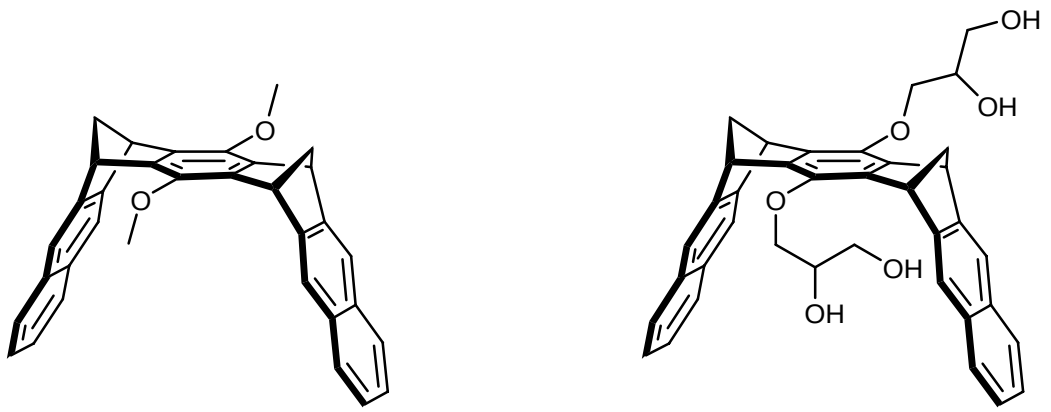

18d **28**

Figure 2.40: The similar structure of the substituents at the central benzene spacer unit makes the dimethoxy clip **18d** an appropriate reference to evaluate the effect of the hyperbranched polyglycerol substituents of clips **98**, **99** and **28**.

Since the dimethoxy clip **18d** does not show significant complex formation with various guest molecules such as tetracyanobenzene **85** and Kosower salt **84**,[78, 115] the conclusion that can be drawn from the findings described for the hyperbranched polyglycerol substituted clips **98**, **99** and **28** that the dendritic side chains of these clips substantially stabilize the host-guest complexes with TCNB **85** and KS **84**. The relatively small $\Delta\delta_{max}$ values observed for the complexes of Kosower salt **84** and *N*-methylnicotinamide iodide **33** with clips **98**, **99** and **28** indicate that the aromatic rings of the guest molecule is no longer positioned inside the clip cavity differently to their position in the corresponding complexes with the diacetoxy clip **18b** and the G_1-TEG substituted clip **27**. Evidently, in the complexes **KS@99** and **NMNA@99** in D_2O the guests are at least partially pulled out of the clip cavity in order to experience bonding interactions, most likely with the OH groups of the side chains of the substituents of clip **99**.

2.5.3 Comparison among the thermodynamic data of the complexes of 28, 98 and 99

Table 2.24 shows the comparison of the complex stability with caffeine **34**, *N*-methyl-nicotinamide **33** and Kosower salt **84** with the clips **28**, **98**, **27** and **18g** in methanol-d_4 solution. According to these data the perfectly-structured clip **28** (first generation) is, evidently, a considerably weaker receptor than **98** and **99**, substituted by higher generations of polyglycerol. This result indicates that the size of the polyglycerol substituent has a significant influence on the complex stability. The larger the substituents are, the better is the complex stabilization by hydrogen bonds between the receptor side chains and the guest.

The association constant with caffeine (**34**) is of the special interest, as it is up to 25 times larger for the receptor **98** than for the receptor **28** (K_a= 1035 and 41 M^{-1}, respectively). This difference confirms the hydrogen-bond stabilization hypothesis mentioned before; the

caffeine molecule has a total of six atoms able to serve as hydrogen-bond acceptors but it has no atoms that can serve as hydrogen-bond donors. Since the clip **98** has much more hydroxyl groups than the clip **28**, the complex with clip **98** is better stabilized having the larger K_a value. Moreover the receptor **27** has no hydrogen-bond donors and consequently, the complex **34@27** is less stabilized and its association constant is lower than that for the complex **34@98**. The complex **34@27** is, however, more stable than the complex **34@28** by a factor of 10, which is in agreement with the observation that clips and tweezers substituted by –OCOR ester groups in the central spacer unit form more stable complexes with electron-withdrawing aromatic guest molecules than clips and tweezers with $–OCH_2R$ ether groups in the central spacer unit.[79, 115]

Guest	Clip 28 K_a [M^{-1}]	Clip 98 K_a [M^{-1}]	Clip 27 K_a [M^{-1}]	Clip 18g K_a [M^{-1}]
Caffeine **34**	41	1035	415	9550 [a]
NMNA **33**	60	230	65	1660
Kosower salt **84**	45	85	235	3200

[a] Measured at 25 ºC in D_2O-Buffer (pH= 7.2)[132]

Table 2.24: Association constants comparison chart among the polyglycerol clips **28**, **98,** the TEG-dendrimer substituted clip **27** and the dilithium phosphonate clip **18g** in methanol-d_4 at 25 ºC.

The comparison of association constants of the complex formation of clip **99** with those of clips **18h** and **18g** in aqueous solution show that the complexes of the neutral receptor are much less stable than those of the negatively charged molecular clips. There are two main factors to take into account in order to understand these results. First of all, the anionic clips **18h** and **18g** are able to stabilize the positive charged guests inside the cavity by means of electrostatic interactions (Coulomb forces), which are much stronger than the hydrogen-bonding stabilization the clip **99** is able to accomplish. Secondly, assuming that the folding of the polyglycerol side chains of high generation does occur, it inhibits the complex formation with clip **99**.

Guest	Clip 99 K_a [M^{-1}]	Clip 18h K_a [M^{-1}]	Clip 18g K_a [M^{-1}]
Caffeine **34**	175	42700 [a]	9550 [a]
NMNA **33**	40	29400 [a]	83000
Kosower salt **84**	50	19000 [a]	4800

[a] Measured at 25 ºC in D_2O-Buffer (pH= 7.2)[132]

Table 2.25: Association constants comparison chart among the polyglycerol clip **99**, the tetralithium phosphate clip **18h** and the dilithium phosphonate clip **18g** in D_2O (and buffer as indicated) at 25 ºC.

2.5.4 Comparison of the maximum complexation-induced chemical shifts, $\Delta\delta_{max}$, of 28 with the calculated structures of the complexes

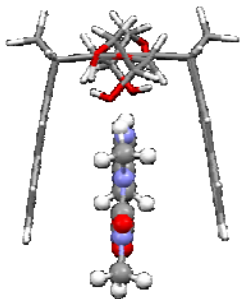

34@28, front view

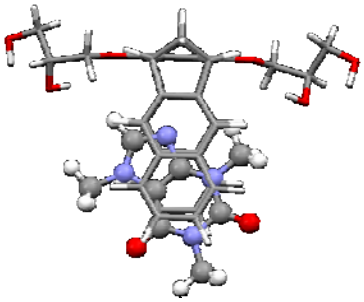

34@28, side view

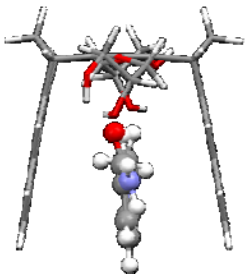

NMNA@28, front view

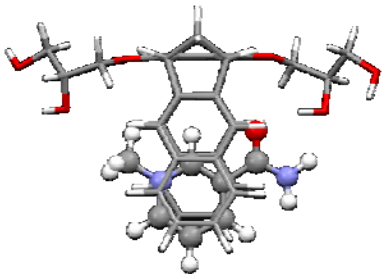

NMNA@28, side view

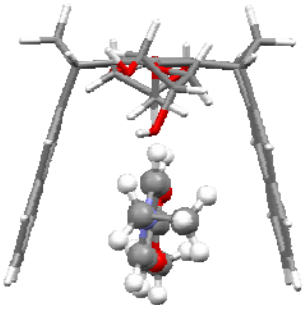

KS@28, front view

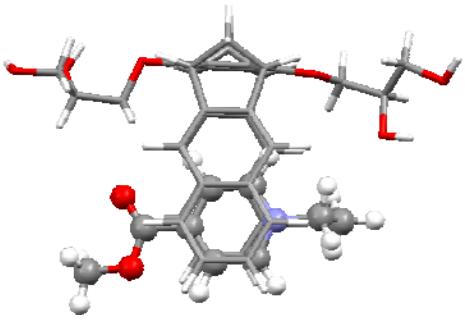

KS@28, side view

Figure 2.41: Calculated minimum-energy structures (MacroModel 9.0, Monte-Carlo simulation, AMBER*, *n*-octanol, 5000 structures) of the complexes **34@28**, **NMNA@28** and **KS@28**.

The calculated structures of the complexes **34@28**, **NMNA@28** and **KS@28** in *n*-octanol differ from those of analogous complexes with the clip **27** (page 88), allowing us to conclude that the nature of the substituent attached to the central spacer unit of the clip does have an influence on its structure. However, none of the structures resulting from the

conformational analyses showed the guest molecules to be pulled out of the cavity in order to undergo interactions with the dendritic substituents.

The calculated minimum-energy complex structures of **28** with caffeine, NMNA and KS as guest molecules are, however, not in agreement with the experimental data of maximum complexation-induced chemical shifts, $\Delta\delta_{max}$. For instance, none of the guest protons of the complex **34@28** is calculated to be located inside the receptor cavity whereas the observed values of $\Delta\delta_{max}$ are relatively large (Table 2.20) and in the same range as those observed for other complexes. Evidently, other conformers and not only the calculated minimum-energy structure, contribute to the overall structure of complex **34@28**. A similar conclusion can be drawn for the complex **NMNA@28**, where the experimental values of $\Delta\delta_{max}$ are not in agreement with the calculated minimum-energy structure of the complex. In this case the experimental values, especially the $\Delta\delta_{max}$ value found for proton H_a (0.60 ppm) pointing toward the central benzene spacer unit according to the calculation, are certainly too small for a complex structure in which the NMNA guest molecule is positioned inside the clip cavity. The calculated structure of **NMNA@28** also differs, in terms of relative orientation of the guest in the clip cavity, from that of **NMNA@27**, in which the methyl group is located inside the cavity. The reason for this difference in the calculated structures is that in the complex **NMNA@28** the NMNA molecule is additionally stabilized by a hydrogen bond between one of the hydroxyl groups of the substituent and the amide group of the NMNA whereas this stabilization is not possible in the complex **NMNA@27** and therefore it adopts a different conformation.

The $\Delta\delta_{max}$ values of the complex **KS@28** are consistent with its calculated structures. Both kinds of aromatic protons (H_a and H_b) are located completely inside the clip cavity and, accordingly, these groups of protons show higher values of complexation-induced up-field chemical shifts than those protons situated outside the cavity.

2.6 Host-guest complex formation with sulphate substituted clips.

2.6.1 Self-association properties of sulphate substituted clips. Comparison with phosphate and phosphonate substituted clips

The ^{1}H NMR spectra of **36** and **38** are unexpectedly different in methanol-d_4 and D_2O. This finding supplies an experimental evidence for a self-association of both clips in aqueous solution. By changing the solvent from methanol-d_4 to D_2O, the signals assigned to the naphthalene sidewalls of the clip **36** are significantly up-field shifted, broad and without multiplicity, whereas the signals assigned to the other protons of the clip appear to be less solvent-dependent. The anthracene clip **38** shows an even more dramatic solvent dependence of the chemical shifts of the anthracene protons when the solvent is changed from methanol-d_4 to D_2O. In this case the signal of the proton H_b, at the central benzene ring of the anthracene sidewall, shows the strongest up-field shift of δ_c= 2.26 ppm.

We observed that in methanol-d_4 solution the ^{1}H NMR spectra of both naphthalene and anthracene clips are not significantly concentration-dependent within the limits of NMR detection (Δ[**36**]= 7.5-0.3 mM and Δ[**38**]= 5.9-0.2 mM), whereas in D_2O solution the

chemical shifts are dependent on the clip concentration. The changes observed in the ^{1}H NMR spectra of clip **36** and **38** by replacing methanol with water as a solvent provide good evidence that in aqueous solution the clips **36** and **38** tend to self-assemble, forming distinct supramolecular structures in which the ^{1}H NMR signals of the protons on the naphthalene and anthracene sidewalls are strongly influenced by the magnetic anisotropy of the arene systems of the neighbour clip molecules. The effect of solvent change on the aromatic region of ^{1}H NMR spectra of **36** and **38** is shown in Figure 2.42 and Figure 2.43 respectively.

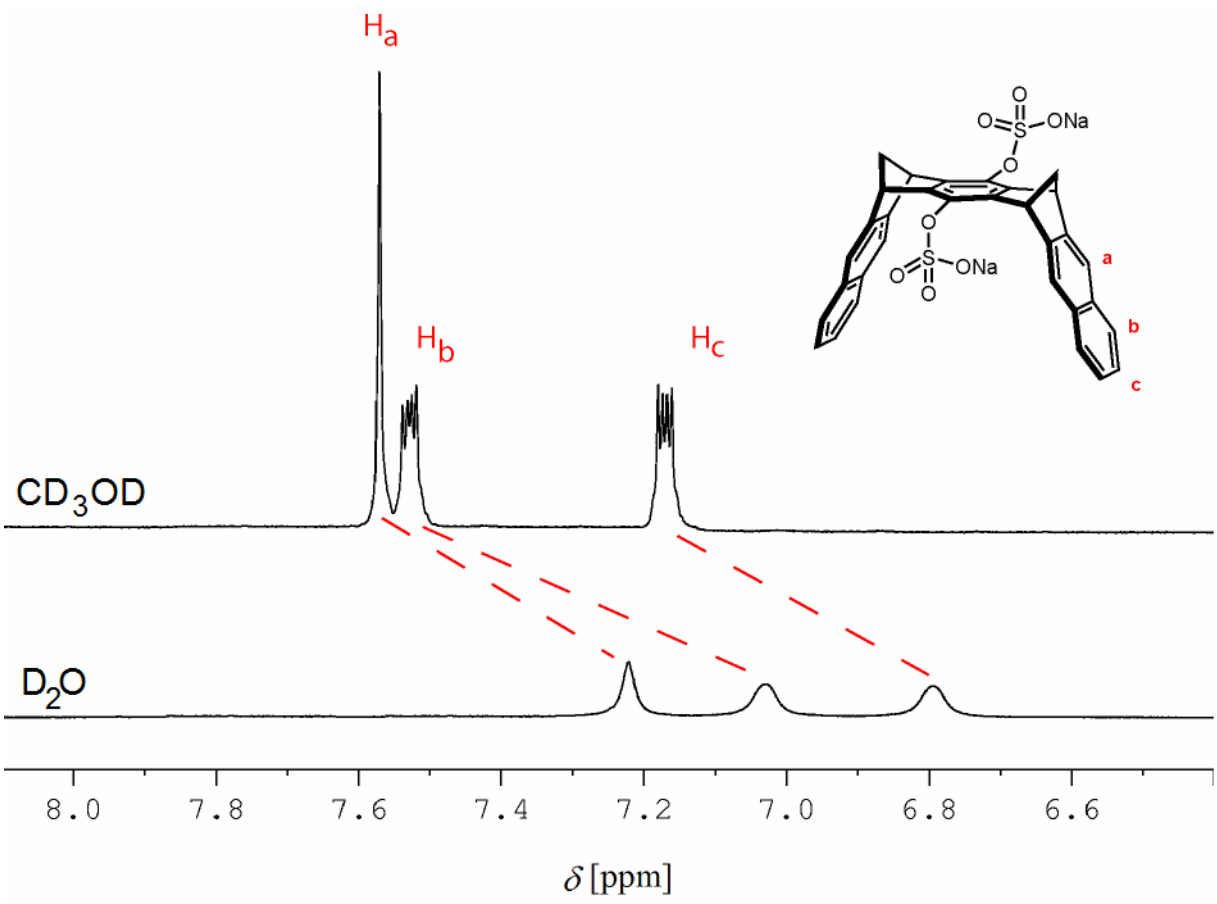

Figure 2.42: Solvent change effect on the ^{1}H NMR spectrum (500 MHz) of **36**.

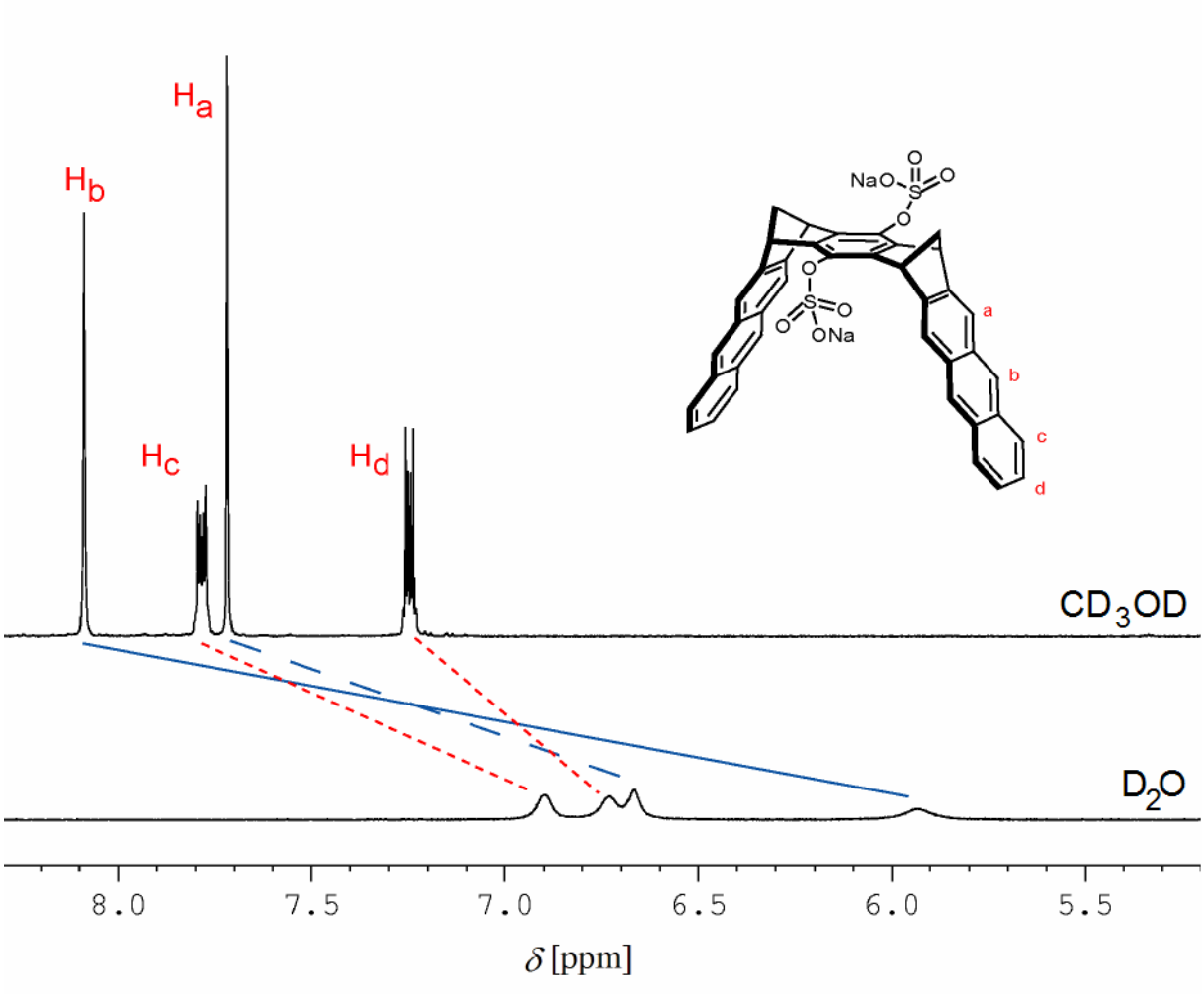

Figure 2.43: Solvent change effect on the ^{1}H NMR spectrum (500 MHz) of **38**.

Similar results were obtained for the phosphate substituted naphthalene clip **18h** and the phosphonate substituted anthracene clip **20g**. Also in these cases the ^{1}H NMR signals of the protons assigned to the naphthalene and anthracene sidewalls protons experience a large up-field shift by the change of the solvent from methanol to water. A survey of all the water-soluble molecular tweezers and clips prepared up to date and their corresponding constants of self-association is shown in Figure 2.46.

In order to elucidate the self-assembled structures of clips **36** and **38**, force-field calculations were performed for the monomeric (**36** and **38**) and dimeric forms (**36**$_2$ and **38**$_2$, respectively) of both clips by means of conformational search (MacroModel 9.0, Monte-Carlo simulation, AMBER*, H_2O, 5000 structures). The low-energy conformers resulted from these calculations are shown in Figure 2.44.

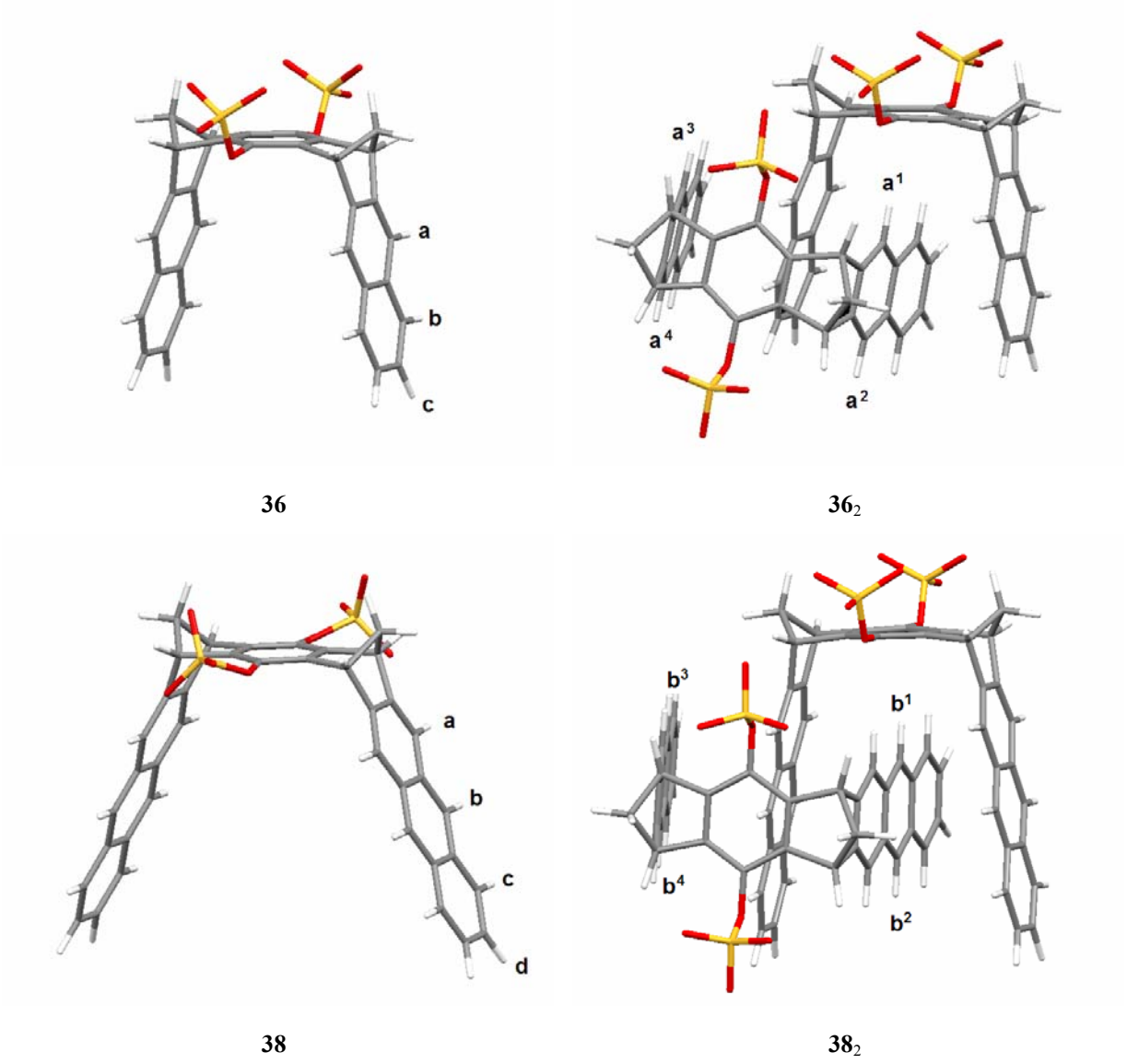

Figure 2.44: Low-energy conformers of the monomer and dimer forms of **36** and **38** resulting from the conformational search (MacroModel 9.0. Monte-Carlo simulation, AMBER*, H_2O, 5000 structures).

The calculated structures of the dimers $\mathbf{36}_2$ and $\mathbf{38}_2$ indicate that the corresponding aromatic protons are no longer chemically equivalent to each other contrary to the structures of the respective monomers. In both dimer structures, one of the sidewalls of one clip is located inside the cavity of the second clip molecule and, additionally, the protons of each sidewall are located with different orientation relative to the central spacer unit. In the ^{1}H NMR spectra in D_2O of both clips, however, only one signal for each kind of aromatic protons is observed but with a remarkable broadening, which indicates that a fast exchange between these protons takes place in solution (for instance $H_b^1 \rightleftharpoons H_b^2 \rightleftharpoons H_b^3 \rightleftharpoons H_b^4$) leading to the observed averaged signal. The indicated fast proton exchange results clearly from a fast association-dissociation process $\mathbf{36}_2 \rightleftharpoons 2\cdot\mathbf{36}$ or $\mathbf{38}_2 \rightleftharpoons 2\cdot\mathbf{38}$, with dimers $\mathbf{36}_2$ and $\mathbf{38}_2$ as the predominant species in their corresponding equilibrium. According to the

broadening of the ^{1}H NMR signals at room temperature each equilibration proceeds at a rate comparable to the NMR time scale.

In aqueous solution at room temperature the ^{1}H NMR signals of **38** do not show a large concentration dependence whereas the signals of **36** are significantly more affected by diluting the solution. This finding is an indication that the equilibrium constant of dimerization, K_{dim}, of **38** is significantly higher than that of **36**.

$$2\cdot\text{Clip} \rightleftharpoons \text{Clip}_2$$

$$K_{dim} = \frac{[\text{dimer}]}{[\text{monomer}]} = \frac{[\text{Clip}_2]}{[\text{Clip}]^2}$$

Scheme 2.27: Representation of the self-association equilibrium and definition of the association constant of dimerization.

The equilibrium constant of dimerization, K_{dim}, and the maximum chemical shift differences, $\Delta\delta_{max} = (\delta_{monomer}-\delta_{dimer})$, of **36** and **37** were determined by means of ^{1}H NMR dilution titration, assuming $\delta_{monomer}$ to be equal to δ_{obs} found in methanol-d_4 solution. The results of these titrations are shown in the Figure 2.45.

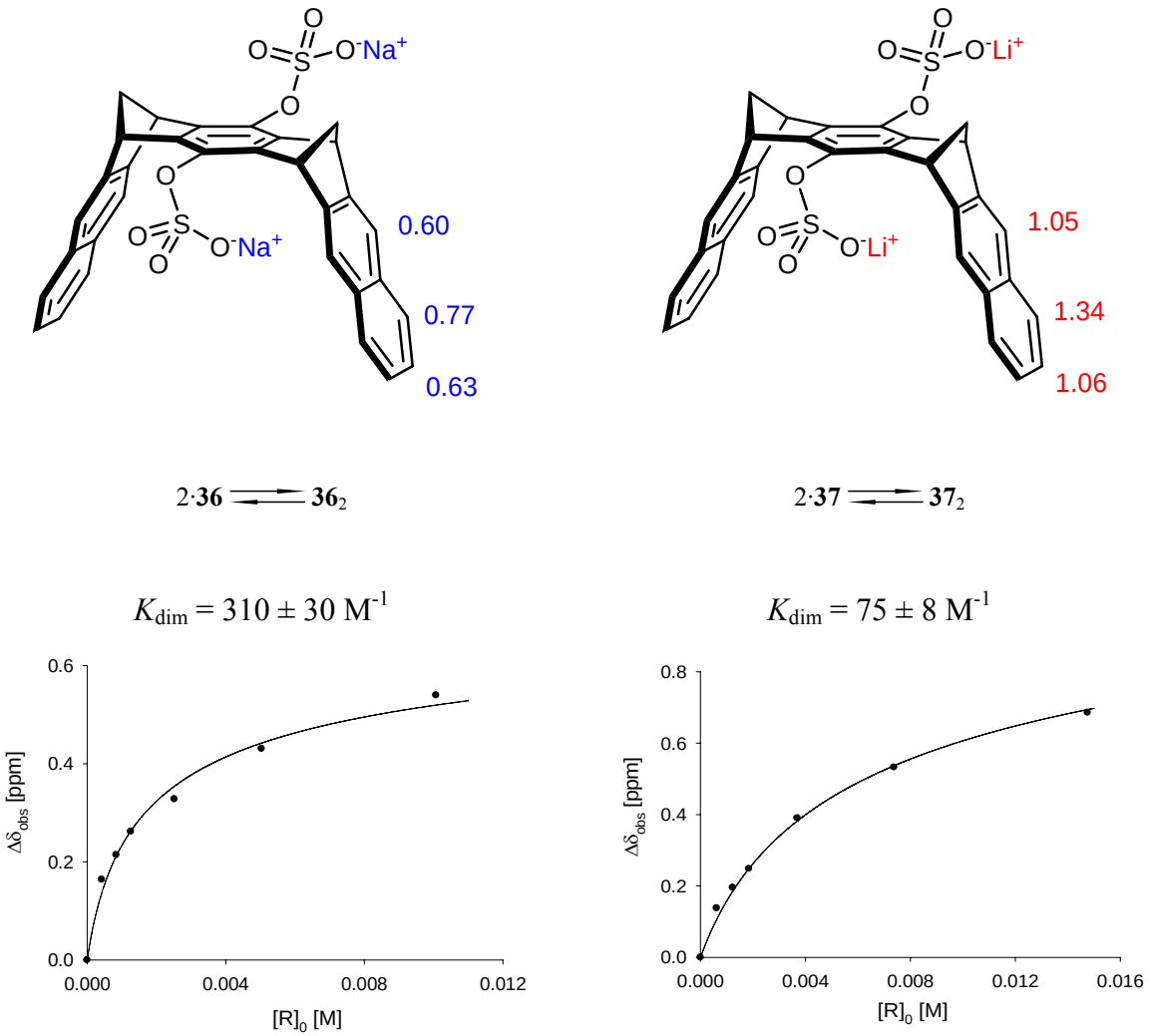

Figure 2.45: Values of self-association constant, K_{dim}, and maximum complexation-induced ^{1}H NMR shifts, $\Delta\delta_{max}$, for the sulphate substituted naphthalene clips **36** and **37** determined by dilution titration (298 K in D_2O) and the corresponding titration curves.

Within similar concentration ranges (from 14.8 mM to 0.5 mM), both sodium and lithium sulphate clips (**36** and **37** respectively) show significantly different values of K_{dim}, being for **36** four times larger than that of **37**. Due to its charge and ionic radius, lithium cations tend to form more stable bonds with oxygen than sodium cations, being the bond Li-O partially covalent.[134] Therefore in the lithium sulphate clip **37** the negative charges of the sulphate groups are much better compensated by the lithium cations than what they are by the sodium cations in the analogous clip **36**. Hence the difference between the hydrophilic nature of the sidewalls and the lipophilic nature of the sulphate groups is considerably larger in the sodium sulphate clip **36** than in the analogous lithium clip **37** and, consequently, the tendency of **37** to form self-aggregates is not as noticeable as that of **36**.

In order to evaluate the temperature dependence of K_{dim} and hence the thermodynamic parameters ΔH, ΔS and ΔG, temperature-dependent titration measurements were carried out

with the anthracene clip **38**. A linear relationship between the values of $\ln K_{dim}$ and the inverse of the temperature (T^{-1}) is observed, which indicates that the change of heat capacity for the self-association process is equal to zero ($\Delta C_p = 0$). By the linear representation of van't Hoff equation (van't Hoff plot), the thermodynamic parameters ΔG, ΔH and ΔS for the self-association process at room temperature can be determined (Table 2.26).

$2 \cdot \mathbf{38} \rightleftharpoons \mathbf{38}_2$ Self-aggregation equilibrium

$R \cdot \ln K_{dim} = \Delta S - \Delta H / T$ van't Hoff's equation

T [K]	$\Delta\delta_{max}(H_a)$ [ppm]	K_{dim} [$10^3 \cdot M^{-1}$]	T^{-1} [K^{-1}]	$R \cdot \ln K_{dim}$ [kcal·mol^{-1}·K^{-1}]
298	1.11	194 ± 20	0.00335570	0.024188442
318	1.10	544 ± 5	0.00314465	0.021665645
338	1.08	17.1 ± 2	0.00295858	0.019367540
358	1.06	5.91 ± 0.6	0.00279330	0.017257921
368	1.05	3.70 ± 0.4	0.00271739	0.016323218

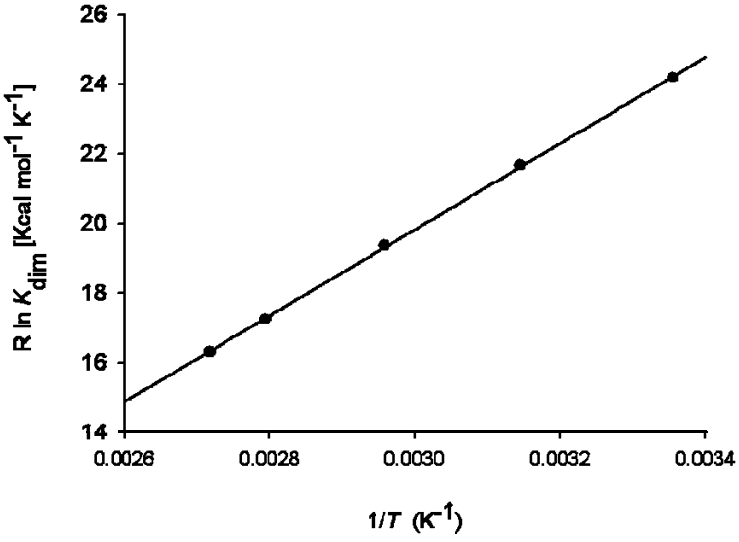

$R \cdot \ln K_{dim} = -16.19 - 11937.54 / T$ ($R^2 = 0.9998$)

$\Delta H = -12.4 \pm 0.1$ kcal·mol^{-1}

$T \cdot \Delta S^a = -5.2 \pm 0.3$ kcal·mol^{-1}

$\Delta G^a = -7.2 \pm 0.2$ kcal·mol^{-1}

$K_{dim}{}^a = (1.94 \pm 0.2) \cdot 10^5$ M^{-1}

[a] The indicated values are calculated for a temperature of 298 K (24.85 ºC)

Table 2.26: Temperature-dependent association constants, K_{dim}, maximum complexation-induced chemical shifts, $\Delta\delta_{max}$, determined, by dilution ^{1}H NMR titrations, for the self-association process of **38** in aqueous solution and the thermodynamic parameters at room temperature obtained by the use of the van't Hoff equation.

Hydrophobic interactions tend to increase gradually as the surface of the molecules is enlarged compared to the highly structured water molecules in aqueous solution. The release of water molecules into the solvent bulk through the aggregation of the solute leads, usually, to an increase in entropy.[135] In good agreement with the results obtained for the self-assembly of the analogous phosphonate substituted anthracene clip **20g**,[89] we found negative values of ΔH and $T \cdot \Delta S$ indicating an enthalpically controlled binding in the self-assembled dimers and an unfavourable entropy contribution contrary to the expectations described previously for hydrophobic interactions. Our results are well in accord with the results obtained for protein aggregation and host-guest complex formation in aqueous solutions relying on aromatic interactions and can be explained by the so-called non-classical hydrophobic effect.[20, 136-139]

The self-association constants, K_{dim}, shown in Table 2.26 were determined by evaluating the change of the chemical shift, $\Delta\delta$, of the proton H_a in relation to the clip concentration. The analysis of the proton H_b was not possible because the broadening of its ^{1}H NMR signal in dilute solutions was too large to determine accurate values. The ^{1}H NMR signal of H_b at [**38**] = 3.30 mM (first titration step, most concentrated sample) is broad but still detectable, whereas the signal of H_b at [**38**] = 0.83 mM (third titration step) and in further diluted solutions cannot be detected. However, the values of $\Delta\delta_{max}$ (H_a) and the chemical shift differences observed in the first titration step for H_a and H_b ($\Delta\delta_1$ (H_a) and $\Delta\delta_1$ (H_b) respectively) allowed us to calculate the values of maximum complexation-induced chemical shift for the proton H_b by the use of $\Delta\delta_{max}$ (H_a), according to Equation 2.4.

$$\Delta\delta_{max}(H_b) = \Delta\delta_1(H_b) \times \frac{\Delta\delta_{max}(H_a)}{\Delta\delta_1(H_a)} \qquad \text{Equation 2.4}$$

The values obtained with the Equation 2.4 for the proton H_b and the comparison with the experimentally obtained values for the proton H_a are shown in Table 2.27.

Temperature [K]	$\Delta\delta_{max}$ (H_b) [ppm]	$\Delta\delta_{max}$ (H_a) [ppm]
298	2.26	1.11
318	2.33	1.10
338	2.34	1.08
358	2.32	1.06
368	2.31	1.05

Table 2.27: Calculated maximum complexation-induced chemical shifts for the proton H_b, $\Delta\delta_{max}$ (H_b), of **38** obtained with the Equation 2.4 and the comparison with the experimental values obtained for the proton H_a, $\Delta\delta_{max}$ (H_a).

The values of $\Delta\delta_{max}$ for the proton H_b (central benzene ring of the anthracene sidewall) are significantly higher than those of the proton H_a. This result is in good accord with the calculated minimum-energy conformer of the dimer $\mathbf{38}_2$ in aqueous solution, shown in Figure 2.44. In this calculated structure the proton H_b^1 of one clip is directly pointing towards the central benzene spacer unit of the second clip, whereas the proton H_a is slightly outside the cavity. Consequently, the proton H_b is influenced directly by the magnetic anisotropy of the benzene spacer unit and, hence, its maximum complexation-induced chemical shift is significantly larger that that of H_a.

Other anionic water-soluble molecular clips, substituted by phosphate and phosphonate groups, also show self-aggregation in water.[89] For instance, the self-association constant, K_{dim}, of the anthracene phosphonate lithium clip **20g** at room temperature (298 K) is calculated, by means of a van't Hoff plot, to be $K_{dim} = 1.60 \cdot 10^5\ M^{-1}$ whereas, surprisingly, the analogous naphthalene clip **18g** shows no evidence of self-aggregation within the limits of ^{1}H NMR detection.

The larger values of K_{dim} obtained for the anthracene clips **38** and **20g** in comparison to the analogous naphthalene clips **36** and **18g**, respectively, provide good evidence that the size of the sidewalls of the clips plays an important role. The bigger the aromatic sidewall is, the more hydrophobic the clip is and therefore it tends to the formation of self-aggregates.

Figure 2.46 summarizes all water soluble receptors substituted by anionic functions, the binding constants and the values of $\Delta\delta_{max}$ for the formation of their self-assembled dimers.

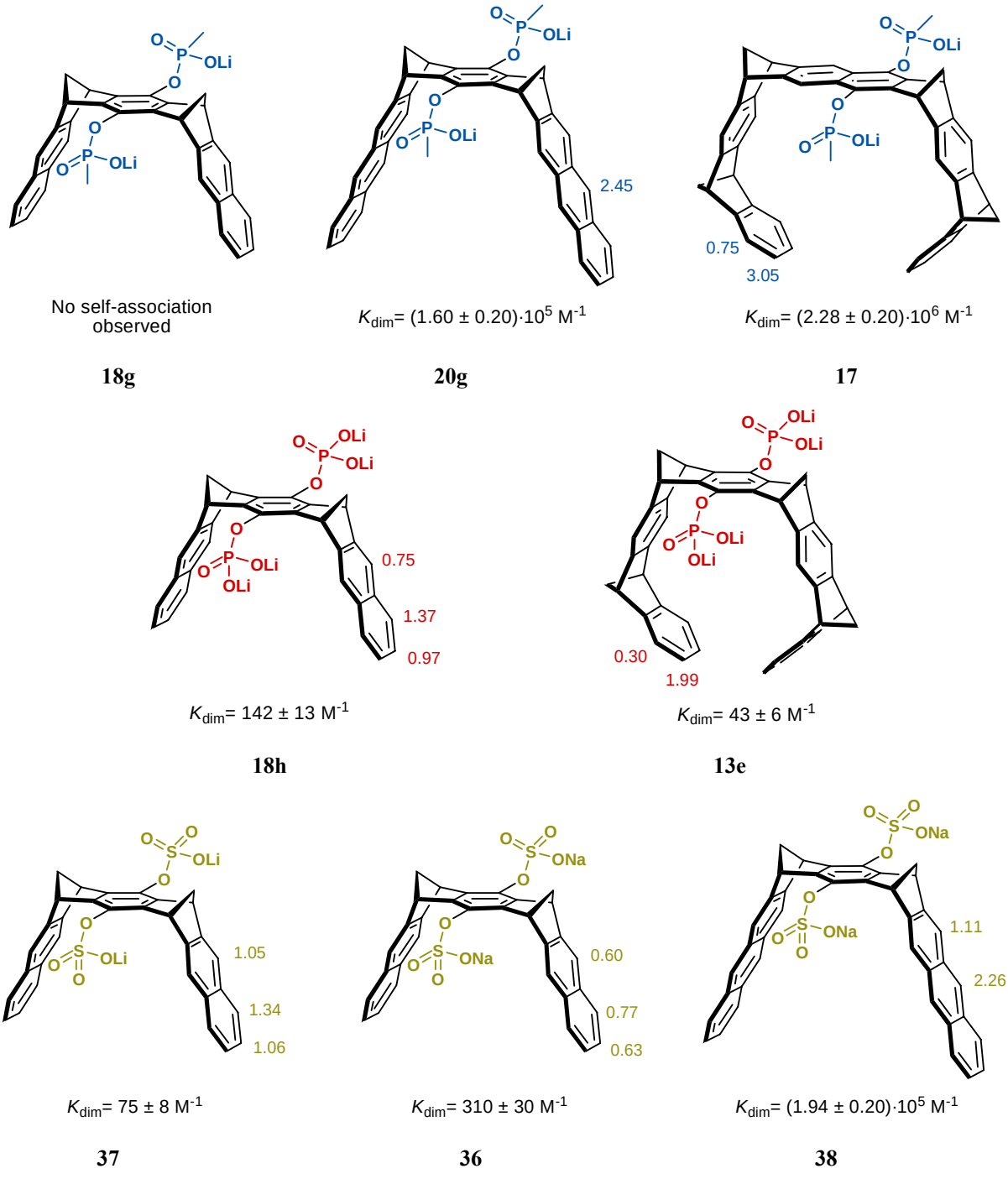

Figure 2.46: Water soluble molecular clips and tweezers synthesized to date and their binding constants of self-aggregation, K_{dim} at 298 K. The values of $\Delta\delta_{max}$ indicated in the structures are expressed in ppm.[89, 128, 129, 140]

2.6.2 Complexation properties of 36 with small aromatic guests molecules

The efficient self-association processes of the sulphate substituted molecular clips **36**, **37** and **38** are overruled if a proper guest molecule is added to an aqueous solution of these receptors. An exceedingly strong binding of guest molecules inside the clip cavity is observed in most of the cases.

For the evaluation of the receptor properties of the molecular clip **36**, the association constants with the guests shown in Figure 2.47 in water and methanol were investigated by means of ^{1}H NMR titration. The results obtained with these guest molecules are shown in Table 2.28 whereas the detailed titration experiment data are described in chapter 4.5.

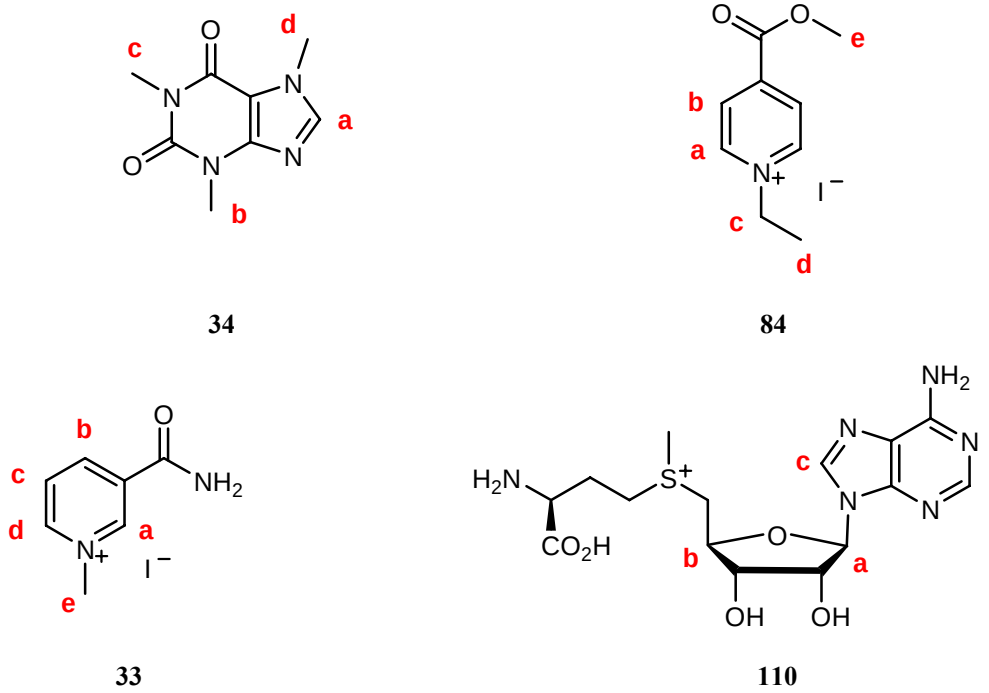

Figure 2.47: Guest molecules used for the study of the complexation properties of **36**.

Guest	Solvent	K_a [M^{-1}]	ΔG [kcal·mol^{-1}]	$\Delta\delta_{max}$ [ppm]
Caffeine **34**	D_2O/Buffer[a]	2900 ± 300	-4.72	2.94 (H_a) 0.47 (H_c)
Kosower salt **84**	Methanol-d_4	(6.84 ± 0.70)·10^4	-6.60	1.23 (H_a) 1.68 (H_b) 0.66 (H_c) 0.42 (H_d)
Kosower salt **84**	D_2O	(8.16 ± 0.82)·10^4	-6.70	1.38 (H_a) 2.11 (H_b) 0.52 (H_c) 0.41 (H_d)
Kosower salt **84**	D_2O/Buffer[a]	c.p.[b]	-	-
NMNA **33**	Methanol-d_4	(1.76 ± 0.18)·10^5	-7.16	1.10 (H_a) 1.11 (H_b) 1.79 (H_c) 0.93 (H_d)
NMNA **33**	D_2O and D_2O/Buffer[a]	c.p.[b]	-	-
SAM **110**	D_2O/Buffer[a]	940 ± 95	-4.06	0.50 (H_a) 1.10 (H_b) 0.52 (H_c)

[a] Aqueous phosphate buffer (pH= 7.2)[132]

[b] Complex Precipitation: precipitation of the 1:1, host-guest complex.

Table 2.28: Association constants, K_a [M^{-1}], Gibbs energy, ΔG [kcal·mol^{-1}], and maximum induced chemical shifts of the guest protons, $\Delta\delta_{max}$ [ppm], of the host-guest complexes of **36** in different solvents at 25 ºC.

2.6.2.1 Comparison among the thermodynamic data of the complexes of 36, 18h and 18g

Guest	Host		
	36 K_a [M^{-1}]	**18h K_a [M^{-1}]**	**18g K_a [M^{-1}]**
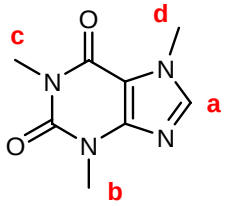 Caffeine **34**	2900	42700	9550
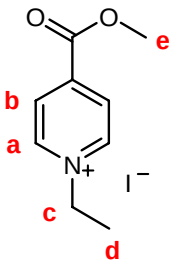 Kosower salt **84**	81600 [a] 68400 [b]	19000	840 4800 [a,c] 43000 [b,c]
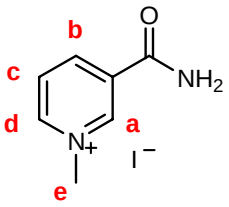 NMNA **33**	176000 [b]	33800 34100 [b,d] 218000 [a]	11300 82800 [a] 700 [b]
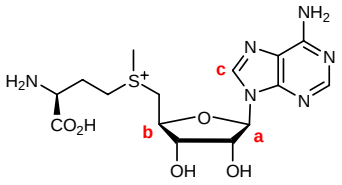 SAM **110**	940	5400	1200

[a] Measured in pure D_2O

[b] Measured in methanol-d_4.

[c] Measured with clip **18f** (R= -OP(O)(CH_3)O^-·N^+(nBu)$_4$)

[d] Measured with the clip **18i** (R= -OP(OH)O_2^-·Li^+)

Table 2.29: Association constants comparison among the sodium sulphate naphthalene clip **36,** the tetralithium phosphate clip **18h** and the dilithium phosphonate clip **18g** in buffered water solution (pH= 7.2). All the association constants were measured by means of ^{1}H NMR titration experiments carried out at 25 ºC.

We were surprised to observe that structurally similar receptors such as the sulphate, phosphonate and phosphate substituted naphthalene clips (**36**, **18g** and **18h** respectively) show rather different binding constants with one and the same guest (Table 2.29). It is important to consider that the sulphate and phosphonate clips, **36** and **18g**, react neutral, pH≈ 7, in aqueous solution, but the phosphate clip **18h** reacts basic, pH≈ 9. Therefore, both the sulphate and phosphonate clip, exist as salts when they are dissolved in aqueous phosphate buffer at pH= 7.2 whereas the phosphate clip **18h**, R= $-OPO_3^{2-}$, is partially protonated to R= $-OPO(OH)O_2^-$ when it is dissolved in aqueous buffer.

In the case of caffeine **34** as guest molecule in aqueous buffered solution (pH= 7.2) the complex with the sulphate clip **36** is substantially less stable that those with the phosphonate clip **18g** and phosphate clip **18h**. Evidently, the interaction of this neutral guest molecule with the partially protonated phosphate groups of clip **18h** leads to a large stabilization of the complex **36@18h**. In the case of the positively charged pyridinium guest molecules such as Kosower salt **84** and NMNA **33**, the host-guest complexes with the sulphate clip **36** are more stable than the corresponding complexes with the phosphonate and phosphate clips, **18g** and **18h** respectively. A detailed quantitative comparison of the binding constants, however, is here difficult since in some cases it was not possible to determine the binding constants all under the same conditions because, for example, some of the complexes of the sulphate clip **36** (*e.g.* **KS@36** or **NMNA@36**) precipitate in aqueous buffer or even in aqueous solution. But the comparison of the data determined in one and the same solvent, for example, of the NMNA complexes **NMNA@36**, **NMNA@18h** and **NMNA@18g** in methanol-d_4 show the extraordinary stability of the complex with the sulphate clip **36**. The sequence of stability of the complexes with S-adenosyl methionine (SAM, **110**) as another cationic guest molecule in aqueous buffer is, however, reversed in comparison to that of the pyridinium guest molecules. Here the complexes **SAM@36** is the least and **SAM@18h** the most stable one. The influence of the anionic substituents on the complex stability shown in Table 2.29 cannot be explained currently. There are several factors that can influence the complex stability:

1. The number of negative charges in each substituent: -2 in $-OPO_3^{2-}$ (phosphate clip **18h**) *vs*. -1 in $-OPO(OH)O_2^-$ (partially protonated clip **18h** or clip **18i**), $-OP(CH_3)O_2^-$ (phosphonate clip **18g**) and $-OSO_3^-$ (sulphate clip **36**).
2. The distribution of the negative charge on oxygen atoms by various resonance structures.

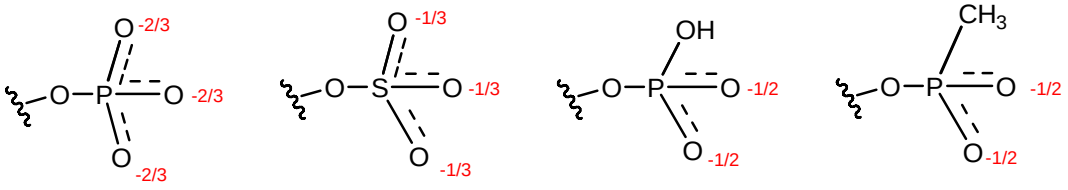

phosphate sulphate partially protonated phosphate phosphonate

3. The positive counterions which are certainly differently bound to the anion and differently solvated as already pointed out.

The thus far existing data do not allow the decision which of these factors is particularly important for the complex stability with a certain guest molecule.

2.6.2.2 Comparison of the maximum complexation-induced chemical shifts, $\Delta\delta_{max}$, of 36 with the calculated structures of the complexes

The structures of the complexes of **36** with the guest molecules caffeine **34**, Kosower salt **84** and NMNA **33** were calculated by conformer search using the AMBER*/H_2O force-field. The structure of the complex **SAM@36** could not be calculated by this method because force field parameters for the sulphonium cation are missing in the parameters implemented in MacroModel 9.0. For that reason we calculated this structure with the MMFF94 (gas phase) force-field implemented in Spartan. The calculated complex structures are shown in Figure 2.48.

In contrast to the calculated structure of complex **34@28**, the structure of complex **34@36** shows no guest proton inside the cavity of the clip and the carbonyl group at C-2 points towards the benzene spacer unit of clip **36**. This is not consistent with the experimental values of the maximum complexation-induced chemical shifts, $\Delta\delta_{max}$, of the protons H_a ($\Delta\delta_{max}$= 2.94 ppm) and H_c ($\Delta\delta_{max}$= 0.47 ppm) indicating that these protons are strongly influenced by the magnetic anisotropy of the clip arene units and, therefore, certainly are positioned inside the clip cavity. Evidently, other conformers than the calculated energy-minimum structure contribute to the overall complex structure.

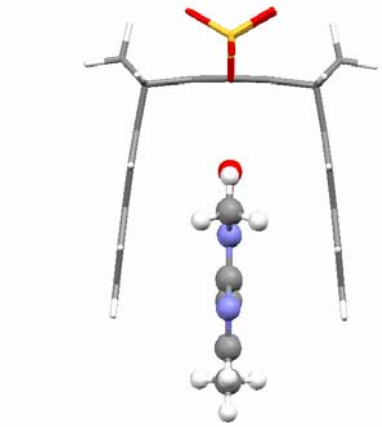

34@36, front view

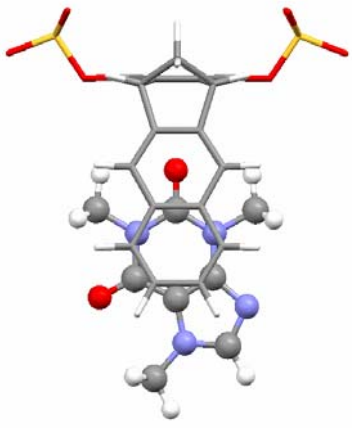

34@36, side view

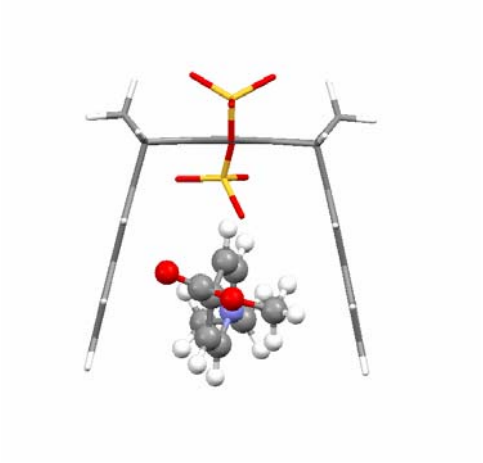

KS@36, front view

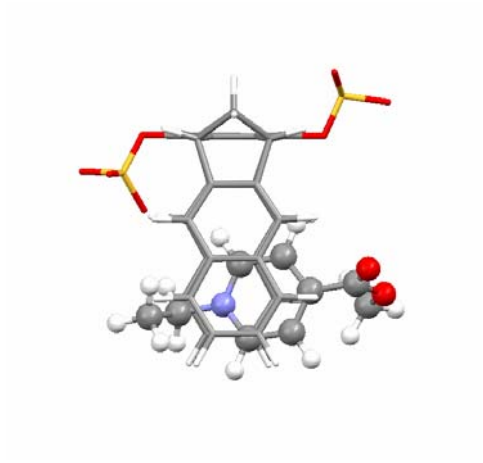

KS@36, side view

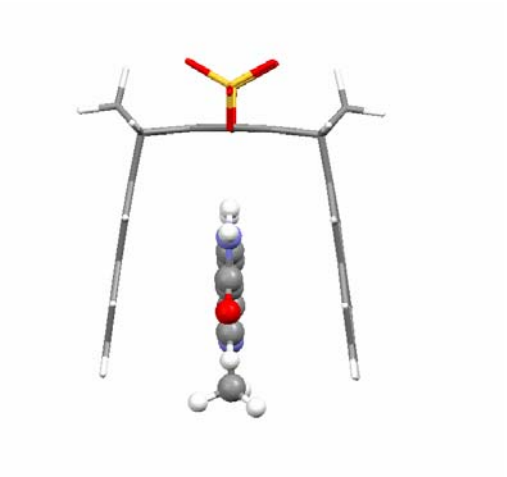

NMNA@36, front view

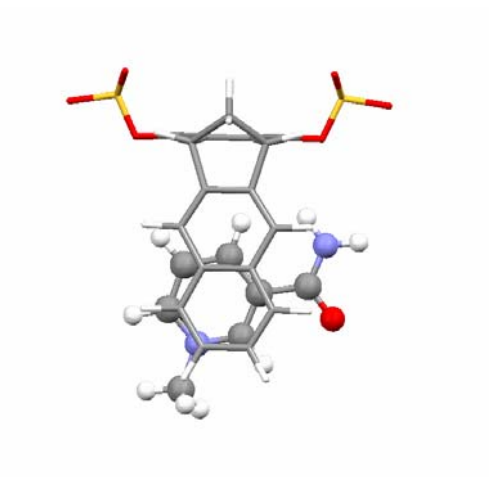

NMNA@36, side view

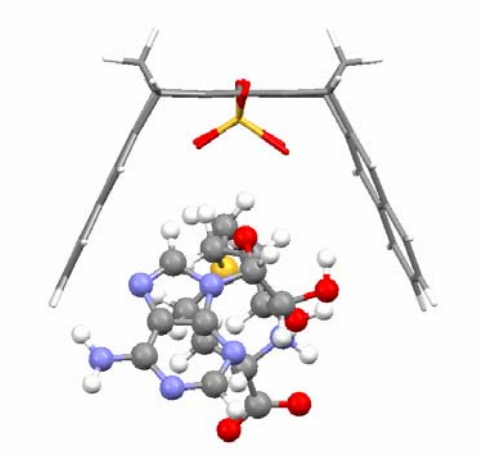

SAM@36 [a], front view

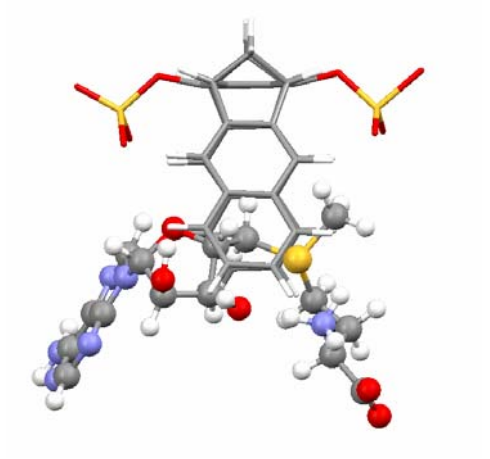

SAM@36 [a], side view

[a] Structure calculated in Spartan'04[141] (MMFF94, gas phase). MacroModel 9.0 does not support sulphonium cations.

Figure 2.48: Calculated structures (MacroModel 9.0, Monte-Carlo simulation, AMBER*, water, 5000 structures) of the complexes **34@36**, **KS@36**, **NMNA@36** and **SAM@36**.

The calculated complex **KS@36** is similar to that of the complex **KS@28** (page 106), with the positively charged nitrogen centered between the sidewalls and the protons H_b positioned inside the clip cavity. The experimental values of $\Delta\delta_{max}$ of the complex **KS@36** in water are, in this case, in good agreement with the calculated structure, as the value for H_b ($\Delta\delta_{max}$= 2.11 ppm) is significantly larger than that of H_a ($\Delta\delta_{max}$= 1.38 ppm). Since the ethyl group is not electron-deficient enough to be inside the clip cavity. The finding that $\Delta\delta_{max}$ values of the ethyl group of Kosower salt are considerably smaller than those of the aromatic ring, indicates that the ethyl group is outside the clip cavity as expected from the results of other clip molecules with aliphatic chains.[115]

According to the calculated complex structure for **NMNA@36** (in *n*-octanol) the pyridinium ring of NMNA is located inside the cavity of the clip, similarly to complex **KS@36**. Furthermore, none of the protons is directly positioned towards the benzene ring of the spacer unit. These results are in accord with the maximum complexation-induced chemical shifts, $\Delta\delta_{max}$, obtained by means of the ^{1}H NMR titration, which show similar values for all the protons (from 1.10 to 1.70 ppm).

MacroModel 9.0 does not support sulphonium cation and therefore the structure of the complex **SAM@36** was calculated with the Spartan'04 software[141] (MMFF94, gas phase). The obtained minimum-energy conformer found is similar to that of the complex of SAM with phosphonate clip, **SAM@18g**, calculated with the same method.[142] Due to steric interactions of the methyl attached to the sulphonium cation, it cannot be fully placed inside the clip cavity and it is slightly shifted outside it. The experimental values of $\Delta\delta_{max}$ confirm this calculated geometry as the proton H_b shows a significantly higher value of maximum complexation-induced chemical shift ($\Delta\delta_{max}$= 1.10 ppm) than those of H_a ($\Delta\delta_{max}$= 0.50 ppm) and H_c ($\Delta\delta_{max}$= 0.52 ppm), due to a stronger influence of the magnetic anisotropy created by the arene system of the clip.

2.6.3 Binding properties of 38 with small aromatic guests molecules

Due to the different structure of the anthracene system of **38**, different binding properties were expected in comparison to those of the clip **36**. As standard guest molecules for the study of the binding properties of **38**, *N*-methylnicotinamide iodide **33** and Kosower salt **84** were chosen. The values of K_a and $\Delta\delta_{max}$ obtained by ^{1}H NMR dilution titrations are shown in Table 2.30.

Guest	Solvent	K_a [M^{-1}]	ΔG [kcal·mol^{-1}]	$\Delta\delta_{max}$ [ppm]
Kosower salt **84**	Methanol-d_4	$(1.78 \pm 0.20)\cdot 10^4$	-5.80	1.63 (H_a) 2.38 (H_b) 0.69 (H_c)
Kosower salt **84**	D_2O	c.p.[a]	-	-
Kosower salt **84**	D_2O/Buffer[a]	c.p.[a]	-	-
NMNA **33**	Methanol-d_4	$(3.69 \pm 0.40)\cdot 10^4$	-6.23	2.09 (H_a) 1.41 (H_b) 2.48 (H_c) 0.30 (H_d)
NMNA **33**	D_2O	c.p.[a]	-	-
NMNA **33**	D_2O/Buffer[a]	c.p.[a]	-	-

[a] Complex Precipitation: precipitation of the 1:1 host-guest complex.

Table 2.30: Association constants, K_a [M^{-1}], Gibbs energy, ΔG [kcal·mol^{-1}], and maximum complexation-induced chemical shifts of the guest protons, $\Delta\delta_{max}$ [ppm], of the **KS@38**, **NMNA@38** and **NAD@38** complexes at 25 ºC.

All the complexes precipitated in both pure D_2O and D_2O/buffer solutions in a 1:1 stoichiometry. This fact could be an indication of very stable complex structures, but at the same time does not permit us to calculate the association, K_a.

In methanol the association constants of the complexes **NMNA@38** and **KS@38**, although being considerably large, are smaller by a factor of 4 and 5, respectively, than those found for the naphthalene sidewalled clip **36** (Table 2.31).

Guest	Host 38 K_a [M^{-1}]	Host 36 K_a [M^{-1}]
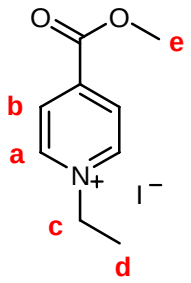 Kosower salt **84**	$1.78 \cdot 10^4$	$6.84 \cdot 10^4$
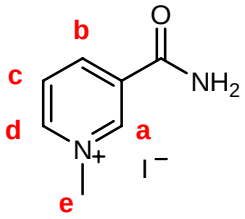 NMNA **33**	$3.69 \cdot 10^4$	$1.76 \cdot 10^5$

Table 2.31: Association constants comparison between the sulphate naphthalene clip **36** and sulphate anthracene clip **38** measured in methanol-d_4 at 25 ºC.

To bind small guest molecules such as NMNA and KS, the anthracene clips must contract the distance between sidewalls in order to optimize the arene-arene interactions, which is a low-energy process.[79, 140] For the previously synthesized anthracene clips (acetoxy, hydroxy and methoxy substituted) the larger van der Waals contact surfaces of the anthracene units were used to explain the higher stabilization of the host-guest complexes in chloroform compared to the complexes of the corresponding naphthalene clips.[79] A similar trend was found for the complexes of the phosphonate substituted anthracene and naphthalene clips **20g** and **18g** with NMNA in methanol-d_4. The complex **NMNA@20g** is more stable by a factor of 6 than the complex **NMNA@18g** (K_a= $1.04 \cdot 10^4$ and $0.17 \cdot 10^4$ M^{-1} respectively). Thus, it is surprising that the complexes of the sulphate substituted anthracene clip **KS@38** and **NMNA@38** are less stable than those of the naphthalene clip **36**. Up to now there is no explanation for this finding.

The calculated complex structures of the anthracene clip **38** (Figure 2.49) show that the guest molecule is better embraced by the larger anthracene sidewalls than in the corresponding complexes of **36** by the smaller naphthalene sidewalls (Figure 2.48).

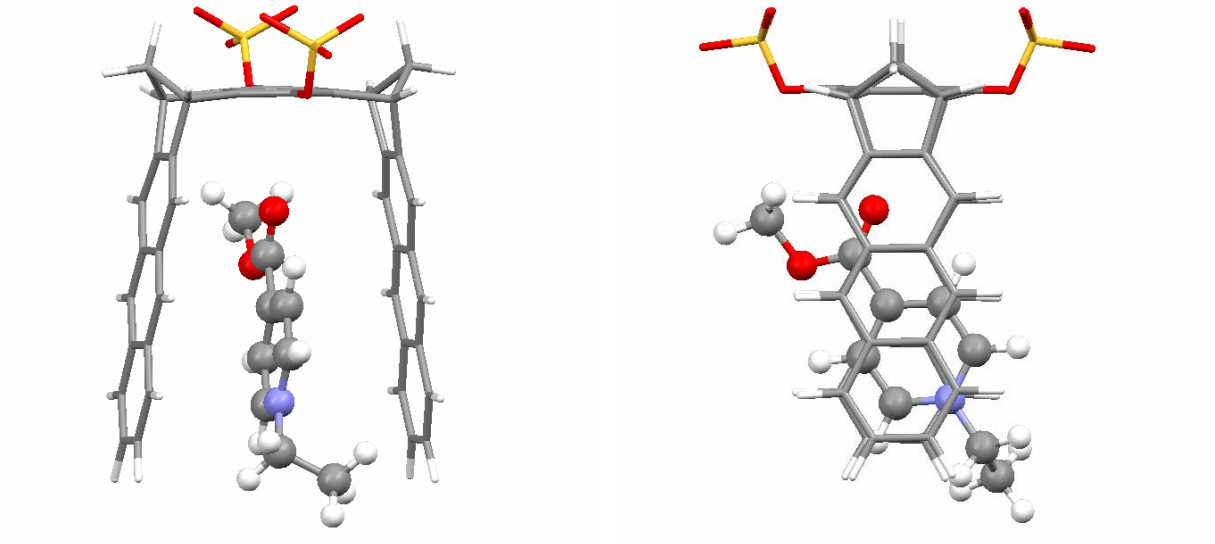

KS@38, front view

KS@38, side view

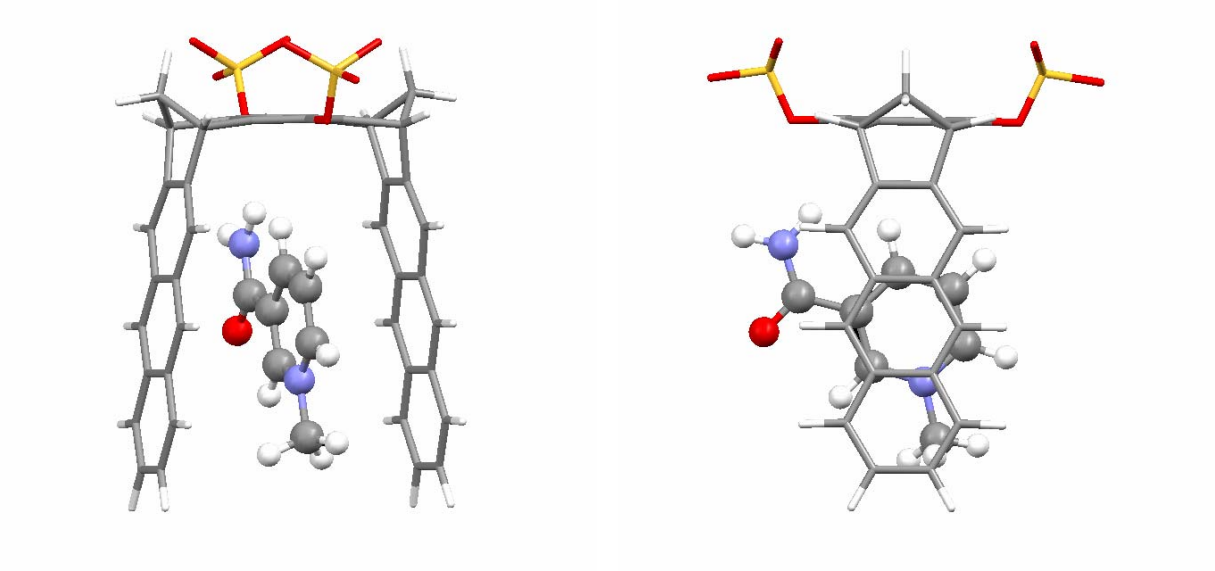

NMNA@38, front view

NMNA@38, side view

Figure 2.49: Calculated structures (MacroModel 9.0, Monte-Carlo simulation, AMBER*, water, 5000 structures) of the complexes **KS@38**, **NMNA@38**.

2.7 Binding of NAD^+ with sulphate substituted clips 36, 37 and 38

NAD^+ is an exceptional guest molecule for molecular clips. Besides its biological relevance (NAD^+ is the cofactor in many enzymatic reactions), the structure of NAD^+ is of

special interest since it has two potential binding sites, the nicotinamide ring (pyridinum salt) and the adenine fused aromatic bicycle. Despite both binding sites are aromatic systems, *a priori*, we predict a notable selectivity of the clips for the nicotinamide ring, since its cationic nature creates a higher electron deficiency than that of the adenine system. We shall be able to observe this selectivity by means of the values of $\Delta\delta_{max}$ of the different protons. For instance, according to this hypothesis, the protons of the nicotinamide ring are expected to show larger $\Delta\delta_{max}$ values than the protons of the adenine unit in the 1:1 host-guest complex.

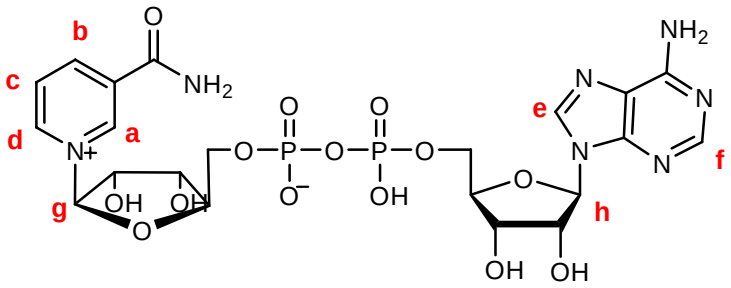

NAD^+, **35**

Figure 2.50: Structure and proton designation of nicotinamide adenine dinucleotide (NAD^+), **35**.

2.7.1 Chiral transfer resulting from NAD^+ binding

In the NAD^+ complex **NAD@36** a remarkable splitting is observed for the ^1H NMR signals (Figure 2.51) of the host protons assigned to the naphthalene sidewalls of **36**, which are equivalent in the free clip (Figure 2.52). In the complexed clip the isolated naphthalene protons H^a and H^f show two singlets and the protons H^b – H^d an ABCD spectrum instead of one singlet and an A_2B_2 spectrum, respectively as found in the free clip. The spectrum of the protons H^b – H^d calculated for an ABCD spin system is in good accord with the experimental data. Evidently, complex dissociation and association as well as conformational equilibration between the different complex structures proceed rapidly with respect to the NMR time scale. These dynamic processes lead to an averaging of the NMR signals of the complex and make the corresponding protons at the two naphthalene sidewalls of complexed clip **36** equivalent to each other, whereas the front- and backside protons of each naphthalene sidewall remain non-equivalent. This finding can be explained with a chirality transfer of the chiral guest NAD^+ to the achiral clip **36** as depicted in Figure 2.52 for one complex structure including the adenine system inside the clip cavity.

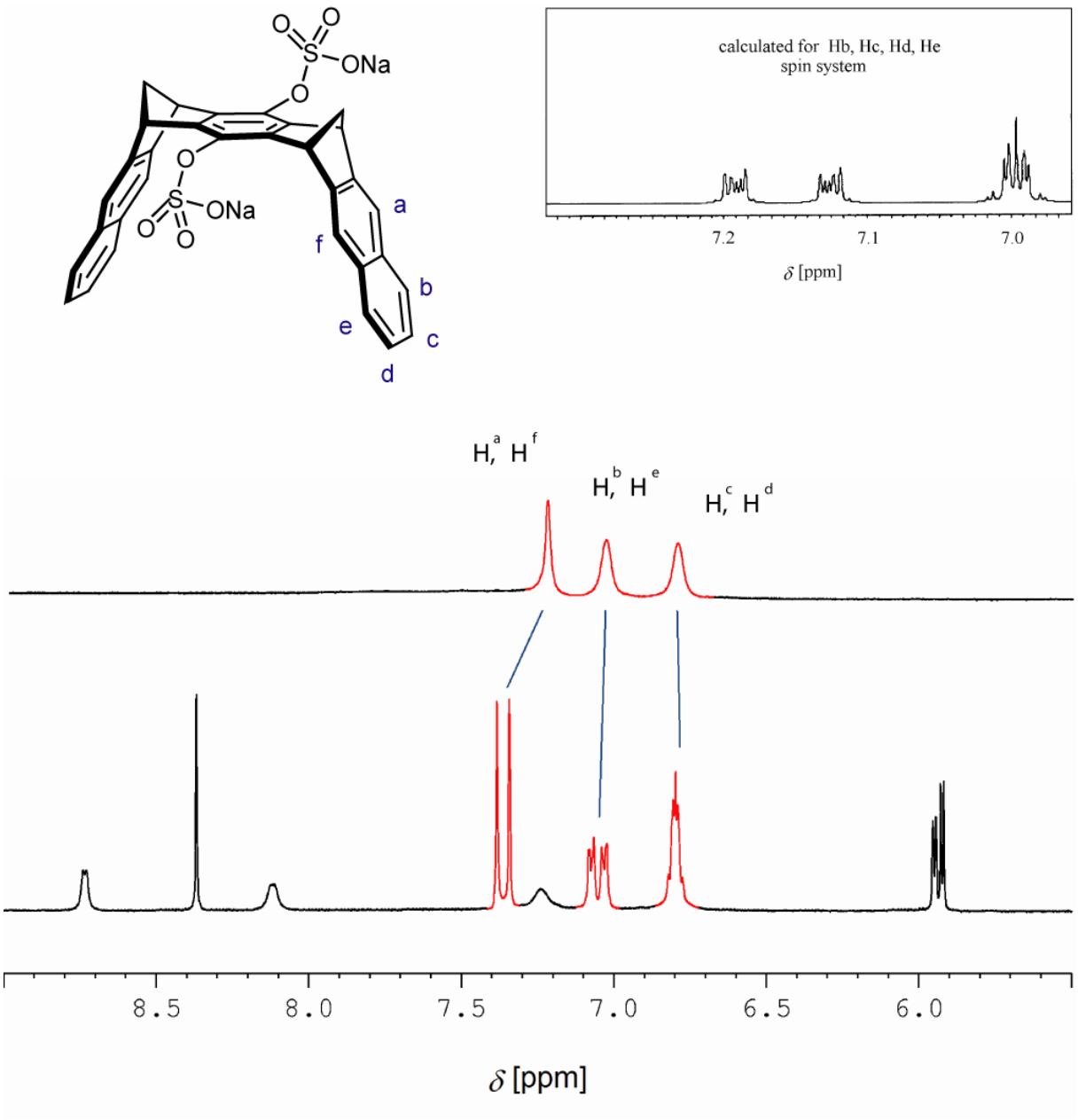

Figure 2.51: Bottom: comparison of the aromatic region of the experimental ^{1}H NMR spectra in D_2O of the free clip **36** and the 1:1 complex **NAD@36**. The signals of the naphthalene sidewall are highlighted in red. Top: calculated spectrum for a H^b, H^c, H^e, H^e spin system.

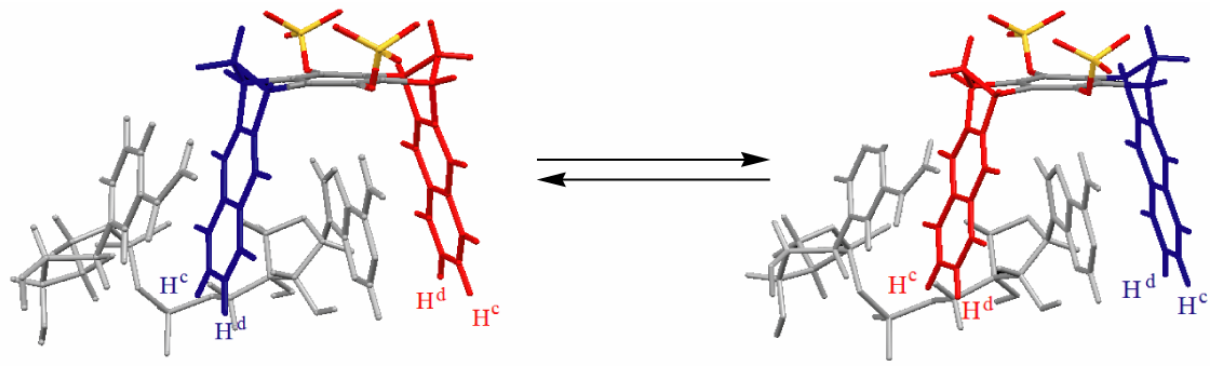

Figure 2.52: A formal 180° rotation around the C_2 axis through the central benzene spacer-unit of the clip molecule leads to a pair-wise exchange of the host protons (e. g. H^c and H^d) at the naphthalene sidewall marked in blue with those of the other ones marked in red as it is shown for one complex structure including the adenine inside the clip cavity calculated for complex **NAD@36** by force field (MacroModel 9.0, Monte-Carlo simulation, AMBER*, water, 5000 structures). Similar conclusions can be drawn for other complex structures, e. g. for those including the nicotinamide ring inside the clip cavity. In any case the corresponding host protons at one and the same naphthalene sidewall remain non-equivalent.

2.7.2 Binding properties of 36 and 37 with NAD^+

The binding experiments carried out with the naphthalene sulphate clips **36** and **37** as well as the data for the phosphonate and phosphate clips, **18g** and **18h**, are summarized in Table 2.32. All these data were obtained from ^1H NMR dilution experiments.

Clip	Cond.	$\Delta\delta_{max}$ [ppm]						K_a [M^{-1}]	ΔG [kcal·mol^{-1}]
		H_a	H_b	H_c	H_d	H_e	H_f		
36	D_2O	0.50	0.93	1.19	0.62	0.27	-	8040±810	-5.33
37	D_2O	0.60	1.13	2.04	0.76	0.32	-	6240±630	-5.18
36	NaOD[a]	0.83	1.78	-	1.15	0.17	-	945±95	-4.06
37	NaOD[a]	1.03	2.19	-	1.42	0.21	0.38	920±90	-4.04
36	Buffer[b]	0.79	1.71	-	1.07	0.18	0.30	1420±130	-4.30
18g	Buffer[b]	1.20	2.88	3.17	1.54	1.61	0.52	4200±315	-4.94
18h	Buffer[b]	1.22	2.75	3.17	1.51	0.90	0.41	5630±570	-5.12

[a] NAD^+ neutralized until pH= 7 with NaOD.

[b] Aqueous phosphate buffer (pH= 7.2).[132]

Table 2.32: Association constants and maximum complexation-induced chemical shifts of the complexes between NAD^+ and naphthalene sulphate clips **36** and **37** and the phosphate clip **18h** and phosphonate clip **18g** in aqueous solution.

NAD^+ shows an acid value of pH in water solution (pH≈ 3). In order to observe how the pH affects the value of the association constants, three different experiments were performed: first, the association constants were measured with both host and guest as they are, secondly NAD^+ was used after its neutralization with NaOD and finally the association constant was measured in buffer aqueous solution (pH= 7.2). This last experiment is particularly important as most enzymatic reactions, where NAD^+ acts as cofactor, take place in buffered aqueous solution under analogous conditions.

The complex formation between the molecular clips and NAD^+ is complicated by the fact that NAD^+ forms a higher self-aggregate in aqueous solution.[81] Most recent results of ITC measurements[90] indicate that NAD^+ exists in monomeric form in buffered aqueous solution at pH= 7.2. From the small complexation-induced ^{1}H NMR shifts of the NAD^+ protons observed in aqueous solution, it can be assumed that the sulphate clips **36** and **37** investigated in this work bind NAD^+ without cleaving the self-aggregate.

The smaller association constants obtained for the complexes with neutralized NAD^+ can be explained by the structure resulting from that neutralization. This structure is doubly negatively charged at the diphosphate group (highlighted in red in Figure 2.53) and, according to the mentioned ITC measurement, NAD^+ exists in its monomeric form. Thus by folding of the guest molecule around the naphthalene sidewalls (Figure 2.54), repulsive interactions are created between the electron-rich sidewalls of the clip and the negatively charged oxygens of the diphosphate unit of NAD^+, which obviously destabilize the complex. These interactions are not as strong in the case of the monoprotonated diphosphate bridge of NAD^+ because in this case there is only one negative charge at this diphosphate group, but a quantitative comparison is difficult because NAD^+ exists as self-aggregate in pure water.

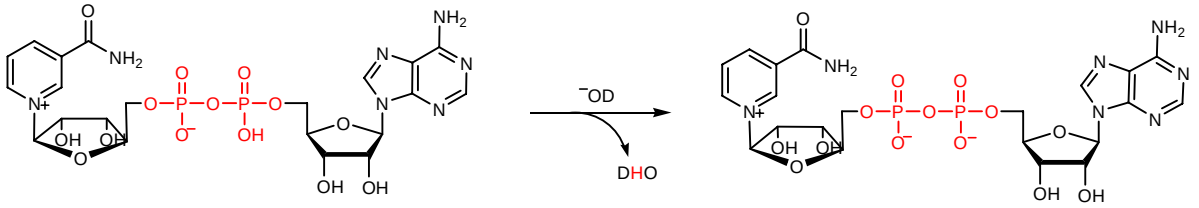

Figure 2.53: Structure of the NAD^+ (left side) and the resulting structure of its neutralization with NaOD.

The ^{1}H NMR dilution titration measured in aqueous phosphate buffer solution led to an association constant only slightly higher than those measured with the neutralized NAD^+, which is not surprising, since the pH of the both solutions are not significantly different. For instance the pH of the solutions with neutralized NAD^+ was pH= 7, while the phosphate buffer solutions are standardized to the physiological pH= 7.2.

More significant is the difference between the association constants of NAD^+ in buffer solution of the sulphate clip **36** and the phosphate clip **18h** (1420 M^{-1} and 5630 M^{-1} respectively). As explained before the phosphate groups of **18h** are partially protonated at pH= 7.2 and thus these groups are able to further stabilize the complex by means of hydrogen bonds with the guest. Since the sulphate clips are already neutral in water solution, the use of buffer at pH= 7.2 does not partially protonate the negatively charged oxygen and finally the

hydrogen-bonding does not take place and the complex is not extra stabilized, as reflected by the values of K_a.

Surprisingly, the phosphonate clip **18g** also shows a larger association constant with NAD^+ in buffer solution than that of the sulphate clip **36**. As shown in Figure 2.46, phosphonate clip **18g** does not show self-aggregation in aqueous solution. Therefore, although the phosphonate substituents in clip **18g** could create a certain degree of steric repulsion with the guest (due to the methyl groups), this is compensated by the absence of the self-aggregation process observed in the other water-soluble anionic clips.

2.7.2.1 Calculated structure of the NAD@36 complex in water

The values of the maximum complexation-induced chemical shifts, $\Delta\delta_{max}$, resulting from the ^{1}H NMR dilution titrations show that, in all the cases, the values determined for the protons at the nicotinamide ring are significantly larger than those obtained for the adenine protons. This finding is good evidence that the clip binds selectively the pyridinium ring as it was expected due to the cationic nature of the nicotinamide ring. Additionally the $\Delta\delta_{max}$ values for each proton appear to be similar for all the receptors, which suggest similar relative position inside the clip cavity.

The conformational search (MacroModel 9.0, Monte-Carlo simulation, AMBER*, water, 5000 structures) for the complex **NAD@36** led to an unexpected structure of minimum energy, with the adenine ring inside the clip cavity (Figure 2.54). While the ability of the clip to bind adenine systems is actually not surprising, the unusual fact about the calculated structure is the selectivity of **36** for adenine versus the positively charged (and therefore more electron-deficient) pyridinium ring of nicotinamide.

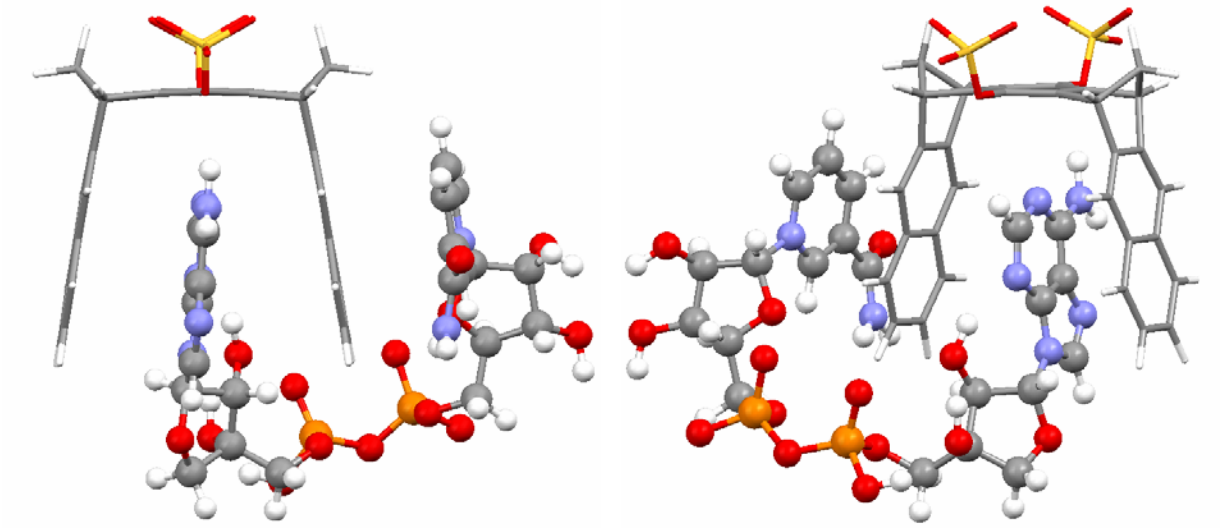

NAD@36, front view **NAD@36**, side view

Figure 2.54: Minimum energy conformer (MacroModel 9.0, Monte-Carlo simulation, AMBER*, water, 5000 structures) of the complex **NAD@36**.

For a better understanding of this result, further conformational searches in MM3*, OPLS and MMFF force-fields (in water as a solvent) were carried out, leading always to a similar structure as that shown in Figure 2.54. These results obtained by the calculations were surprising particularly because the force-field calculation of the NAD^+ complexes with the phosphonate and phosphate substituted clips, **18g** and **18h**, led in each case to complex structures in which both active sites, the adenine unit as well as the nicotinamide ring, were included in the clip cavity. Furthermore we repeated the calculation with several starting structures including either the nicotinamide ring or the adenine unit inside the clip cavity and structures in which the proton at the diphosphate unit of NAD^+ is shifted from one to the other phosphate moiety. In all cases only structures were found in which the adenine unit is included into the clip cavity. In the studied energy range of 50 kcal·mol-1 no structure was found including the nicotinamide ring into the clip cavity. We repeated the calculation with a new modified NAD^+ starting structure: since the ^1H NMR titrations were made in buffer solution, the NAD^+ was completely deprotonated (Figure 2.53, right side). Therefore the input structure was replaced by that with the NAD^+ with the diphosphate group completely deprotonated, as it is in better accord with the experimental conditions. Surprisingly, the structure of minimum energy resulting from the new calculation (conformational search in MacroModel 9.0, Monte-Carlo simulation, AMBER*, water, 5000 structures) was not significantly different from that obtained initially (Figure 2.54), being the relative orientation of the adenine ring inside the cavity only slightly altered (Figure 2.55).

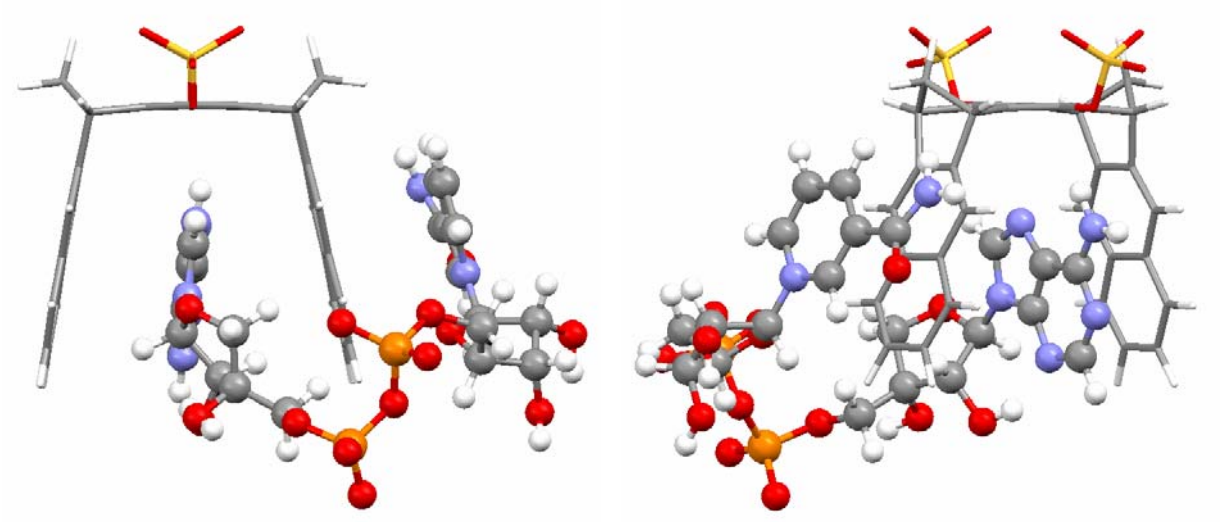

NAD@36, front view

NAD@36, side view

Figure 2.55: Minimum energy conformer (MacroModel 9.0, Monte-Carlo simulation, AMBER*, water, 5000 structures) of the complex **NAD@36** with the anionic form of NAD^+.

In order to gain further insight into the complex structure of sulphate clips **36** and **37**, we studied the complexation of the mononucleotides NMN **111** and adenosine **31**, the two fragments of NAD^+ (Figure 2.56).

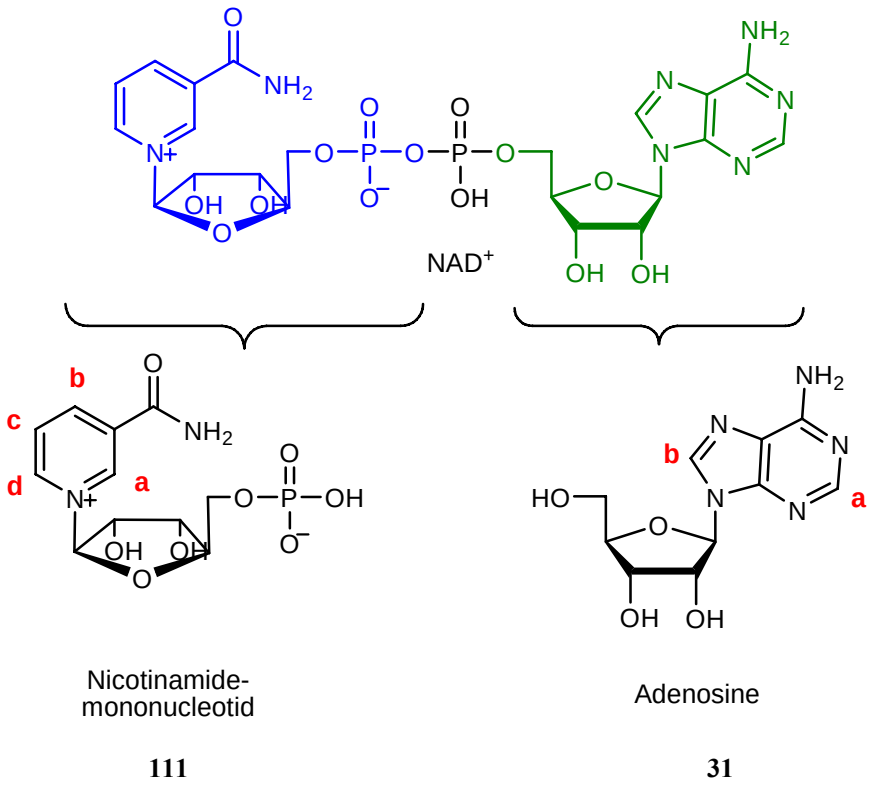

Figure 2.56: Molecules chosen as individual subunits of NAD^+.

The values of association constant, K_a, and maximum complexation induced chemical shifts, $\Delta\delta_{max}$, obtained by means of these ^{1}H NMR titration experiments are summarized in Table 2.33. The nearly identical data gained for the sodium and lithium sulphate clips (**36** and **37** respectively), clearly confirm that the cation plays no role in the complexation properties of the sulphate clips, when the measurement is carried out in buffer solution.

Clip	Guest	K_a [M^{-1}]	ΔG [kcal·mol^{-1}]	$\Delta\delta_{max}$ [ppm]
36	**111**	1225 ± 130	-4.21	0.90 (H_a) 1.80 (H_b) 1.22 (H_d)
36	**31**	260 ± 25	-3.29	0.94 (H_a) 0.78 (H_b)
37	**111**	1330 ± 130	-4.26	1.20 (H_a) 3.43 (H_c) 1.64 (H_d)
37	**31**	210 ± 20	-3.17	1.29 (H_a) 1.06 (H_b)

Table 2.33: Association constants, K_a [M^{-1}], Gibbs energy, ΔG [kcal·mol^{-1}], and maximum complexation-induced chemical shifts of the guest protons, $\Delta\delta_{max}$ [ppm], of the host-guest complexes of **36** and **37** with the individual subunits of NAD^+, nicotinamide mononucleotide and adenosine, in D_2O/buffer solution (pH= 7.2).

The association constants of the complexes with nicotinamide mononucleotide are clearly in the same range as those observed for NAD^+ and, significantly larger, than those obtained for adenosine. Therefore we can assert, that the calculated structure of the **NAD@36** complex shown in Figure 2.54 does not reflect the real structure, as the clip **36** selectively binds the nicotinamide fragment of NAD^+. The similar values of $\Delta\delta_{max}$ gained for NAD^+ and its individual components **31** and **111** also suggest that the pyridinium ring of the nicotinamide mononucleotide is positioned inside the clip cavity in a similar manner as observed in the complex with NAD^+. The calculated structures obtained from a conformational search (MacroModel 9.0, Monte-Carlo simulation, AMBER*, water, 5000 structures) of the complexes **111@36** and **31@36** are shown in Figure 2.57.

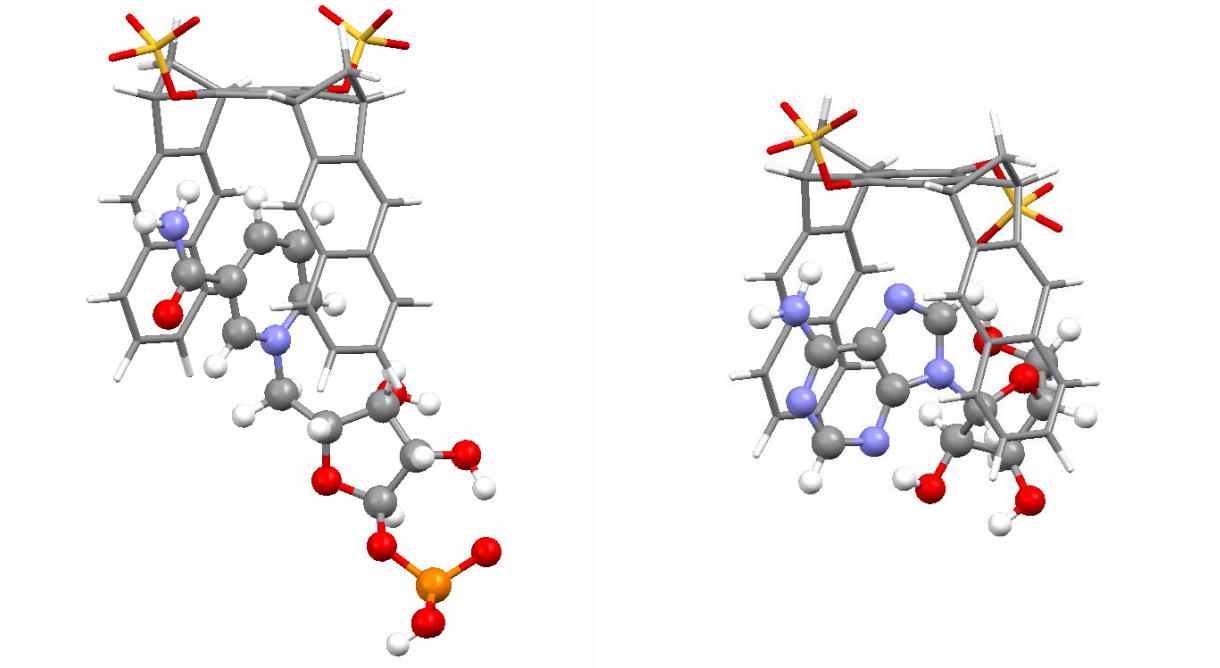

111@36 **31@36**

Figure 2.57: Conformers of minimum energy of the complexes **111@36** and **31@36** (MacroModel 9.0, Monte-Carlo simulation, AMBER*, water, 5000 structures).

Finally, we can only conclude that it is not possible to evaluate the structure of the system **NAD@36** in either water or buffer solution with our resources as the calculated structures do not agree with the experimental evidences ($\Delta\delta_{max}$) obtained for this structure.

2.7.3 Binding properties of 38 with NAD^+

The van-der-Waals contact surfaces of the sidewalls are larger in the anthracene clip **38** than in the analogous naphthalene clip **36**. Thus, in this case more stable host-guest complexes are expected with NAD^+. However, the anthracene clip **38** forms a stable self-aggregate dimer in aqueous solution which has to be cleaved during the complex formation with NAD^+. We explained the result, that NMNA **33** forms with the anthracene clip **38** a less stable host-guest complex than the naphthalene clip **36**, with the self-aggregation of **38**. Therefore, it was interesting to find out whether the anthracene clip **38** forms a stable host-guest complex with NAD^+ or not.

The results of the ^1H NMR dilution titration in phosphate buffer solution (D_2O, pH= 7.2) are shown in Table 2.34.

Guest	Solvent	K_a [M^{-1}]	ΔG [kcal·mol^{-1}]	$\Delta\delta_{max}$ [ppm]
NAD^+ **35**	D_2O/Buffer	$(1.74 \pm 0.20)\cdot 10^4$	-5.78	0.79 (H_a) 1.17 (H_b) 1.08 (H_d) 0.30 (H_e) 0.17 (H_f)

Table 2.34: Association constant, K_a [M^{-1}], Gibbs energy, ΔG [kcal·mol^{-1}], and maximum induced chemical shifts of the guest protons, $\Delta\delta_{max}$ [ppm], of **NAD@38** complex at 25 ºC.

The association constant of the complex **NAD@38** determined by ^{1}H NMR titration is, surprisingly, ten times larger than that determined for the naphthalene sulphate clip **36**. The values of maximum complexation-induced chemical shifts, $\Delta\delta_{max}$, are comparable to those obtained for the complex **NAD@36**, which indicates a similar relative orientation of the guest molecule inside the clip cavity. Again in the minimum energy conformer found for the complex **NAD@38** the adenine ring is bound inside the cavity of the clip (Figure 2.58). This calculated structure again is in disagreement with the experimental observations reflected in the values of $\Delta\delta_{max}$, which show larger shifts for the nicotinamide ring, than for the adenine unit. This finding again suggests the nicotinamide ring to be included into the cavity of clip **38**.

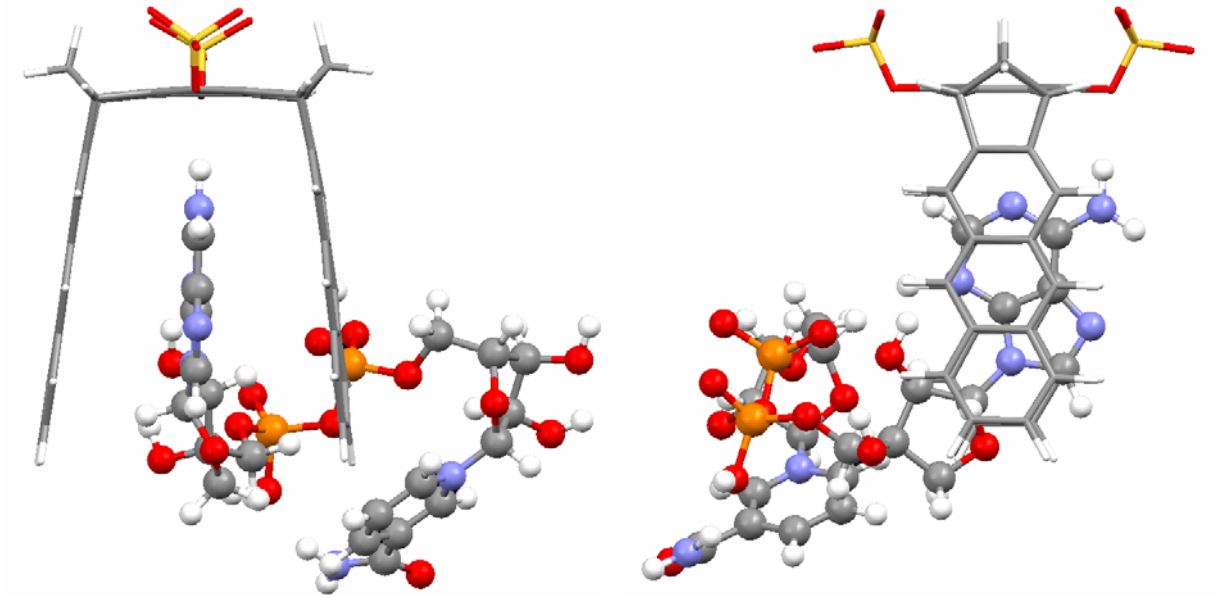

NAD@38, front view **NAD@38**, side view

Figure 2.58: Calculated structures (MacroModel 9.0, Monte-Carlo simulation, AMBER*, water, 5000 structures) of the complex **NAD@38**.

Compared to the $\Delta\delta_{max}$ values determined for the nicotinamide protons of NAD^+ complexes of phosphonate and phosphate substituted clips **18g** and **18h** (Table 2.32), the

$\Delta\delta_{max}$ values of these protons in complex **NAD@38** (Table 2.34) are relatively small indicating a complex structure which is different from a 1:1 host-guest complex structure including the nicotinamide ring into the clip cavity. Moreover, there is a discrepancy to the behaviour of the corresponding phosphonate substituted anthracene clip **20g** which also exists as a highly stable self-assembled dimer in aqueous solution and only forms a weak complex with NAD^+ in aqueous buffered solution at 65 ºC ($K_a \approx$ 100-300 M^{-1}).[143] For that reason we tried to determine the binding constants of the NAD^+ complexes with the anthracene clips **20g** and **38** by the use of fluorimetric titrations. The fluorimetric titrations are usually performed at much lower host-guest concentrations (700-1000 μM) than the ^1H NMR titrations which require host-guest concentrations in the mM range. Indeed, the fluorescence of the anthracene clips **20g** and **38** appearing at m_{axi}= 504 nm (on excitation at e_{xec}= 354nm) is quenched by the addition of NAD^+ (Figure 2.59).

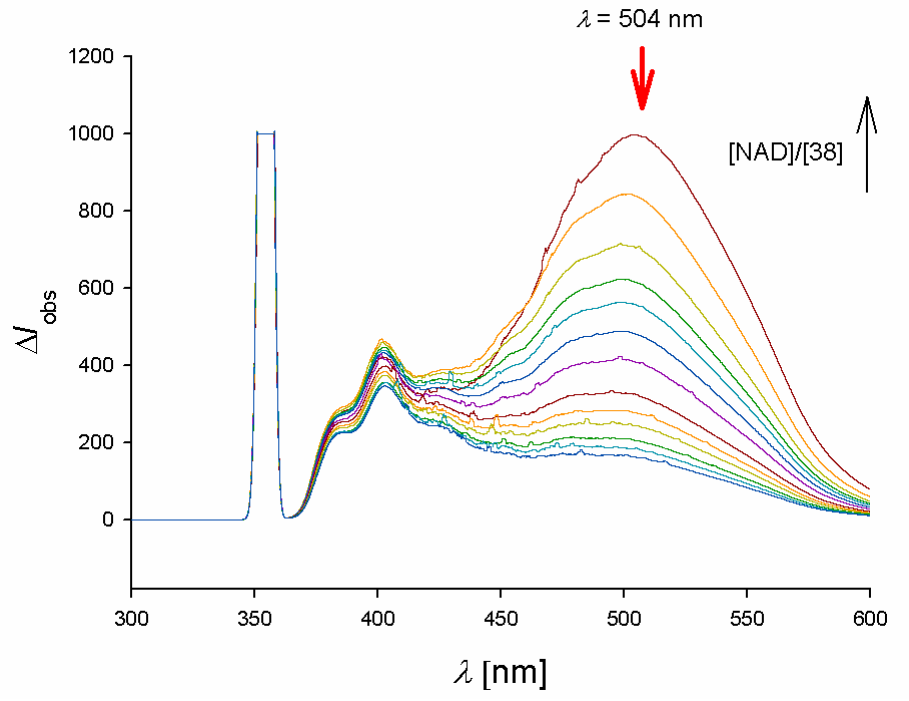

sulphate anthracene clip **38**

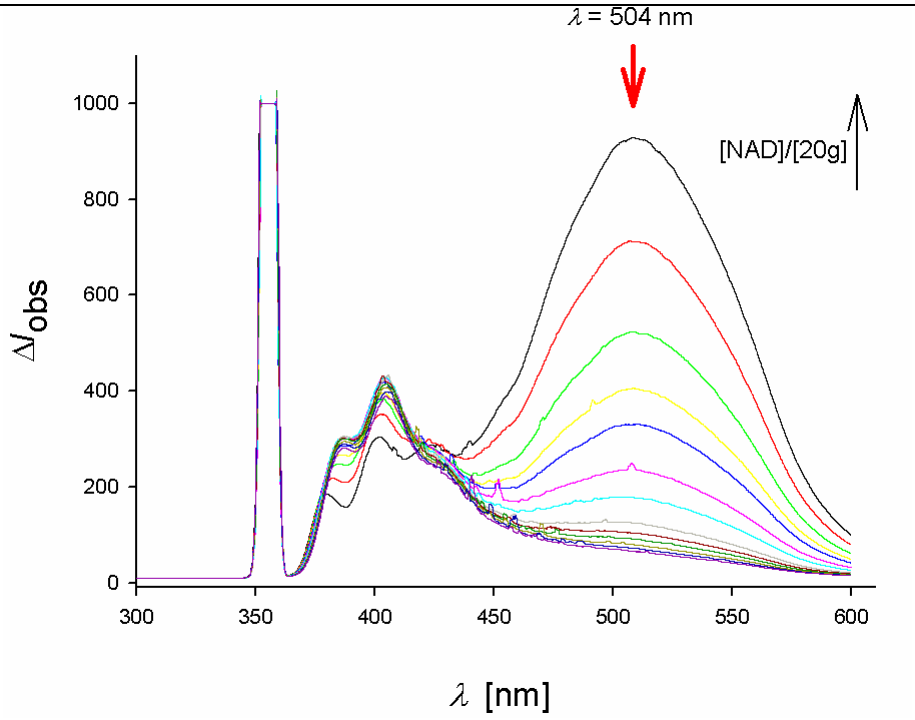

phosphonate anthracene clip **20g**

Figure 2.59: Evolution of the fluorescence spectrum of a mixture of **NAD**$^+$ and **38** (top) and a mixture of **NAD**$^+$ and **20g** (bottom) at different host-guest ratios in a buffer solution (pH= 7.2). The Ib_{os} (I_{max}-I) decreases at higher [**NAD**$^+$]/[**host**] ratios due to the quenching of the naphthalene fluorescence by the NAD$^+$, induced by complexation. Excitation of clip fluorescence at e_{xec}= 354nm.

The representation of the maximum of emission intensity at λ= 504 nm (Figure 2.59) versus the **[NAD$^+$]/[host]** ratio, led to the titration curves shown in Figure 2.60, from which the association constants were calculated to be K_a= 3600 M^{-1} for the complex **NAD@38** and K_a= 8800 for the complex **NAD@20g**.

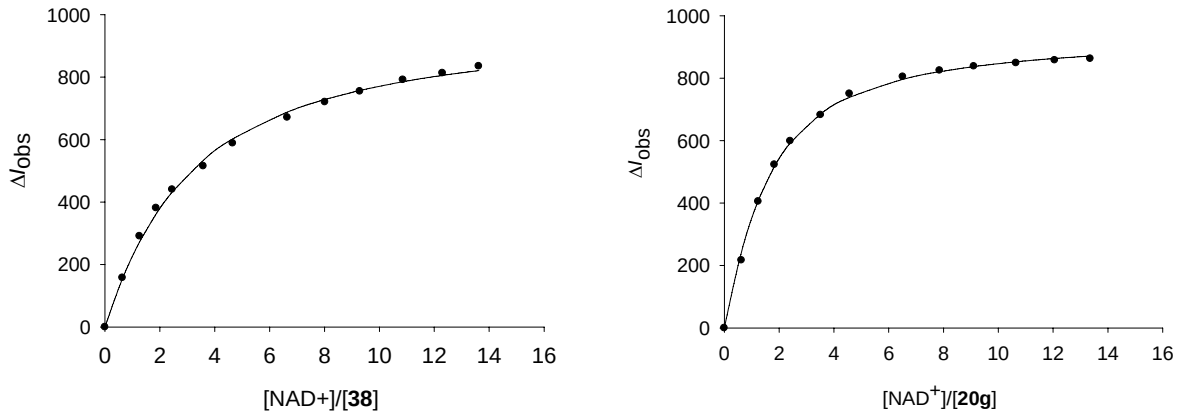

sulphate anthracene clip **38**

K_a= 3600 ± 200 M^{-1}

phosphonate anthracene clip **20g**

K_a= 8800 ± 370 M^{-1}

Figure 2.60: Plot of the variation of emission intensity at λ= 504 nm versus different **[NAD$^+$]/[38]** ratios (left) and **[NAD$^+$]/[20g]** ratios (right) and the value of association constant obtained for the **NAD@38** and **NAD@20g** complexes.

The association constant for the complex **NAD@38** calculated by fluorescence spectroscopy differs from that determined by ^{1}H NMR dilution titration by a factor 1/5.

The binding constant determined for complex **NAD@38** is smaller by a factor of 1/2.5 than that obtained for the phosphonate substituted anthracene clip **20g** (-OP(O)(CH_3)O$^-$) with NAD$^+$ under the same conditions by the use of fluorescence spectroscopy (Figure 2.60).[144] See chapter 4.5.3, page 234, for the detailed data regarding fluorescence titrations.

In the case of clip **20g** the binding constant determined by fluorimetric titration is much higher, by a factor of 40, than that derived from the ^{1}H NMR titration experiment. These discrepancies between the values determined either by fluorimetric or ^{1}H NMR titration experiments, evidently, result from the self-aggregation processes of the anthracene clips **38** and **20g**. At the low concentrations of clip **38** or **20g** and NAD$^+$ used for the fluorimetric titrations the equilibria **38**$_2$ $\rightleftharpoons$ 2·**38** and **20g**$_2$ $\rightleftharpoons$ 2·**20g** are shifted toward the monomeric clip that is able to form the 1:1 host-guest complexes with NAD$^+$. At the higher concentrations used for the ^{1}H NMR titrations the clips exist almost exclusively as self-assembled dimers. The association with NAD$^+$ occurs either with clip dimer, as it seems to be the case with sulphate substituted clip **38**, or with monomer which has to be formed prior to the complexation as it seems to be the case with the phosphonate substituted clip **20g**. Therefore, the binding constants determined in highly diluted titrations are certainly the more reliable values.

3 Summary and outlook

3.1 Summary

3.1.1 Molecular tweezers substituted by a G_1-TEG group

The molecular naphthalene spaced tweezer substituted by one TEG dendrimer of first generation **26** was successfully synthesized starting from the well known diacetoxy naphthalene tweezer **15** (Scheme 3.1).

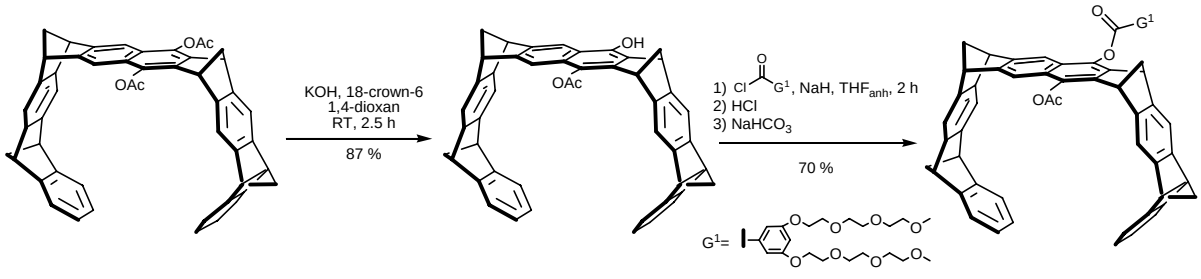

15 **58** **26**

Scheme 3.1: Synthesis of the G_1-TEG tweezer **26** from the diacetoxy tweezer **15**.

The tweezer **26** was obtained in 70 % yield as a racemic mixture, which was confirmed by HPLC using a chiral column. Due to the relatively low C/O ratio the tweezer **26** is not water-soluble and only slightly soluble in methanol (2.8 mg/mL, 2.7 mmol/mL).

The evaluation of the binding properties of **26** by means of ^{1}H NMR was not possible due to the overlapping of the signals corresponding to the guest molecules and those signals corresponding to the TEG branches of the tweezer substituent. Furthermore, isothermal titration microcalorimetry binding experiments did not lead to successful results showing, at best, a highly scattered representation of the measured heat of binding.

Due to the impossibility of synthesizing the tweezer substituted by two G_1-TEG groups at the central naphthalene spacer unit, we focused our efforts on the synthesis and study of molecular clips substituted by neutral hydrophilic groups.

3.1.2 Molecular clips substituted by neutral hydrophilic groups

3.1.2.1 Syntheses

The easily available benzene spaced hydroquinone clip **18c** allowed us to prepare three different types of molecular clips substituted by neutral hydrophilic groups.

Molecular clip **27**, substituted by two G_1-TEG groups, was obtained from the reaction of hydroquinone clip **18c** and the benzoyl chloride **59** (Scheme 3.2) under different conditions as those used for the synthesis of the tweezer **26** and in a significantly lower overall yield (37 %).

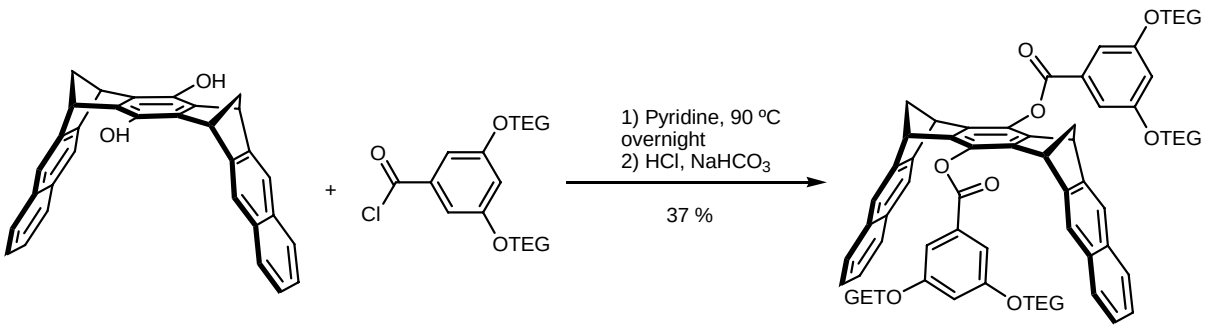

18c **59** **27**

Scheme 3.2: Optimized reaction conditions for the coupling reaction between the dihydroxy clip **18c** and the dendrimer substituent **59**.

All attempts of preparing analogous clips substituted by the second generation of the TEG substituent (G_2-TEG) were not successful, obtaining in most of the cases, the starting materials in conversions between 40 and 92 %. This dissatisfactory result disabled us to study the effect of different generations of the TEG substituents on the supramolecular properties of the corresponding clip.

In cooperation with Prof. Haag and his research group we could study another type of hydrophilic substituents, the hyperbranched polyglycerol groups. Starting, once again, from the hydroquinone clip **18c** as initiator molecule, and submitting it to a polymerization reaction with glycidol **97** as monomer unit, two molecular clips of type **96** of different sizes, substituted by hyperbranched polyglycerol units were obtained (Scheme 3.3).

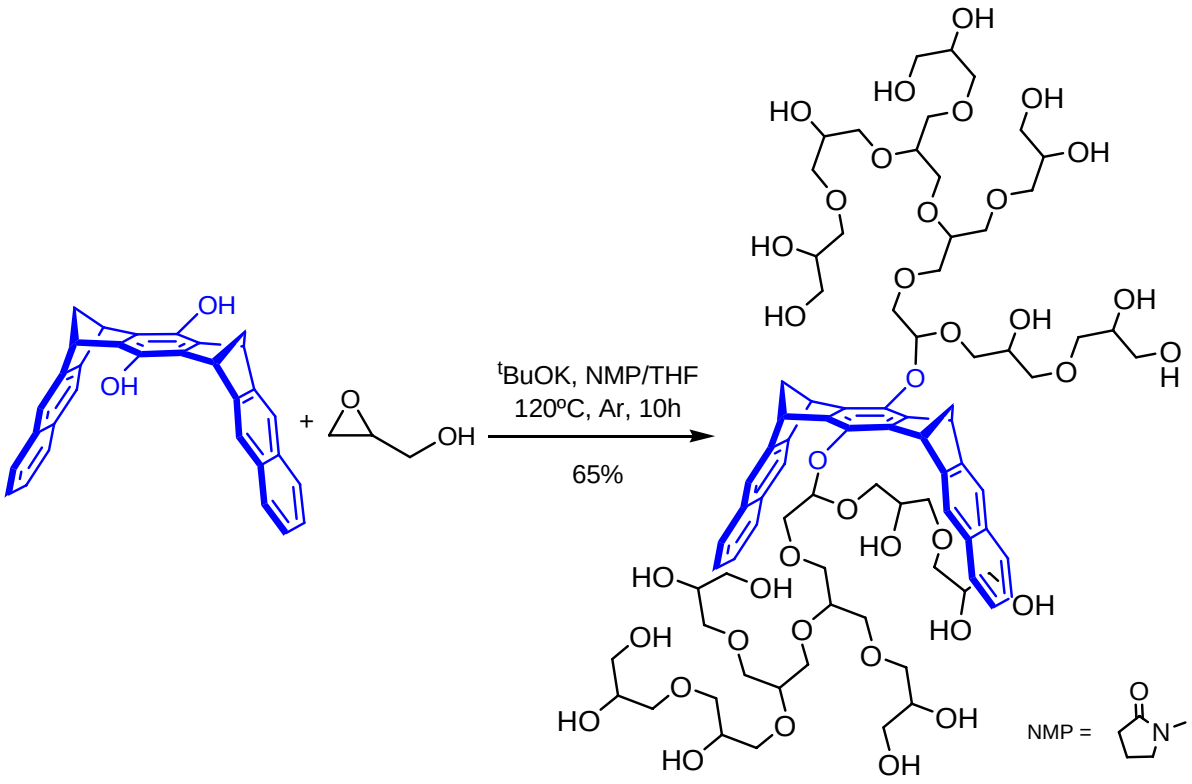

Scheme 3.3: Synthesis of the polyglycerol substituted molecular clips. The clip **96** is one structural model of the hyperbranched polyglycerol substituted clip and does not correspond to any synthesized clip.

The clip **98** was obtained in 65 % yield by the use of 27 equivalents of glycidol with the intention to obtain 1 kD of glycidol units at each side of the central benzene spacer unit. Analogously clip **99** was obtained, in 63 % yield, by using 81 equivalents of glycidol and with the intention to obtain 3 kD of glycidol at each side of the central benzene spacer unit.

Since clips **98** and **99** are products of a polymerization reaction, they have not well defined structures. The MALDI-TOF MS spectrum of **98** shows a distribution of peaks corresponding to clips with 1 up to 22 equivalents of glycidol attached to the central benzene spacer unit.

By means of a stepwise synthesis and in further cooperation with the research group of Prof. Haag, we were able to synthesize the clip **28**, substituted by the first generation of hyperbranched polyglycerol at the central benzene spacer unit. Contrary to the clips of type **96**, clip **28** has a well defined structure.

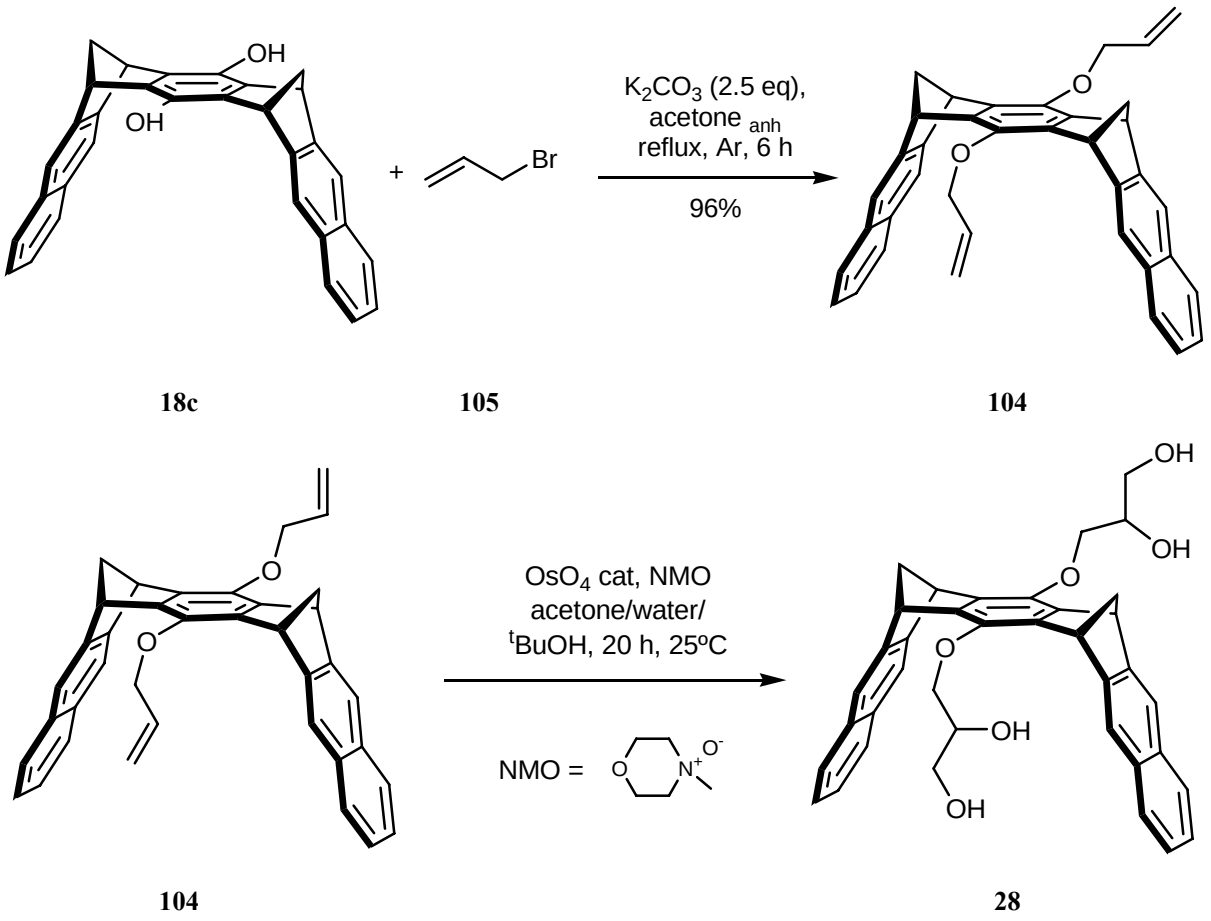

Scheme 3.4: Stepwise synthesis of molecular clip **28**, substituted by the first generation hyperbranched polyglycerol group.

The diallyloxy substituted clip **104** was prepared in our laboratory in Essen, whereas the dihydroxylation of the allyloxy groups in order to obtain clip **28** was carried out in Berlin in the research group of Prof. Haag.

3.1.2.2 Properties

While hyperbranched polyglycerol substituted clips **98** and **99** turned out to be soluble in water, the perfectly structured polyglycerol substituted clip **28** and the G_1-TEG substituted clip **27** did not. G1-TEG substituted clip **27** is soluble in both methanol and chloroform, whereas clip **28** is only soluble in methanol.

By means of conformational search (MacroModel, Monte-Carlo simulation, AMBER*, 5000 structures) it was found that clips **27**, **98** and **99**, with long aliphatic branches at the central benzene spacer unit, do have a tendency to include them inside the clip cavity whereas clip **28**, with shorter branches at the central benzene spacer unit, does not.

The binding properties of clips **27**, **98**, **99** and **28** with the guests show on Figure 3.1 were studied by means of ^{1}H NMR titrations (both standard and dilution).

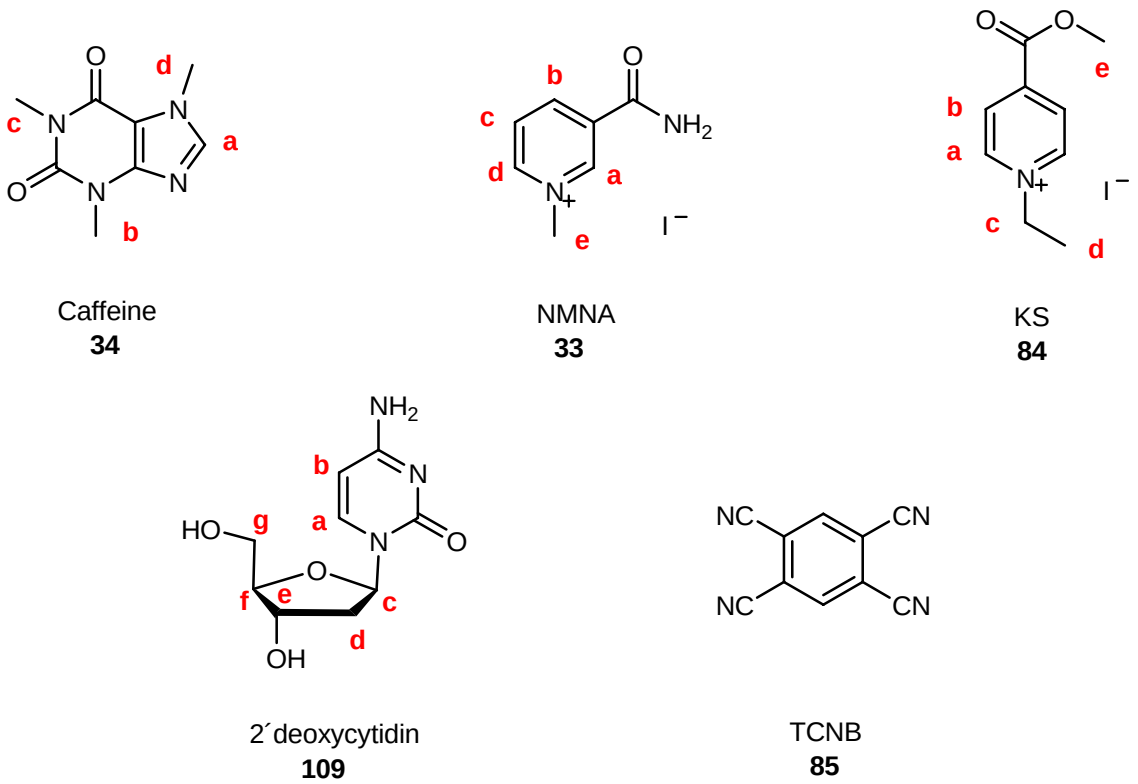

Figure 3.1: Guest molecules used for the study of binding properties of clips **27**, **98**, **99** and **28**.

The most relevant values of association constants gained from these ^{1}H NMR titration experiments with clips **27**, **98**, **99** and **28** are summarized in Table 3.1. Clips **27**, **98** and **28** were evaluated in methanol-d_4, whereas clip **99** was evaluated in D_2O.

	Host			
Guest	**27 K_a [M^{-1}]**	**98 K_a [M^{-1}]**	**99 K_a [M^{-1}]**[a]	**28 K_a [M^{-1}]**
Caffeine **34**	415	1065	175	41
NMNA **33**	65	230	40	60
Kosower salt **84**	235	85	60	45

[a]Measured in D_2O at 25 ºC

Table 3.1: Association constants, K_a [M^{-1}] of the host-guest complexes of **27**, **98**, **99** and **28** in methanol-d_4 at 25 ºC.

Clip **98** appears to be, in general terms, a better receptor for electron-withdrawing guest molecules in comparison to **27**, most likely due to the hydrogen-bond interactions between the guest and the OH groups of the polyglycerol branches of the clip molecule.

3.1.3 Molecular clips substituted by sulphate groups

Molecular clips with both naphthalene and anthracene sidewalls substituted by sulphate groups at the central benzene spacer units were also synthesized in this work. Similar to the clips with hydrophilic neutral substituents, the starting substrates for the synthesis of these sulphate clips are the corresponding hydroquinone clips **18c** (naphthalene sidewalls) and **20c** (anthracene sidewalls).

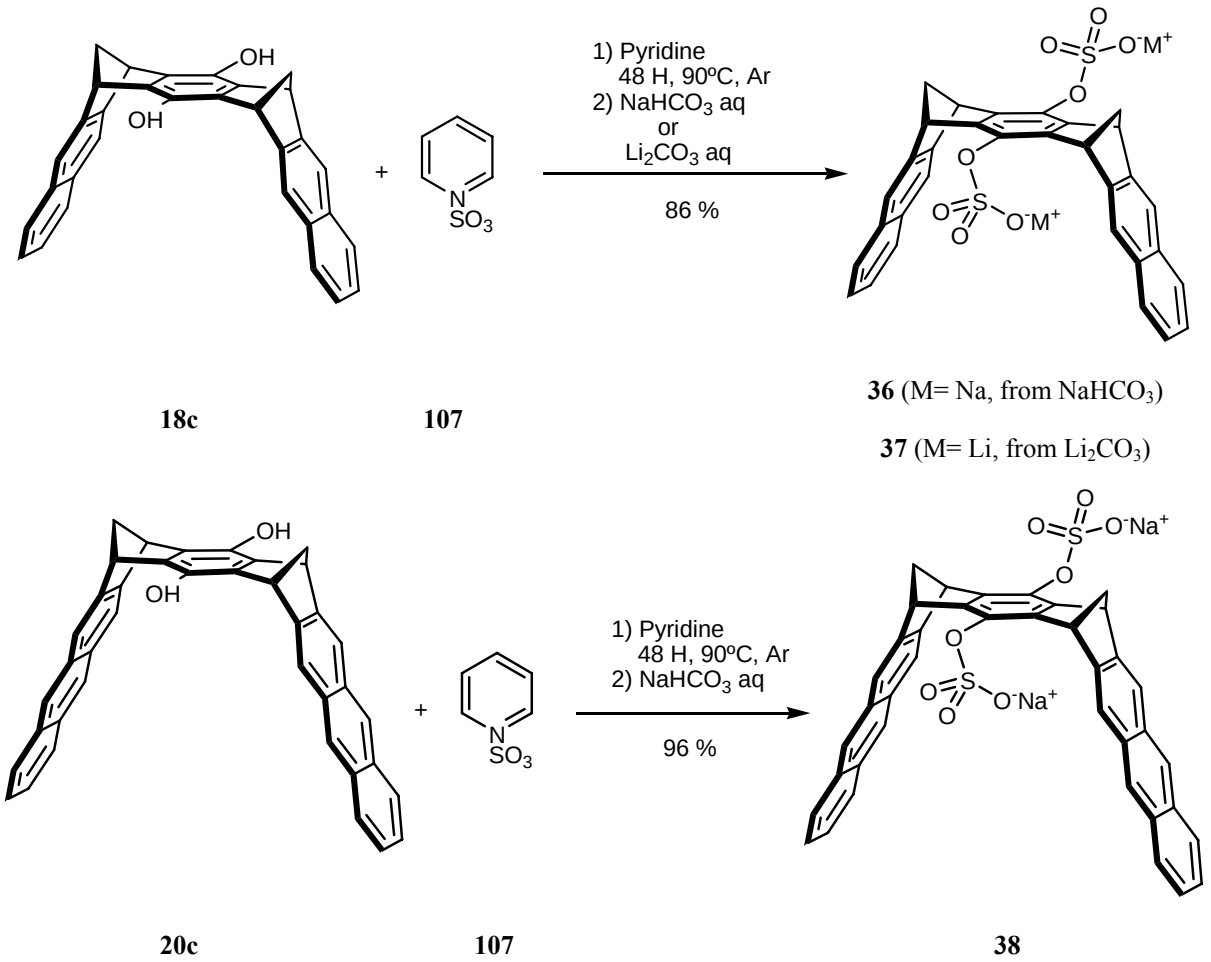

Scheme 3.5: Synthesis of the sulphate substituted clips **36**, **37** and **38**.

All three synthesized sulphate clips **36**, **37** and **38** are completely soluble in water and methanol. When the solvent is changed from methanol-d_4 to D_2O, the ^{1}H NMR signals assigned to the aromatic sidewalls are significantly up-field shifted, broad and without multiplicity. We assumed this phenomenon is caused by a spontaneous self-assembly in water solution, which was further confirmed by the calculated minimum-energy conformations of

the dimer (MacroModel, Monte-Carlo simulation, AMBER*, 5000 structures). The constants of self-assembly for clips **36**, **37** and **38** were experimentally determined by means of dilution ^{1}H NMR titrations, to be 310 M^{-1}, 175 M^{-1} and $1.98 \cdot 10^5$ M^{-1} respectively. Temperature-dependent ^{1}H NMR titrations of **38** allowed us to conclude that the non-classical hydrophobic effect is the driving force for the self-assembly process (ΔH= -12.4 kcal·mol^{-1}, $T \cdot \Delta S_{298\,K}$= -5.2 kcal·mol^{-1} and $\Delta G_{298\,K}$= -7.2 kcal·mol^{-1}).

Similar to the previously described phosphate substituted clip **18g** and the phosphonate clip **20h** the self-aggregation process of the sulphate substituted clips is overruled by the addition of a suitable guest molecule to an aqueous solution of the clip. The binding properties of these clips were studied by means of ^{1}H NMR titration experiments with the guest molecules shown in Figure 3.2.

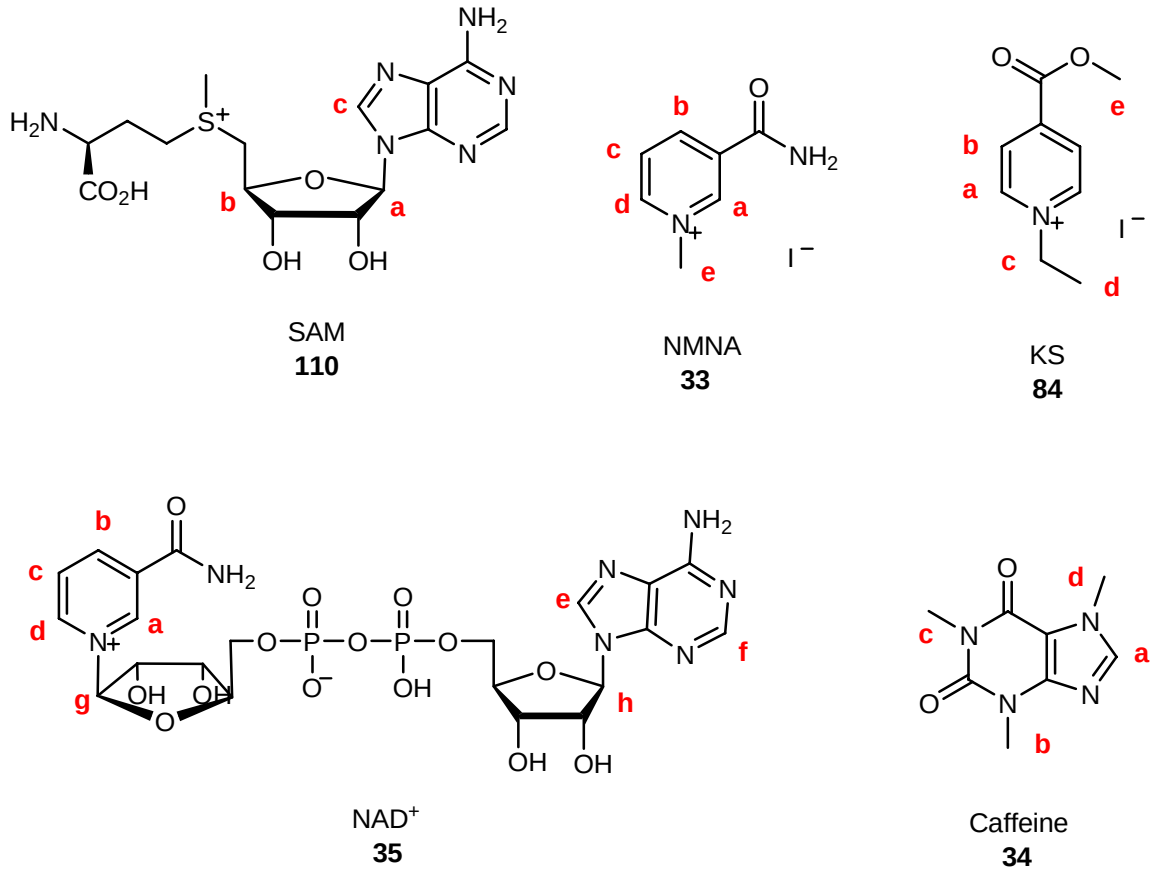

Figure 3.2: Guest molecules used for the study of binding properties of clips **36**, **37**, and **38**.

The most relevant values of association constants gained from these ^{1}H NMR titration experiments with clips **36** and **38** are summarized in Table 3.2.

Guest	Host	
	36 K_a [M^{-1}]	**38 K_a [M^{-1}]**[a]
Caffeine **34**	2900	n.y.e.
NMNA **33**	$1.76 \cdot 10^{5}$ [b]	$3.69 \cdot 10^{4}$ [b]
Kosower salt **84**	$8.16 \cdot 10^{4}$ [a]	$1.78 \cdot 10^{4}$ [b]
SAM **110**	940	n.y.e.
NAD^+ **35**	1420	3800[c]

n.y.e.: not yet evaluated

[a] Measured in pure D_2O

[b] Measured in methanol-d_4 at 25 ºC, the 1:1 host-guest complexes precipitate in both D_2O and D_2O/Buffer (pH=7.2)

[c] Spectrofluorimetric titration

Table 3.2: Association constants, K_a [M^{-1}] of the host-guest complexes of **36** and **38** in D_2O/Buffer (pH= 7.2) at 25 ºC.

3.2 Outlook

3.2.1 Molecular clips substituted by neutral lipophilic groups

Molecular clips substituted by higher generation of both, triethyleneglycol-based and polyglycerol-based, dendrimer substituents shall be further synthesized. For instance, we expect the molecular clips substituted with the second generation of the TEG dendrimer (G_2-TEG, **94**) and the second generation of the hyperbranched polyglycerol **29** (Figure 3.3) to be, finally, water soluble.

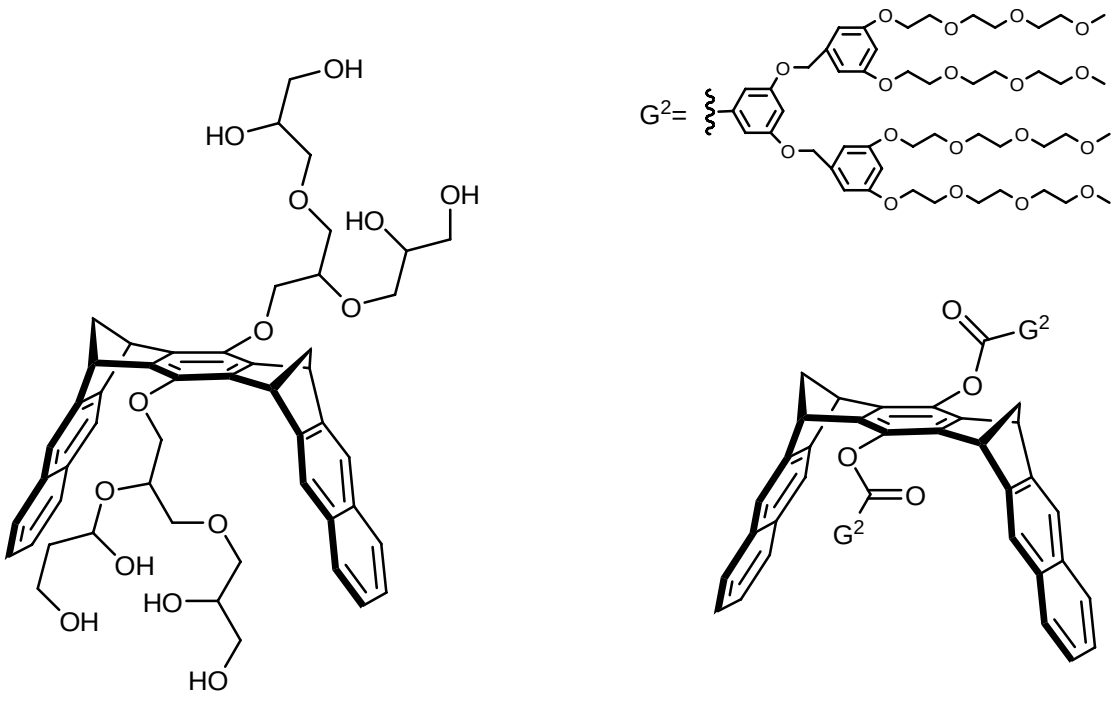

29 **94**

Figure 3.3: Molecular clips substituted by the second generation of hyperbranched polyglycerol dendrimer, **29**, and the second generation of TEG-based dendrimers, **94**.

The binding properties of **29** and **94** shall be evaluated by means of ^{1}H NMR titration experiments with the same guests we used for the already synthesized clips in order to make a rational comparison and evaluation of the effect of the substituents at the central benzene spacer unit on the supramolecular properties.

3.2.2 Molecular clips substituted by sulphate groups

Molecular clips substituted by sulphate groups shall be evaluated as receptors for additional bio relevant guest molecules, for instance NADH (**113**), nicotinamide adenine dinucleotide phosphate (NADP, **114**) and SAM **110**.

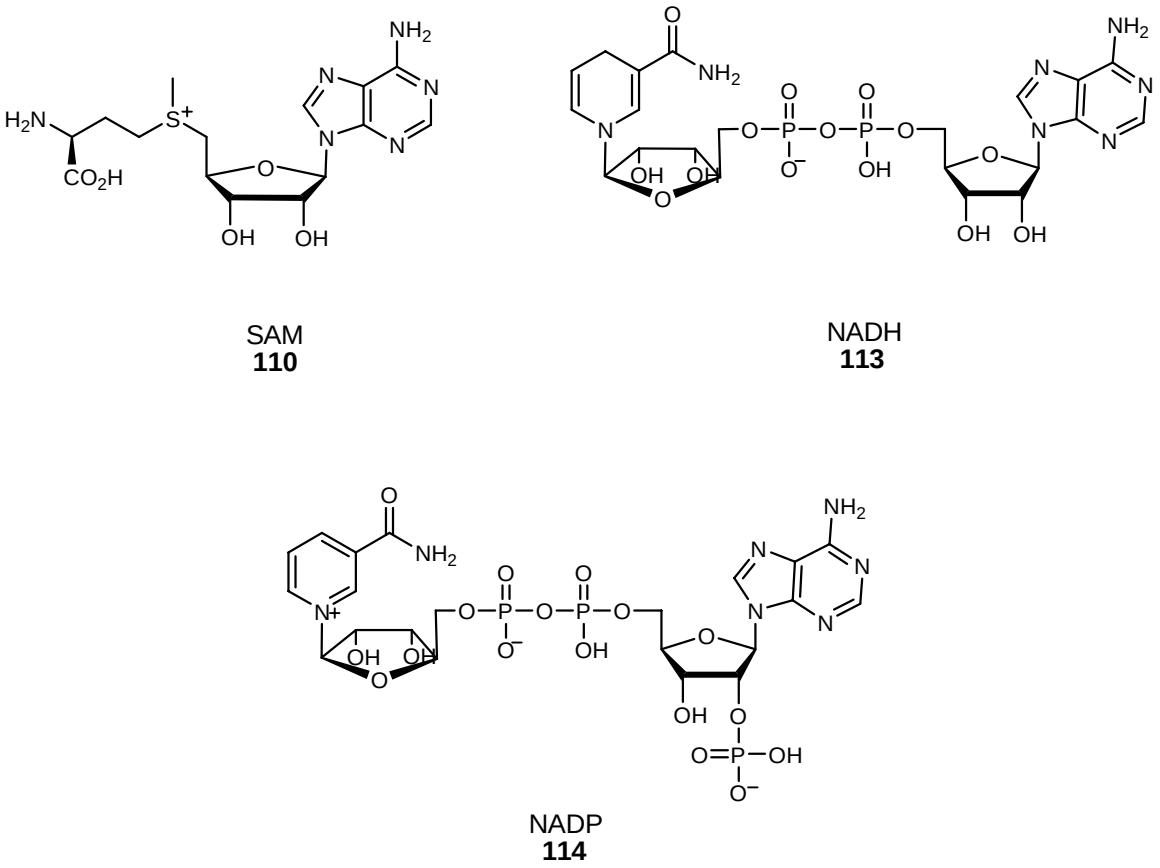

Figure 3.4: Additional bio relevant potential guest molecules for sulphate substituted molecular clips.

Molecular clips substituted by phosphate and phosphonate groups have been recently shown to be inhibitors in enzymatic reactions which include NAD^+ and $NADP^+$ as cofactors (Scheme 3.6).[145]

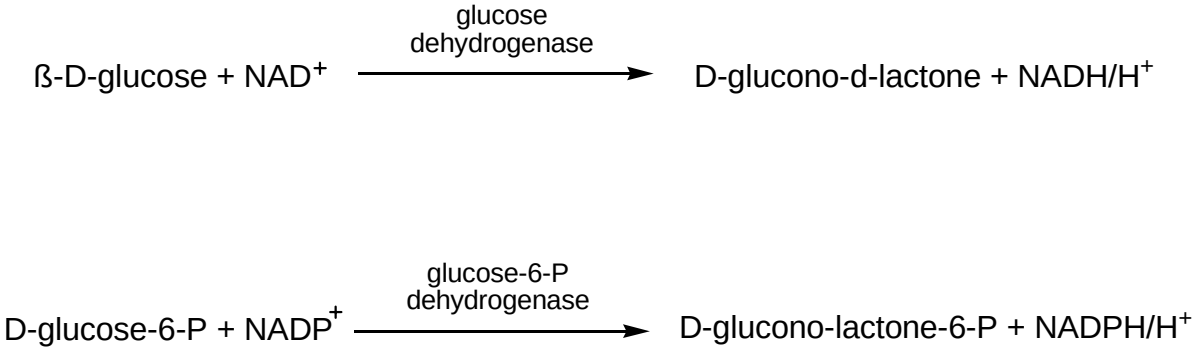

Scheme 3.6: Enzymatic reactions including NAD^+ and $NADP^+$ as cofactors.

Sulphate substituted molecular clips shall be tested as inhibitors, in these enzymatic reactions in order to evaluate the effect of the substituent on the inhibitor properties.

4 Experimental section

4.1 General processes

All the solvents were distilled prior use. When necessary, the solvents were dried following the processes from the literature. In case an oxygen-free solvent or solution was needed, it was put into an ultrasound bath for ten minutes followed by an argon flow for ten minutes more.

Thermolysis:

The glass ampoule was filled, as maximum 2/3 of the whole capacity, with the reaction mixture. The process to evacuate the oxygen from the solution was the following: The ampoule was put into the ultrasound bath for fifteen minutes and after that into an isopropanol/dry-ice cooling bath (-78 ºC). After cooling for ten minutes, an oil-pump vacuum was connected for fifteen minutes. This process was repeated up to three times before the ampoule was sealed under vacuum.

Chromatography:

TLC-sheets with fluorescence indicator SIL g/UV_{254} from the brand Machery und Nagel were employed for thin-layer chromatography (TLC). The detection was carried out with the fluorescence indicator at 254 nm, anisaldehid revealer or iodide.

Silica gel 60 (mesh size 0.0063-0.2 mm) from the brand Fluka was used as stationary phase for the preparative column chromatography.

Melting points:

The melting points were carried out in a Reichert Termovar apparatus and are uncorrected.

4.2 General processes for analytical and spectroscopic methods

NMR Spectroscopy:

A Varian Gemini 200 XL spectrometer was used for the routine ^{1}H NMR spectra . The 1D and 2D NMR experiments for the characterization of new products were carried out by Herrn Dipl.-Ing. Heinz Bandmann and Herrn Dr. Torsten Schaller in a Bruker Advance DRX 500 spectrometer. The 2D experiments for the characterization were: HH-COSY, CH-COSY, HMQC (Heteronuclear Multiple Quantum Coherence) and HMBC (Heteronuclear Multiple Bond Connectivity).

The chemical shifts are given in δ (ppm) in reference to tetramethylsilane (TMS, 0 ppm). The signal of the traces of undeuterated solvent were used as internal reference

($CDCl_3$: 7.24 ppm, methanol-d_4: 3.34 ppm) for ^1H NMR and the signal of the solvent was used for ^{13}C NMR. The multiplicity of the signals is assigned by the following abbreviations and combination of those: s: singlet, d: doublet, t: triplet, q: quadruplet, m: multiplet and br for broad signals. All the coupling constants are given in Hertz (Hz).

Mass Spectrometry:

All the mass spectra (MS and HR-MS) were carried out by Herrn Dipl.-Ing. Werner Karow in a Bruker Bio TOF II using ESI as technique in most of the cases.

IR-Spectroscopy:

The IR spectra were carried out in a FTS 135 (Bio-Rad) spectrometer, using film (in the case of oils) and KBr pill (in the case of solids).

Single-crystal structure:

The analysis of the single-crystal structure was carried out in the working group of Prof. Dr. Roland Boese in the University of Duisburg-Essen (Campus Essen) by Herrn Dipl.-Ing. Dieter Bläser.

4.3 Syntheses

4.3.1 Preparation of dendrimer substituents

Synthesis of Toluene-4-sulfonic acid 2-[2-(2-methoxy-ethoxy)-ethoxy]-ethyl ester, 62[87]

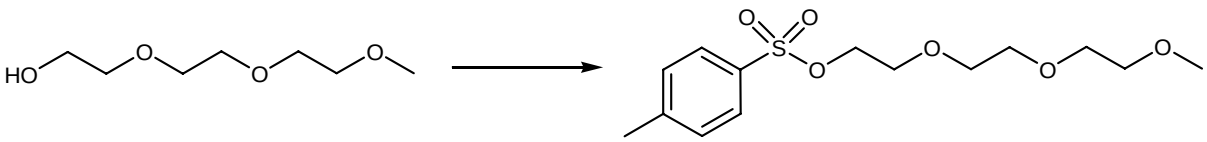

112 **62**

25.5 g (0.65 mol) of NaOH and 72 g (0.44 mol) of the alcohol **112** in a mixture of water (125 mL) and THF (1015 mL) was cooled using an ice bath with magnetic stirring. A solution of *p*-toluenesulfonyl chloride (92 g, 0.48 mol) in THF (125 mL) was added dropwise to the mixture, while maintaining the temperature bellow 5 ºC. The resulting mixture was stirred at 0 ºC for another 3 hours and then poured into an ice-water mixture (250 mL). The mixture was extracted three times with methylene chloride (250 mL), and the combined organic layers were washed twice with diluted HCl solution (pH=1) and once more with brine. After drying with sodium sulphate, the solvent was evaporated *in vacuo* to give 136 g (0.43 mol) of pure desired product **62** as colourless oil in 96 % yield.

Molecular Formula: $C_{14}H_{22}O_6S$ (318.11 g/mol)

MS (ESI-TOF): m/z (%) = 341.2 $[M+Na]^+$

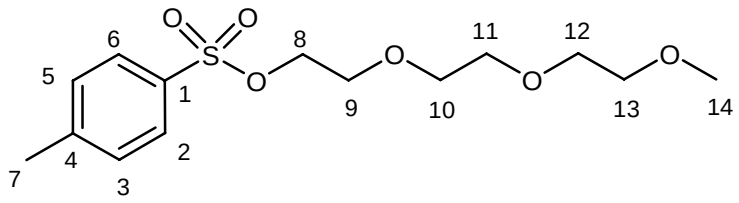

^{1}H NMR (500 MHz, $CDCl_3$) δ[ppm]: 2.43 (s, 3H, H-7), 3.35 (s, 3H, H-14), 3.51 (t, 2H, ^3J(H-13, H-12)=2.9 Hz, H-13), 3.59 (m, 6H, H-12+ H-11+H-10), 3.67 (t, 2H, ^3J(H-8, H-9)=4.9 Hz, H-9), 4.14 (t, 2H, H-8), 7.32 (d, 2H, ^3J(H-2, H-3)=8.2 Hz, H-2+H-6), 7.78 (d, 2H, H-3+H-5).

^{13}C NMR (126 MHz, $CDCl_3$) δ[ppm]: 21.58 (C-7), 58.98 (C-14), 68.63 (CH_2), 69.18 (CH_2), 70.50 (CH_2), 70.52 (CH_2), 70.70 (CH_2), 71.86 (CH_2), 127.93 (C-3+ C-5), 129.77 (C-2+ C-6), 132.99 (C-4), 144.73 (C-1).

IR (Film) $\tilde{\nu}$ [cm^{-1}]: 3064 (st, Csp^2-H), 2877 (st, Csp^3-H), 1598 (ring st), 1452 (scissors vibration, -CH_2-), 1352 (st, S=O), 1177 (antisym st, S-O-C), 1018 (antisym st, C-O-C), 817.

Synthesis of methyl 3,5-Bis-{2-[2-(2-methoxy-ethoxy)-ethoxy]-ethoxy}-benzoate, 61

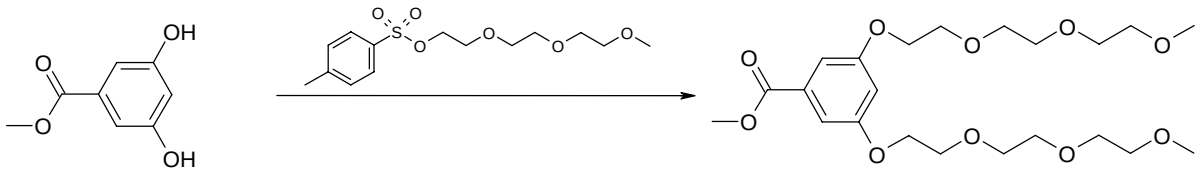

63 **61**

1st Variant[87]

1.31 g (32.7 mmol) of sodium hydride (60 % suspension in mineral oil) was suspended in 15 mL of dry dimethylformamide and then cooled-down into an ice-water bath under argon flow. A solution of methyl 3,5-dihydroxy-benzoate **63** (2.50 g, 14.9 mmol) in dry dimethylformamide (10 mL) was added dropwise and then the resulting mixture was heated to 60 ºC for two hours. Then the mixture was cooled until 0 ºC again and a solution of tosylate **62** (11.8 g, 37.2 mmol) in dry dimethylformamide (10 mL) was added dropwise and the resulting mixture was heated to 55 ºC for 20 hours. After allow room temperature, 150 mL of ethyl acetate and 25 mL of water were added to give a clear 2-phase solution. The organic layer was separated and washed two times with 25 mL of water, dried with sodium sulphate, filtrated and the solvent removed *in vacuo* to give 10 g of crude. This crude was purified by column chromatography on silica gel using ethyl acetate/methanol (9:1) as eluant to give, finally, 3.52 g (7.7 mmol) of the desired product **61** as pale-yellow oil in 51 % yield.

2nd Variant

5.0 g (30.1 mmol) of methyl 3,5-dihydroxy-benzoate **63**, 19.2 g (60.2 mmol) of the tosylate **62** and 10.0 g (72.3 mmol) of potassium carbonate were dissolved in 35 mL of dry dimethylformamide and heated, under argon, at 80 ºC for three hours. After cooled down to room temperature water (50 mL) and dichloromethane (50 mL) were added to the mixture. The aqueous layer was washed three times with 50 mL of dichloromethane and the combined organic layers were dried with sodium sulphate, filtered and the solvent removed under reduced pressure. 13.3 g (28.9 mmol) the desired **61** product was obtained in 96 % yield.

Molecular Formula: $C_{22}H_{36}O_{10}$ (460.23 g/mol)

MS (ESI-TOF): m/z (%) = 483.2 (100 %) $[M+Na]^+$

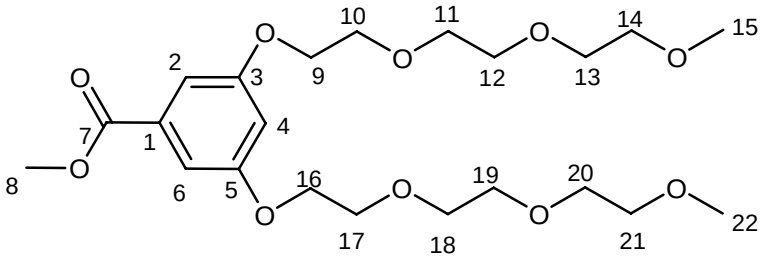

^{1}H NMR (500 MHz, $CDCl_3$) δ[ppm]: 3.35 (s, 6H, H-15+H-22), 3.53 (m, 4H, H-14+H-21), 3.64 (m, 8H, H-11+H-12+H-18+H-19), 3.71 (m, 4H, H-13+H-20), 3.83 (t, 4H, ^{3}J(H-10, H-9)=4.8 Hz, H-10+H-17), 3.87 (s, 3H, H-8), 4.17 (t, 4H, H-9+H-16), 6.67 (t, 1H, ^{4}J(H-4, H-2)=2.3 Hz, H-4), 7.17 (d, 2H, H-2+H-6).

^{13}C NMR (126 MHz, $CDCl_3$) δ[ppm]: 52.19 (C-8), 59.02 (C-15+C-22), 67.73 (CH_2), 69.58 (CH_2), 70.57 (CH_2), 70.65 (CH_2), 70.84 (CH_2), 71.92 (CH_2), 106.90 (C-4), 108.01 (C-2+C-6), 131.86 (C-1), 159.74 (C-3+C-5), 166.75 (C-7).

IR (Film) $\tilde{\nu}$ [cm^{-1}]: 2878 (st, Csp^3-H), 1722 (st, C=O), 1598 (ring st), 1446 (scissors vibration, -CH_2-), 1243 (st, C-O-C), 1111 (antisym st, C-O-C), 857, 768.

Synthesis of 3,5-Bis-{2-[2-(2-methoxy-ethoxy)-ethoxy]-ethoxy}-benzoic acid, 23

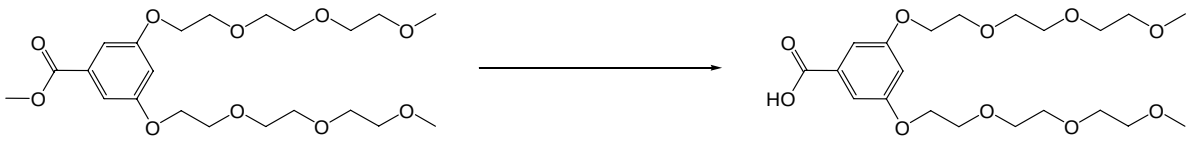

61 **23**

3.5 g (7.6 mmol) of the ester **61**, 1.28 g (22.8 mmol) of potassium hydroxide were dissolved in 100 mL of a mixture of ethanol and water (1:1) and heated until reflux overnight. Concentrated hydrochloric acid was added under reflux until pH=2 and then the mixture was poured into an ice-water mixture. The aqueous layer was separated and extracted two times with dichloromethane. The combined organic layers were washed with brine (pH=2), dried with sodium sulphate, filtered and the solvent was removed *in vacuo* to give 3.10 g (7.0 mmol) of the acid **23**, as a colourless oil in 91 % yield.

Molecular Formula: $C_{21}H_{34}O_{10}$ (446.22g/mol)

HR-MS (ESI-TOF, MeOH, positive ionization), m/z = 469.2033 $[M+Na]^+$ (Calculated for $C_{21}H_{34}NaO_{10}$= 469.2050)

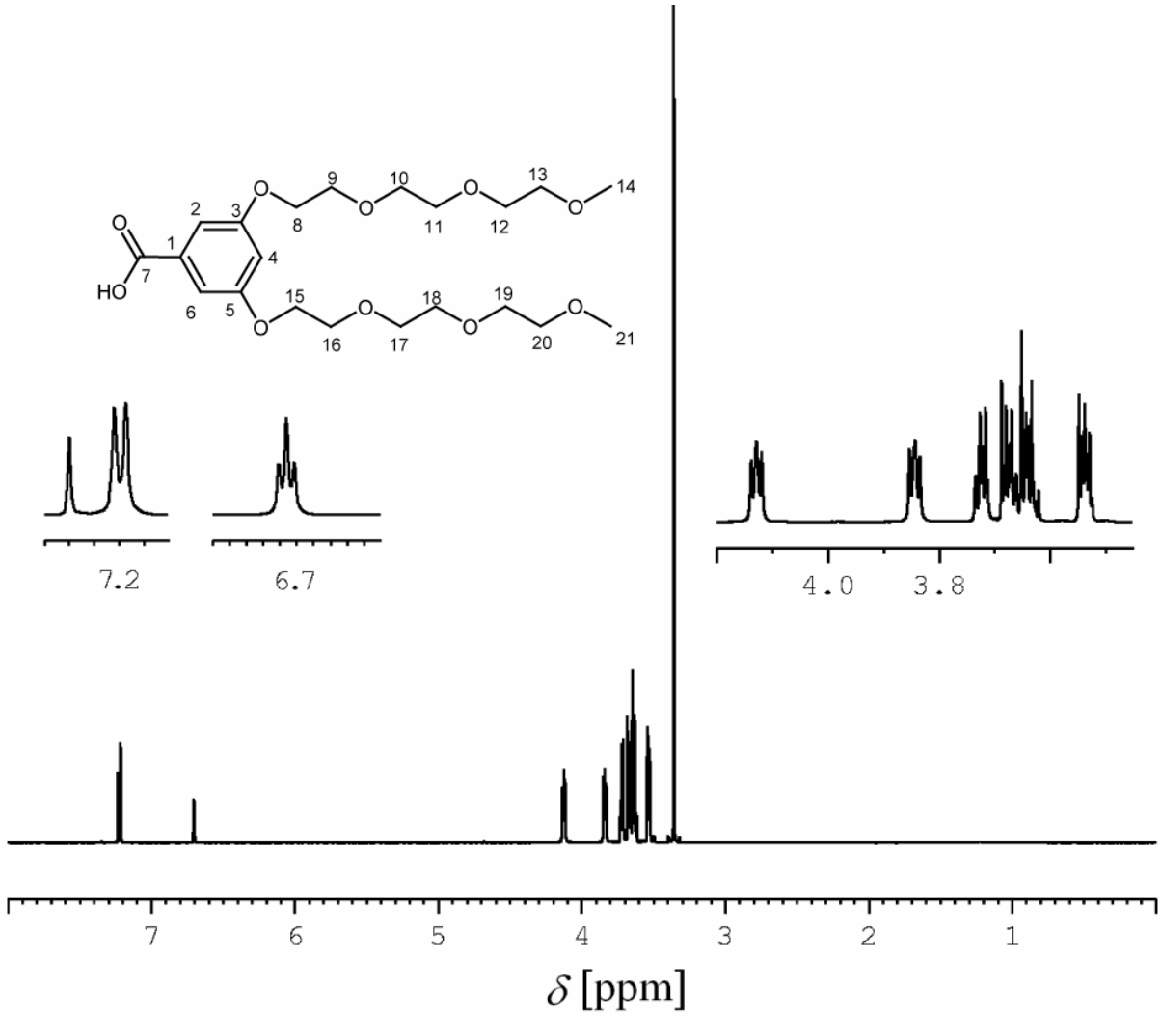

^{1}H NMR (500 MHz, $CDCl_3$) δ[ppm]: 3.36 (s, 6H, H-14+H-21), 3.54 (m, 4H, H-13+H-20), 3.66 (m, 8H, H-10+H-11+H-17+H-18), 3.72 (m, 4H, H-12+H-19), 3.84 (t, 4H, ^{3}J(H-9, H-8)=4.7 Hz, H-9+H-16), 4.13 (t, 4H, H-8+H-15), 6.71 (t, 1H. ^{4}J(H-4, H-2)=2.4 Hz, H-4), 7.22 (d, 2H, H-2+H-6).

^{13}C NMR (126 MHz, $CDCl_3$) δ[ppm]: 59.01 (C-14+C-21), 67.76 (CH_2), 69.60 (CH_2), 70.56 (CH_2), 70.65 (CH_2), 70, 83 (CH_2), 71.92 (CH_2), 107.58 (C-4), 108.51 (C-1+C-6), 131.05 (C-1), 159.79 (C-3+C-5), 170.12 (C-7).

IR (Film) $\tilde{\nu}$ [cm^{-1}]: 3491 (st, -COO-H), 2880 (st, Csp^3-H), 1717 (st, C=O), 1598 (ring st), 1448 (scissors vibration, -CH_2-), 1297 (st, C-O-C), 1105 (antisym st, C-O-C), 855, 707.

Synthesis of 3,5-bis(2-(2-(2-methoxyethoxy)ethoxy)ethoxy)benzoyl chloride, 59

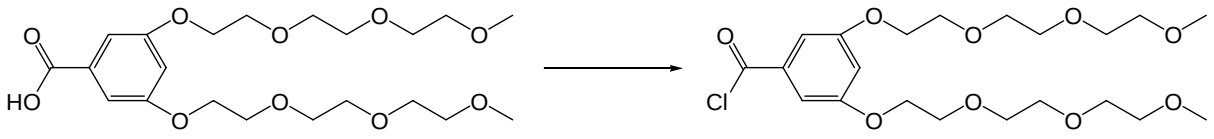

23 **59**

1st Variant

1.0 g (2.24 mmol) of the acid **23**, 1.87 g (15.7 mmol) of thionyl chloride in 1.14 mL of dry toluene were heated up at 90 ºC under argon. After 18 hours the reaction mixture was concentrated under reduced pressure. 5 mL of toluene were added and removed in the rotatory evaporator. This process was repeated for four times to remove the excess of thionyl chloride and finally dried under vacuum giving 1.04 g (2.24 mmol) of the desired chloride **59** as dark oil 99 % yield.

2nd Variant

Under argon atmosphere 1.15 mL (1.70 g, 13.30 mmol) of oxallyl chloride were added into a solution 1.99 g (4.46 mmol) of the acid **23** and 0.80 mL (0.78 g, 9.93 mmol) of pyridine in 1 mL of toluene (0.22 mL/mmol). The solution was stirred 2.5 hours at room temperature and then 10 mL of diethyl ether were added. The resulting solid was removed by filtration and the organic phase was concentrated under reduced pressure giving 1.63 g (3.51 mmol) of the desired product **59** as light-yellow oil in 79 % yield.

Molecular Formula: $C_{21}H_{33}ClO_9$ (464.93 g/mol)

HR-MS (ESI-TOF, MeOH, positive ionization), m/z = 487.1747 $[M+Na]^+$ (Calculated for $C_{21}H_{33}NaClO_9$= 487.1711).

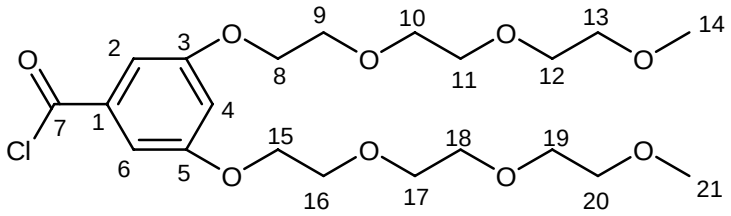

^{1}H NMR (500 MHz, $CDCl_3$) δ[ppm]: 3.39 (s, 6H, H-14+H-21), 3.56 (m, 4H, H-13+H-20), 3.53 (m, 8H, H-10+H-11+H-17+H-18), 3.75 (m, 4H, H-12+H-19), 3.88 (t, 4H, ^3J(H-9, H-8)=4.9 Hz, H-9+H-16), 4.16 (t, 4H, H-8+H-15), 6.81 (t, 1H. ^4J(H-4, H-2)=2.3 Hz, H-4), 7.27 (d, 2H, H-2+H-6).

^{13}C NMR (126 MHz, $CDCl_3$) δ[ppm]: 59.04 (C-14+C-21), 67.98 (CH_2), 69.50 (CH_2), 70.60 (CH_2), 70.66 (CH_2), 70, 88 (CH_2), 71.93 (CH_2), 108.99 (C-4), 109.89 (C-1+C-6), 134.84 (C-1), 159.99 (C-3+C-5), 168.16 (C-7).

IR (Film) $\widetilde{\nu}$ [cm^{-1}]: 2878 (st, Csp^3-H), 1757 (st, C=O), 1593 (ring st), 1444 (scissors vibration, -CH_2-), 1297 (st, C-O-C), 1110 (antisym st, C-O-C), 856, 757, 670.

Synthesis of (3,5-bis(2-(2-(2-methoxyethoxy) ethoxy) ethoxy) phenyl) methanol, 65

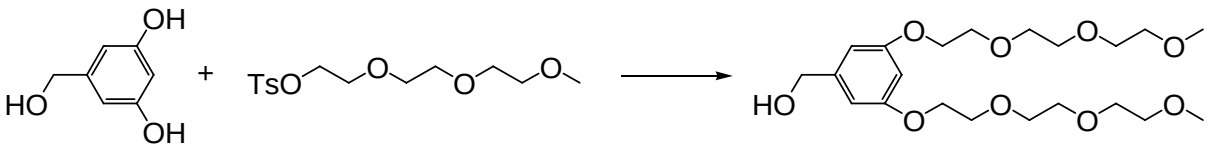

66 **62** **65**

2.0 g (14.3 mmol) of 5-(hydroxymethyl) benzene-1,3-diol, 9.3 g (29.3 mmol) of the tosylate **62**, 5.0 g (36 mmol) of potassium carbonate and 0.76 g (2.8 mmol) of 18-crown-6 were dissolved with 15 mL of dry acetone and the mixture was heated under reflux under argon atmosphere for 14 hours. After cooling to room temperature, the reaction mixture was diluted with dichloromethane. After filtration of the salts the solution was washed with NaOH 1M, HCl 2M and finally with water. The organic layer was dried with sodium sulphate and the solvent was removed under reduced pressure to give 6.17 g of the desired alcohol **65** as yellow oil in 99% yield.

Molecular formula: $C_{21}H_{36}O_9$ (432.51 g/mol)

HR-MS (ESI-TOF, MeOH, positive ionization), m/z = 455.2278 $[M+Na]^+$ (Calculated for $C_{21}H_{36}NaO_9$= 455.2257)

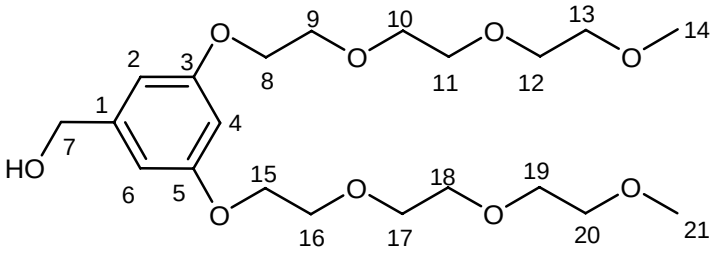

^{1}H-RMN (500 MHz, $CDCl_3$) δ[ppm]: 3.36 (s, 6H, H-14+H-21), 3.53 (m, 4H, H-13+H-20), 3.67 (m, 12H, H-10+H-11+H-12+H-17+H-18+H-19), 3.82 (t, 4H, ^3J(H-9, H-8)=4.8 Hz, H-9+H-16), 4.09 (t, 4H, H-8+H-15), 4.59 (s, 2H, H-7), 6.39 (t, 1H, ^4J(H-4, H-2)=2.3 Hz), 6.52 (d, 2H, H-2+H-6)

^{13}C NMR (126 MHz, $CDCl_3$) δ[ppm]: 59.13 (C-15+C-22), 65.31 (C-7), 67.61 (2*CH_2), 69.82 (2*CH_2), 70.65 (2*CH_2), 70.78 (2*CH_2), 70.92 (2*CH_2), 72.04 (2*CH_2), 101.00 (C-4), 105.58 (C-2+C-6), 143.57 (C-1), 160.19 (C-3+C-5)

IR (Film) $\widetilde{\nu}$ [cm^{-1}]: 3449 (st, O-H), 2922 (st, Csp-H), 2875 (st, Csp^3-H), 1596 (ring st), 1450 (scissors vibration, -CH_2-), 1294 (st, C-O-C), 1110 (antisym st, C-O-C), 848, 684

Synthesis of 1,3-bis(2-(2-(2-methoxyethoxy)ethoxy)ethoxy)-5-(bromomethyl)benzene, 64[87]

65 **64**

2.68 g (6.20 mmol) of the alcohol **65** and 3.08 g (9.30 mmol) of tetrabromomethane were dissolved in 6 mL of dry THF and cooled with an ice-bath. When the mixture reached 0 ºC a solution of 1.85 g (4.65 mmol) 1-(phenyl (2-(diphenylphosphino) ethyl) phosphino) benzene in 6 mL of THF was added dropwise and the resulting mixture was stirred for 15 minutes at 0 ºC. After cooling to room temperature the reaction mixture was stirred for 10 additional minutes and 0.25 mL of water were added. The solvent was removed *in vacuo* and the resulting crude material was purified by column chromatography on silica gel and a mixture of ethyl acetate/methanol 9:1 as eluant giving finally 2.41 g (4.87 mmol) of the desired product as a yellow oil in 79 % yield.

Molecular formula: $C_{21}H_{35}BrO_8$ (495.40 g/mol)

HR-MS (ESI-TOF, MeOH, positive ionization), m/z = 519.2 (100 %) $[M+Na]^+$ (Calculated for $C_{21}H_{35}BrNaO_8$= 519.1)

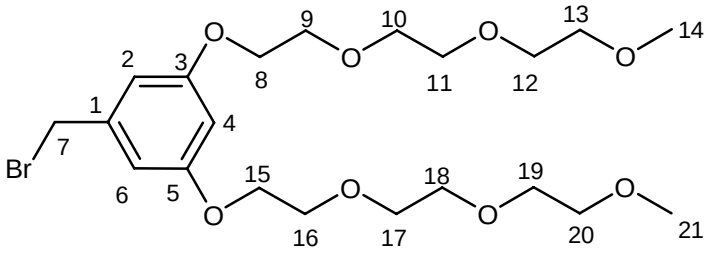

^{1}H-RMN (500 MHz, $CDCl_3$) δ[ppm]: 3.38 (s, 6H, H-14+H-21), 3.55 (m, 4H, H-13+H-20), 3.69 (m, 12H, H-10+H-11+H-12+H-17+H-18+H-19), 3.84 (t, 4H, ^3J(H-9, H-8)=4.8 Hz, H-

9+H-16), 4.10 (t, 4H, H-8+H-15), 4.39 (s, 2H, H-7), 6.42 (t, 1H, ^{4}J(H-4, H-2)=2.3 Hz), 6.54 (d, 2H, H-2+H-6)

^{13}C NMR(126 MHz, $CDCl_3$) δ[ppm]: 33.55 (C-7), 59.03 (C-15+C-22), 67.56 (2*CH_2), 70.58 (2*CH_2), 70.67 (2*CH_2), 70.71 (2*CH_2), 70.84 (2*CH_2), 72.94 (2*CH_2), 101.75 (C-4), 107.88 (C-2+C-6), 139.60 (C-1), 160.00 (C-3+C-5)

IR(Film) $\widetilde{\nu}$ [cm^{-1}]: 3013 (st, Csp-H), 2875 (st, Csp^3-H), 1595 (ring st), 1449 (scissors vibration, -CH_2-), 1297 (st, C-O-C), 1108 (antisym st, C-O-C), 850, 657

Synthesis of 3,5- bis (2-(2-(2-methoxyethoxy)ethoxy)ethoxy)benzyl *p*-toluenesulphonate, 72

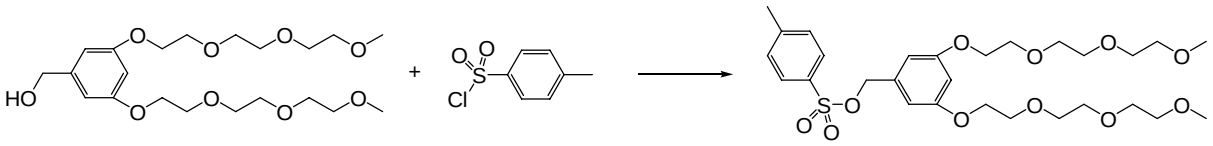

65 **70** **72**

8.73 g (20.2 mmol) of the alcohol **65**, and 5.75 g (147.5 mmol) of sodium hydroxide were dissolved in 6 mL of water and 27 mL of THF. The mixture was stirred and cooled at 0 ºC. After 30 minutes a solution of 3.85 g (20.2 mmol) of *p*-toluenesulphonyl-chloride, **70** in 25 mL of THF was added dropwise. When the addition was complete, the mixture was stirred for 3 hours at 0 ºC (the solution became pink) and then poured into a ice-water mixture and extracted 3 times with 75 mL of dichloromethane. The organic layer was washed two times with HCl 2M (the solutions became yellow) and one time with brine and finally dried with sodium sulphate and filtrated. The solvent was removed *in vacuo* to give 10.10 g of the desired product tosylate **72** as yellow oil in 85 % yield.

Molecular formula: $C_{28}H_{42}O_{11}S$ (586.69 g/mol)

HR-MS (ESI-TOF, MeOH, positive ionization), m/z = 469.2430 [M-$C_7H_7O_3S$+CH_3O+Na]$^+$ (Calculated for $C_{22}H_{38}NaO_9$= 469.2414)

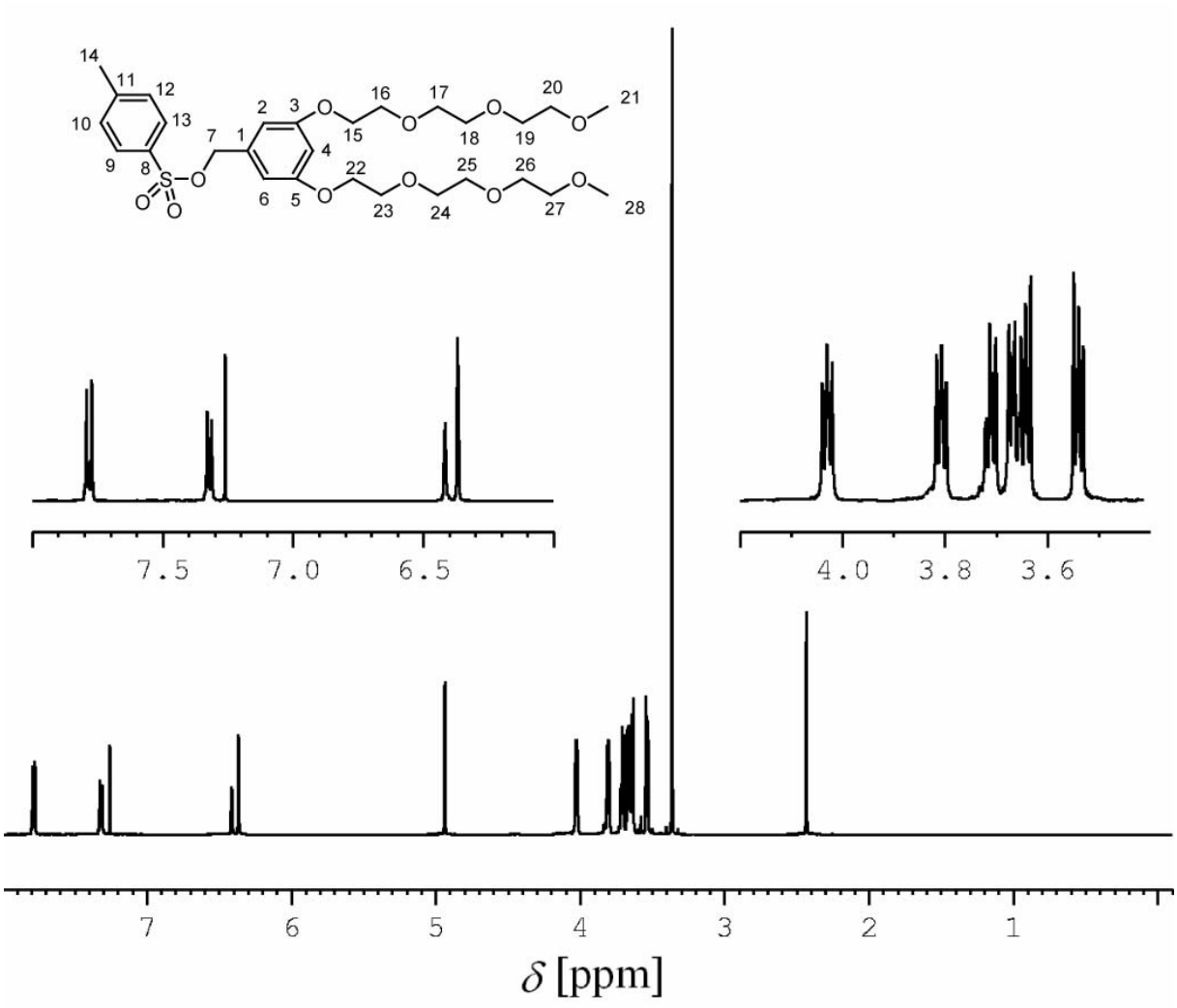

^{1}H-RMN (500 MHz, $CDCl_3$) δ[ppm]: 2.44 (s, 3H, H-14), 3.37 (s, 6H, H-21+H-28), 3.54 (m, 4H, H-20+H-27), 3.67 (m, 12H, H-17+H-18+H-19+H-24+H-25+H-26), 3.81 (t, 4H, ^{3}J(H-16, H-15)=4.8 Hz, H-16+H-25), 4.03 (t, 4H, H-15+H-22), 4.94 (s, 2H, H-7), 6.37 (d, 2H, ^{4}J(H-2, H-4)=2.2 Hz, H-2+H-6), 6.42 (t, 1H, H-4), 7.32 (d, 2H, ^{3}J(H-10, H-9)=8.6 Hz, H-10+H-12), 7.78 (d, 2H, H-9+H-13)

^{13}C NMR (126 MHz, $CDCl_3$) δ[ppm]: 21.74 (C-14), 59.15 (C-21+C-28), 67.67 (2*CH_2), 69.71 (2*CH_2), 70.69 (2*CH_2), 70.77 (2*CH_2), 70.94 (2*CH_2), 71.83 (C-7), 72.05 (2*CH_2), 102.27 (C-4), 107.14 (C-2+C-6), 128.09 (C-9+C-13), 129.96 (C-10+C-12), 133.35 (C-11), 135.41 (C-8), 144.94 (C-1), 160.14 (C-3+C-5)

IR (Film) $\tilde{\nu}$ [cm^{-1}]: 3052 (st, Csp-H), 2877 (st, Csp^3-H), 1598 (ring st), 1450 (scissors vibration, -CH_2-), 1359 (antisym st SO_2), 1177 (st, C-O-C), 1111 (antisym st, C-O-C), 1072 (sym st SO_2), 934, 850, 666

Synthesis of methyl 3,5-bis(3,5-bis(2-(2-(2-methoxyethoxy) ethoxy) ethoxy)benzyloxy) benzoate, 67

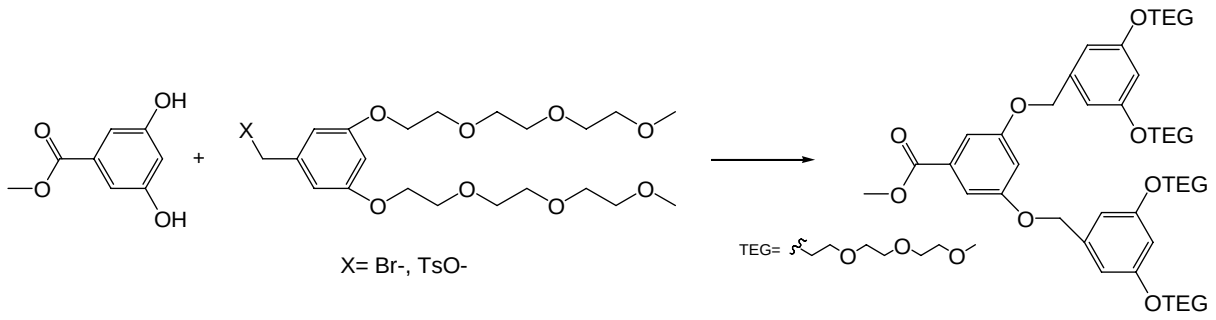

23 **64** or **72** **67**

1st Variant (X= Br-)[87]

3.0 g (6.06 mmol) of bromide **64**, 0.49 g (2.89 mmol) of methyl 3,5-dihydroxy-benzoate **23**, 0.153 g (0.58 mmol) of 18-crown-6 and 1.00 g (7.23 mmol) of potassium carbonate were dissolved with 60 mL of dry acetone and heated at reflux under argon. After 18 hours, the reaction mixture was cooled down to room temperature, diluted with dichloromethane and filtered. After removal of the solvent under reduced pressure the crude reaction mixture was purified with column chromatography on silica gel using ethyl acetate/Methanol (9:1) as eluant to give, finally, 1.08 g (1.08 mmol) of the desired product **67** as pale-yellow oil in 37 % yield.

2nd Variant (X= TsO-)

0.70 g (4.15 mmol) of methyl 3,5-dihydroxybenzoate **23**, 4.85 g (8.29 mmol) of the tosylate **72**, 0.22 g (0.83 mmol) of 18-crown-6 and 1.14 g (8.29 mmol) of potassium carbonate were submitted to the same procedure as the 1st variant giving, finally 3.74 g (3.75 mmol) of the desired product **67** in 91% yield.

Molecular Formula: $C_{50}H_{76}O_{20}$ (997.13 g/mol)

HR-MS (ESI-TOF, MeOH, positive ionization), m/z = 997.5003 $[M+H]^+$ (Calculated for $C_{50}H_{76}O_{20}$= 977.5008), 1019.4822 $[M+Na]^+$ (Calculated for $C_{50}H_{76}NaO_{20}$= 1019.4828).

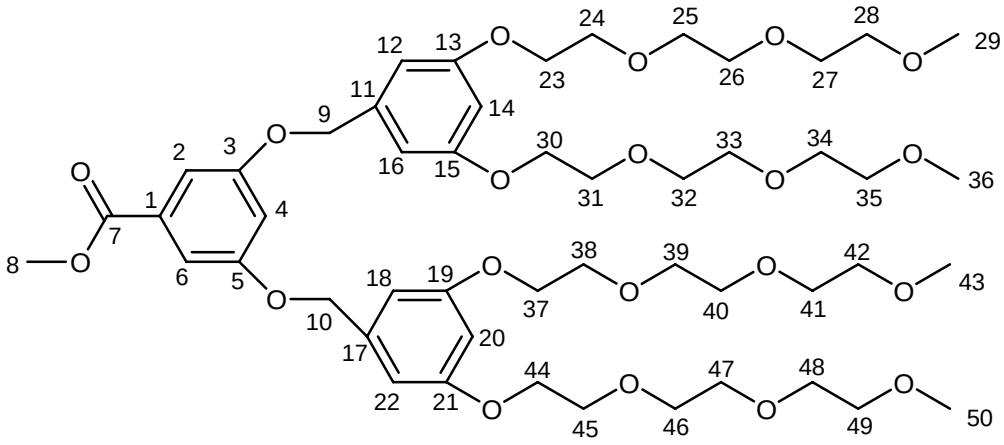

^{1}H NMR (500 MHz, $CDCl_3$) δ[ppm]: 3.38 (s, 12H, H-29+H36+H-43+H50), 3.56 (m, 8H, H-28+H-35+H-42+H-49), 3.67 (m, 16H, H-25+H-26+H-32+H-33+H-39+H-40+H-46+H-47), 3.74 (m, 8H, H-27+H-34+H-41+H-48), 3.85 (t, 8H, ^3J(H-24, H-23)=4.9 Hz, H-24+H-31+H-38+H-45), 3.91 (s. 3H, H-8), 4.12 (t, 8H, H-23+H-30+H-37+H-44), 4.99 (s, 4H, H-9+H-10), 6.45 (t, 2H, ^4J(H-14, H-12)=2.2 Hz, H-14+H-20), 6.59 (d, 4H, H-12+H-16+H-18+H-22), 6.78 (t, 1H, ^4J(H-4, H-2)= 2.3 Hz, H-4), 7.27 (d, 2H, H-2+H-6).

^{13}C NMR (126 MHz, $CDCl_3$) δ[ppm]: 52.40 (C-8), 59.18 (C-29+C-36+C-43+C-50), 67.67 (4*CH_2), 69.82 (4*CH_2), 70.29 (C-9+C-10), 70.72 (4*CH_2), 70.81 (4*CH_2), 70.97 (4*CH_2), 72.09 (4*CH_2), 101.40 (C-14+C-20), 106.25 (C-12+C-16+C-18+C-22), 107.33 (C-4), 108.51 (C-2+C-6), 132.19 (C-1), 138.86 (C-11+C-17), 159.86 (C-3+C-5), 160.27 (C-13+C-15+C-19+C-21), 166.88 (C-7).

IR (Film) $\widetilde{\nu}$ [cm^{-1}]: 2876 (st, Csp^3-H), 1722 (st, C=O), 1595 (ring st), 1446 (scissors vibration, -CH_2-), 1295 (st, C-O-C), 1109 (antisym st, C-O-C), 849, 769, 684.

Synthesis of 3,5-bis (3,5-bis (2- (2- (2-methoxyethoxy) ethoxy) ethoxy) benzyloxy) benzoic acid, 24

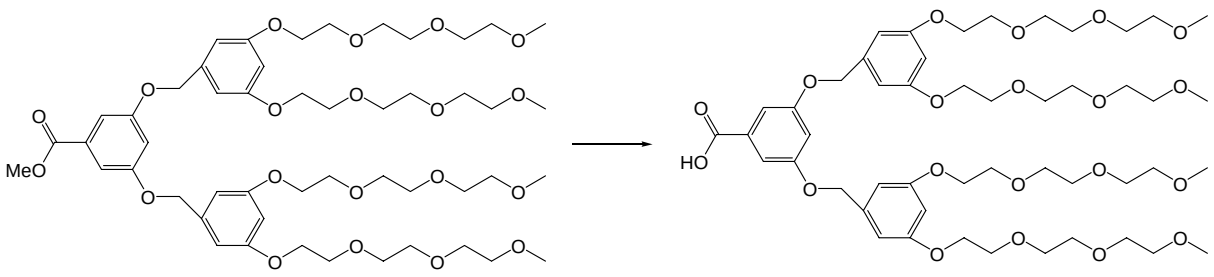

67 **24**

1.08 g (1.08 mmol) of the ester **67** and 0.17 g (3.01 mmol) of potassium hydroxide were dissolved in 13 mL of a mixture of ethanol and water (1:1) and heated at reflux

overnight. Concentrated hydrochloric acid was added to the refluxing mixture until pH=2. Then the mixture was poured into an ice-water mixture. The aqueous layer was separated and extracted two times with dichloromethane. The combined organic layers were washed with brine (pH=2), dried with sodium sulfate, filtered and the solvent was removed *in vacuo* to give 1.05 g (1.07 mmol) of the acid **24** as a pale yellow oil in 99 % yield.

Molecular Formula: $C_{49}H_{74}O_{20}$ (983.10 g/mol)

HR-MS (ESI-TOF, MeOH, positive ionization), m/z = 1005.4689 $[M+Na]^+$ (Calculated for $C_{59}H_{76}NaO_{20}$= 1005.4671).

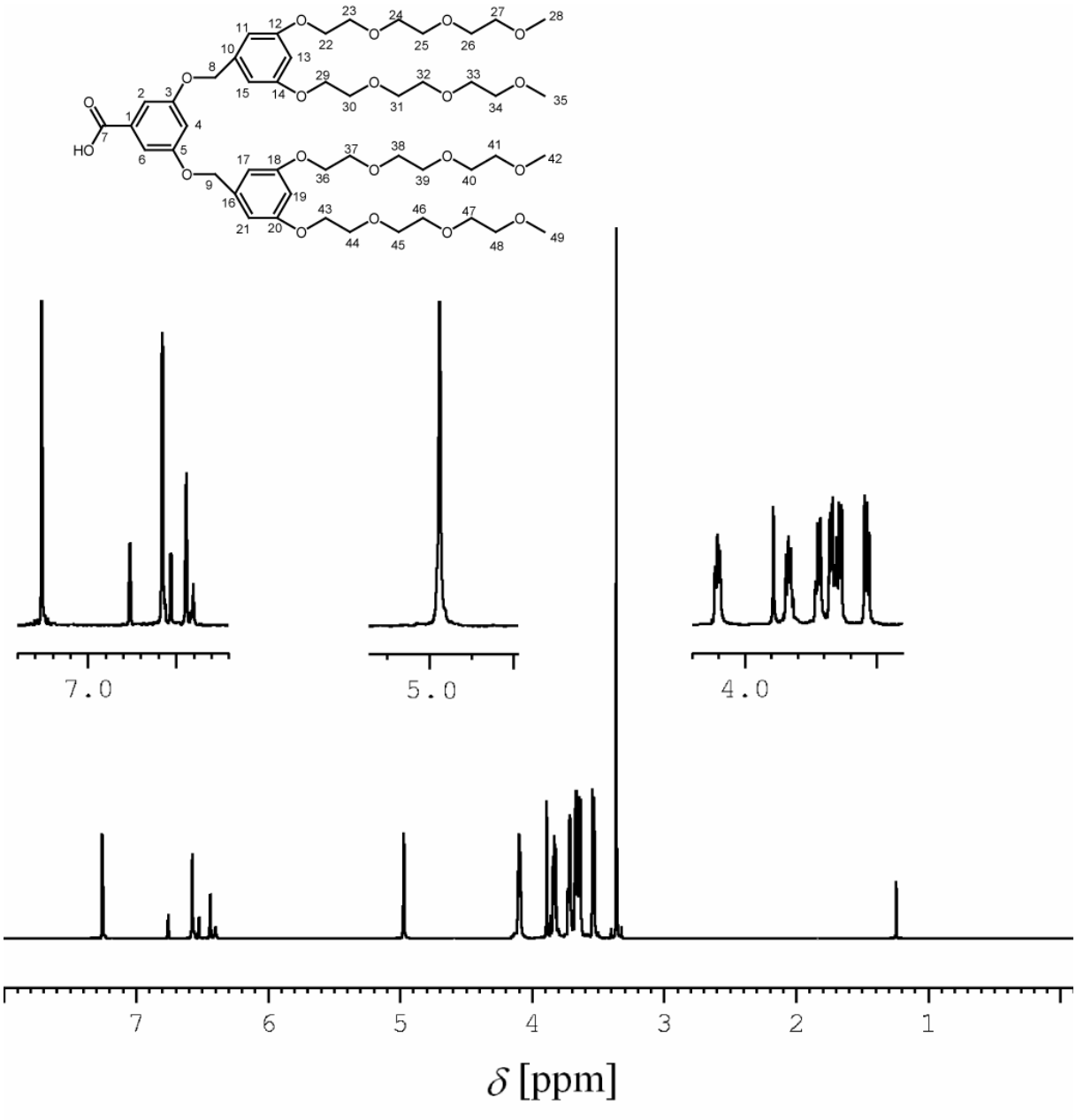

^{1}H NMR (500 MHz, $CDCl_3$) δ[ppm]: 3.38 (s, 12H, H-28+H35+H-42+H49), 3.55 (m, 8H, H-27+H-34+H-41+H-48), 3.67 (m, 16H, H-24+H-25+H-31+H-32+H-38+H-39+H-45+H-46), 3.73 (m, 8H, H-26+H-30+H-37+H-44), 3.83 (t, 8H, ^{3}J(H-23, H-22)=4.9 Hz, H-23+H-30+H-37+H-44), 4.11 (t, 8H, H-22+H-29+H-36+H-43), 4.99 (s, 4H, H-8+H-9), 6.43 (t, 2H, ^{4}J(H-13, H-11)=2.1 Hz, H-13+H-19), 6.58 (d, 4H, H-11+H-15+H-17+H-21), 6.78 (t, 1H, ^{4}J(H-4, H-2)= 2.3 Hz, H-4), 7.29 (d, 2H, H-2+H-6).

^{13}C NMR (126 MHz, $CDCl_3$) δ[ppm]: 59.98 (C-28+C-35+C-42+C-49), 67.50 (4*CH_2), 69.62 (4*CH_2), 70.18 (C-8+C-9), 70.50 (4*CH_2), 70.65 (4*CH_2), 70.78 (4*CH_2), 71.91 (4*CH_2), 101.34 (C-13+C-19), 106.18 (C-11+C-15+C-17+C-21), 108.12 (C-4), 108.81 (C-2+C-6), 131.43 (C-1), 138.73 (C-10+C-16), 159.62 (C-3+C-5), 160.07 (C-12+C-14+C-18+C-20), 169.05 (C-7).

IR (Film) $\tilde{\nu}$ [cm^{-1}]: 3487 (st, -COO-H), 2877 (st, Csp^3-H), 1718 (st, C=O), 1596 (ring st), 1448 (scissors vibration, -CH_2-), 1297 (st, C-O-C), 1145 (antisym st, C-O-C), 848, 732, 684.

Synthesis of 3,5-bis(3,5-bis(2-(2-(2-methoxyethoxy)ethoxy)ethoxy)benzyloxy)benzoyl chloride, 60

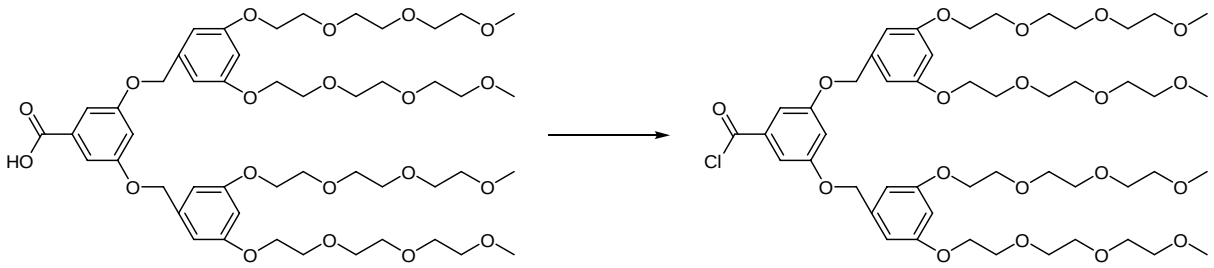

24 **60**

1st Variant

2.2 g (2.24 mmol) of the acid **24** and 0.64 g (0.39 mL, 5.4 mmol) of thionyl chloride were dissolved in 50 mL of toluene and heated at 40 ºC under Ar for 14.5 hours. After cooling to room temperature, the solvent was removed *in vacuo*. 10 mL of toluene were added and removed *in vacuo*. This procedure was repeated three additional times in order to remove the excess of thionyl chloride. Finally, the residue was dried in an oil pump vacuum to give 2.2 g (2.21 mmol) of the desired chloride **60** product as dark oil in 99 % yield.

2nd Variant

Under argon atmosphere 1.59 mL (2.55 g, 19.98 mmol) of oxallyl chloride were added to a solution of 6.59 g (6.70 mmol) of the acid **24** and 1.20 mL (1.17 g, 14.92 mmol) of pyridine in 3.30 mL of toluene (0.22 mL/mmol). The solution was stirred 2.5 hours at room temperature and then 15 mL of diethyl ether were added. The resulting solid was removed by filtration and the organic phase was concentrated under reduced pressure, giving 5.01 g (5.09 mmol) of the desired product **60** as light-yellow oil in 76 % yield.

Molecular Formula: $C_{49}H_{73}ClO_{19}$ (1001.55 g/mol)

HR-MS (ESI-TOF, MeOH, positive ionization), m/z = 1033.4699 $[M+MeOH+H]^+$ (Calculated for $C_{50}H_{78}ClO_{20}$= 1033.4775), 521.2395 $[M+ACN+H]^{2+}$ (Calculated for $C_{51}H_{77}ClNO_{19}$= 1042.4778/2 = 521.2389)

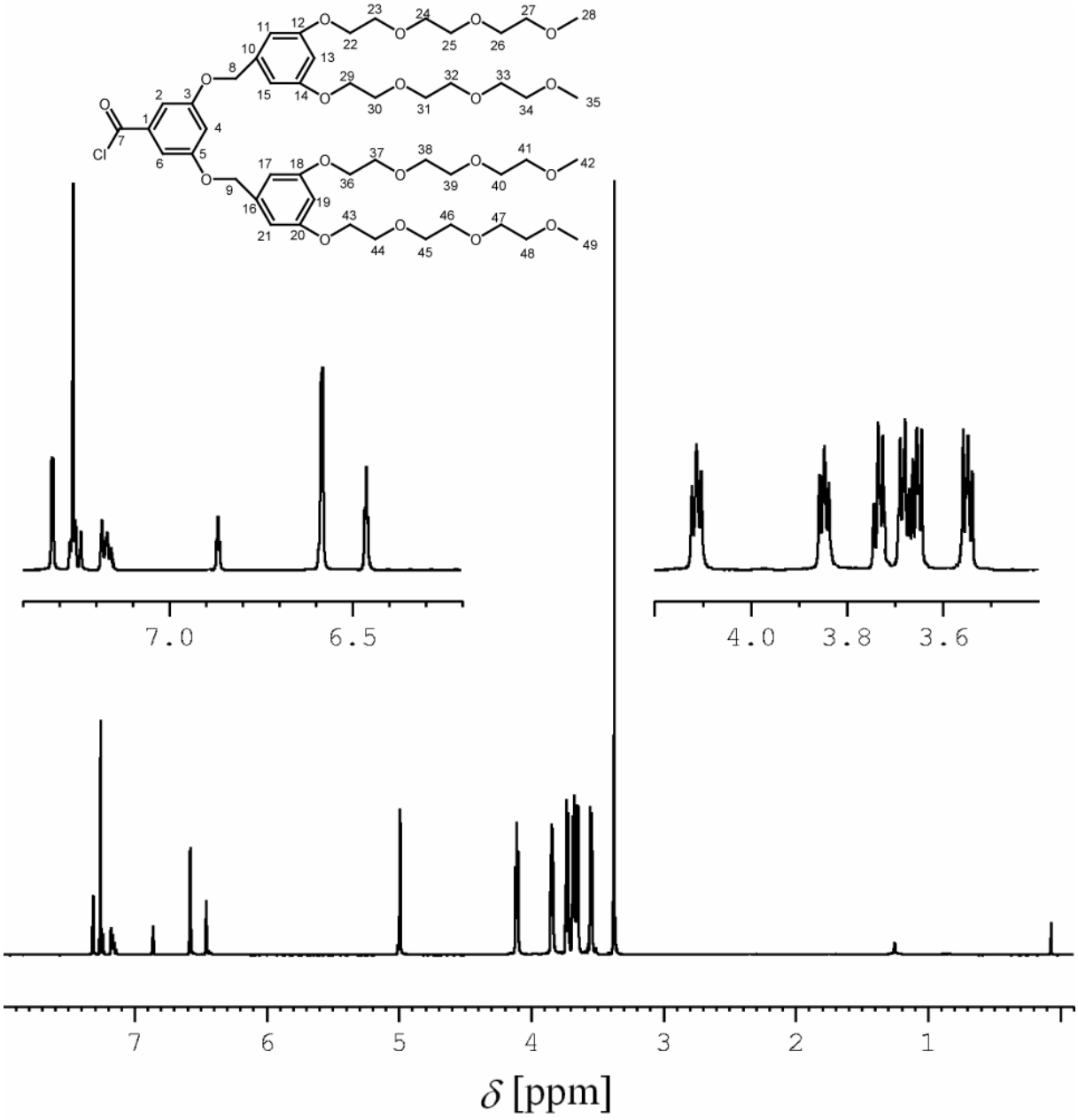

^{1}H NMR (500 MHz, $CDCl_3$) δ[ppm]: 3.37 (s, 12H, H-28+H35+H-42+H49), 3.55 (m, 8H, H-27+H-34+H-41+H-48), 3.67 (m, 16H, H-24+H-25+H-31+H-32+H-38+H-39+H-45+H-46), 3.73 (m, 8H, H-26+H-30+H-37+H-44), 3.85 (t, 8H, ^{3}J(H-23, H-22)=4.8 Hz, H-23+H-30+H-37+H-44), 4.11 (t, 8H, H-22+H-29+H-36+H-43), 5.00 (s, 4H, H-8+H-9), 6.46 (t, 2H, ^{4}J(H-13, H-11)=2.1 Hz, H-13+H-19), 6.58 (d, 4H, H-11+H-15+H-17+H-21), 6.86 (t, 1H, ^{4}J(H-4, H-2)= 2.1 Hz, H-4), 7.32 (d, 2H, H-2+H-6).

^{13}C NMR (126 MHz, $CDCl_3$) δ[ppm]: 59.02 (C-28+C-35+C-42+C-49), 67.55 (4*CH_2), 69.66 (4*CH_2), 70.38 (C-8+C-9), 70.58 (4*CH_2), 70.67 (4*CH_2), 70.83 (4*CH_2), 71.94 (4*CH_2), 101.38 (C-13+C-19), 106.17 (C-11+C-15+C-17+C-21), 109.38 (C-4), 110.20 (C-2+C-6), 134.97 (C-1), 128.22 (C-10+C-16), 159.86 (C-3+C-5), 160.21 (C-12+C-14+C-18+C-20), 168.10 (C-7).

IR (Film) $\tilde{\nu}$ [cm^{-1}]: 2921 (st, Csp^2-H), 2876 (st, Csp^3-H), 1751 (st, C=O), 1597 (ring st), 1448 (scissors vibration, -CH_2-), 1297 (st, C-O-C), 1174 (antisym st, C-O-C), 989, 953, 849.

4.3.2 Preparation of molecular tweezers

Synthesis of 5-Acetoxy-12-{3′,5′-bis(2-(2-(2-methoxyethoxy)ethoxy)ethoxy)benzoate}-(1α, 4α, 7α, 10α) 1,4,7,10-tetrahydro-1,4:7,10-tetramethanodecacen, 48

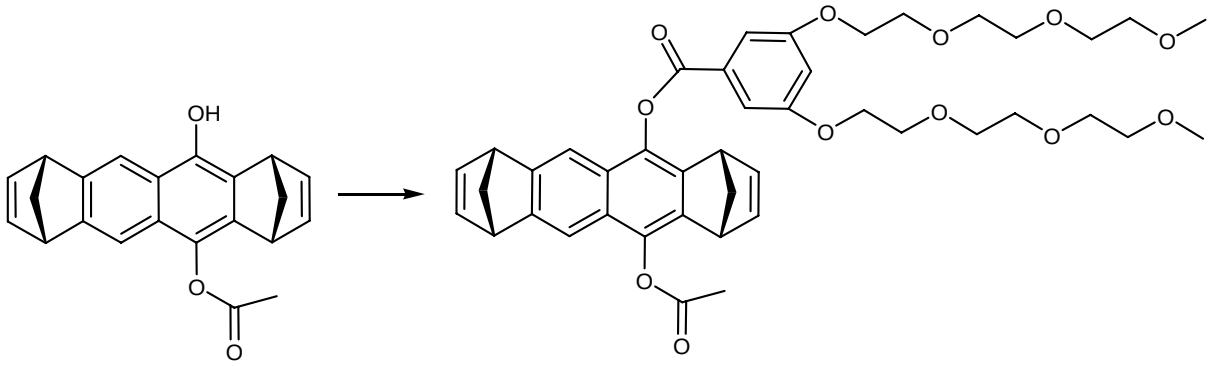

78 **48**

24 mg (0.91 mmol) of sodium hydride without paraffin oil were suspended into 1.5 mL of dry THF under argon. After 10 minutes a solution of 100 mg (0.303 mmol) of spacer **78** in 2 mL of dry tetrahydrofuran was added and the mixture was stirred at room temperature for 30 minutes. A solution of 183 mg (0.303 mmol) of the chloride **59** in 1.5 mL of dry tetrahydrofuran was added to the stirred solution and the mixture was stirred for 2 additional hours. The solvent was evaporated under reduced pressure and the crude residue was redissolved in ethyl acetate and then washed with HCl 2.5 M, water, $NaHCO_3$ sat. and water. The organic layer was dried with anhydrous sodium sulphate, filtered and, after removal of the solvent, the crude was purified by column chromatography on silica gel using ethyl acetate as eluant giving, finally, 210 mg (0.28 mmol) of the desired product **48** as brown oil and in 91 % yield.

Molecular Formula: $C_{43}H_{50}O_{12}$ (748.85 g/mol)

HR-MS (ESI-TOF, MeOH, positive ionization), m/z = 781.3247 $[M+Na]^+$ (Calculated for $C_{43}H_{50}NaO_{12}$= 781.3200).

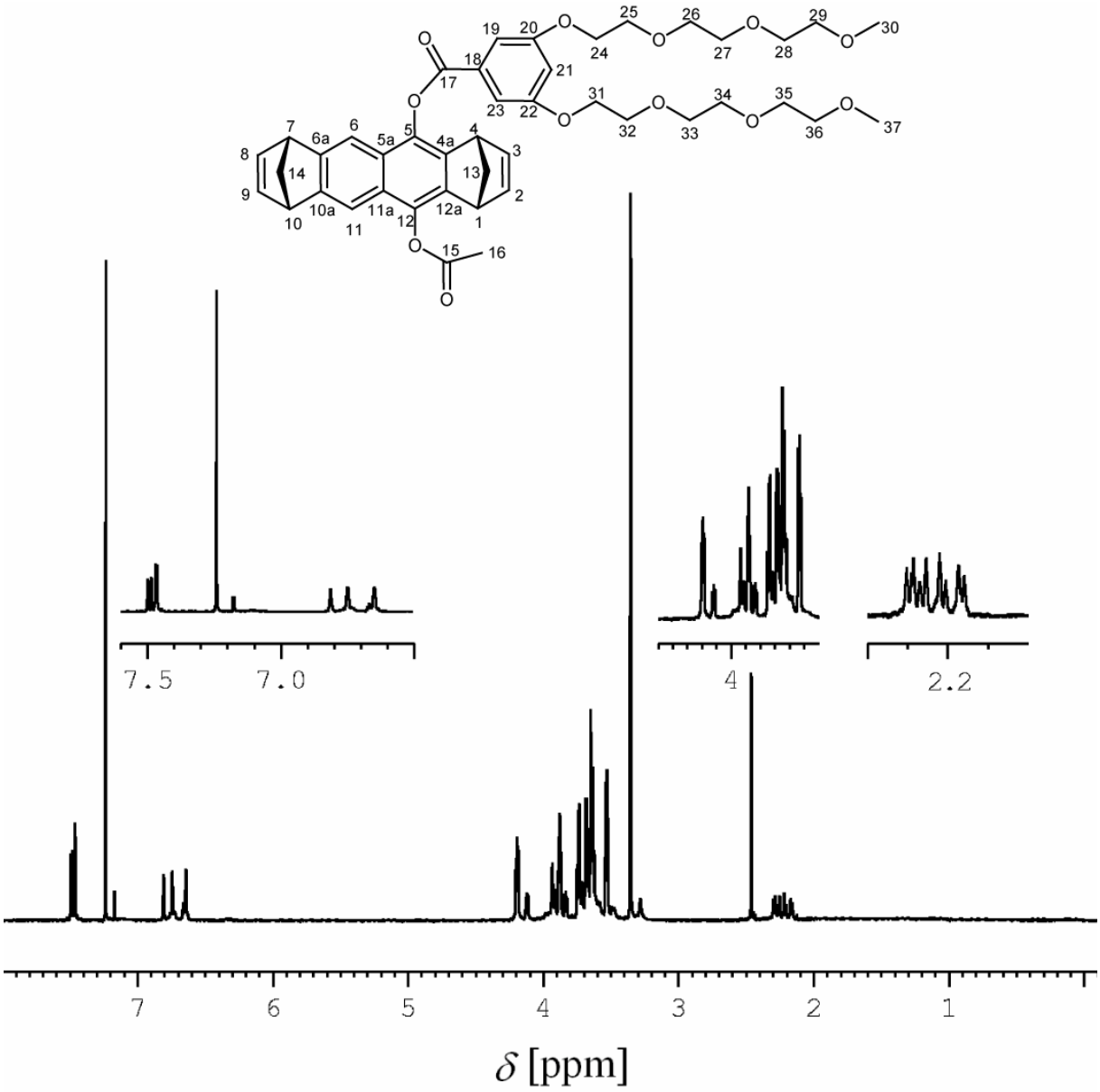

^{1}H NMR (500 MHz, $CDCl_3$) δ[ppm]: 2.26 (m, 4H, H-13+H-14), 2.46 (s, 3H, H-16), 3.36 (s, 6H, H-30+H-37), 3.53 (m, 4H, H-29+H-36), 3.64 (m, 4H, H-28+H-35), 3.68 (m, 4H, H-27+H-34), 3.75 (m, 4H, H-26+H-33), 3.88 (t, 4H, ^{3}J(H-25, H-24)=4.3 Hz, H-25+H-32), 3.93 (m, 4H, H1+H4+H7+H10), 4.20 (t, 4H, H-24+H-31), 6.66 (m, 2H, H8+H9), 6.75 (m, 2H, H-2+H-3), 6.81 (t, ^{4}J(H-21, H-19)=2.3 Hz, H-21), 7.47(d, 2H, H19+H-23), 7.48 (s, 1H, H-6), 7.50 (s, 1H, H-11).

^{13}C NMR (126 MHz, $CDCl_3$) δ[ppm]: 20.82 (C16), 47.52 (C1+C4), 49.73 (C7), 49.77 (C10), 59.04 (C30+C37), 65.43 (C14), 67.02 (C13), 67.90 (CH_2), 69.62 (CH_2), 70.60 (CH_2), 70.68 (CH_2), 70.87 (CH_2), 71.94 (CH_2), 107.44 (C21), 108.82 (C19+C23), 113.12 (C6), 113.32 (C11), 124.73 (C11a), 124.79 (C5a), 131.06 (C18), 137.30 (C12a), 137.37 (C4a), 139.00 (C12), 139.04 (C5), 141.72 (C9), 141.86 (C8), 142.05 (C2), 142.20 (C3), 149.47 (C10a), 149.50 (C6a), 160.06 (C20+C22), 164.51 (C17), 169.15 (C15).

IR (Film) $\tilde{\nu}$ [cm^{-1}]: 2930 (st, Csp^2-H), 2874 (st, Csp^3-H), 1765 (st, C=O), 1739 (st, C=O), 1594 (ring st), 1445 (scissors vibration, -CH_2-), 1302 (st, C-O-C), 1107 (antisym st, C-O-C), 829.

Synthesis of 8-Acetoxy-21-{3´, 5´-bis(2-(2-(2-methoxyethoxy) ethoxy) ethoxy) benzoate}-(5α, 7α, 10α, 12α, 17α, 19α, 22α, 24α) 5, 7, 10, 12, 17, 19, 22, 24-octahydro-5,24:7,22:10,19:12,17-tetramethanodecacen, 26

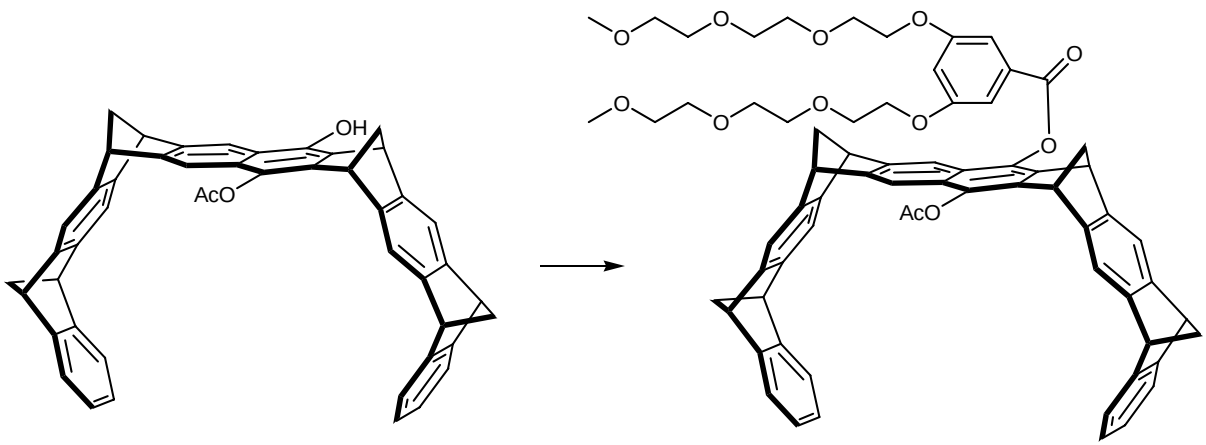

58 **26**

5.4 mg (0.23 mmol) of sodium hydride without paraffin oil were suspended in 0.5 mL of dry THF under argon. After 10 minutes a solution of 59.5 mg (0.09 mmol) of tweezer **58** in 0.8 mL of dry tetrahydrofuran was added and the mixture was stirred at room temperature for 30 minutes. A solution of 41.8 mg (0.09 mmol) of the chloride **59** in 0.5 mL of dry tetrahydrofuran was added to the stirred solution and the mixture was stirred for 2 additional hours. The solvent was evaporated *in vacuo* and the crude residue was redissolved in ethyl acetate, washed with HCl 2.5 M, water, $NaHCO_3$ sat. and finally with water. The organic layer was dried with sodium sulphate anh., filtered and, after removal of the solvent, the crude residue was purified by MPLC on silica gel using ethyl acetate as eluant giving finally 63.5 mg (0.058 mmol) of the desired tweezer **26** as yellow solid in 70 % yield.

Molecular Formula: $C_{69}H_{66}O_{12}$ (1087.26 g/mol)

Melting point *T* [ºC]= 127

HR-MS (ESI-TOF, MeOH, positive ionization), m/z = 1109.4398 $[M+Na]^+$ (Calculated for $C_{69}H_{66}NaO_{12}$= 1109.4452).

HR-MS (EI 70 eV, MeOH), m/z = Not suitable to the technique.

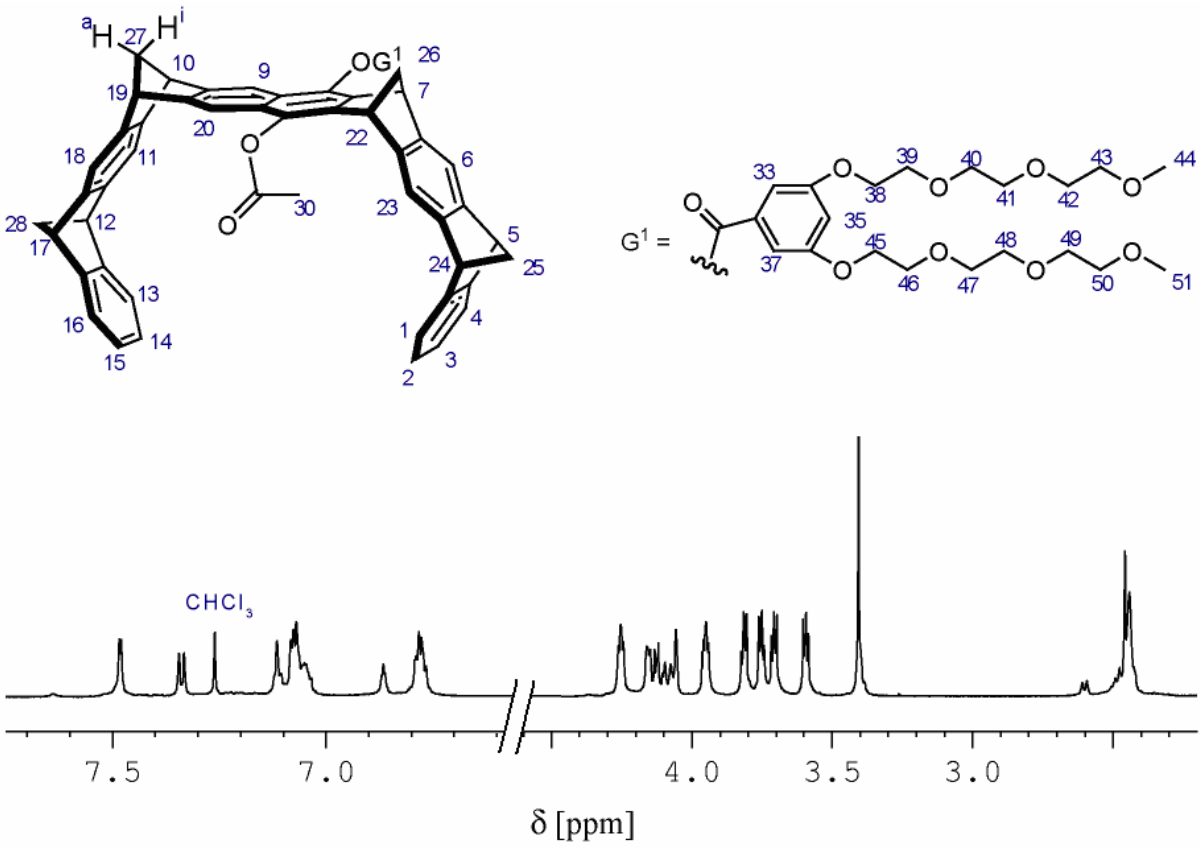

^{1}H NMR (500 MHz, $CDCl_3$) δ[ppm]: 2.41 (m, 2H, H-26^{a}+H-27^{i}), 2.42 (m, 4H, H-25+H-28), 2.46 (s, 3H, H-30), 2.46 (d, 1H, ^{2}J(H-27^{a}, H-27^{i})= 8.1 Hz, H-27^{a}), 2.58 (d, 1H, 2J(H-26^{i}, H-26^{a})= 7.9 Hz, H-26^{i}), 3.38 (s, 6H, H-44+H-51), 3.57 (t, 4H, ^{3}J(H-43, H-42)= 4.7 Hz, H-43+H-50), 3.69 (t, 4H, H-42+H-49), 3.73 (m, 4H, H-41+H-48), 3.80 (m, 4H, H-40+H-47), 3.93 (t, 4H, ^{3}J(H-39, H-38)= 4.6 Hz, H-39+H-46), 4.04 (s, 1H, H-17), 4.07 (m, 2H, H-5+H-24), 4.08 (m, 1H, H-12), 4.10 (m, 1H, H-19), 4.13 (m, 1H, H-10), 4.14 (m, 2H, H-7+H-22), 4.23 (t, 4H, H-38+H-45), 6.76 (m, 4H, H-2+H-3+H-14+H-15), 6.85 (t, 1H, ^{4}J(H-35, H-33)= 2.1 Hz, H-35), 7.05 (m, 6H, H-1+H-4+H-11+H-18+H-13+H-16), 7.09 (s, 1H, H-6), 7.09 (s, 1H, H-23), 7.32 (s, 2H, H-9+H-20), 7.46 (d, 2H, H-33+H-37).

^{13}C NMR (126 MHz, $CDCl_3$) δ[ppm]: 20.85 (C-30), 48.21 (C-7), 48.25 (C-22), 50.56 (C-10), 50.65 (C-19), 51.03 (C-24), 51.05 (C-17), 51.06 (C-12), 51.06 (C-5), 59.07 (C-44+C-51), 64.03 (C-26), 64.83 (C-27), 67.64 (C-28), 67.70 (C-25), 67.96 (C-38+C-45), 70.64 (C-42+C-49), 70.73 (C-41+C-48), 70.92 (C-40+C-47), 71.97 (C-43+C-50), 107.35 (C-35), 108.84 (C-33+C-37), 113.04 (C-20), 113.35 (C-9), 116.22 (C-18), 116.39 (C-11), 116.76 (C-23), 116.84 (C-6), 121. 54 (C-16), 121.60 (C-1), 121.60 (C-13), 121.67 (C-4), 124.10 (C-15), 124.10 (C-2), 124.24 (C-14), 124.25 (C-13), 124.97 (C-8a), 125.06 (C-20a), 131.14 (C-32), 137.22 (C-8), 137.31 (C-21), 137.87 (C-7a), 137.98 (C-21a), 145.68 (C-22a), 145.69 (C-6a), 146.60 (C-18a), 146.61 (C-10a), 147.76 (C-17a), 147.77 (C-11a), 147.91 (C-23a), 147.95 (C-5a), 148.39 (C-19a), 148.46 (C-9a), 150.55 (C12a+C-16a), 150.57 (C-4a+C-24a), 160.04 (C-34+C-36), 164.36 (C-31), 168.88 (C-29).

IR (Diffuse reflection) $\tilde{\nu}$ [cm^{-1}]: 2930 (st, Csp^2-H), 2864 (st, Csp^3-H), 1737 (st, C=O), 1594 (ring st), 1443 (scissors vibration, -CH_2-), 1297 (st, C-O-C), 1196 (antisym st, C-O-C), 996, 834, 753

UV/vis ($CHCl_3$): λ_{max} [nm] (log ε)= 247 (4.43), 294 (4.18).

4.3.3 Preparation of molecular clips

Synthesis of 7, 16-bis{3´,5´-bis(2-(2-(2-methoxyethoxy)ethoxy)ethoxy)benzoate}- (6α, 8α, 15α, 17α)-6, 8, 15 ,17-tetrahydro-6,17:8,15-di-methanoheptacen, 27

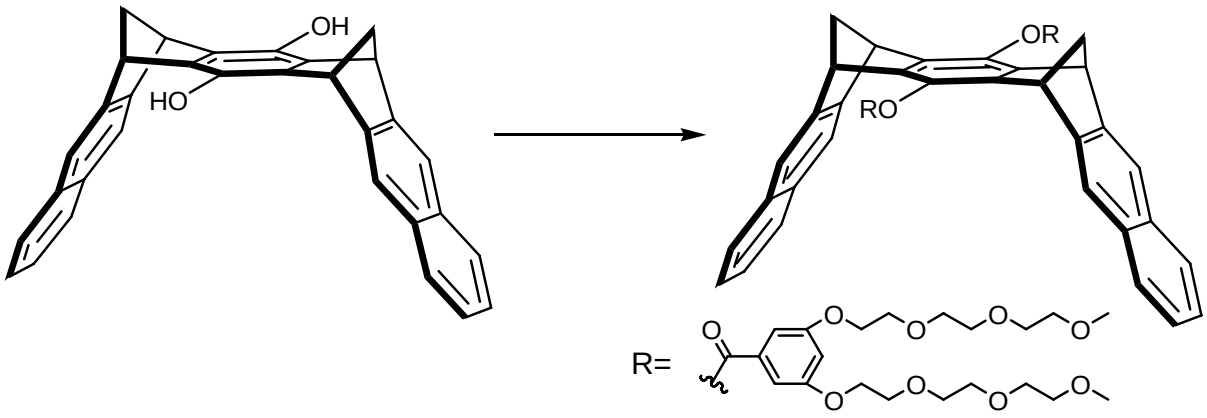

18c **27**

320 mg (0.73 mmol) of dihydroxy clip **18c** was dissolved in 15 mL of dry pyridine and stirred under argon. After 20 min. 679 mg (1.46 mmol) of the chloride **59** dissolved in 3 mL of dry pyridine were added to the solution and the mixture was heated at 90 ºC overnight under argon. Most of the solvent was removed in the rotatory evaporator under reduced pressure and the resulting crude residue was dissolved in chloroform and washed twice with diluted hydrochloric acid and twice with a saturated solution of sodium hydrogencarbonate. The organic layer was dried over sodium sulphate, filtered and the solvent was removed *in vacuo*. The crude residue was purified by column chromatography over silica gel and a mixture of ethyl acetate methanol 1:1 as eluant. After clean the column with pure methanol 350 mg (0.27 mmol) of the desired product were obtained as black viscose oil in 37% yield.

Molecular formula: $C_{74}H_{86}O_{20}$ (1295.46 g/mol)

HR-MS (ESI-TOF, MeOH, positive ionization), m/z = 1317.5625 $[M+Na]^+$ (Calculated for $C_{74}H_{86}NaO_{20}$= 1317.5610), 670.2767 $[M+2\cdot Na]^{2+}$ (Calculated for $C_{74}H_{86}Na_2O_{20}$= 670.2754)

HR-MS (EI 70 eV, MeOH), m/z = Not suitable to the technique.

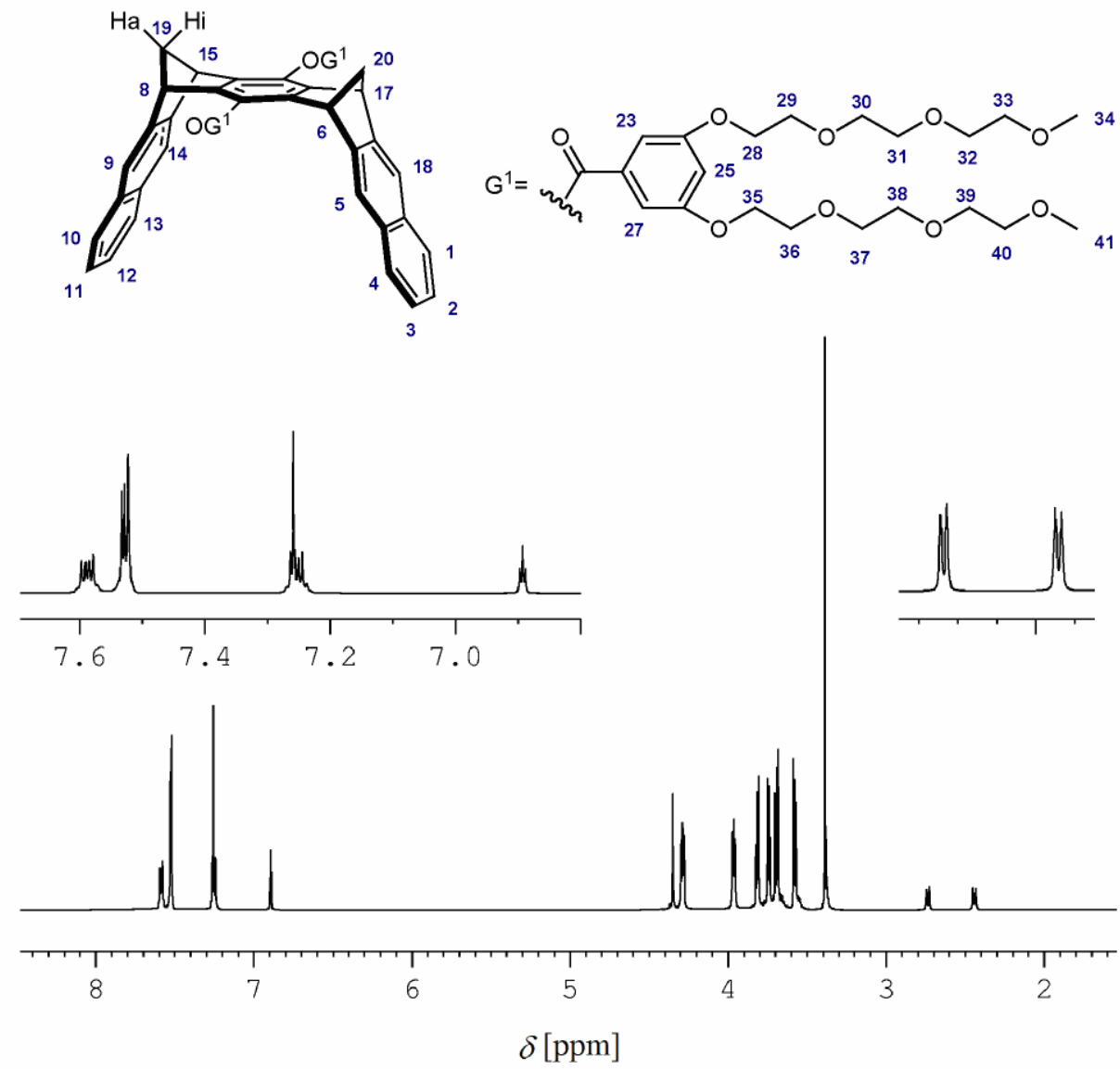

^{1}H NMR (500 MHz, $CDCl_3$) δ[ppm]: 2.44 (dt, 2H, ^{2}J(H-19a,H-19i)= 8.0 Hz, ^{3}J(H-19a, H-8)= 1.4 Hz, H-19a+H-20a), 2.74 (dt, 2H, ^{3}J(H-19i, H-8)= 1.4 Hz, H-19i+H-20i), 3.39 (s, 12H, H-34+H-41), 3.58 (m, 8H, H-33+H-40), 3.69 (m, 8H, H-32+H-39), 3.74 (m, 8H, H-31+H-38), 3.81 (m, 8H, H-30+H-37), 3.96 (t, 8H, ^{3}J(H-29, H-28)= 4.6 Hz, H-29+H-36), 4.29 (t, 8H, H-28+H-35), 4.35 (m, 4H, H-6+H-8+H-15+H-17), 6.89 (t, 2H, ^{4}J(H-25, H-23)= 2.3 Hz, H-25), 7.25 (m, 4H, H-2+H-3+H-12+H-11), 7.52 (s, 4H, H-5+H-9+H-14+H-18), 7.53 (d, 4H, H-23+H-27), 7.59 (dd, 4H, ^{3}J(H-1, H-2)= 6.1 Hz, ^{4}J(H-1, H-3)= 3.3 Hz, H-1+H-4+H-10+H-13)

^{13}C NMR (126 MHz, $CDCl_3$) δ[ppm]: 48.27 (C-6+C-8+C-15+C-17), 59.19 (C-34+C-41), 65.09 (C-19+C-20), 68.12 (C-29+C-36), 69.81 (C-28+C-35), 70.76 (C-32+C-39), 70.85 (C-31+C-38), 71.06 (C-30+C-37), 72.09 (C-33+C40), 107.68 (C-25), 108.98 (C-23+C-27), 120.30 (C-5+C-9+C-14+C-18), 125.31 (C-2+C-3+C-11+C-12), 127.82 (C-1+C-4+C-10+C-13), 131.22 (C-22), 132.27 (C-4a+C-9a+C-13a+C-18a), 137.64 (C-7+C-16), 141.12 (C-6a+C-7a+C-15a+C-16a), 145.99 (C-5a+C-8a+C-14a+C-7a), 160.28 (C-24+C-26), 164.30 (C-21)

IR (Film) $\tilde{\nu}$ [cm^{-1}]: 2878 (st, Csp^3-H), 1742 (st, C=O), 1594 (ring st), 1456 (scissors vibration, -CH_2-), 1302 (st, C-O-C), 1126 (antisym st, C-O-C), 860, 667.

4.3.4 Synthesis of allyloxy substituted clip 104

General procedure for allylation of 1,4-hydroquinones

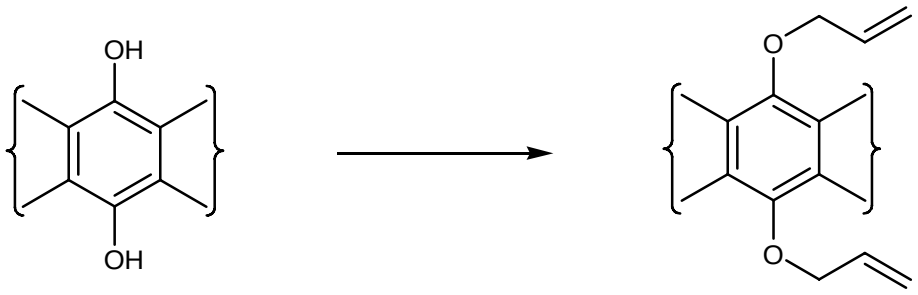

1,4 hydroquinone (1 eq) is added to a stirred mixture of K_2CO_3 (2.5 eq), and allyl bromide (3.3 eq) in dry acetone (2mL/mmol). The reaction mixture is heated up to reflux under argon atmosphere. After 6 hours the reaction is cooled down and the inorganic salts are filtered off over a filtration plate (pour 4). The acetone is removed in a rotatory evaporator under reduced pressure and the remaining solid is recrystallized with *n*-hexane at -20 ºC giving the desired product in an average yield of 80%.

Synthesis of 1,4-bis(allyloxy)benzene, 103[126]

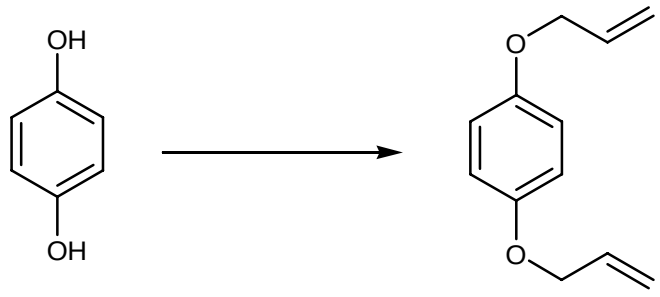

92 **103**

The general procedure was carried out with hydroquinone **92** (11 g, 0.10 mol), K_2CO_3 (34.5 g, 0.25 mol) and allyl bromide (40 g, 0.33 mol) dissolved in 200 mL of dry acetone giving finally 13.4 g (0.07 mol) of the 1,4-bis(allyloxy) benzene **103** in 70% yield.

Molecular formula: $C_{12}H_{14}O_2$ (190.24 g/mol)

Melting point *T* [ºC]= 29

HR-MS (ESI-TOF, MeOH, positive ionization), m/z = 191.1064 $[M+H]^+$ (Calculated for $C_{12}H_{15}O_2$= 1901.1072)

HR-MS (EI 70 eV, MeOH), m/z (%)= 190.1012 (17) $[M]^+$, 148.9692 (75) $[M\text{-}C_3H_5]^+$, 109.0290 (16) $[M\text{-}2\cdot C_3H_5+H]^+$

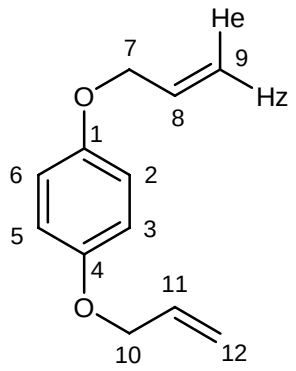

^{1}H NMR (500 MHz, $CDCl_3$) δ[ppm]: 4.48 (dt, 4H, ^3J(H-7,H-8)= 5.5 Hz, ^4J(H-8, H-9)= 1.5 Hz, H-7+H-10), 5.27 (ddt, 2H, ^3J(H-9$_Z$, H-8)= 10.5 Hz, ^2J(H-9z, H-9e)= 1.5 Hz ^4J(H-9z, H-7)= 1.0 Hz, H-9z+H-12z), 5.40 (ddt, 2H, ^3J(H-9e, H-8)= 17.0 Hz, ^4J(H-9e, H-7)= 1.5 Hz, H-9e+H-12e), 6.05 (m, 2H, H-8+H-11), 6.85 (s, 4H, H-2+H-3+H-5+H-6)

^{13}C NMR (126 MHz, $CDCl_3$) δ[ppm]: 69.46 (C-7+C-10), 115.64 (C-2+C-3+C-5+C-6), 117.47 (C-9+C-12), 133.58 (C-8+C-11), 152.87 (C-1+C-4)

IR (KBr) $\tilde{\nu}$ [cm^{-1}]: 3084 (st Csp^2-H), 2912 (st Csp^3-H), 1508 (ring st), 1231 (ArC-O st), 1023 (oop def, =CH), 826 (oop wag, CH^2), 790.

Synthesis of 7, 16-diallyloxy-(6α, 8α, 15α, 17α)-6, 8, 15, 17-tetrahydro-6, 17:8, 15-dimethanoheptacen, 104

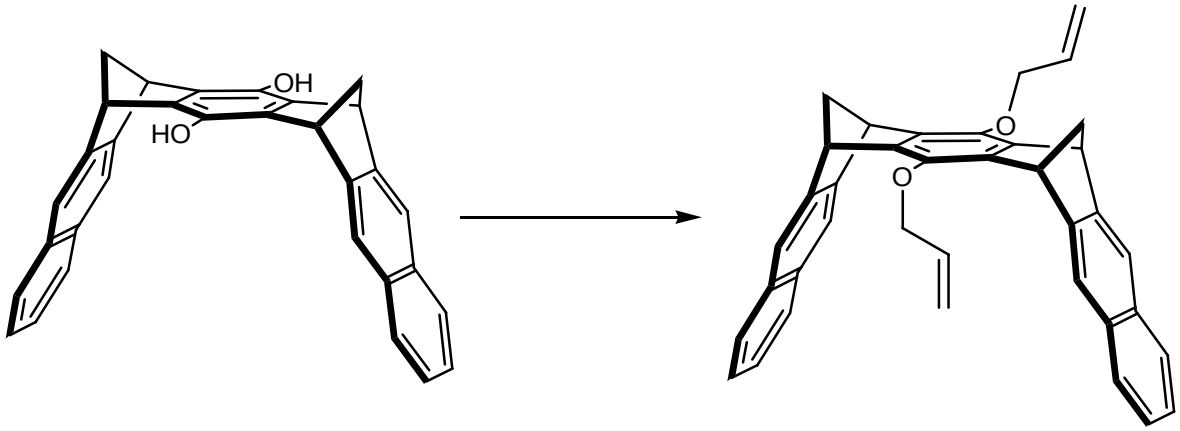

18c **104**

The general procedure was carried out with the dihydroxy clip **18c** (1.4 g, 3.21 mmol), K_2CO_3 (1.1 g, 8.05 mmol) and allyl bromide (1.3 g, 10.60 mmol) dissolved in 65 mL of dry acetone giving finally 1.66 g (3.21 mmol) of the desired allyloxy clip **104** in 96% yield.

Molecular formula: $C_{38}H_{30}O_2$ (518.22 g/mol)

Melting point *T* [ºC]= 242

HR-MS (ESI-TOF, MeOH, positive ionization), m/z = 519.2275 $[M+H]^+$ (Calculated for $C_{38}H_{31}O_2$= 519.2324), 536.2542 $[M+H_2O]^+$ (Calculated for $C_{38}H_{32}O_3$= 536.2351), 578.2821 $[M+{}^{i}PrOH]^+$ (Calculated for $C_{41}H_{38}O_3$= 578.2821)

HR-MS (EI 70 eV, MeOH), m/z (%)= 518.2277 (67) $[M]^+$, 477.1720 (100) $[M-C_3H_5]^+$, 436.1383 (28) $[M-2\cdot C_3H_5]^+$, 166.0828 (30) $[C_{13}H_{10}]^+$

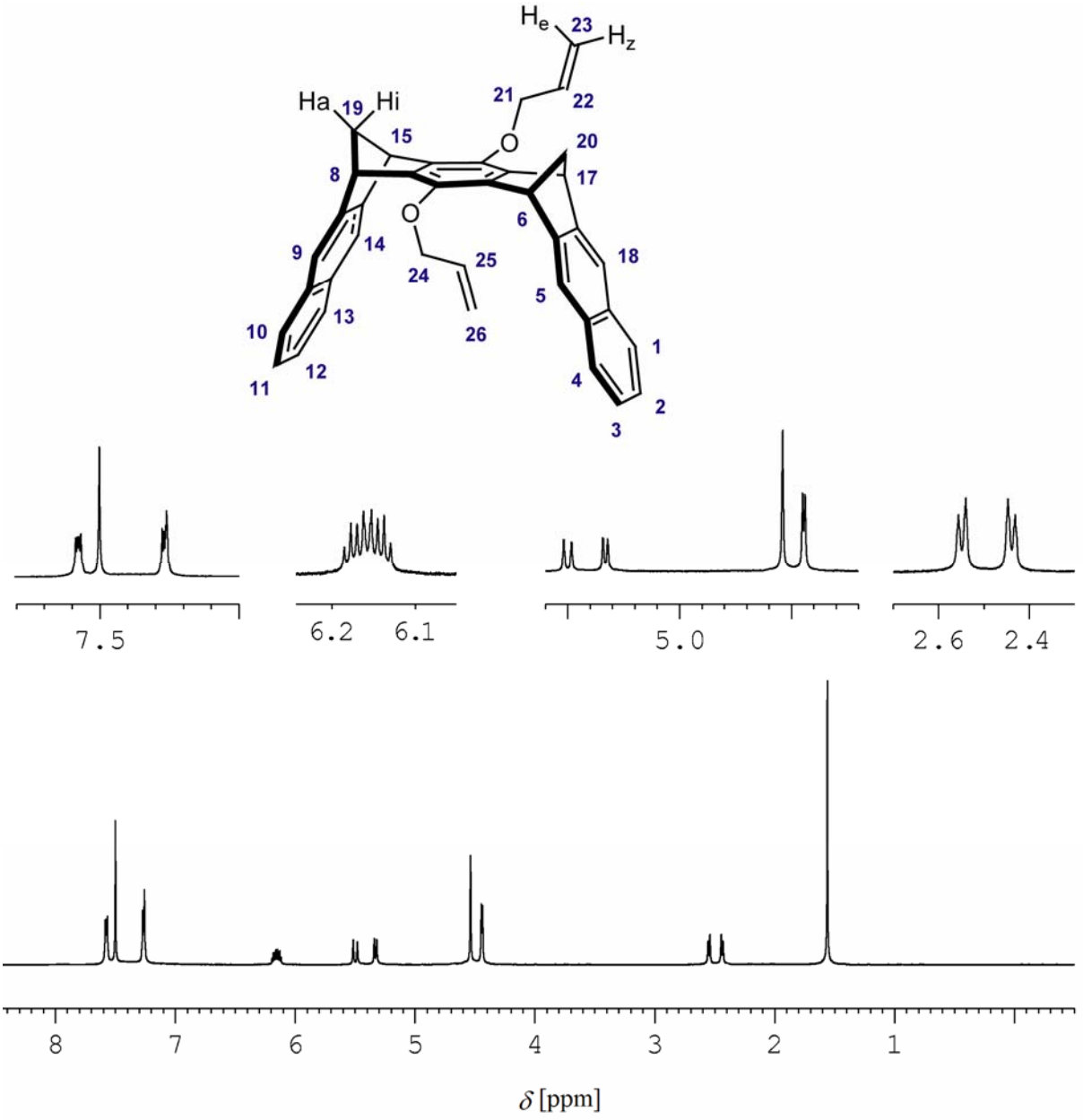

^{1}H NMR (500 MHz, $CDCl_3$) δ[ppm]: 2.44 (d, 2H, ^{2}J(H-19a,H-19i)= 8.0 Hz, H-19a+H-20a), 2.55 (d, 2H, H-19i+H-20i), 4.44 (dt, 2H, ^{3}J(H-21,H-22)= 5.4 Hz, ^{4}J(H-21, H-23)= 1.7 Hz, H-21+H-24), 4.54 (s, 4H, H-6+H-8+H-15+H-17), 5.33 (dd, 2H, ^{3}J(H-23z, H-22)= 10.8 Hz, ^{2}J(H-23z, H-23e)= 2.1 Hz, H-23z+H-26z), 5.50 (dd, 2H, ^{3}J(H-23e, H-22)= 17.3 Hz, H-23e+H-23e), 6.15 (m, 2H, H-22+H-24), 7.27 (dd, 4H, ^{3}J(H-2,H-1)= 6.3 Hz, ^{4}J(H-2,H-4)= 3.3 Hz, H-2+H-3+H-12+H-11), 7.50 (s, 4H, H-5+H-9+H-14+H-18), 7.58 (dd, 4H, H-1+H-4+H-10+H-13)

^{13}C NMR (126 MHz, $CDCl_3$) δ[ppm]: 47.64 (C-6+C-8+C-15+C-17), 64.26 (C-19+C-20), 74.53 (C-21+C-24), 117.23 (C-23+C-26), 119.43 (C-5+C-9+C-14+C-18), 125.21 (C-2+C-3+C-11+C-12), 127.55 (C-1+C-4+C-10+C-13), 132.04 (C-22+C-25), 134.43 (C-4a+C-9a+C-13a+C-18a), 140.02 (C-7+C-16), 144.45 (C-6a+C-7a+C-15a+C-16a), 147.21 (C-5a+C-8a+C-14a+C-17a)

IR (Diffuse reflection) $\tilde{\nu}$ [cm^{-1}]: 3002 (st Csp^2-H), 2931 (st Csp^3-H), 1476 (ring st), 1281 (ArC-O st), 1002 (oop def, =CH), 835 (oop wag, CH_2), 751, 619

UV/vis ($CHCl_3$): λ_{max} [nm] (log ε)= 240 (4.68), 255 (4.71), 309 (3.28), 324 (3.35).

4.3.5 Synthesis of glycerol substituted clips

4.3.5.1 Polymerization reactions

Synthesis of 7, 16-dipolyglycerol-(6α, 8α, 15α, 17α)-6, 8, 15, 17-tetrahydro-6, 17:8, 15-dimethanoheptacen, 98 and 99

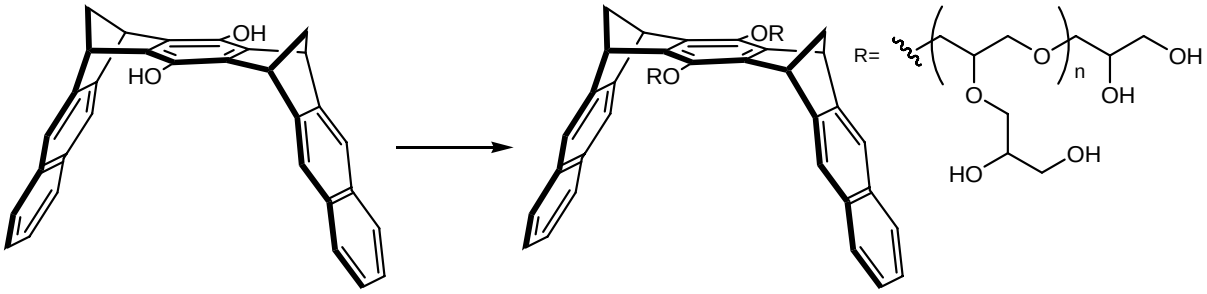

18c **98**

Synthesis carried out by Ewelina Burakowska in the working group of Prof. Dr. Rainer Haag (Freie Universität Berlin). Refer to page 57 for general description of the synthesis.

Molecular formula: Unknown

HR-MS = no suitable to any of the available methods in Essen. MALDI-TOF MS of **98** is shown in page 64.

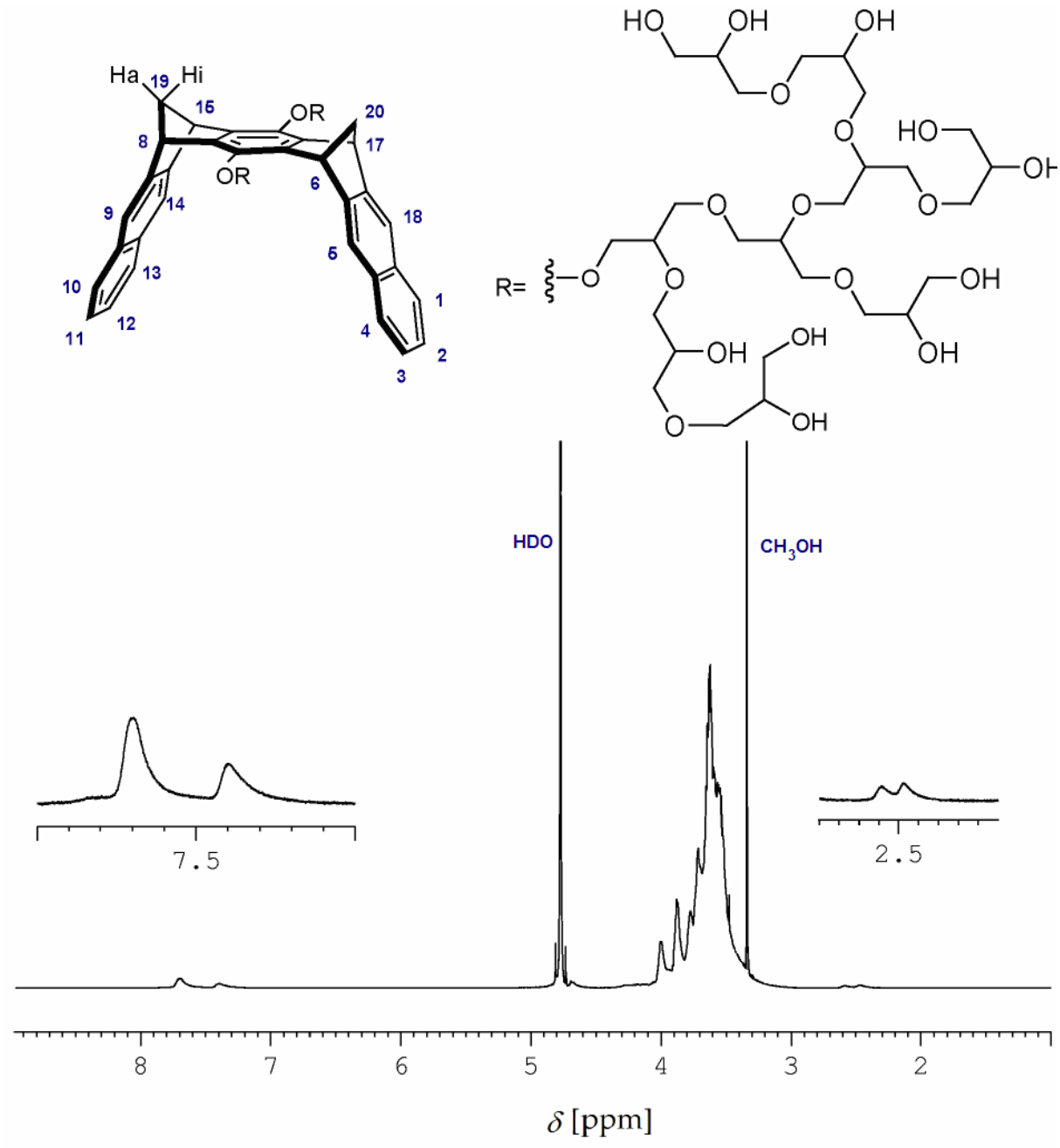

^{1}H NMR (99) (500 MHz, D_2O) δ[ppm]: 2.44 (br, 2H, H-19a+H-20a), 2.54 (br, H-19i+H-20i), 4.54 (br, 4H, H-6+H-8+H-15+H-17), 7.33 (br, 4H, H-2+H-3+H-12+H-11), 7.65 (br, 8H, H-5+H-9+H-14+H-18+H-1+H-4+H-10+H-13)

^{13}C NMR (99) (126 MHz, D_2O) δ[ppm]: 17.00, 29.36, 30.74, 47.53 (C-6+C-8+C-15+C-17), 48.94, 50.27, 60.81, 62.66, 66.93 (C-19+C-20), 68.93, 68.92, 69.21, 70.47, 70.78, 772.15, 77.97, 79.48, 119.68 (C-5+C-9+C-14+C-18), 125.91 (C-2+C-3+C-11+C-12), 127.78 (C-1+C-4+C-10+C-13), 131.86 (C-22+C-25), 147.18 (C-5a+C-8a+C-14a+C-17a)

IR (99) (Difusse reflection) $\tilde{\nu}$ [cm^{-1}]: 3359 (st O-H), 2871 (st Csp^2-H and Csp^3-H), 1453 (CH_2 scissors vibration), 1283 (ArC-O st), 1039 (st C-OH), 930, 862, 655

UV/vis (99) (H_2O): λ_{max} [nm] (log ε)= 228 (4.87), 257 (4.69), 308 (3.40), 322 (3.37).

4.3.5.2 Stepwise synthesis of glycerol substituted clips

Synthesis of 3,3'-(1,4-phenylenebis(oxy))dipropane-1,2-diol, 106

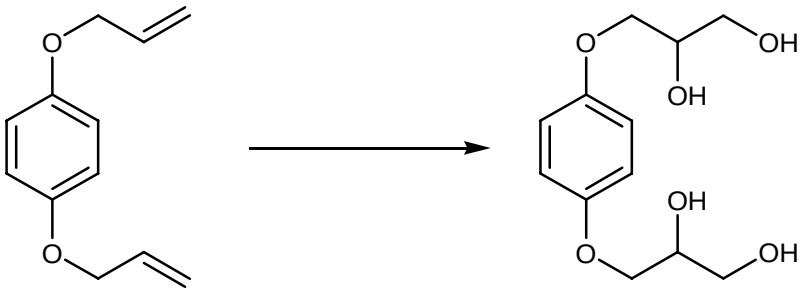

103 **106**

Synthesis carried out by Ewelina Burakowska in the working group of Prof. Dr. Rainer Haag (Freie Universität Berlin). Refer to page 69 for general description of the synthesis.

Molecular formula: $C_{12}H_{18}O_6$ (258.27 g/mol)

Melting point *T* [ºC]= 123

HR-MS (ESI-TOF, MeOH, positive ionization), m/z = 281.0992 $[M+Na]^+$ (Calculated for $C_{12}H_{18}NaO_6$= 281.1001), 539.2102 $[2\cdot M+Na]^+$ (Calculated for $C_{24}H_{36}NaO_{12}$= 539.2104)

HR-MS (ESI-TOF, MeOH, negative ionization), m/z = 257.1009 $[M-H]^-$ (Calculated for $C_{12}H_{17}O_6$= 257.1025), 515.2091 $[2\cdot M-H]^-$ (Calculated for $C_{24}H_{35}O_{12}$= 515.2129)

HR-MS (EI 70 eV, MeOH), m/z (%)= 258.1232 (14) $[M]^+$, 184.0790 (11) $[M-C_3H_7O_2+H]^+$, 110.0515 (67) $[M-2\cdot C_3H_7O_2+2\cdot H]^+$

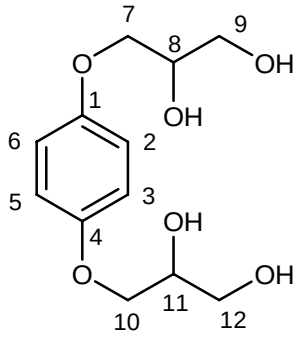

^{1}H NMR (500 MHz, D_2O) δ[ppm]: 3.68 (dd, 2H, ^{2}J(H-9r, H-9s)= 11.8 Hz, ^{3}J(H-9r, H-8)= 6.1 Hz, H-9r+H-12r), 3.74 (dd, 2H, ^{3}J(H-9s, H-8)= 4.6 Hz, H-9s+H-12s), 4.00 (dd, 2H, ^{2}J(H-7r, H-7s)= 9.8 Hz, ^{3}J(H-7r, H-8)= 6.2 Hz, H-7r+H-10r), 4.06 (m, 2H, H-8+H-11), 4.10 (dd, 2H, ^{3}J(H-7s, H-8)= 3.5 Hz, H-7s+H-10s), 7.00 (s, 4H, H-2+H-3+H-5+H-6)

^{13}C NMR (126 MHz, $CDCl_3$) δ[ppm]: 63.70 (C-9+C-12), 70.49 (C-7+C-10), 70.79 (C-8+C-11), 116.81 (C-2+C-3+C-5+C-6), 153.49 (C-1+C-4)

IR (Difusse reflection) $\tilde{\nu}$ [cm^{-1}]: 3302 (st O-H), 2920 (st Csp^2-H), 2872 (st Csp^3-H), 1511 (ring st), 1232 (ArC-O st), 1114 (st C-O), 1023 (st C-O), 818, 790, 719

Synthesis of 7, 16-bis{dihydroxypropyl}-(6α, 8α, 15α, 17α)-6, 8, 15, 17-tetrahydro-6, 17:8, 15-di-methanoheptacen, 28

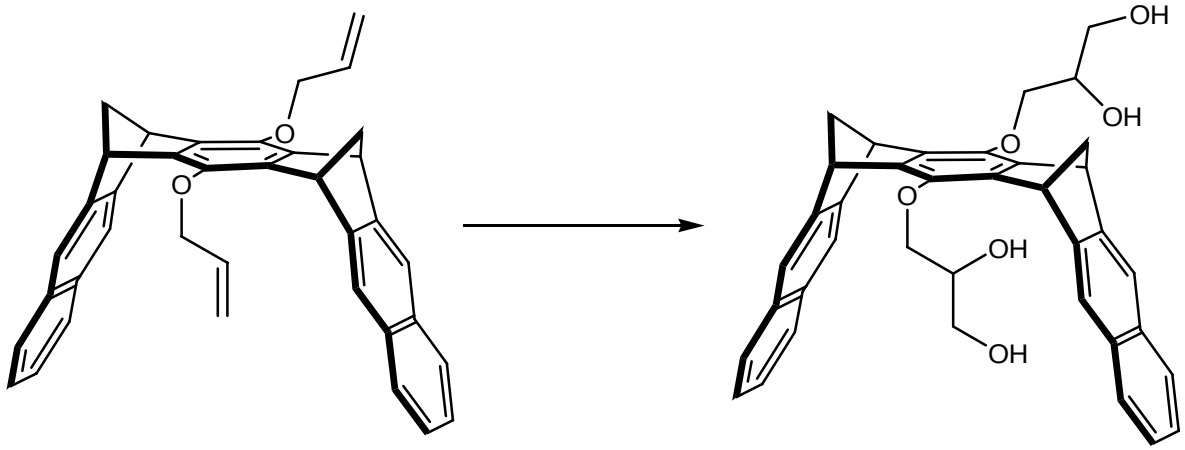

104 **28**

Synthesis carried out by Ewelina Burakowska in the working group of Prof. Dr. Rainer Haag (Freie Universität Berlin). Refer to page 57 for general description of the synthesis.

Molecular formula: $C_{38}H_{34}O_6$ (586.24 g/mol)

Melting point *T* [ºC]= 118

HR-MS (ESI-TOF, MeOH, positive ionization), m/z = 609.2264 $[M+Na]^+$ (Calculated for $C_{38}H_{34}NaO_6$= 609.2253), 1195.4635 $[2\cdot M+Na]^+$ (Calculated for $C_{76}H_{68}NaO_{12}$= 1195.4608)

HR-MS (ESI-TOF, MeOH, negative ionization), m/z = 585.2251 $[M-H]^-$ (Calculated for $C_{38}H_{33}O_6$= 585.2277)

HR-MS (EI 70 eV, MeOH), m/z (%)= 586.2374 (63) $[M]^+$, 512.1971 (25) $[M-C_3H_7O_2+H]^+$, 437.1520 (69) $[M-2\cdot C_3H_7O_2+H]^+$

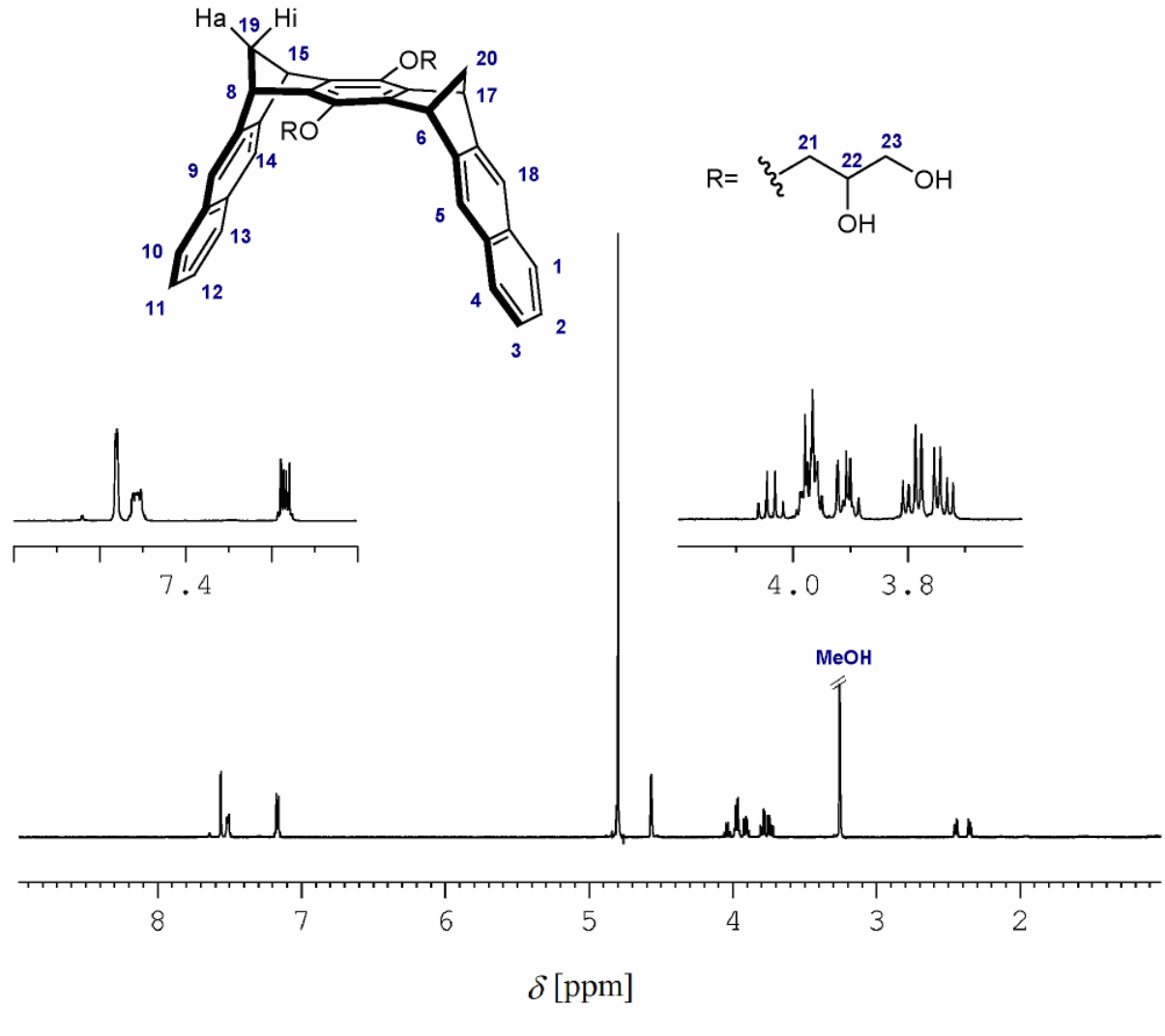

^{1}H NMR (500 MHz, CD_3OD) δ[ppm]: 2.41 (d, 2H, ^2J(H-19a,H-19i)= 8.0 Hz, H-19a+H-20a), 2.50 (d, 2H, H-19i+H-20i), 3.79 (dd, 2H, ^2J(H-23r, H-23s)= 11.3 Hz, ^3J(H-23r, H-22)= 5.4 Hz, H-23r+H-26r), 3.85 (dd, 2H, ^3J(H-23r, H-22)= 5.2 Hz, H-23s+H-26s), 3.99 (m, 6H, H-21+H-22+H-24+H-25), 4.62 (d, 4H, ^4J(H-6,H-5)= 2.0 Hz, H-6+H-8+H-15+H-17), 7.22

(dd, 4H, ^{3}J(H-2,H-1)= 6.0 Hz, ^{4}J(H-2,H-4)= 3.0 Hz, H-2+H-3+H-12+H-11), 7.57 (ddd, 4H, ^{4}J(H-1,H-18)= 1.9 Hz,H-1+H-4+H-10+H-13). 7.62 (d, 4H, H-5+H-9+H-14+H-18)

^{13}C NMR (126 MHz, CD_3OD) δ[ppm]: 48.93 (C-6+C-8+C-15+C-17), 64.29 (C-19+C-20), 65.18 (C-23+C-26), 72.40 (C-21+C-24), 76.21 (C-22+C-25), 120.55 (C-5+C-9+C-14+C-18), 126.17 (C-2+C-3+C-11+C-12), 128.59 (C-1+C-4+C-10+C-13), 133.58 (C-22+C-25), 133.59 (C-4a+C-9a+C-13a+C-18a), 141.51 (C-7+C-16), 145.77 (C-6a+C-7a+C-15a+C-16a), 148.51 (C-5a+C-8a+C-14a+C-17a)

IR (Difusse reflection) $\tilde{\nu}$ [cm^{-1}]: 3387 (st O-H), 2933 (st Csp^2-H), 2868 (st Csp^3-H), 1708 (st C=C), 1478 (ring st), 1281 (ArC-O st), 1242 (st C-O-C), 1116 (st C-O), 1039 (st C-O), 889, 747, 649

UV/vis (MeOH): λ_{max} [nm] (log ε)= 216 (4.60), 271 (3.24), 285 (3.28)

4.3.6 Preparation of sulphate substituted molecular clips

General procedure for sulphanation

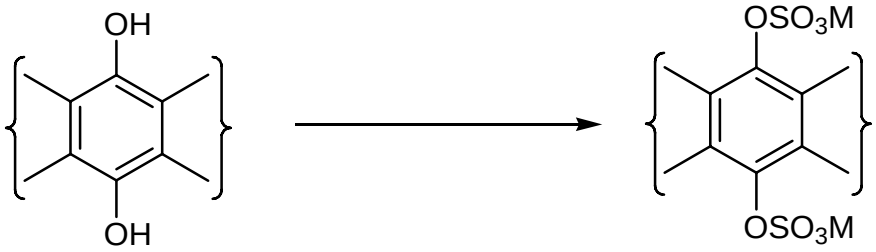

A mixture of the hydroquinone derivative (1 eq) and sulphur trioxide pyridinium complex (4 eq) are dissolved in dry pyridine (31 mL/mmol) and stirred under argon at 90 ºC. After 24 hours additional sulphur trioxide pyridinium complex (3 eq) is added and after 24 hours of additional reaction time the mixture is cooled to room temperature and quenched with an aqueous saturated solution of either $NaHCO_3$ or Li_2CO_3. The excess of inorganic salt is filtered off over a filtration plate (pour 4). The solution is washed three times with diethyl ether and the aqueous phase is concentrated *in vacuo*. The resulting dark solid is redissolved in ethanol and filtered again. The ethanolic solution is diluted with isopropanol and the organic solvents are removed in the rotatory evaporator under reduced pressure. A light brown solid is obtained. The yield of the reactions oscillates between 85 and 99%.

Synthesis of sodium 1,4-phenylene disulfate, 108

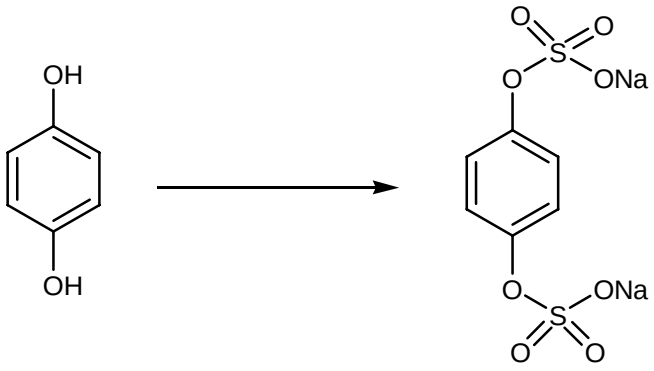

92 **108**

The general procedure carried out with hydroquinone **92** (110 mg, 1.0 mmol) and $NaHCO_3$ gave 310 mg (0.99 mmol) of the sodium sulphate benzene derivative **108** in 96% yield.

Molecular formula: $C_6H_4Na_2O_8S_2$ (291.21 g/mol)

Melting point *T* [ºC]> 300

HR-MS (ESI-TOF, MeOH, negative ionization), m/z = 290.9248 $[M\text{-}Na]^-$ (Calculated for $C_6H_4NaO_8S_2$= 290.9254), 133.9669 $[M\text{-}2\cdot Na]^{2-}$ (Calculated for $C_6H_4O_8S_2^{2-}$= 267.9348/2 = 133.9674)

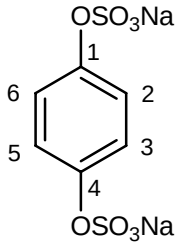

^{1}H NMR (500 MHz, CD_3OD) δ[ppm]: 6.99 (s, 4H, H-2+H-3+H-5+H-6)

^{13}C NMR (126 MHz, CD_3OD) δ[ppm]: 130.42 (C-2+C-3+C-5+C-6), 158.61 (C-1+C-4)

IR (KBr) $\tilde{\nu}$ [cm^{-1}]: 2962 (st, Csp^2-H), 1638 (st, C=C), 1513 (ring st), 1261 (ArC-O st), 1054 (oop def, =CH), 877, 703, 624, 570

Synthesis of sodium-(6α, 8α, 15α, 17α)-6, 8, 15, 17- tetrahydro- 6:17, 8:15-dimethano-heptacen-7, 16-bissulphate, 36

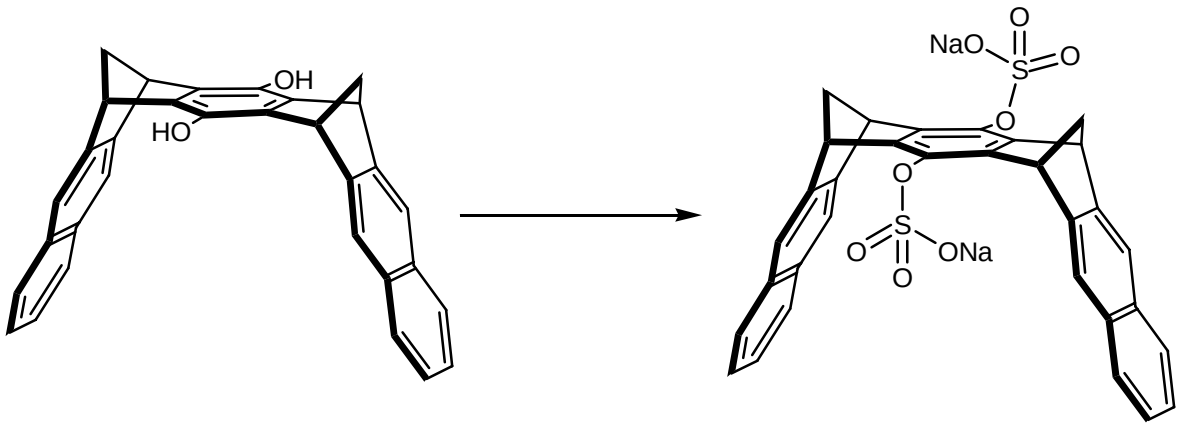

18c **36**

The general procedure carried out with dihydroxy clip **18c** (290 mg, 0.66 mmol) and $NaHCO_3$ gave 364.3 mg (0.57 mmol) of the sodium sulphate substituted clip **36** in 86% yield.

Molecular formula: $C_{32}H_{20}Na_2O_8S_2$ (642.61 g/mol)

Melting point *T* [ºC]> 300

HR-MS (ESI-TOF, MeOH, negative ionization), m/z = 298.0295 $[M-2\cdot Na]^{2-}$ (Calculated for $C_{32}H_{20}O_8S_2^{2-}$= 596.0600/2 = 298.0300), 619.0487 $[M-Na]^-$(Calculated for $C_{32}H_{20}NaO_8S_2$= 619.0497)

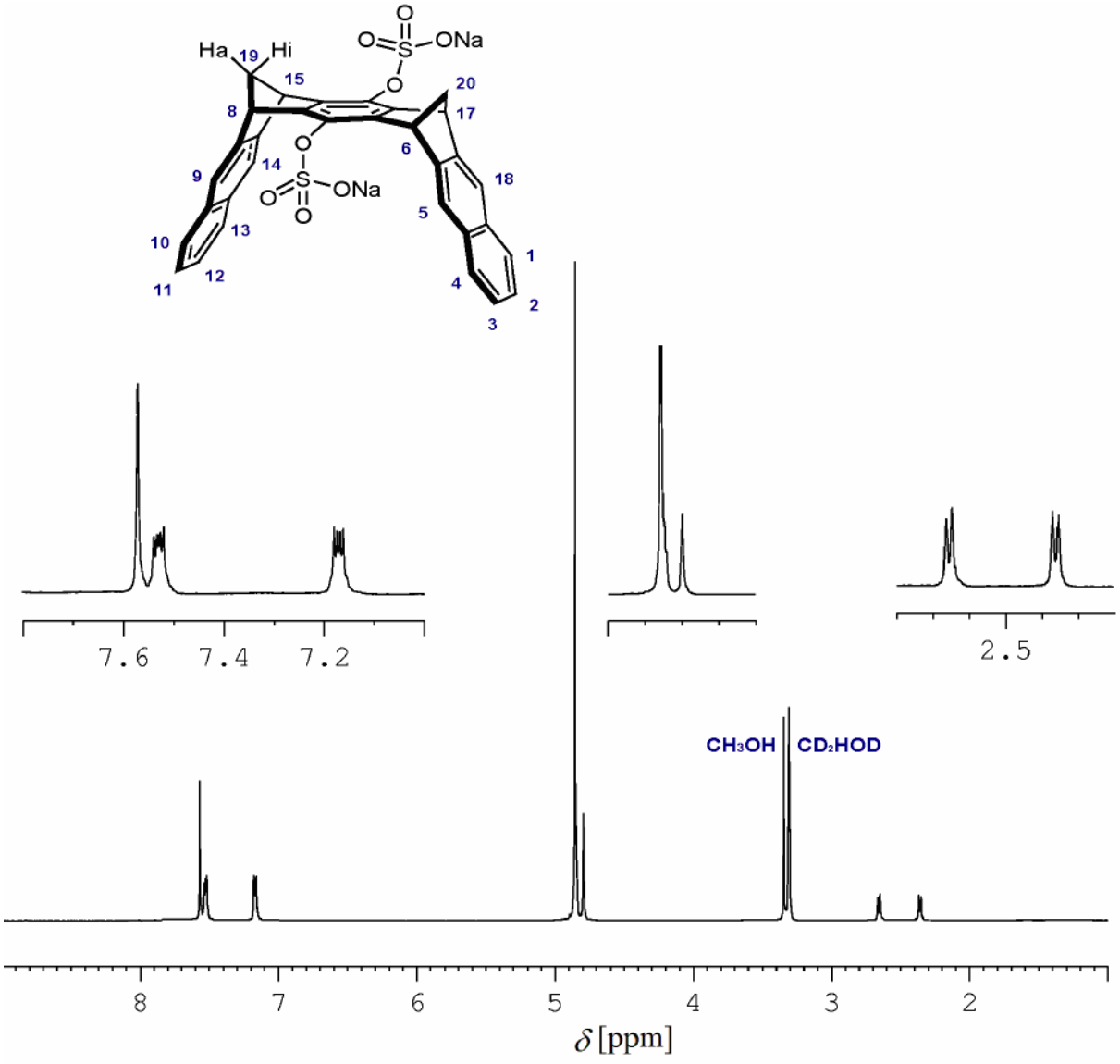

^{1}H NMR (500 MHz, CD_3OD) δ[ppm]: 2.36 (d, 2H, ^{2}J(H-19a,H-19i)= 7.9 Hz, H-19a+H-20a), 2.65 (d, 2H, H-19i+H-20i), 4.80 (s, 4H, H-6+H-8+H-15+H-17), 7.17 (dd, 4H, ^{3}J(H-2,H-1)= 6.3 Hz, ^{4}J(H-2,H-4)= 3.3 Hz, H-2+H-3+H-12+H-11), 7.53 (dd, 4H, H-1+H-4+H-10+H-13), 7.57 (s, 4H, H-5+H-9+H-14+H-18)

^{13}C NMR (126 MHz, CD_3OD) δ[ppm]: 49.66 (C-6+C-8+C-15+C-17), 65.74 (C-19+C-20), 120.97 (C-5+C-9+C-14+C-18), 125.79 (C-2+C-3+C-11+C-12), 128.57 (C-1+C-4+C-10+C-13), 133.55 (C-4a+C-9a+C-13a+C-18a), 139.64 (C-7+C-16), 144.02 (C-6a+C-7a+C-15a+C-16a), 148.59 (C-5a+C-8a+C-14a+C-17a)

^{1}H NMR (500 MHz, D_2O) δ[ppm]: 2.37 (d, 2H, ^{2}J(H-19a,H-19i)= 8.1 Hz, H-19a+H-20a), 2.63 (d, 2H, H-19i+H-20i), 4.70 (s, 4H, H-6+H-8+H-15+H-17), 6.78 (br, 4H, H-2+H-3+H-12+H-11), 7.01 (br, 4H, H-1+H-4+H-10+H-13), 7.20 (s, 4H, H-5+H-9+H-14+H-18)

^{13}C NMR (126 MHz, D_2O) δ[ppm]: 50.28 (C-6+C-8+C-15+C-17), 66.11 (C-19+C-20), 121.20 (C-5+C-9+C-14+C-18), 126.31 (C-2+C-3+C-11+C-12), 128.56 (C-1+C-4+C-10+C-13), 132.67 (C-4a+C-9a+C-13a+C-18a), 139.26 (C-7+C-16), 144.45 (C-6a+C-7a+C-15a+C-16a), 147.48 (C-5a+C-8a+C-14a+C-17a)

IR (Diffuse reflection) $\tilde{\nu}$ [cm^{-1}]: 2870 (st, Csp^3-H), 1232 (st S=O), 1622 (st C=C), 1044 (st S=O), 945, 835, 743

UV/vis (H_2O): λ_{max} [nm] (log ε)= 219 (4.87), 274 (4.17), 308 (3.37), 322 (3.34).

Synthesis of lithium-(6α, 8α, 15α, 17α)-6, 8, 15, 17- tetrahydro- 6:17, 8:15-dimethano-heptacen-7, 16-bissulphate, 37

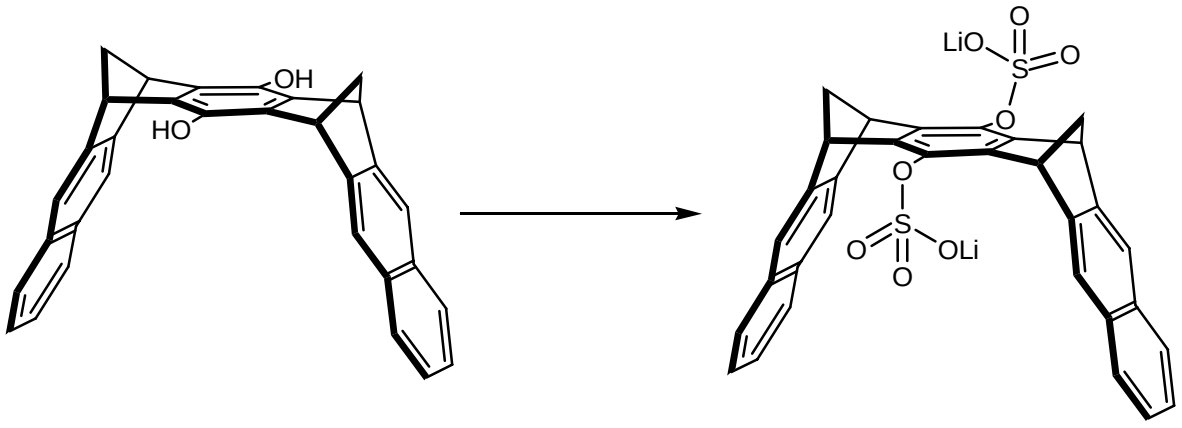

18c **37**

The general procedure carried out with dihydroxy clip **18c** (271 mg, 0.62 mmol) and Li_2CO_3 gave 346 mg (0.57 mmol) of the lithium sulphate substituted clip in 91% yield.

Molecular formula: $C_{32}H_{20}Li_2O_8S_2$ (610.50 g/mol)

Melting point *T* [ºC]> 300

HR-MS (ESI-TOF, MeOH, negative ionization), m/z = 298.0295 $[M-2\cdot Li]^{2-}$ (Calculated for $C_{32}H_{20}O_8S_2^{2-}$= 596.0600/2= 298.0300), 603.0743 $[M-Na]^-$ (Calculated for $C_{32}H_{20}LiO_8S_2$= 603.0760)

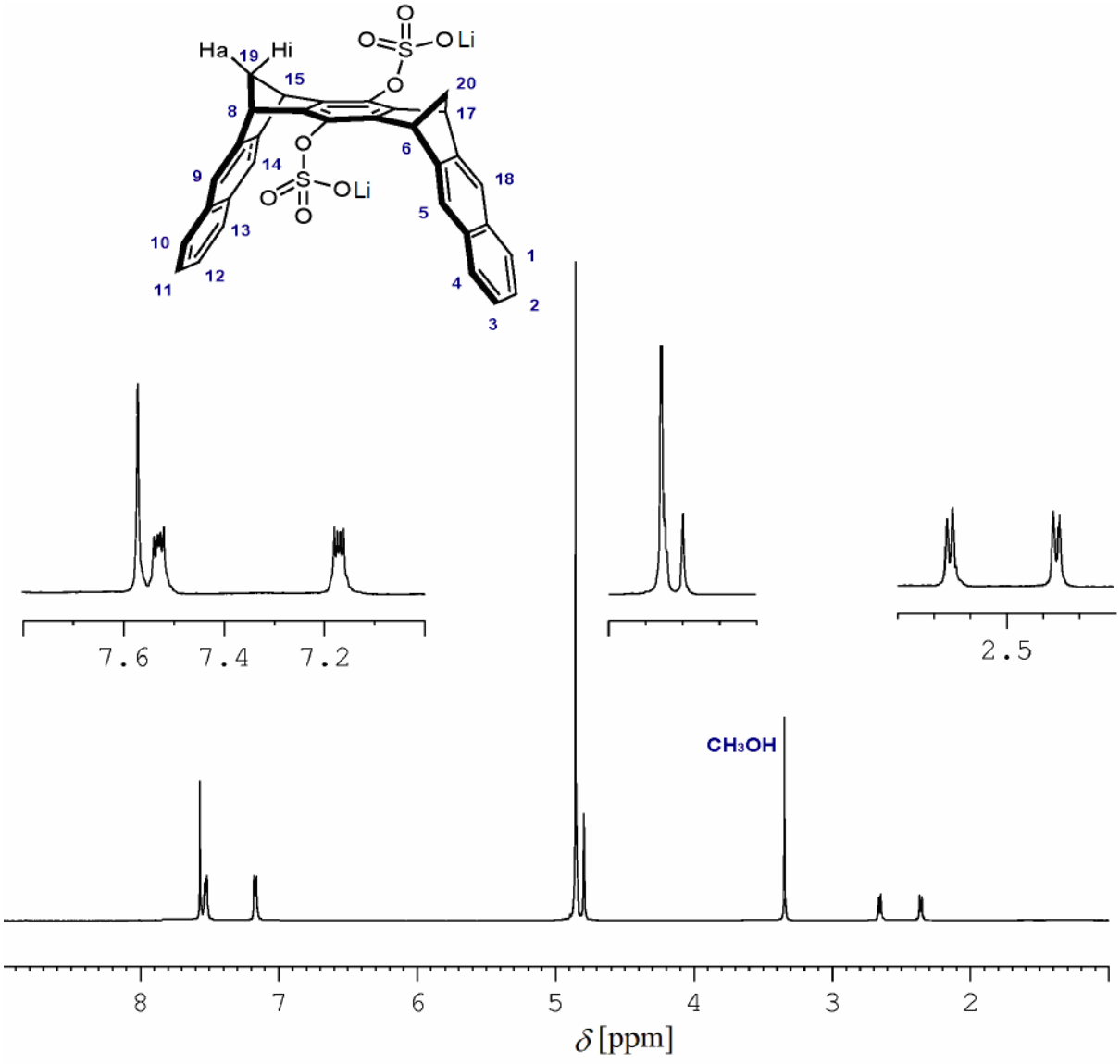

^{1}H NMR (500 MHz, CD_3OD) δ[ppm]: 2.36 (dt, 2H, ^{2}J(H-19a,H-19i)= 7.6 Hz, ^{3}J(H-19a,H-8)= 1.6 Hz, H-19a+H-20a), 2.66 (dt, 2H, ^{3}J(H-19i,H-8)= 1.6 Hz, H-19i+H-20i), 4.80 (t, 4H, H-6+H-8+H-15+H-17), 7.18 (dd, 4H, ^{3}J(H-2,H-1)= 5.9 Hz, ^{4}J(H-2,H-4)= 3.0 Hz, H-2+H-3+H-12+H-11), 7.54 (dd, 4H, H-1+H-4+H-10+H-13), 7.58 (s, 4H, H-5+H-9+H-14+H-18)

^{13}C NMR (126 MHz, CD_3OD) δ[ppm]: 49.68 (C-6+C-8+C-15+C-17), 65.75 (C-19+C-20), 120.95 (C-5+C-9+C-14+C-18), 125.76 (C-2+C-3+C-11+C-12), 128.60 (C-1+C-4+C-10+C-13), 133.58 (C-4a+C-9a+C-13a+C-18a), 139.63 (C-7+C-16), 144.00 (C-6a+C-7a+C-15a+C-16a), 148.60 (C-5a+C-8a+C-14a+C-17a)

^{1}H NMR (500 MHz, D_2O) δ[ppm]: 2.33 (d, 2H, ^{2}J(H-19a,H-19i)= 8.0 Hz, H-19a+H-20a), 2.63 (d, 2H, H-19i+H-20i), 4.68 (s, 4H, H-6+H-8+H-15+H-17), 6.28 (br, 4H, H-2+H-3+H-12+H-11), 6.59 (br, 4H, H-1+H-4+H-10+H-13), 6.97 (s, 4H, H-5+H-9+H-14+H-18)

^{13}C NMR (126 MHz, D_2O) δ[ppm]: 48.18 (C-6+C-8+C-15+C-17), 64.78 (C-19+C-20), 119.79 (C-5+C-9+C-14+C-18), 124.59 (C-2+C-3+C-11+C-12), 126.88 (C-1+C-4+C-10+C-13), 131.14 (C-4a+C-9a+C-13a+C-18a), 137.92 (C-7+C-16), 143.18 (C-6a+C-7a+C-15a+C-16a), 145.76 (C-5a+C-8a+C-14a+C-17a)

IR (Diffuse reflection) $\tilde{\nu}$ [cm^{-1}]: 2970 (st, Csp^3-H), 1627 (st C=C), 1235 (st S=O), 1050 (st S=O), 946, 890, 837, 745, 697

UV/vis (H_2O): λ_{max} [nm] (log ε)= 219 (4.97), 274 (4.25), 308 (3.31), 322 (3.32).

Synthesis of sodium-(7α, 9α, 18α, 20α)-7, 9, 18, 20-tetrahydro-7, 20:9, 18-dimethanononacen-8, 19-bissulphate, 38

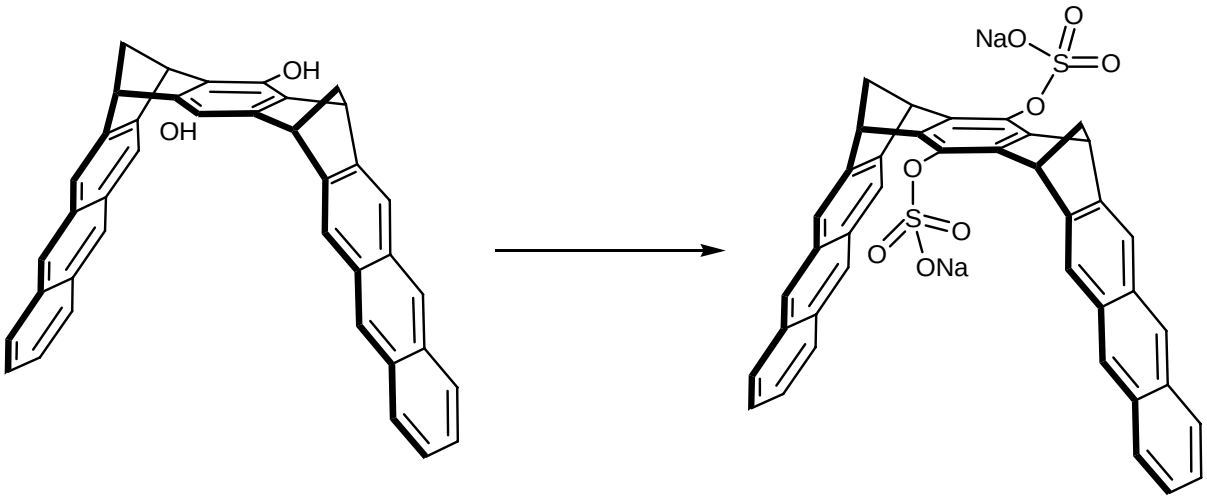

112 **38**

The general procedure carried out with dihydroxy anthracene clip **112** (173.7 mg, 0.32 mmol) and $NaHCO_3$ gave 220 mg (0.30 mmol) of the sodium anthracene sulphate substituted clip **38** in 92% yield.

Molecular formula: $C_{40}H_{24}Na_2O_8S_2$ (742.07 g/mol)

Melting point *T* [ºC]> 300

HR-MS (ESI-TOF, MeOH, negative ionization), m/z = 348.0484 $[M-2\cdot Na]^{2-}$ (Calculated for $C_{40}H_{24}O_8S_2^{2-}$= 696.0918/2= 348.0459), 719.0870 $[M-Na]^-$ (Calculated for $C_{40}H_{24}NaO_8S_2$= 719.0816)

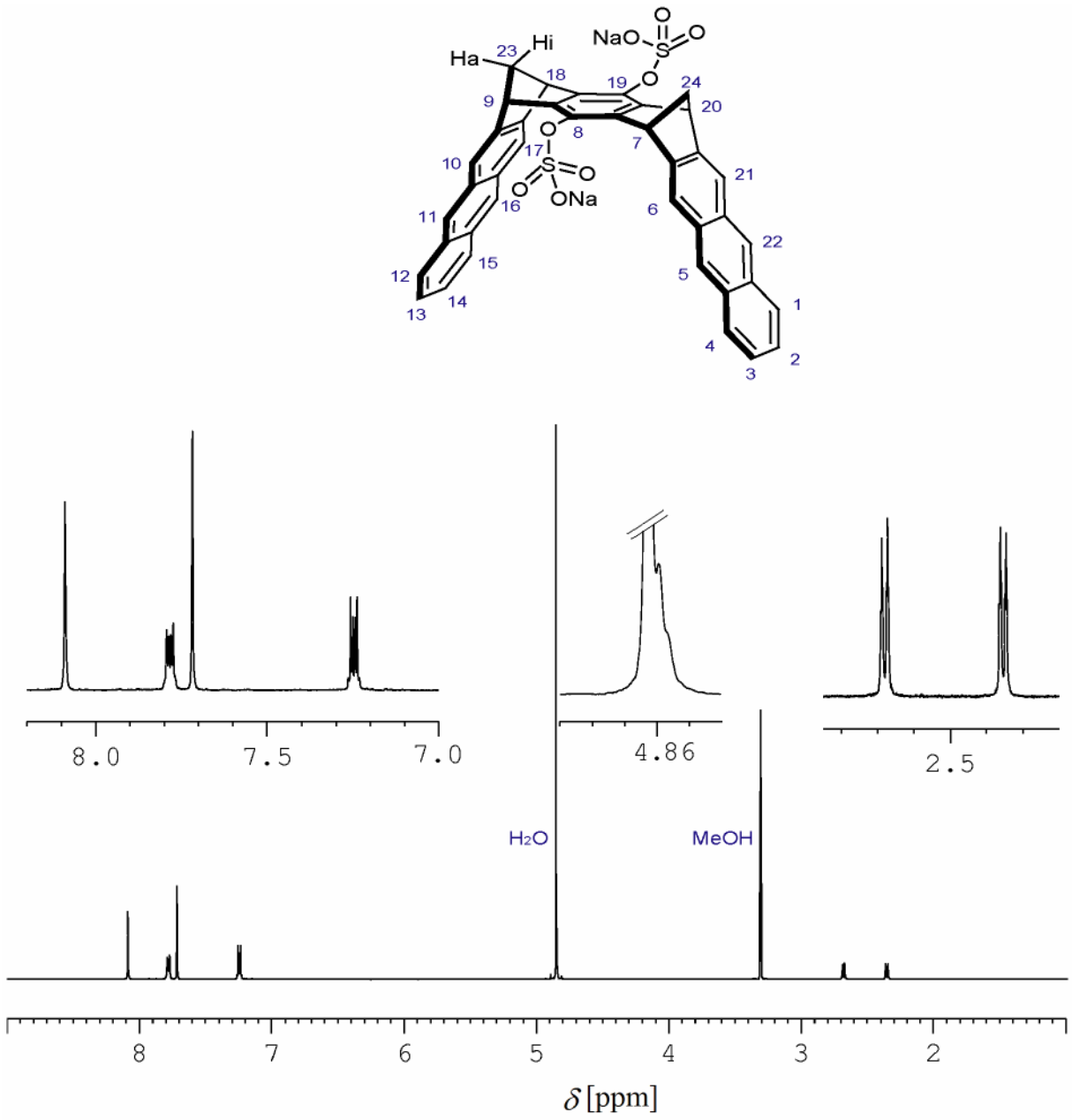

^{1}H NMR (500 MHz, CD_3OD) δ[ppm]: 2.70 (dt, 2H, ^{2}J(H-23a,H-23i)= 7.8 Hz, ^{3}J(H-23a,H-9)= 1.5 Hz, H-23a+H-24a), 2.68 (dt, 2H, ^{3}J(H-23i,H-9)= 1.3 Hz, H-23i+H-24i), 4.85 (s, 4H, H-7+H-9+H-18+H-20), 7.25 (dd, 4H, ^{3}J(H-2,H-1)= 6.5 Hz, ^{4}J(H-2,H-4)= 3.2 Hz, H-2+H-3+H-13+H-14), 7.72 (s, 4H, H-6+H-10+H-17+H-21), 7.78 (dd, 4H, H-1+H-4+H-12+H-15), 8.09 (s, 4H, H-5+H-11+H-16+H-22)

^{13}C NMR (126 MHz, CD_3OD) δ[ppm]: 64.33 (C-23+C-24), 64.80 (C-7+C-9+C-18+C-20), 120.58 (C-6+C-10+C-17+C-21), 125.52 (C-2+C-3+C-13+C-14), 126.60 (C-5+C-11+C-16+C-22), 128.85 (C-1+C-4+C-12+C-15), 132.54 (C-5a+C-10a+C-16a+C-21a), 132.82 (C-4a+C-11a+C-15a+C-22a), 139.69 (C-8+C-19), 143.62 (C-7a+C-8a+C-18a+C-19a), 147.72 (C-6a+C-9a+C-17a+C-20a)

^{1}H NMR (500 MHz, D_2O) δ[ppm]: 2.44 (br, 2H, H-23i+H-24i), 2.75 (br, 2H, H-23^{a}+H-24^{a}), 4.76 (s, 4H, H-7+H-9+H-18+H-20), 5.95 (br, 4H, H-5+H-11+H-16+H-22), 6.65 (br, 8H, H-1+H-4+H-6+H-10+H-12+H-15+H-17+H-21), 6.79 (br, 4H, H-2+H-3+H-13+H-14)

^{13}C NMR (126 MHz, D_2O) δ[ppm]: 48.57 (C-7+C-9+C-18+C-20), 62.54 (C-23+C-24), , 120.03 (C-6+C-10+C-17+C-21), 124.28 (C-2+C-3+C-13+C-14), 124.73 (C-5+C-11+C-16+C-22), 127.63 (C-1+C-4+C-12+C-15), 129.88 (C-5a+C-10a+C-16a+C-21a), 130.47 (C-4a+C-11a+C-15a+C-22a), 138.65 (C-8+C-19), 143.72 (C-7a+C-8a+C-18a+C-19a), 144.58 (C-6a+C-9a+C-17a+C-20a)

IR (Diffuse reflection) $\tilde{\nu}$ [cm^{-1}]: 2944 (st, Csp^3-H), 1626 (st C=C), 1231 (st S=O), 1041 (st S=O), 946, 902, 839, 768, 739

UV/vis (H_2O): λ_{max} [nm] (log ε)= 252 (4.93), 337 (3.76), 354 (3.82), 371 (3.68).

4.4 Evaluation of receptor solubility

4.4.1 Evaluation of solubility by ^{1}H NMR

A known amount of receptor is poured into a flask together with 0.7 mL of the deuterated solvent to evaluate. The flask is sealed and the mixture is heated up to 50 ºC for two hours. After cooling down the solution is transferred into a NMR tube through a syringe filter in order to separate it from the remaining solid. After the addition of a known amount of an internal standard (another solvent) a ^{1}H NMR is measured and the solubility is calculated by the relative integrals (internal standard *vs*. receptor).

Receptor	Solvent	mg of receptor	Internal Standard	Solubility [mg/mL]
26	$CDCl_3$	4.1	CH_2Cl_2	Complete
26	CD_3OD	3.5	CH_2Cl_2	2.8
26	D_2O	5.3	1,4-dioxane	Not detected
27	$CDCl_3$	6.2	CH_2Cl_2	Complete
27	CD_3OD	5.2	CH_2Cl_2	Complete
27	D_2O	5.7	1,4-dioxane	Not detected

4.4.2 Evaluation of water solubility by UV-vis

A known amount of receptor is poured into a flask together with a measured volume of water (X mL). The mixture is heated up to 50 ºC in the ultrasound bath for one and a half hours. The solution is filtered off into another flask and the water is removed *in vacuo*. The remaining solid is dissolved with 2 mL of a solvent in which the UV-vis spectrum of the receptor is already known (usually methanol). The UV-vis of this solution is measured and the unknown concentration of the receptor is evaluated by the Lambert-Beer law:[146]

$$A = \varepsilon \cdot c \cdot l$$

Where:

- A: Absorbance [unitless]
- ε: Molar absorptivity [$L \cdot mol^{-1} \cdot cm^{-1}$]
- c: Concentration [$mol \cdot L^{-1}$]
- l: Length of the measuring cell [cm]

The concentration measured is that of the methanol solution and it must be corrected with the volume of water used in the extraction:

$$C_{water} = C_{MeOH} \times \frac{2\ \text{mL MeOH}}{\text{X mL } H_2O}$$

Receptor	Solvent	mg of receptor	mL of Solvent	Solubility [mg/mL]	Solubility [mmol/mL]
28	H_2O	2.12	0.80	$6.16 \cdot 10^{-3}$	$1.05 \cdot 10^{-5}$
27	H_2O	4.73	1.60	$6.62 \cdot 10^{-3}$	$5.11 \cdot 10^{-6}$

4.5 Determination of association constants K_a

The determination of the association constants, K_a, was carried out following the description given in the chapter 2.1.3.5.4 (page 36) via NMR titrations using a Bruker DRX 500 NMR spectrometer. For the analysis of the data the program Table Curve 2D was used. All the determined association constants are rounded as shown in chapter 2. The indicated errors are located at 95% of confidence limit in the non-linear regression. The abbreviations used in the following tables are shown below.

m_R and. m_G	Weighed portion of receptor and guest respectively
M_R and. M_G	Molecular weight of the receptor and guest respectively
V_0	Volume of the stock solution
V	Volume of the titration solution
$[R]_0$	Total concentration of the receptor
$[G]_0$	Total concentration of the guest
δ_0	Chemical shift of the free guest
δ_{obs}	Chemical shift of the guest in presence of the receptor
$\Delta\delta_{obs} = \delta_0 - \delta_{obs}$	Observed complexation-induced up-field shift of the guest protons
$\Delta\delta_{calc}$	Calculated complexation-induced up-field shift of the guest protons
$\Delta\delta_{max}$	Maximum complexation-induced shift of the guest protons
K_a	Association constant
n. d.	Not detected

4.5.1 ^{1}H NMR titrations with constant guest concentration

Receptor:	**27**	M_R [g/mol]:	1295.46
Solvent:	CD_3OD	M_G [g/mol]:	194.19
T [°C]:	25	m_R [mg]:	13.61
Substrat:	Caffeine (**34**)	m_G [mg]:	3.25
		V_0 [mL]:	3.15
		$[G]_0$ [mM]:	5.26

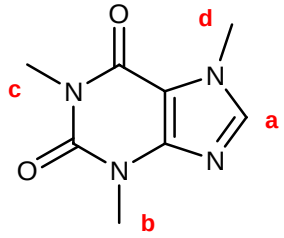

δ_0 (H_a) [ppm] = 7.8603

δ_0 (H_b) [ppm] = 3.5334

V [mL]	$[R]_0$ [M]	δ_{obs} (H_a) [ppm]	$\Delta\delta_{obs}$ (H_a) [ppm]	$\Delta\delta_{calc}$ (H_a) [ppm]
0.60	0.017510	7.6714	0.1889	0.1827
0.65	0.016163	7.6762	0.1841	0.1796
0.70	0.015008	7.6800	0.1803	0.1765
0.75	0.014008	7.6834	0.1769	0.1735
0.80	0.013132	7.6853	0.1750	0.1704
0.85	0.012360	7.6901	0.1702	0.1674
0.90	0.011673	7.6937	0.1666	0.1644
0.95	0.011059	7.6968	0.1635	0.1615
1.00	0.010506	7.6988	0.1615	0.1557
1.10	0.009551	7.7069	0.1534	0.1501
1.20	0.008755	7.7134	0.1469	0.1446
1.30	0.008081	7.7158	0.1445	0.1395
1.40	0.007504	7.7242	0.1361	0.1345
1.50	0.007004	7.7261	0.1342	0.1298
1.60	0.006566	7.7302	0.1301	0.1253
1.70	0.006180	7.7343	0.1260	0.1210
1.80	0.005837	7.7364	0.1239	0.1170

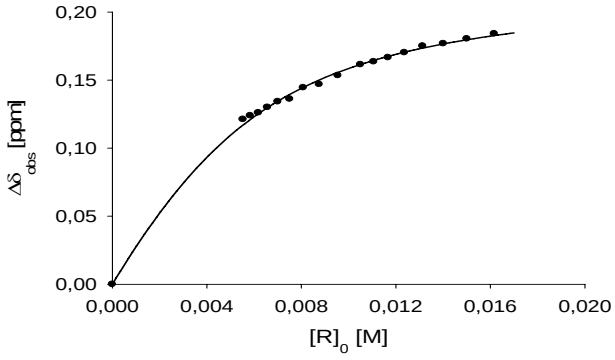

K_a [M^{-1}] = 415 ± 45

$\Delta\delta_{max}$ (H_a) [ppm] = 0.22

$\Delta\delta_{max}$ (H_b) [ppm] = 0.05

34@**27** ^{1}H NMR (500 MHz, CD_3OD) δ[ppm]: 2.34 (dt, 2H, H-19a+H-20a), 2.56 (dt, 2H, H-19i+H-20i), 3.49 (s, 3H, Caffeine, H_b), 4.37 (s, 4H, H-6+H-8+H-15+H-17), 6.96 (t, 2H, H-25), 7.11 (dd, 4H, H-2+H-3+H-12+H-11), 7.42 (dd, 4H, H-1+H-4+H-10+H-13), 7.43 (s, 4H, H-5+H-9+H-14+H-18), 7.53 (d, 4H, H-23+H-27), 7.64 (s, 1H, Caffeine, H_a)

Receptor:	**27**	M_R [g/mol]:	1295.46
Solvent:	CD_3OD	M_G [g/mol]:	246.06
T [°C]:	25	m_R [mg]:	22.45
Substrat:	NMNA (**33**)	m_G [mg]:	6.40
	δ_0 (H_a) [ppm] = 9.3690	V_0 [mL]:	3.00
	δ_0 (H_b) [ppm] = 8.9371	$[G]_0$ [mM]:	8.67
	δ_0 (H_c) [ppm] = 8.1813		
	δ_0 (H_d) [ppm] = 9.0334		
	δ_0 (H_e) [ppm] = 4.4804		

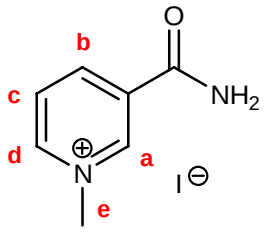

V [mL]	$[R]_0$ [M]	δ_{obs} (H_c) [ppm]	$\Delta\delta_{obs}$ (H_c) [ppm]	$\Delta\delta_{calc}$ (H_c) [ppm]
0.60	0.028883	6.4480	1.7330	1.7406
0.65	0.026661	6.5120	1.6690	1.6724
0.70	0.024757	6.5710	1.6100	1.6088
0.75	0.023106	6.6250	1.5560	1.5495
0.80	0.021662	6.6800	1.5010	1.4941
0.85	0.020388	6.7390	1.4420	1.4423
0.90	0.019255	6.7880	1.3930	1.3937
0.95	0.018242	6.8360	1.3450	1.3481
1.00	0.017330	6.8750	1.3060	1.3052
1.10	0.015754	6.9370	1.2440	1.2267
1.20	0.014441	7.0170	1.1640	1.1568
1.30	0.013331	7.0970	1.0840	1.0941
1.40	0.012378	7.1600	1.0210	1.0377

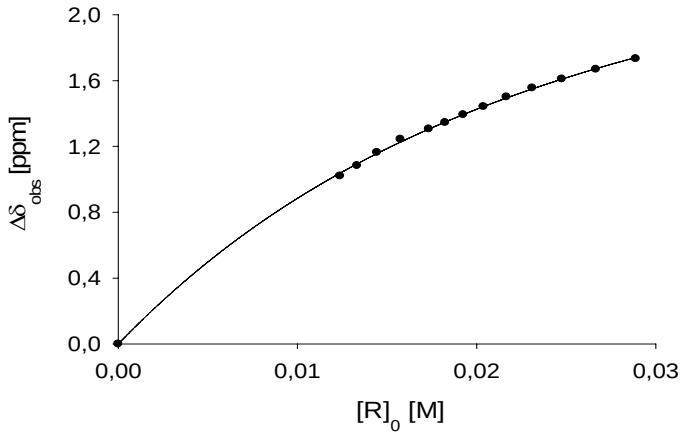

K_a [M^{-1}]	=	65 ± 7
$\Delta\delta_{max}$ (H_a) [ppm]	=	2.50
$\Delta\delta_{max}$ (H_b) [ppm]	=	2.75
$\Delta\delta_{max}$ (H_c) [ppm]	=	3.12
$\Delta\delta_{max}$ (H_d) [ppm]	=	2.04
$\Delta\delta_{max}$ (H_e) [ppm]	=	2.93

33@**27** ^{1}H NMR (500 MHz, CD_3OD) δ[ppm]: 1.55 (s, 3H, NMNA, H_e), 2.18 (dt, 2H, H-19a+H-20a), 2.37 (dt, 2H, H-19i+H-20i), 4.41 (s, 4H, H-6+H-8+H-15+H-17), 5.06 (t, 1H, NMNA, H_c), 6.18 (d, 1H, NMNA, H_b), 6.68 (dd, 4H, H-1+H-4+H-10+H-13), 6.70 (dd, 4H, H-2+H-3+H-12+H-11), 6.87 (s, 1H, NMNA, H_a), 7.03 (d, 1H, NMNA, H_d), 7.04 (s, 4H, H-5+H-9+H-14+H-18), 7.04 (t, 2H, H-25), 7.60 (d, 4H, H-23+H-27)

Receptor:	**27**	M_R [g/mol]:	1295.46
Solvent:	CD_3OD	M_G [g/mol]:	293.10
T [°C]:	25	m_R [mg]:	14.47
Substrat:	Kosower Salt (**84**)	m_G [mg]:	5.17
		V_0 [mL]:	3.06
		$[G]_0$ [mM]:	5.59

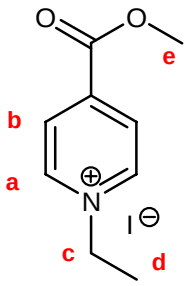

δ_0 (H_a) [ppm] = 9.2004

δ_0 (H_b) [ppm] = 8.5463

δ_0 (H_c) [ppm] = 4.7677

δ_0 (H_d) [ppm] = 1.2246

V [mL]	$[R]_0$ [M]	δ_{obs} (H_a) [ppm]	$\Delta\delta_{obs}$ (H_a) [ppm]	$\Delta\delta_{calc}$ (H_a) [ppm]
0.60	0.018616	8.0323	1.1678	1.1528
0.65	0.017184	8.0580	1.1421	1.1263
0.70	0.015957	8.0966	1.1035	1.1003
0.75	0.014893	8.1278	1.0723	1.0750
0.80	0.013962	8.1588	1.0413	1.0503
0.85	0.013141	8.1809	1.0192	1.0263
0.90	0.012411	8.2099	0.9902	1.0029
0.95	0.011758	8.2366	0.9635	0.9803
1.00	0.011170	8.2615	0.9386	0.9583
1.30	0.008592	8.3712	0.8289	0.8400
1.40	0.007978	8.3885	0.8116	0.8056
1.50	0.007447	8.4060	0.7941	0.7733
1.60	0.006981	8.4333	0.7668	0.7432

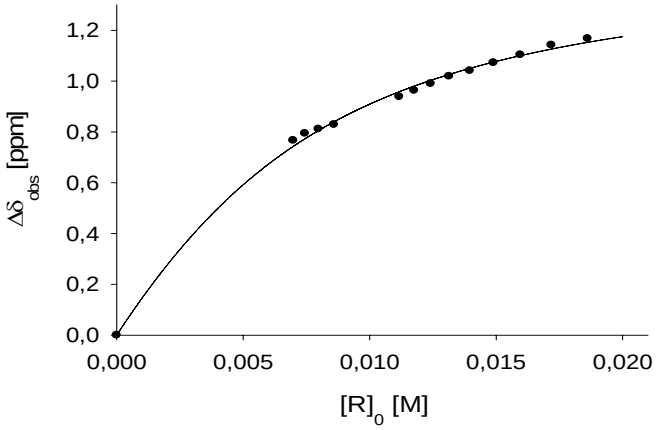

K_a [M^{-1}] = 235 ± 25

$\Delta\delta_{max}$ (H_a) [ppm] = 1.50

$\Delta\delta_{max}$ (H_b) [ppm] = 1.28

$\Delta\delta_{max}$ (H_c) [ppm] = 0.87

$\Delta\delta_{max}$ (H_d) [ppm] = 0.60

84@**27** ^{1}H NMR (500 MHz, CD_3OD) δ[ppm]: 1.09 (t, 3H, KS, H_d), 2.37 (dt, 2H, H-19a+H-20a), 2.62 (dt, 2H, H-19i+H-20i), 3.90 (q, 2H, KS, H_c), 4.37 (s, 4H, H-6+H-8+H-15+H-17), 6.97 (t, 2H, H-25), 7.12 (dd, 4H, H-1+H-4+H-10+H-13), 7.27 (d, 2H, KS, H_b), 7.38 (dd, 4H, H-2+H-3+H-12+H-11), 7.40 (s, 4H, H-5+H-9+H-14+H-18), 7.56 (d, 4H, H-23+H-27), 7.70 (d, 2H, KS, H_a)

Receptor:	**27**	M_R [g/mol]:	1295.46
Solvent:	$CDCl_3$	M_G [g/mol]:	293.10
T [°C]:	25	m_R [mg]:	13.74
Substrat:	Kosower Salt (**84**)	m_G [mg]:	6.30
		V_0 [mL]:	3.90
		$[G]_0$ [mM]:	5.35

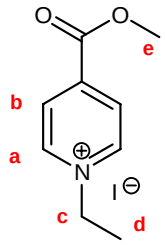

δ_0 (H_a) [ppm] = 9.5955

δ_0 (H_b) [ppm] = 8.5365

δ_0 (H_c) [ppm] = 4.0743

δ_0 (H_e) [ppm] = 1.7826

V [mL]	$[R]_0$ [M]	δ_{obs} (H_a) [ppm]	$\Delta\delta_{obs}$ (H_a) [ppm]	$\Delta\delta_{calc}$ (H_a) [ppm]
0.60	0.017677	8.0670	1.5285	1.5296
0.65	0.016317	8.1102	1.4853	1.4804
0.70	0.015152	8.1581	1.4374	1.4337
0.75	0.014142	8.2016	1.3939	1.3894
0.80	0.013258	8.2470	1.3485	1.3472
0.85	0.012478	8.2902	1.3053	1.3072
0.90	0.011785	8.3290	1.2665	1.2691
0.95	0.011164	8.3656	1.2299	1.2329
1.00	0.010606	8.4044	1.1911	1.1985
1.10	0.009642	8.4630	1.1325	1.1345
1.20	0.008839	8.5280	1.0675	1.0763
1.30	0.008159	8.5791	1.0164	1.0234
1.40	0.007576	8.6254	0.9701	0.9750
1.50	0.007071	8.6630	0.9325	0.9308
1.60	0.006629	8.6958	0.8997	0.8901
1.80	0.005892	8.7762	0.8193	0.8182
2.00	0.005303	8.8229	0.7726	0.7565

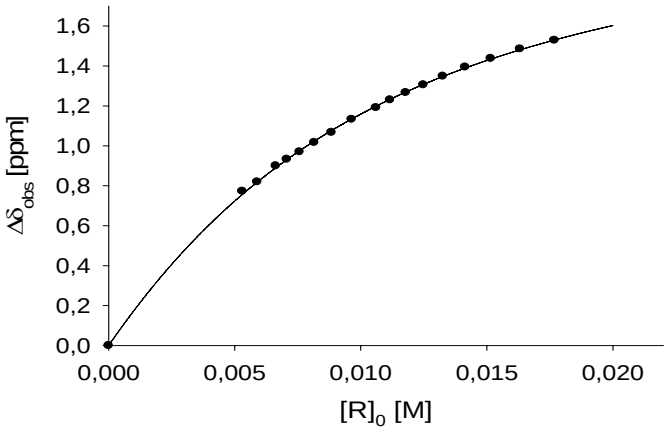

K_a [M^{-1}] = 135 ± 15

$\Delta\delta_{max}$ (H_a) [ppm] = 2.33

$\Delta\delta_{max}$ (H_b) [ppm] = 1.96

$\Delta\delta_{max}$ (H_c) [ppm] = 0.02

$\Delta\delta_{max}$ (H_e) [ppm] = 0.82

84@27 ^{1}H NMR (500 MHz, $CDCl_3$) δ[ppm]: 0.96 (t, 3H, KS, H_e), 2.19 (dt, 2H, H-19a+H-20a), 2.35 (dt, 2H, H-19i+H-20i), 4.06 (q, 2H, KS, H_c), 4.43 (s, 4H, H-6+H-8+H-15+H-17), 6.58 (d, 2H, KS, H_b), 6.79 (dd, 4H, H-1+H-4+H-10+H-13), 6.90 (dd, 4H, H-2+H-3+H-12+H-11), 7.12 (s, 4H, H-5+H-9+H-14+H-18), 7.15 (t, 2H, H-25), 7.26 (d, 2H, KS, H_a),7.63 (d, 4H, H-23+H-27)

Receptor:	**27**	M_R [g/mol]:	1295.46
Solvent:	$CDCl_3$	M_G [g/mol]:	178.15
T [°C]:	25	m_R [mg]:	9.09
Substrat:	Tetracyanobenzene (**85**)	m_G [mg]:	1.86
		V_0 [mL]:	3.00
		$[G]_0$ [mM]:	3.48

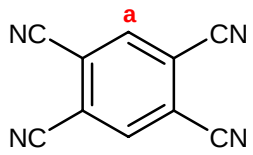

δ_0 (H) [ppm] = 8.2528

V [mL]	$[R]_0$ [M]	δ_{obs} (H) [ppm]	$\Delta\delta_{obs}$ (H) [ppm]	$\Delta\delta_{calc}$ (H) [ppm]
0.60	0.011695	5.5698	2.6830	2.6785
0.65	0.010795	5.6356	2.6172	2.6108
0.70	0.010024	5.7013	2.5515	2.5451
0.75	0.009356	5.7673	2.4855	2.4814
0.80	0.008771	5.8314	2.4214	2.4198
0.85	0.008255	5.8950	2.3578	2.3602
0.90	0.007796	5.9550	2.2978	2.3027
0.95	0.007386	6.0097	2.2431	2.2471
1.00	0.007017	6.0692	2.1836	2.1935
1.10	0.006379	6.1734	2.0794	2.0920
1.20	0.005847	6.2727	1.9801	1.9977
1.30	0.005398	6.3567	1.8961	1.9102
1.40	0.005012	6.4179	1.8349	1.8288
1.50	0.004678	6.5177	1.7351	1.7532
1.60	0.004386	6.5571	1.6957	1.6829
1.80	0.003898	6.6476	1.6052	1.5564

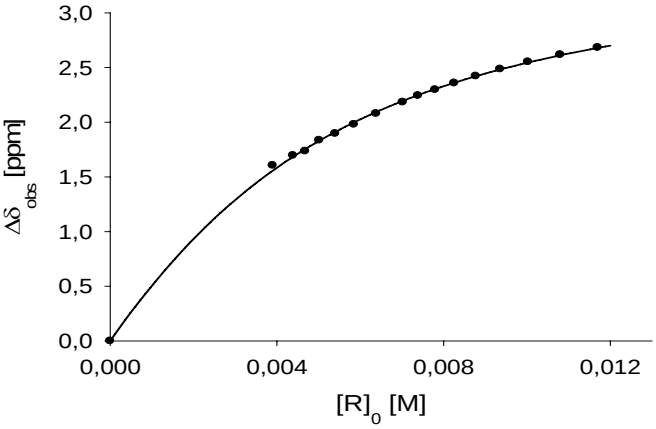

K_a [M^{-1}] = 315 ± 35

$\Delta\delta_{max}$ (H) [ppm] = 3.61

85@**27** ^{1}H NMR (500 MHz, $CDCl_3$) δ[ppm]: 2.46 (dt, 2H, H-19a+H-20a), 2.76 (dt, 2H, H-19i+H-20i), 4.46 (s, 4H, H-6+H-8+H-15+H-17), 4.65 (s, 2H, TCNB), 6.91 (t, 2H, H-25), 7.20 (dd, 4H, H-1+H-4+H-10+H-13), 7.56 (dd, 4H, H-2+H-3+H-12+H-11), 7.54 (s, 4H, H-5+H-9+H-14+H-18), 7.79 (d, 4H, H-23+H-27)

Receptor:	**28**	M_R [g/mol]:	586.24
Solvent:	CD_3OD	M_G [g/mol]:	194.19
T [°C]:	25	m_R [mg]:	6.80
Substrat:	Caffeine (**34**)	m_G [mg]:	3.34
		V_0 [mL]:	3.00
		$[G]_0$ [mM]:	5.73

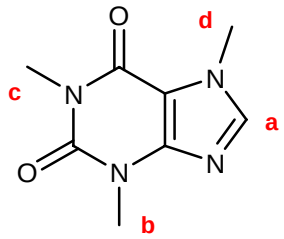

δ_0 (H_a) [ppm] = 7.8606

δ_0 (H_b) [ppm] = 3.5341

δ_0 (H_c) [ppm] = 3.3528

δ_0 (H_d) [ppm] = 3.9753

V [mL]	$[R]_0$ [M]	δ_{obs} (H_a) [ppm]	$\Delta\delta_{obs}$ (H_a) [ppm]	$\Delta\delta_{calc}$ (H_a) [ppm]
0.60	0.019332	7.1896	0.6710	0.6553
0.65	0.017845	7.2322	0.6284	0.6230
0.70	0.016570	7.2662	0.5944	0.5936
0.75	0.015466	7.2965	0.5641	0.5669
0.80	0.014499	7.3262	0.5344	0.5423
0.85	0.013646	7.3501	0.5105	0.5198
0.90	0.012888	7.3698	0.4908	0.4991
0.95	0.012210	7.3937	0.4669	0.4799
1.00	0.011599	7.4127	0.4479	0.4621
1.10	0.010545	7.4296	0.4310	0.4301
1.20	0.009666	7.4627	0.3979	0.4023
1.30	0.008923	7.4755	0.3851	0.3778
1.40	0.008285	7.4988	0.3618	0.3561
1.50	0.007733	7.5122	0.3484	0.3367
1.60	0.007250	7.5221	0.3385	0.3193

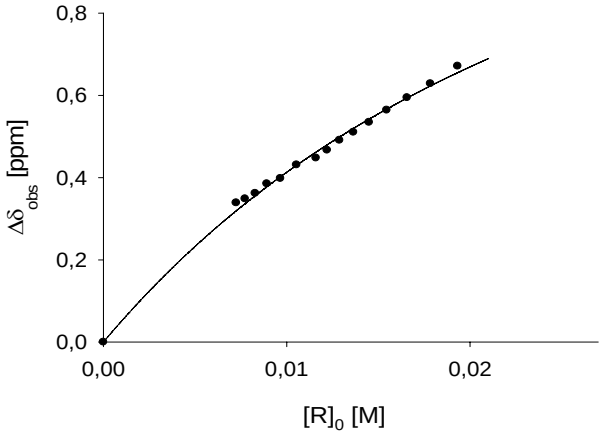

K_a [M^{-1}] = 41 ± 4

$\Delta\delta_{max}$ (H_a) [ppm] = 1.60

$\Delta\delta_{max}$ (H_b) [ppm] = 0.64

$\Delta\delta_{max}$ (H_c) [ppm] = 0.53

$\Delta\delta_{max}$ (H_d) [ppm] = 1.14

28@**34** ^{1}H NMR (500 MHz, CD_3OD) δ[ppm]: 2.34 (dt, 2H, H-19a+H-20a), 2.50 (dt, 2H, H-19i+H-20i), 2.82 (s, 3H, Caffeine, H_c), 2.83 (s, 3H, Caffeine, H_d), 2.90 (s, 3H, Caffeine, H_b), 3.49 (s, 3H, Caffeine, H_b), 3.89 (dd, 2H, H-23r+H-26r), 3.91 (dd, 2H, H-23s+H-26s), 4,30 (m, 6H, H-21+H-22+H-24+H-25), 4.63 (s, 4H, H-6+H-8+H-15+H-17), 6.26 (1H, Caffeine, H_a), 6.90 (dd, 4H, H-2+H-3+H-11+H-12), 7.26 (dd, 4H, H-1+H-4+H-10+H-13), 7.47 (s, 4H, H-5+H-9+H-14+H-18)

Receptor:	**28**	M_R [g/mol]:	586.24
Solvent:	CD_3OD	M_G [g/mol]:	246.06
T [°C]:	25	m_R [mg]:	4.71
Substrat:	NMNA (**33**)	m_G [mg]:	3.09
	δ_0 (H_a) [ppm] = 9.3797	V_0 [mL]:	3.00
	δ_0 (H_b) [ppm] = 8.9489	$[G]_0$ [mM]:	4.19
	δ_0 (H_c) [ppm] = 8.1908		
	δ_0 (H_d) [ppm] = 9.0401		
	δ_0 (H_e) [ppm] = 4.4811		

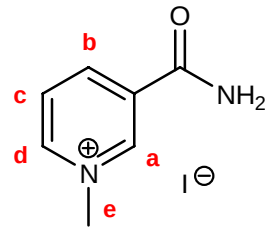

V [mL]	$[R]_0$ [M]	δ_{obs} (H_a) [ppm]	$\Delta\delta_{obs}$ (H_a) [ppm]	$\Delta\delta_{calc}$ (H_a) [ppm]
0.65	0.012360	9.0771	0.3026	0.2958
0.70	0.011478	9.0948	0.2849	0.2820
0.75	0.010712	9.1105	0.2692	0.2693
0.80	0.010043	9.1241	0.2556	0.2577
0.85	0.009452	9.1371	0.2426	0.2471
0.90	0.008927	9.1451	0.2346	0.2372
0.95	0.008457	9.1567	0.2230	0.2282
1.00	0.008034	9.1639	0.2158	0.2197
1.10	0.007304	9.1805	0.1992	0.2046
1.20	0.006695	9.1910	0.1887	0.1914
1.30	0.006180	9.1964	0.1833	0.1798
1.40	0.005739	9.2069	0.1728	0.1695
1.50	0.005356	9.2152	0.1645	0.1603
1.60	0.005021	9.2195	0.1602	0.1520

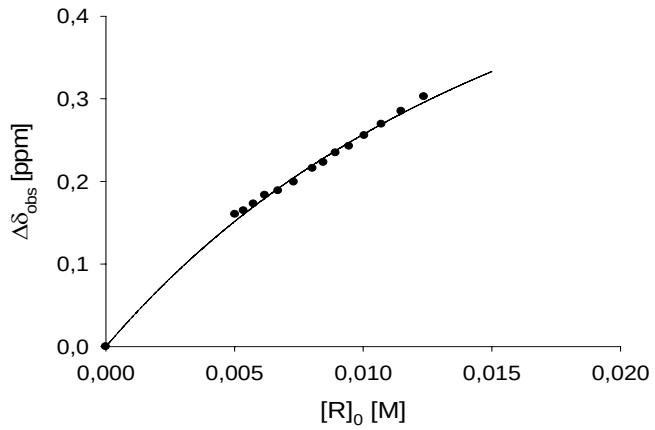

K_a [M^{-1}] = 60 ± 6

$\Delta\delta_{max}$ (H_a) [ppm] = 0.75

$\Delta\delta_{max}$ (H_b) [ppm] = 0.64

$\Delta\delta_{max}$ (H_c) [ppm] = 0.53

$\Delta\delta_{max}$ (H_d) [ppm] = 1.14

$\Delta\delta_{max}$ (H_e) [ppm] = 1.14

28@**33** ^{1}H NMR (500 MHz, CD_3OD) δ[ppm]: 2.38 (dt, 2H, H-19a+H-20a), 2.55 (dt, 2H, H-19i+H-20i), 3.84 (s, 3H, NMNA, H_e), 3.87 (dd, 2H, H-23r+H-26r), 3.90 (dd, 2H, H-23s+H-26s), 4,33 (m, 6H, H-21+H-22+H-24+H-25), 4.67 (s, 4H, H-6+H-8+H-15+H-17), 6.72 (t, 1H, NMNA, H_c), 7.10 (dd, 4H, H-2+H-3+H-11+H-12), 7.34 (dd, 4H, H-1+H-4+H-10+H-13), 7.48 (s, 4H, H-5+H-9+H-14+H-18), 7.68 (d, 1H, NMNA, H_b), 8.06 (d, 1H, NMNA, H_d), 8.63 (s, 1H, NMNA, H_a)

Receptor:	**28**	M_R [g/mol]:	586.24
Solvent:	CD_3OD	M_G [g/mol]:	293.10
T [°C]:	25	m_R [mg]:	4.71
Substrat:	Kosower salt (**84**)	m_G [mg]:	3.66
		V_0 [mL]:	3.00
		$[G]_0$ [mM]:	4.19

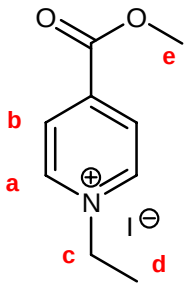

δ_0 (H_a) [ppm] = 9.1981
δ_0 (H_b) [ppm] = 8.5442
δ_0 (H_c) [ppm] = 4.7670
δ_0 (H_d) [ppm] = 1.6945
δ_0 (H_e) [ppm] = 3.3488

V [mL]	$[R]_0$ [M]	δ_{obs} (H_b) [ppm]	$\Delta\delta_{obs}$ (H_b) [ppm]	$\Delta\delta_{calc}$ (H_b) [ppm]
0.65	0.012360	8.0561	0.4881	0.4805
0.70	0.011478	8.0843	0.4599	0.4561
0.75	0.010712	8.1098	0.4344	0.4340
0.80	0.010043	8.1320	0.4122	0.4140
0.85	0.009452	8.1522	0.3920	0.3957
0.90	0.008927	8.1706	0.3736	0.3790
0.95	0.008457	8.1858	0.3584	0.3635
1.00	0.008034	8.2039	0.3403	0.3493
1.10	0.007304	8.2244	0.3198	0.3240
1.20	0.006695	8.2442	0.3000	0.3020
1.30	0.006180	8.2610	0.2832	0.2828
1.40	0.005739	8.2761	0.2681	0.2659
1.50	0.005356	8.2825	0.2617	0.2509
1.60	0.005021	8.2970	0.2472	0.2375

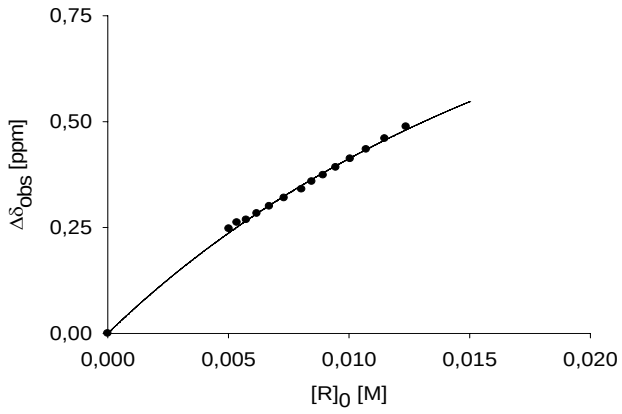

K_a [M^{-1}] = 45 ± 4
$\Delta\delta_{max}$ (H_a) [ppm] = 1.24
$\Delta\delta_{max}$ (H_b) [ppm] = 1.45
$\Delta\delta_{max}$ (H_c) [ppm] = 0.52
$\Delta\delta_{max}$ (H_d) [ppm] = 0.33
$\Delta\delta_{max}$ (H_e) [ppm] = 0.01

28@**84** ^{1}H NMR (500 MHz, CD_3OD) δ[ppm]: 1.36 (t, 3H, KS, H_d), 2.40 (dt, 2H, H-19a+H-20a), 2.56 (dt, 2H, H-19i+H-20i), 3.35 (s, 3H, KS, H_e), 3.88 (dd, 2H, H-23r+H-26r), 3.91 (dd, 2H, H-23s+H-26s), 4.24 (q, 2H, KS, H_c), 4.29 (m, 6H, H-21+H-22+H-24+H-25), 4.69 (s, 4H, H-6+H-8+H-15+H-17), 7.09 (dd, 4H, H-2+H-3+H-11+H-12), 7.09 (d, 2H, KS, H_b), 7.32 (dd, 4H, H-1+H-4+H-10+H-13), 7.46 (s, 4H, H-5+H-9+H-14+H-18), 7.96 (d, 2H, KS. H_a)

Receptor:	**98**	M_R [g/mol]:	2438
Solvent:	CD_3OD	M_G [g/mol]:	293.10
T [°C]:	25	m_R [mg]:	42.07
Substrat:	Kosower Salt (**84**)	m_G [mg]:	8.10
		V_0 [mL]:	4.40
		$[G]_0$ [mM]:	6.28

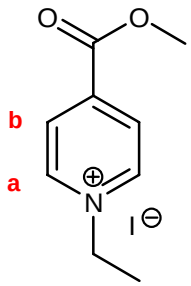

δ_0 (H_a) [ppm] = 9.1982

δ_0 (H_b) [ppm] = 8.5443

V [mL]	$[R]_0$ [M]	δ_{obs} (H_b) [ppm]	$\Delta\delta_{obs}$ (H_b) [ppm]	$\Delta\delta_{calc}$ (H_b) [ppm]
0.60	0.0204	8.0000	0.5440	0.5070
0.65	0.0188	8.0240	0.5200	0.4884
0.70	0.0175	8.0500	0.4940	0.4710
0.75	0.0163	8.0710	0.4730	0.4547
0.80	0.0153	8.0920	0.4520	0.4394
0.85	0.0144	8.1110	0.4330	0.4251
0.90	0.0136	8.1290	0.4150	0.4115
0.95	0.0129	8.1410	0.4030	0.3988
1.00	0.0122	8.1560	0.3880	0.3753
1.10	0.0111	8.1760	0.3680	0.3544
1.20	0.0102	8.1940	0.3500	0.3355
1.30	0.0094	8.2080	0.3360	0.3185
1.40	0.0087	8.2190	0.3250	0.3031
1.50	0.0082	8.2280	0.3160	0.2890

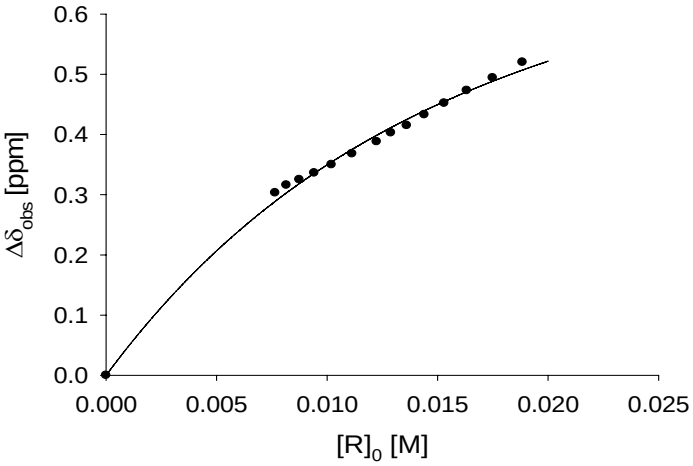

K_a [M^{-1}] = 85 ± 9

$\Delta\delta_{max}$ (H_a) [ppm] = 0.90

$\Delta\delta_{max}$ (H_b) [ppm] = 0.91

Receptor:	**98**	M_R [g/mol]:	2438
Solvent:	CD_3OD	M_G [g/mol]:	194.19
T [°C]:	25	m_R [mg]:	31.64
Substrat:	Caffeine (**34**)	m_G [mg]:	2.92
		V_0 [mL]:	3.20
		$[G]_0$ [mM]:	4.70

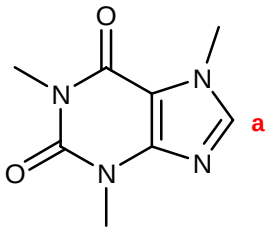

δ_0 (H_a) [ppm] = 7.8992

V [mL]	$[R]_0$ [M]	δ_{obs} (H_a) [ppm]	$\Delta\delta_{obs}$ (H_a) [ppm]	$\Delta\delta_{calc}$ (H_a) [ppm]
0.65	0.014457	6.0151	1.8841	1.8487
0.70	0.013424	6.0434	1.8558	1.8315
0.75	0.012529	6.0672	1.8320	1.8137
0.80	0.011746	6.1001	1.7991	1.7955
0.85	0.011055	6.1399	1.7593	1.7767
0.90	0.010441	6.1639	1.7353	1.7575
0.95	0.009892	6.1872	1.7120	1.7378
1.00	0.009397	6.2112	1.6880	1.7176
1.10	0.008543	6.2450	1.6542	1.6762
1.20	0.007831	6.2812	1.6180	1.6336
1.30	0.007229	6.3249	1.5743	1.5901
1.40	0.006712	6.3484	1.5508	1.5461
1.50	0.006265	6.3871	1.5121	1.5020
1.60	0.005873	6.4372	1.4620	1.4582
1.80	0.005221	6.4715	1.4277	1.3726

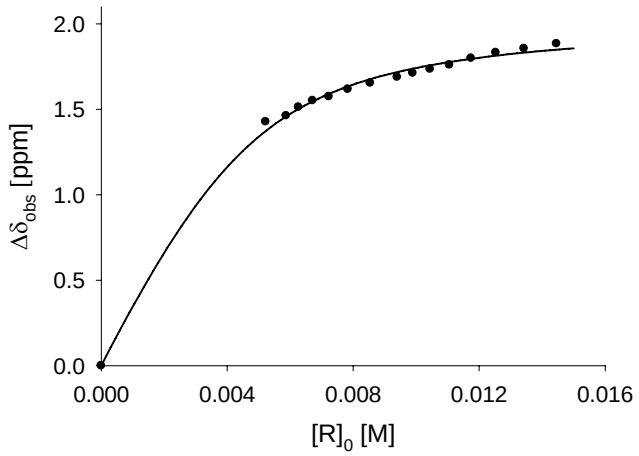

K_a [M^{-1}] = 1035 ± 110

$\Delta\delta_{max}$ (H) [ppm] = 2.02

Receptor:	**98**	M_R [g/mol]:	2438
Solvent:	CD_3OD	M_G [g/mol]:	246.06
T [°C]:	25	m_R [mg]:	40.93
Substrat:	NMNA (**33**)	m_G [mg]:	4.66
		V_0 [mL]:	3.00
		$[G]_0$ [mM]:	6.31

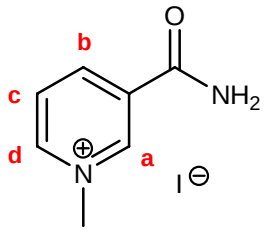

δ_0 (H_a) [ppm] = 9.3813
δ_0 (H_b) [ppm] = 8.9492
δ_0 (H_c) [ppm] = 8.1933
δ_0 (H_d) [ppm] = 9.0441

V [mL]	$[R]_0$ [M]	δ_{obs} (H_d) [ppm]	$\Delta\delta_{obs}$ (H_d) [ppm]	$\Delta\delta_{calc}$ (H_d) [ppm]
0.65	0.018704	8.6560	0.3882	0.3773
0.70	0.017368	8.6689	0.3752	0.3687
0.75	0.016210	8.6827	0.3615	0.3603
0.80	0.015197	8.6952	0.3490	0.3522
0.85	0.014303	8.7061	0.3380	0.3442
0.90	0.013508	8.7158	0.3283	0.3364
0.95	0.012797	8.7211	0.3231	0.3288
1.00	0.012158	8.7314	0.3127	0.3215
1.10	0.011052	8.7379	0.3063	0.3074
1.20	0.010131	8.7560	0.2881	0.2942
1.30	0.009352	8.7623	0.2819	0.2818
1.40	0.008684	8.7704	0.2737	0.2703
1.50	0.008105	8.7774	0.2668	0.2594
1.60	0.007598	8.7823	0.2619	0.2493

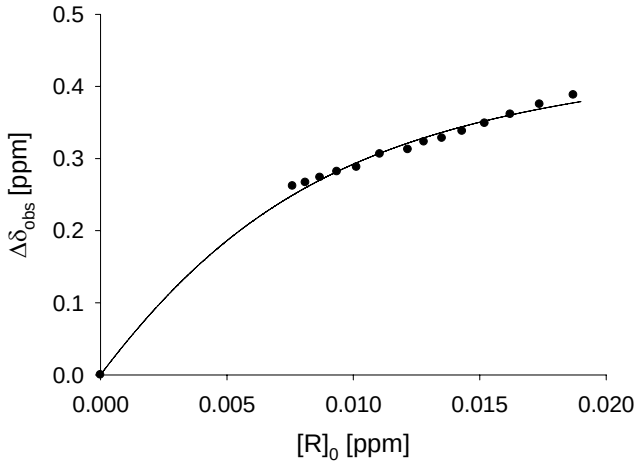

K_a [M^{-1}] = 230 ± 23

$\Delta\delta_{max}$ (H_a) [ppm] = 0.36

$\Delta\delta_{max}$ (H_b) [ppm] = 0.68

$\Delta\delta_{max}$ (H_c) [ppm] = 0.65

$\Delta\delta_{max}$ (H_d) [ppm] = 0.30

Receptor:	**98**	M_R [g/mol]:	2438
Solvent:	D_2O	M_G [g/mol]:	246.06
T [°C]:	25	m_R [mg]:	37.42
Substrat:	NMNA (**33**)	m_G [mg]:	4.52
		V_0 [mL]:	3.00
		$[G]_0$ [mM]:	6.12

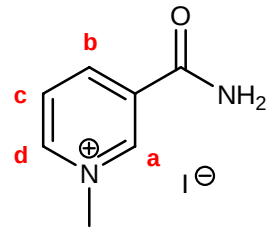

δ_0 (H_a) [ppm] = 9.2848
δ_0 (H_b) [ppm] = 8.8963
δ_0 (H_c) [ppm] = 8.1824
δ_0 (H_d) [ppm] = 8.9705

V [mL]	$[R]_0$ [M]	δ_{obs} (H_d) [ppm]	$\Delta\delta_{obs}$ (H_d) [ppm]	$\Delta\delta_{calc}$ (H_d) [ppm]
0.60	0.018521	8.6700	0.3005	0.2965
0.65	0.017096	8.6770	0.2935	0.2888
0.70	0.015875	8.6873	0.2832	0.2814
0.75	0.014817	8.6952	0.2753	0.2742
0.80	0.013891	8.7041	0.2664	0.2672
0.85	0.013074	8.7163	0.2542	0.2604
0.90	0.012347	8.7226	0.2479	0.2539
0.95	0.011698	8.7274	0.2431	0.2476
1.00	0.011113	8.7317	0.2388	0.2415
1.10	0.010102	8.7444	0.2261	0.2300
1.20	0.009261	8.7490	0.2215	0.2193
1.30	0.008548	8.7626	0.2079	0.2094
1.40	0.007938	8.7701	0.2004	0.2002
1.50	0.007408	8.7794	0.1911	0.1917
1.60	0.006945	8.7816	0.1889	0.1838
1.80	0.006174	8.7960	0.1745	0.1696
2.00	0.005556	8.8080	0.1625	0.1573

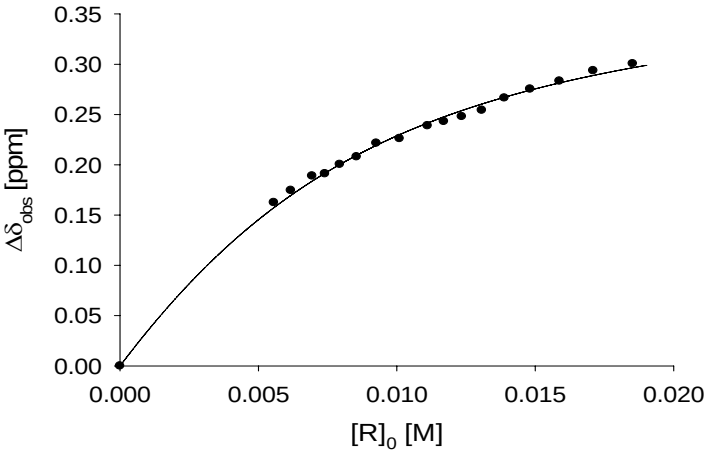

K_a [M^{-1}] = 210 ± 21

$\Delta\delta_{max}$ (H_a) [ppm] = 0.23

$\Delta\delta_{max}$ (H_b) [ppm] = 0.33

$\Delta\delta_{max}$ (H_c) [ppm] = 0.47

$\Delta\delta_{max}$ (H_d) [ppm] = 0.40

Receptor:	**99**	M_R [g/mol]:	6400
Solvent:	D_2O	M_G [g/mol]:	293.10
T [°C]:	25	m_R [mg]:	48.74
Substrat:	Kosower Salt (**84**)	m_G [mg]:	9.98
		V_0 [mL]:	3.20
		$[G]_0$ [mM]:	4.24

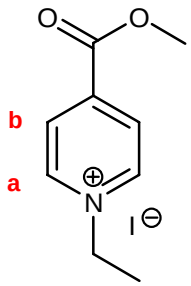

δ_0 (H_a) [ppm] = 9.0735

δ_0 (H_b) [ppm] = 8.5197

V [mL]	$[R]_0$ [M]	δ_{obs} (H_b) [ppm]	$\Delta\delta_{obs}$ (H_b) [ppm]	$\Delta\delta_{calc}$ (H_b) [ppm]
0.60	0.012693	8.2518	0.2679	0.2601
0.65	0.011716	8.2691	0.2506	0.2463
0.70	0.010879	8.2885	0.2312	0.2338
0.75	0.010154	8.2988	0.2209	0.2226
0.80	0.009520	8.3112	0.2085	0.2124
0.85	0.008960	8.3219	0.1978	0.2030
0.90	0.008462	8.3303	0.1894	0.1944
0.95	0.008016	8.3381	0.1816	0.1866
1.00	0.007616	8.3448	0.1749	0.1793
1.10	0.006923	8.3544	0.1653	0.1663
1.20	0.006346	8.3636	0.1561	0.1551
1.30	0.005858	8.3718	0.1479	0.1452
1.40	0.005440	8.3822	0.1375	0.1366
1.50	0.005077	8.3841	0.1356	0.1289
1.60	0.004760	8.3889	0.1308	0.1220

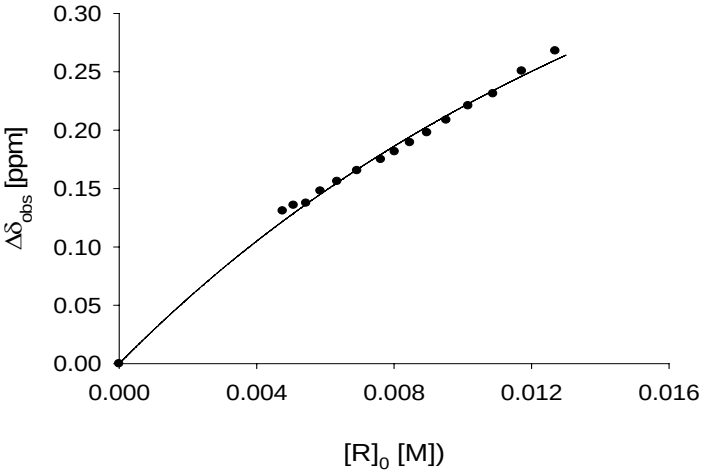

K_a [M^{-1}] = 50 ± 5

$\Delta\delta_{max}$ (H_a) [ppm] = 0.56

$\Delta\delta_{max}$ (H_b) [ppm] = 0.73

Receptor:	**99**	M_R [g/mol]:	6400
Solvent:	D_2O	M_G [g/mol]:	246.06
T [°C]:	25	m_R [mg]:	47.73
Substrat:	NMNA (**33**)	m_G [mg]:	3.60
		V_0 [mL]:	3.30
		$[G]_0$ [mM]:	4.43

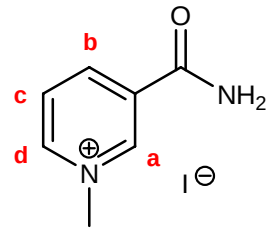

δ_0 (H_a) [ppm] = 9.2848
δ_0 (H_b) [ppm] = 8.8963
δ_0 (H_c) [ppm] = 8.1824
δ_0 (H_d) [ppm] = 8.9705

V [mL]	$[R]_0$ [M]	δ_{obs} (H_d) [ppm]	$\Delta\delta_{obs}$ (H_d) [ppm]	$\Delta\delta_{calc}$ (H_d) [ppm]
0.60	0.012430	8.7501	0.2061	0.2024
0.65	0.011474	8.7648	0.1914	0.1911
0.70	0.010654	8.7730	0.1832	0.1810
0.75	0.009944	8.7830	0.1732	0.1718
0.80	0.009322	8.7933	0.1629	0.1636
0.85	0.008774	8.8046	0.1516	0.1561
0.90	0.008286	8.8102	0.1460	0.1492
0.95	0.007850	8.8171	0.1391	0.1429
1.00	0.007458	8.8218	0.1344	0.1372
1.10	0.006780	8.8312	0.1250	0.1269
1.20	0.006215	8.8406	0.1156	0.1181
1.30	0.005737	8.8472	0.1090	0.1104
1.40	0.005327	8.8512	0.1050	0.1036
1.50	0.004972	8.8550	0.1012	0.0976
1.60	0.004661	8.8605	0.0957	0.0923
1.80	0.004143	8.8686	0.0876	0.0832
2.00	0.003729	8.8768	0.0794	0.0757

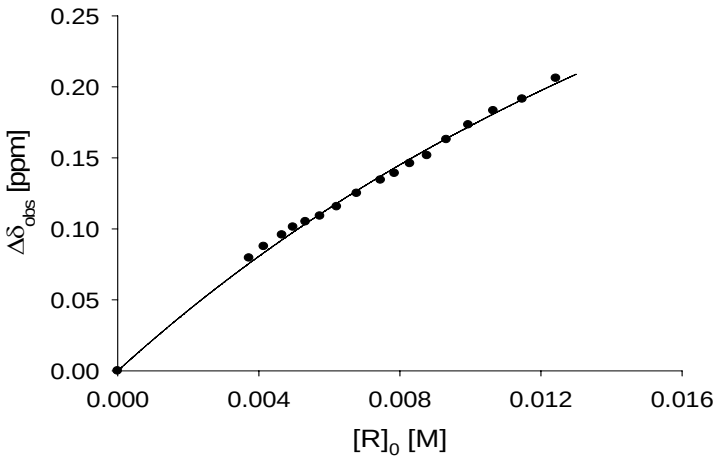

K_a [M^{-1}] = 40 ± 4

$\Delta\delta_{max}$ (H_a) [ppm] = 0.60

$\Delta\delta_{max}$ (H_b) [ppm] = 0.45

$\Delta\delta_{max}$ (H_c) [ppm] = 0.77

$\Delta\delta_{max}$ (H_d) [ppm] = 0.64

Receptor:	**99**	M_R [g/mol]:	6400
Solvent:	D_2O	M_G [g/mol]:	194.19
T [°C]:	25	m_R [mg]:	43.36
Substrat:	Caffeine (**34**)	m_G [mg]:	2.96
		V_0 [mL]:	4.50
		$[G]_0$ [mM]:	3.39

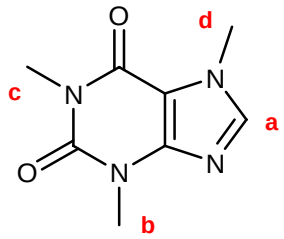

δ_0 (H_a) [ppm] = 7.8811

δ_0 (H_b) [ppm] = 3.3343

δ_0 (H_d) [ppm] = 5.5205

V [mL]	$[R]_0$ [M]	δ_{obs} (H_a) [ppm]	$\Delta\delta_{obs}$ (H_a) [ppm]	$\Delta\delta_{calc}$ (H_a) [ppm]
0.60	0.011292	6.4265	1.4546	1.4357
0.65	0.010423	6.4812	1.3999	1.3854
0.70	0.009679	6.5421	1.3390	1.3379
0.75	0.009033	6.5928	1.2883	1.2932
0.80	0.008469	6.6436	1.2375	1.2510
0.85	0.007971	6.6787	1.2024	1.2112
0.90	0.007528	6.7225	1.1586	1.1736
0.95	0.007132	6.7546	1.1265	1.1381
1.00	0.006775	6.7928	1.0883	1.1044
1.10	0.006159	6.8429	1.0382	1.0424
1.20	0.005646	6.9072	0.9739	0.9864
1.30	0.005212	6.9445	0.9366	0.9358
1.40	0.004839	6.9743	0.9068	0.8899
1.50	0.004517	7.0103	0.8708	0.8481
1.60	0.004234	7.0518	0.8293	0.8099

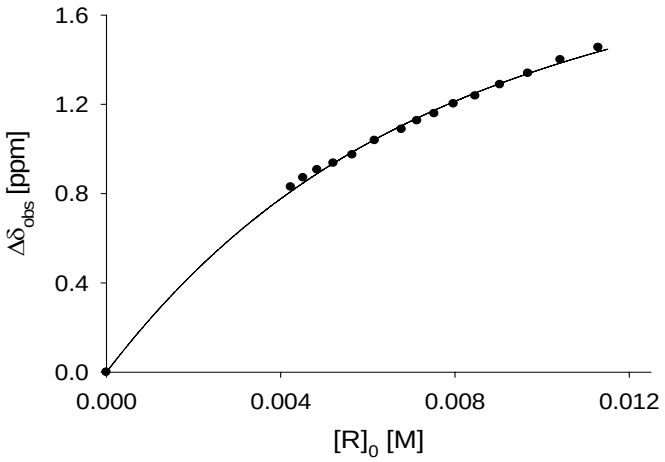

K_a [M^{-1}] = 175 ± 20

$\Delta\delta_{max}$ (H_a) [ppm] = 2.33

$\Delta\delta_{max}$ (H_b) [ppm] = 0.98

$\Delta\delta_{max}$ (H_d) [ppm] = 0.80

4.5.2 ^{1}H NMR dilution titrations

Receptor:	**36**	M_R [g/mol]:	642.61
Solvent:	D_2O	m_R [mg]:	9.70
T [°C]:	25	V_0 [mL]:	1.50
Substrat:	Itself (self-association)	$[R]_0$ [mM]:	10.07

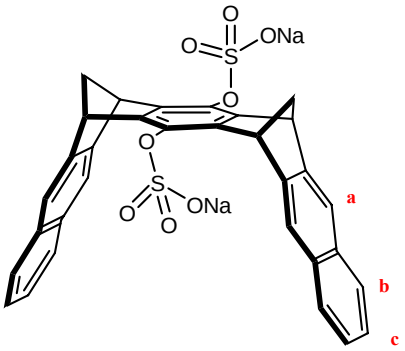

δ_0 (H_a) [ppm] = 7.8132

δ_0 (H_b) [ppm] = 7.7919

δ_0 (H_c) [ppm] = 7.4324

$[R]_0$ [M]	δ_{obs} (H_b) [ppm]	$\Delta\delta_{obs}$ (H_b) [ppm]	$\Delta\delta_{calc}$ (H_b) [ppm]
0.01475	7.2525	0.5394	0.5195
0.007377	7.3612	0.4307	0.4421
0.003688	7.4640	0.3279	0.3541
0.001844	7.5303	0.2616	0.2626
0.000922	7.5777	0.2142	0.2117
0.0004611	7.6630	0.1502	0.1170

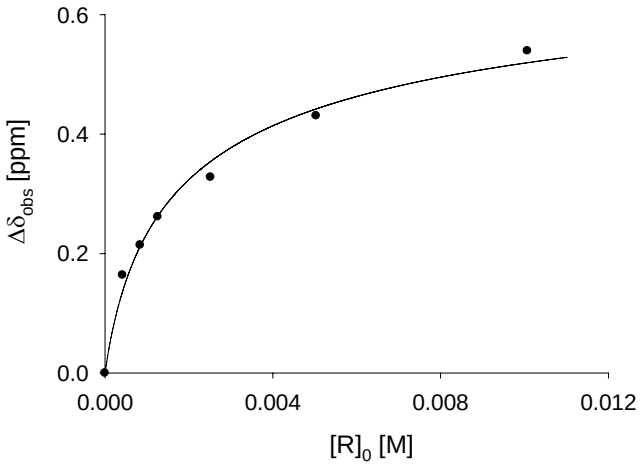

K_{dim} [M^{-1}] = 310 ± 30

$\Delta\delta_{max}$ (H_a) [ppm] = 0.60

$\Delta\delta_{max}$ (H_b) [ppm] = 0.77

$\Delta\delta_{max}$ (H_c) [ppm] = 0.63

Receptor:	**36**	M_R [g/mol]:	642.61
Solvent:	D_2O/Buffer (pH=7.2)	M_G [g/mol]:	194.19
T [°C]:	25	m_R [mg]:	9.70
Substrat:	Caffeine (**34**)	m_G [mg]:	3.05
		V_0 [mL]:	1.50
		$[G]_0$ [mM]:	10.47

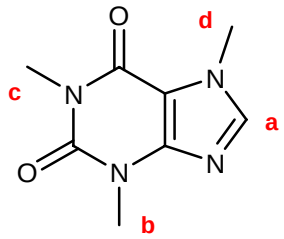

δ_0 (H_a) [ppm] = 7.8811

δ_0 (H_b) [ppm] = 3.3343

δ_0 (H_c) [ppm] = 3.5190

δ_0 (H_d) [ppm] = 5.5205

$[R]_0$ [M]	$[G]_0$ [M]	δ_{obs} (H_c) [ppm]	$\Delta\delta_{obs}$ (H_c) [ppm]	$\Delta\delta_{calc}$ (H_c) [ppm]
0.0050316	0.005235422	3.1453	0.3737	0.3560
0.0025158	0.002617711	3.2004	0.3186	0.3203
0.0012579	0.001308856	3.2478	0.2712	0.2762
0.0008386	0.00087257	3.2678	0.2512	0.2469
0,0004193	0,000436285	3,3041	0,2149	0,1932

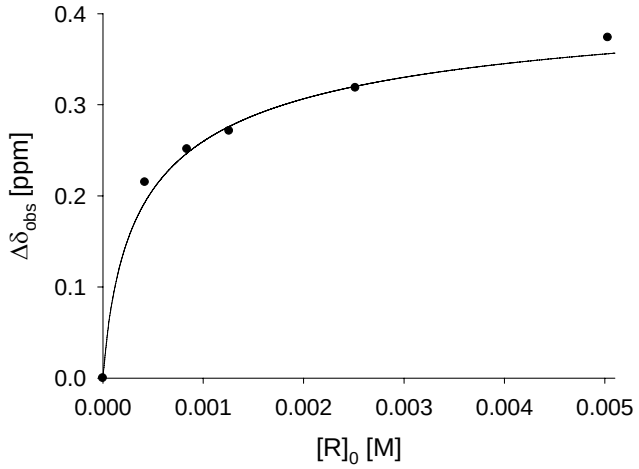

K_a [M^{-1}] = 2900 ± 300

$\Delta\delta_{max}$ (H_a) [ppm] = 2.94

$\Delta\delta_{max}$ (H_c) [ppm] = 0.47

36@**34** ^{1}H NMR (500MHz, D_2O) δ[ppm]: 2.44 (dd, 2H, H-19a+H-20a), 2.67 (d, 2H, H-19i+H-20i), 4.71 (s, 4H, H-6+H-8+H-15+H-17), 6.89 (s, 4H, H-5+H-9+H-14+H-18), 7.05 (dd, 4H, H-2+H-3+H-12+H-11), 7.18 (dd, 4H, H-1+H-4+H-10+H-13)

Receptor:	**36**	M_R [g/mol]:	642.61
Solvent:	D_2O/Buffer (pH=7.2)	M_G [g/mol]:	334.23
T [°C]:	25	m_R [mg]:	10.30
Substrat:	Nicotinanide mononucleotide (**111**)	m_G [mg]:	5.53
		V_0 [mL]:	1.50
		$[G]_0$ [mM]:	10.97

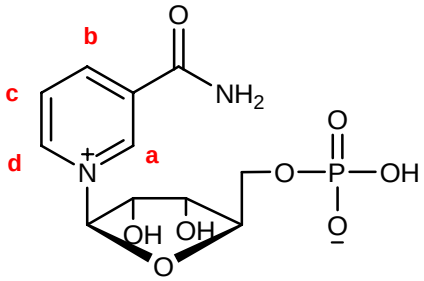

δ_0 (H_a) [ppm] = 9.4635

δ_0 (H_b) [ppm] = 8.9828

δ_0 (H_d) [ppm] = 9.2853

$[R]_0$ [M]	$[G]_0$ [M]	δ_{obs} (H_b) [ppm]	$\Delta\delta_{obs}$ (H_b) [ppm]	$\Delta\delta_{calc}$ (H_b) [ppm]
0.01068566	0.010970489	7.6312	1.3516	1.3356
0.00534283	0.005485245	7.7696	1.2132	1.1941
0.00267141	0.002742622	7.9922	0.9906	1.0212
0.00133571	0.001371311	8.1338	0.8490	0.8231
0.00089047	0.000914207	8.2686	0.7142	0.7013
0.00044524	0.000457104	8.5712	0.4116	0.4985

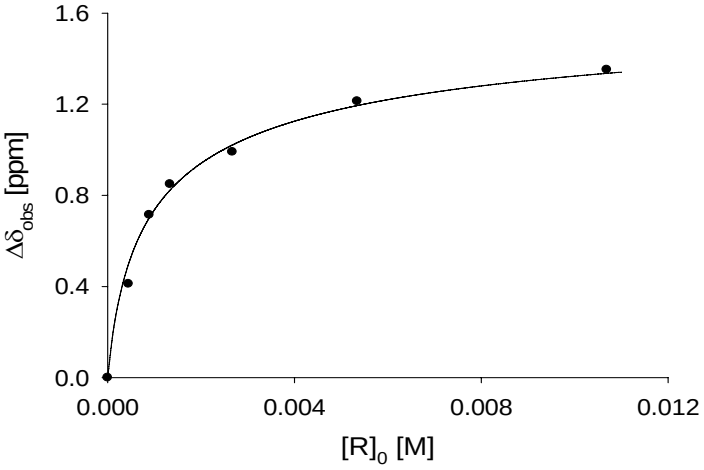

K_a [M^{-1}] = 1225 ± 130

$\Delta\delta_{max}$ (H_a) [ppm] = 0.90

$\Delta\delta_{max}$ (H_b) [ppm] = 1.80

$\Delta\delta_{max}$ (H_d) [ppm] = 1.22

36@111 ^{1}H NMR (500MHz, D_2O) δ[ppm]: 2.47 (dd, 2H, H-19a+H-20a), 2.70 (d, 2H, H-19i+H-20i), 4.59 (s, 4H, H-6+H-8+H-15+H-17), 7.03 (dd, 4H, H-2+H-3+H-12+H-11), 7.18 (d, 1H, NMNAMN, H_a), 7.22 (dd, 4H, H-1+H-4+H-10+H-13), 7.42 (s, 4H, H-5+H-9+H-14+H-18), 8.07 (d, 1H, NMNAMN, H_d), 8.56 (d, 1H, NMNAMN, H_b)

Receptor:	**36**	M_R [g/mol]:	642.61
Solvent:	D_2O/Buffer (pH=7.2)	M_G [g/mol]:	267.24
T [°C]:	25	m_R [mg]:	13.35
Substrat:	Adenosine (**31**)	m_G [mg]:	5.38
	δ_0 (H_a) [ppm] = 8.1848	V_0 [mL]:	1.50
	δ_0 (H_b) [ppm] = 8.2932	$[G]_0$ [mM]:	13.42
	δ_0 (H_c) [ppm] = 6.0388		
	δ_0 (H_d) [ppm] = 4.2763		
	δ_0 (H_e) [ppm] = 4.4099		
	δ_0 (H_g) [ppm] = 3.8583		

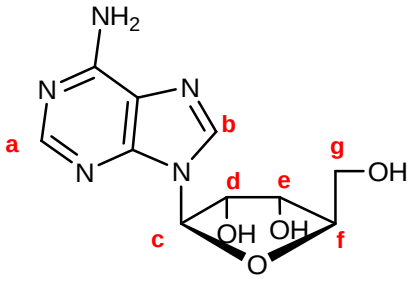

$[R]_0$ [M]	$[G]_0$ [M]	δ_{obs} (H_b) [ppm]	$\Delta\delta_{obs}$ (H_b) [ppm]	$\Delta\delta_{calc}$ (H_b) [ppm]
0.01384986	0.013421145	7.6215	0.5633	0.5641
0.00692493	0.006710572	7.7141	0.4707	0.4578
0.00346246	0.003355286	7.8276	0.3572	0.3452
0.00173123	0.001677643	7.9539	0.2309	0.2386
0.00115415	0.001118429	8.0229	0.1619	0.1843
0.01384986	0.013421145	7.6215	0.5633	0.5641

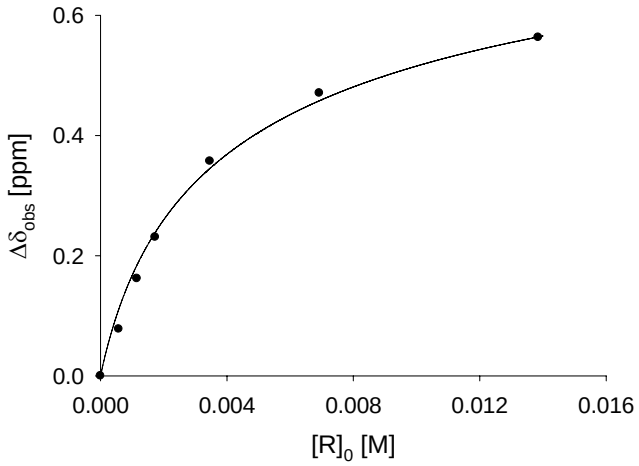

K_a [M^{-1}]	=	260 ± 25
$\Delta\delta_{max}$ (H_a) [ppm]	=	0.94
$\Delta\delta_{max}$ (H_b) [ppm]	=	0.78
$\Delta\delta_{max}$ (H_c) [ppm]	=	0.33
$\Delta\delta_{max}$ (H_d) [ppm]	=	-0.10
$\Delta\delta_{max}$ (H_e) [ppm]	=	0.31
$\Delta\delta_{max}$ (H_g) [ppm]	=	0.06

36@31 ^{1}H NMR (500MHz, D_2O) δ[ppm]: 2.41 (dd, 2H, H-19a+H-20a), 2.66 (d, 2H, H-19i+H-20i), 3.80 (ddd, 2H, Adenosine, H_g), 4.10 (dd, 1H, Adenosine, H_e), 4.37 (dd, 1H, Adenosine, H_d), 4.72 (s, 4H, H-6+H-8+H-15+H-17), 5.70 (d, 1H, Adenosine, H_c), 6.81 (dd, 4H, H-2+H-3+H-12+H-11), 7.13 (dd, 4H, H-1+H-4+H-10+H-13), 7.24 (s, 1H, Adenosine, H_a), 7.36 (s, 4H, H-5+H-9+H-14+H-18), 7.51 (s, 1H, Adenosine, H_b)

Receptor:	**36**	M_R [g/mol]:	642.61
Solvent:	D_2O	M_G [g/mol]:	293.10
T [°C]:	25	m_R [mg]:	6.20
Substrat:	Kosower Salt (**84**)	m_G [mg]:	2.76
		V_0 [mL]:	1.50
		$[G]_0$ [mM]:	6.28

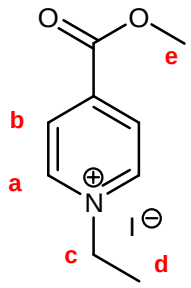

δ_0 (H_a) [ppm] = 9.0837

δ_0 (H_b) [ppm] = 8.5287

δ_0 (H_c) [ppm] = 4.7444

δ_0 (H_d) [ppm] = 1.6736

δ_0 (H_e) [ppm] = 4.0596

$[R]_0$ [M]	$[G]_0$ [M]	δ_{obs} (H_b) [ppm]	$\Delta\delta_{obs}$ (H_b) [ppm]	$\Delta\delta_{calc}$ (H_b) [ppm]
0.00160945	0.001569377	6.5647	1.9640	1.9575
0.00080473	0.000784688	6.6440	1.8847	1.8882
0.00053648	0.000523126	6.7010	1.8277	1.8365
0.00026824	0.000261563	6.7977	1.7310	1.7251

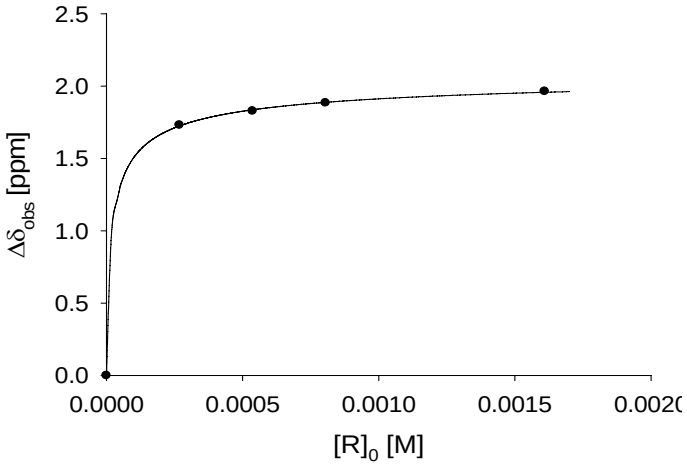

K_a [M^{-1}] = $(8.16 \pm 0.82)\cdot10^4$

$\Delta\delta_{max}$ (H_a) [ppm] = 1.38

$\Delta\delta_{max}$ (H_b) [ppm] = 2.11

$\Delta\delta_{max}$ (H_c) [ppm] = 0.52

$\Delta\delta_{max}$ (H_d) [ppm] = 0.41

36@**84** ^{1}H NMR (500MHz, D_2O) δ[ppm]: 1.43 (t, 3H, KS, H_d), 2.47 (dd, 2H, H-19a+H-20a), 2.71 (d, 2H, H-19i+H-20i), 4.09 (s, 3H, KS, H_e), 4.23 (q, 2H, KS, H_c), 4.70 (s, 4H, H-6+H-8+H-15+H-17), 6.42 (d, 2H, KS, H_b), 7.01 (dd, 4H, H-2+H-3+H-12+H-11), 7.19 (dd, 4H, H-1+H-4+H-10+H-13), 7.37 (s, 4H, H-5+H-9+H-14+H-18), 7.71 (d, 2H, KS, H_a)

Receptor:	**36**	M_R [g/mol]:	642.61
Solvent:	CD_3OD	M_G [g/mol]:	293.10
T [°C]:	25	m_R [mg]:	6.91
Substrat:	Kosower Salt (**84**)	m_G [mg]:	3.34
		V_0 [mL]:	1.50
	δ_0 (H_a) [ppm] = 9.2008	$[G]_0$ [mM]:	7.60
	δ_0 (H_b) [ppm] = 8.5459		
	δ_0 (H_c) [ppm] = 4.7680		
	δ_0 (H_d) [ppm] = 1.6941		

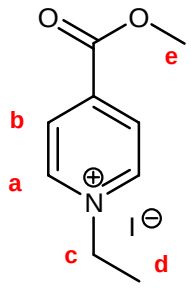

$[R]_0$ [M]	$[G]_0$ [M]	δ_{obs} (H_b) [ppm]	$\Delta\delta_{obs}$ (H_b) [ppm]	$\Delta\delta_{calc}$ (H_b) [ppm]
0.00717505	0.007596693	6.9915	1.5544	1.5479
0.00358753	0.003798346	7.0272	1.5187	1.5230
0.00179376	0.001899173	7.0576	1.4883	1.4864
0.00089688	0.000949587	7.1151	1.4308	1.4345
0.00059792	0.000633058	7.1579	1.3880	1.3954
0.00029896	0.000316529	7.2285	1.3174	1.3105

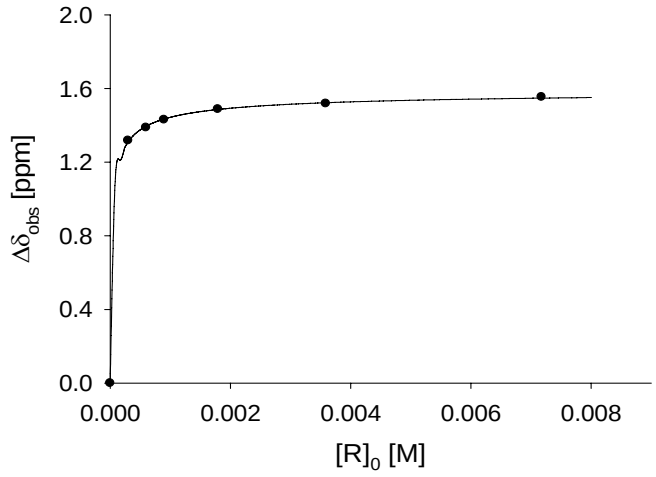

K_a [M^{-1}] = $(6.84 \pm 0.70)\cdot 10^4$

$\Delta\delta_{max}$ (H_a) [ppm] = 1.23

$\Delta\delta_{max}$ (H_b) [ppm] = 1.68

$\Delta\delta_{max}$ (H_c) [ppm] = 0.66

$\Delta\delta_{max}$ (H_d) [ppm] = 0.42

36@**84** ^{1}H NMR (500MHz, CD_3OD) δ[ppm]: 1.27 (t, 3H, KS, H_d), 2.39 (dd, 2H, H-19a+H-20a), 2.67 (d, 2H, H-19i+H-20i), 4.10 (q, 2H, KS, H_c), 4.80 (s, 4H, H-6+H-8+H-15+H-17), 6.87 (d, 2H, KS, H_b), 7.07 (dd, 4H, H-2+H-3+H-12+H-11), 7.35 (dd, 4H, H-1+H-4+H-10+H-13), 7.47 (s, 4H, H-5+H-9+H-14+H-18), 7.98 (d, 2H, KS, H_a)

Receptor:	**36**	M_R [g/mol]:	642.61
Solvent:	CD_3OD	M_G [g/mol]:	260.06
T [°C]:	25	m_R [mg]:	7.20
Substrat:	NMNA (**33**)	m_G [mg]:	3.01
		V_0 [mL]:	1.50
		$[G]_0$ [mM]:	7.47

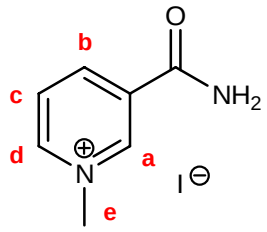

δ_0 (H_a) [ppm] = 9.3827
δ_0 (H_b) [ppm] = 8.9418
δ_0 (H_c) [ppm] = 8.1949
δ_0 (H_d) [ppm] = 9.0472
δ_0 (H_e) [ppm] = 4.4845

$[R]_0$ [M]	$[G]_0$ [M]	δ_{obs} (H_c) [ppm]	$\Delta\delta_{obs}$ (H_c) [ppm]	$\Delta\delta_{calc}$ (H_c) [ppm]
0.00746959	0.00759920	6.4640	1.7309	1.7288
0.00373479	0.00379960	6.4814	1.7135	1.7099
0.00186740	0.00189980	6.5135	1.6814	1.6830
0.00093370	0.00094990	6.5560	1.6389	1.6455
0.00062247	0.00063327	6.5815	1.6134	1.6171
0.00031123	0.00031663	6.6340	1.5609	1.5549

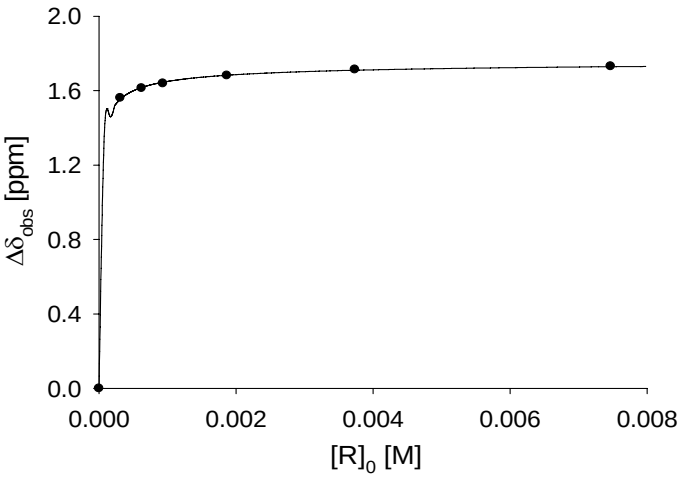

K_a [M^{-1}] = $(1.76 \pm 0.18)\cdot 10^5$
$\Delta\delta_{max}$ (H_a) [ppm] = 1.10
$\Delta\delta_{max}$ (H_b) [ppm] = 1.11
$\Delta\delta_{max}$ (H_c) [ppm] = 1.79
$\Delta\delta_{max}$ (H_d) [ppm] = 0.93
$\Delta\delta_{max}$ (H_e) [ppm] = 0.81

36@33 ^{1}H NMR (500MHz, CD_3OD) δ[ppm]: 2.38 (dd, 2H, H-19a+H-20a), 2.62 (d, 2H, H-19i+H-20i), 3.67 (s, 3H, NMNA, H_e), 4.77 (s, 4H, H-6+H-8+H-15+H-17), 6.40 (t, 1H, NMNA, H_c), 7.10 (dd, 4H, H-2+H-3+H-12+H-11), 7.42 (dd, 4H, H-1+H-4+H-10+H-13), 7.56 (s, 4H, H-5+H-9+H-14+H-18), 7.83 (d, 1H, NMNA, H_b), 8.12 (d, 1H, NMNA, H_d), 8.28 (s, 1H, NMNA, H_a)

Receptor:	**36**	M_R [g/mol]:	642.61
Solvent:	D_2O/Buffer (pH=7.2)	M_G [g/mol]:	507.64
T [°C]:	25	m_R [mg]:	7.84
Substrat:	SAM (**112**)	m_G [mg]:	5.06
		V_0 [mL]:	1.50
		$[G]_0$ [mM]:	6.65

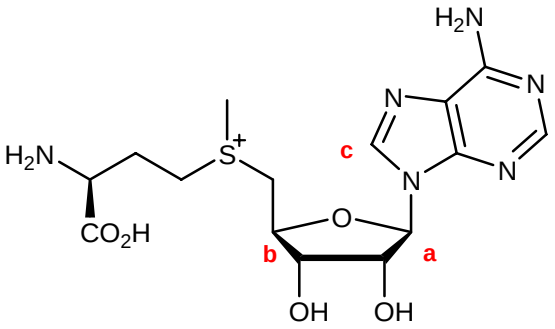

δ_0 (H_a) [ppm] = 6.1094

δ_0 (H_b) [ppm] = 4.8560

δ_0 (H_c) [ppm] = 8.2876

$[R]_0$ [M]	$[G]_0$ [M]	δ_{obs} (H_c) [ppm]	$\Delta\delta_{obs}$ (H_c) [ppm]	$\Delta\delta_{calc}$ (H_c) [ppm]
0.00813355	0.006645142	7.9738	0.3138	0.3132
0.00406677	0.003322571	8.0171	0.2705	0.2726
0.00101669	0.000830643	8.1154	0.1722	0.1718
0.0006778	0.000553762	8.1446	0.1430	0.1413
0.0003389	0.000276881	8.1926	0.0950	0.0941

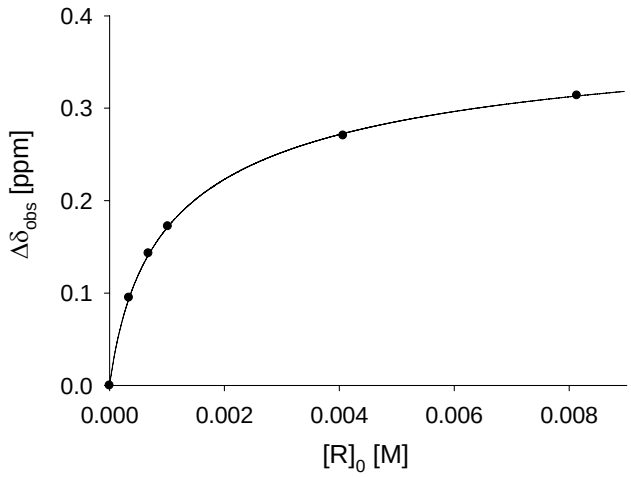

K_a [M^{-1}] = 940 ± 95

$\Delta\delta_{max}$ (H_a) [ppm] = 0.50

$\Delta\delta_{max}$ (H_b) [ppm] = 1.10

$\Delta\delta_{max}$ (H_c) [ppm] = 0.52

36@112 ^{1}H NMR (500MHz, D_2O) δ[ppm]: 2.40(dd, 2H, H-19a+H-20a), 2.59 (d, 2H, H-19i+H-20i), 3.76 (m, 1H, SAM, H_b), 4.70 (s, 4H, H-6+H-8+H-15+H-17), 5.61 (d, 1H, SAM, H_a), 7.04 (dd, 4H, H-2+H-3+H-12+H-11), 7.41 (dd, 4H, H-1+H-4+H-10+H-13), 7.53 (s, 4H, H-5+H-9+H-14+H-18), 7.77 (s, 1H, SAM, H_c)

Receptor:	**36**	M_R [g/mol]	642.61
Solvent:	D_2O	M_G [g/mol]	663.43
T [°C]:	25	m_R [mg]:	10.93
Substrat:	NAD (**35**)	m_G [mg]:	11.26
	δ_0 (H_a) [ppm] = 9.4481	V_0 [mL]:	1.50
	δ_0 (H_b) [ppm] = 8.9572	$[G]_0$ [mM]:	11.31
	δ_0 (H_c) [ppm] = 8.3100		
	δ_0 (H_d) [ppm] = 9.2981		
	δ_0 (H_e) [ppm] = 8.6163		
	δ_0 (H_g) [ppm] = 6.1963		
	δ_0 (H_h) [ppm] = 6.1584		

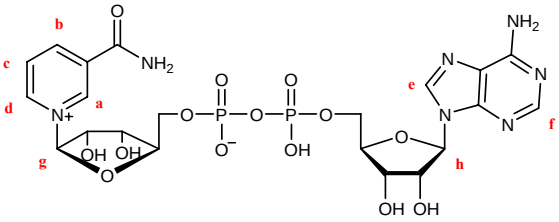

$[R]_0$ [M]	$[G]_0$ [M]	δ_{obs} (H_b) [ppm]	$\Delta\delta_{obs}$ (H_b) [ppm]	$\Delta\delta_{calc}$ (H_b) [ppm]
0.01133925	0.011312422	8.1212	0.8360	0.8387
0.00566962	0.005656211	8.1545	0.8027	0.8032
0.00283481	0.002828105	8.2044	0.7528	0.7555
0.00141741	0.001414053	8.2553	0.7019	0.6932
0.00094494	0.000942702	8.3038	0.6534	0.6491
0.00047247	0.000471351	8.4040	0.5532	0.5605

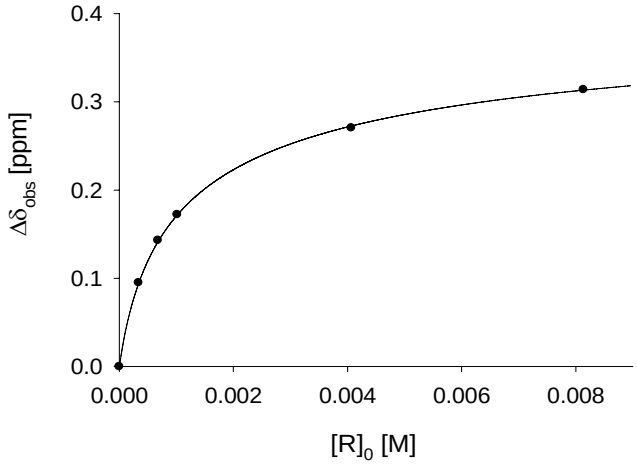

K_a [M^{-1}]	=	8040 ± 810
$\Delta\delta_{max}$ (H_a) [ppm]	=	0.50
$\Delta\delta_{max}$ (H_b) [ppm]	=	0.93
$\Delta\delta_{max}$ (H_c) [ppm]	=	1.19
$\Delta\delta_{max}$ (H_d) [ppm]	=	0.62
$\Delta\delta_{max}$ (H_e) [ppm]	=	0.27
$\Delta\delta_{max}$ (H_g) [ppm]	=	0.27
$\Delta\delta_{max}$ (H_h) [ppm]	=	0.26

36@**35** ^{1}H NMR (500MHz, D_2O) δ[ppm]: 2.49 (dd, 2H, H-19a+H-20a), 2.71 (d, 2H, H-19i+H-20i), 4.75 (s, 4H, H-6+H-8+H-15+H-17), 5.90 (d, 1H, NAD^+, H_h), 5.92 (d, 1H, NAD^+, H_g), 6.80 (dd, 4H, H-2+H-3+H-12+H-11), 7.05 (dd, 4H, H-1+H-4+H-10+H-13), 7.12 (t, 1H, NAD^+, H_c), 7.33 (s, 4H, H-5+H-9+H-14+H-18), 8.03 (d, 1H, NAD^+, H_b), 8.34 (s, 1H, NAD^+, H_e), 8.68 (d, 1H, NAD^+, H_d), 8.95 (s, 1H, NAD^+, H_a)

Receptor:	**36**	M_R [g/mol]	642.61
Solvent:	D_2O	M_G [g/mol]	663.43
T [°C]:	25	m_R [mg]:	11.17
Substrat:	NAD (**35**)	m_G [mg]:	12.18
	δ_0 (H_a) [ppm] = 9.3402	V_0 [mL]:	1.50
	δ_0 (H_b) [ppm] = 8.8380	$[G]_0$ [mM]:	12.23
	δ_0 (H_d) [ppm] = 9.1590		
	δ_0 (H_e) [ppm] = 8.4284		
	δ_0 (H_f) [ppm] = 8.1533		
	δ_0 (H_g) [ppm] = 6.0873		
	δ_0 (H_h) [ppm] = 6.0369		

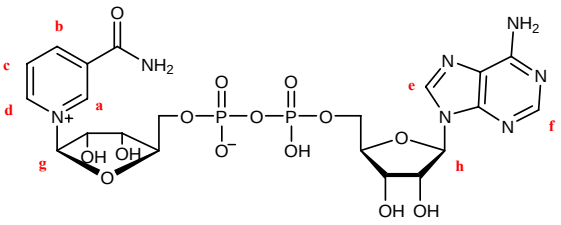

Neutralized with NaOD

$[R]_0$ [M]	**$[G]_0$ [M]**	**δ_{obs} (H_b) [ppm]**	**$\Delta\delta_{obs}$ (H_b) [ppm]**	**$\Delta\delta_{calc}$ (H_b) [ppm]**
0.01158823	0.012234742	7.548	1.290	1.288
0.00579412	0.006117371	7.685	1.153	1.141
0.00289706	0.003058686	7.881	0.957	0.964
0.00144853	0.001529343	8.055	0.783	0.764
0.00096569	0.001019562	8.214	0.624	0.644
0.00048284	0.000509781	8.414	0.424	0.448

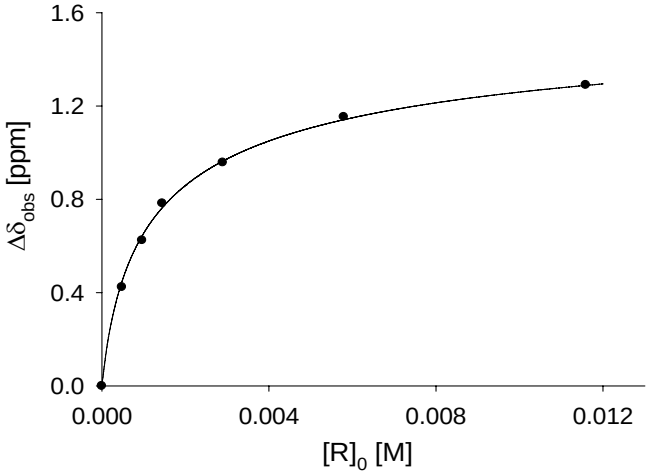

K_a [M^{-1}]	=	945 ± 95
$\Delta\delta_{max}$ (H_a) [ppm]	=	0.83
$\Delta\delta_{max}$ (H_b) [ppm]	=	1.78
$\Delta\delta_{max}$ (H_d) [ppm]	=	1.15
$\Delta\delta_{max}$ (H_e) [ppm]	=	0.17
$\Delta\delta_{max}$ (H_f) [ppm]	=	0.30
$\Delta\delta_{max}$ (H_g) [ppm]	=	0.17
$\Delta\delta_{max}$ (H_h) [ppm]	=	0.33

36@35 ^{1}H NMR (500MHz, D_2O/NaOD) δ[ppm]: 2.50 (dd, 2H, H-19a+H-20a), 2.73 (d, 2H, H-19i+H-20i), 4.76 (s, 4H, H-6+H-8+H-15+H-17), 5.70 (d, 1H, NAD^+, H_h), 5.91 (d, 1H, NAD^+, H_g), 6.94 (dd, 4H, H-2+H-3+H-12+H-11), 7.06 (d, 1H, NAD^+, H_b), 7.10 (dd, 4H, H-1+H-4+H-10+H-13), 7.34 (s, 4H, H-5+H-9+H-14+H-18), 7.85 (s, 1H, NAD^+, H_f), 8.01 (d, 1H, NAD^+, H_d), 8.26 (s, 1H, NAD^+, H_e), 8.51 (s, 1H, NAD^+, H_a)

Receptor:	**36**	M_R [g/mol]	642.61
Solvent:	D_2O/Buffer (pH=7.2)	M_G [g/mol]	663.43
T [°C]:	25	m_R [mg]:	6.14
Substrat:	NAD (**35**)	m_G [mg]:	6.21
	δ_0 (H_a) [ppm] = 9.3350	V_0 [mL]:	1.50
	δ_0 (H_b) [ppm] = 8.8299	$[G]_0$ [mM]:	6.24
	δ_0 (H_d) [ppm] = 9.1482		
	δ_0 (H_e) [ppm] = 8.4205		
	δ_0 (H_f) [ppm] = 8.1527		
	δ_0 (H_g) [ppm] = 6.0850		
	δ_0 (H_h) [ppm] = 6.0315		

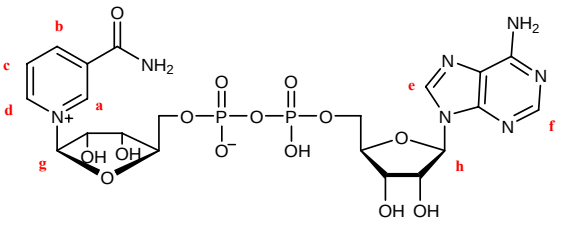

$[R]_0$ [M]	**$[G]_0$ [M]**	**δ_{obs} (H_b) [ppm]**	**$\Delta\delta_{obs}$ (H_b) [ppm]**	**$\Delta\delta_{calc}$ (H_b) [ppm]**
0.0063699	0.006243311	7.5960	1.2339	1.2414
0.00318495	0.003121656	7.7440	1.0859	1.0839
0.00159247	0.001560828	7.9224	0.9075	0.8978
0.00079624	0.000780414	8.1292	0.7007	0.6945
0.00053082	0.000520276	8.2566	0.5733	0.5754
0.00026541	0.000260138	8.4536	0.3763	0.3883

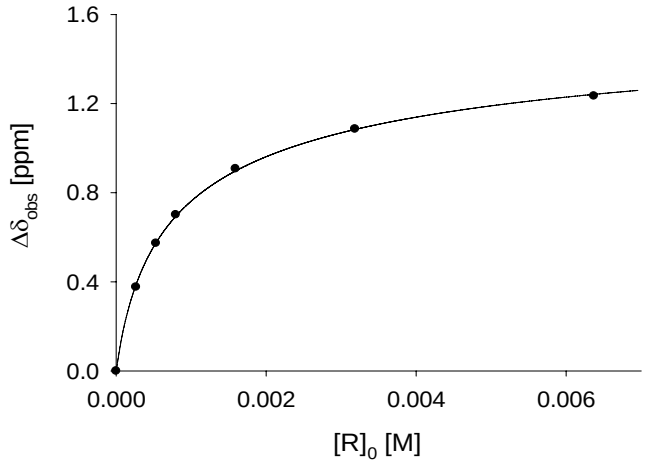

K_a [M^{-1}]	=	1420 ± 130
$\Delta\delta_{max}$ (H_a) [ppm]	=	0.79
$\Delta\delta_{max}$ (H_b) [ppm]	=	1.71
$\Delta\delta_{max}$ (H_d) [ppm]	=	1.07
$\Delta\delta_{max}$ (H_e) [ppm]	=	0.18
$\Delta\delta_{max}$ (H_f) [ppm]	=	0.30
$\Delta\delta_{max}$ (H_g) [ppm]	=	0.18
$\Delta\delta_{max}$ (H_h) [ppm]	=	0.31

36@35 ^{1}H NMR (500MHz, D_2O/Buffer) δ[ppm]: 2.47 (dd, 2H, H-19a+H-20a), 2.70 (d, 2H, H-19i+H-20i), 4.74 (s, 4H, H-6+H-8+H-15+H-17), 5.72 (d, 1H, NAD^+, H_h), 5.91 (d, 1H, NAD^+, H_g), 6.91 (dd, 4H, H-2+H-3+H-12+H-11), 7.08 (dd, 4H, H-1+H-4+H-10+H-13), 7.12 (d, 1H, NAD^+, H_b), 7.30 (s, 4H, H-5+H-9+H-14+H-18), 7.85 (s, 1H, NAD^+, H_f), 8.07 (d, 1H, NAD^+, H_d), 8.25 (s, 1H, NAD^+, H_e), 8.54 (s, 1H, NAD^+, H_a)

Receptor:	**37**	M_R [g/mol]:	610.51
Solvent:	D_2O	m_R [mg]:	13.50
T [°C]:	25	V_0 [mL]:	1.50
Substrat:	Itself (self-association)	$[R]_0$ [mM]:	14.75

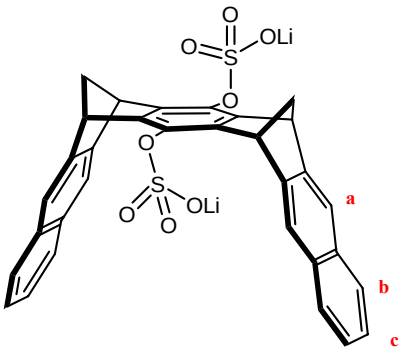

δ_0 (H_a) [ppm] = 7.7999

δ_0 (H_b) [ppm] = 7.7697

δ_0 (H_c) [ppm] = 7.3987

$[R]_0$ [M]	δ_{obs} (H_b) [ppm]	$\Delta\delta_{obs}$ (H_b) [ppm]	$\Delta\delta_{calc}$ (H_b) [ppm]
0.01475	7.0793	0.6854	0.6941
0.007377	7.2324	0.5323	0.5369
0.003688	7.3743	0.3904	0.3821
0.001844	7.5164	0.2483	0.2483
0.000922	7.5690	0.1957	0.1852
0.0004611	7.6266	0.1381	0.1058

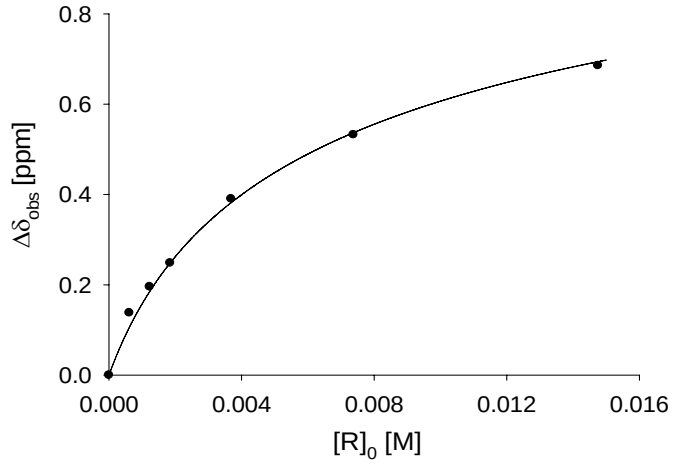

K_{dim} [M^{-1}] = 75 ± 8

$\Delta\delta_{max}$ (H_a) [ppm] = 1.05

$\Delta\delta_{max}$ (H_b) [ppm] = 1.34

$\Delta\delta_{max}$ (H_c) [ppm] = 1.06

Receptor:	**37**	M_R [g/mol]	610.50
Solvent:	D_2O	M_G [g/mol]	663.43
T [°C]:	25	m_R [mg]:	10.42
Substrat:	NAD^+ (**35**)	m_G [mg]:	11.47
	δ_0 (H_a) [ppm] = 9.4481	V_0 [mL]:	1.50
	δ_0 (H_b) [ppm] = 8.9572	$[G]_0$ [mM]:	11.53
	δ_0 (H_c) [ppm] = 8.3100		
	δ_0 (H_d) [ppm] = 9.2981		
	δ_0 (H_f) [ppm] = 8.6163		
	δ_0 (H_g) [ppm] = 6.1963		
	δ_0 (H_h) [ppm] = 6.1584		

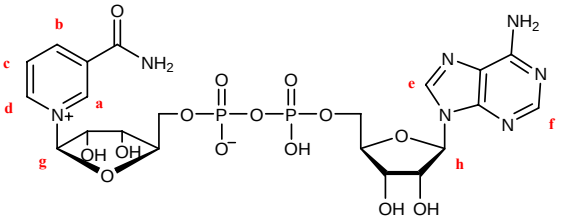

$[R]_0$ [M]	$[G]_0$ [M]	δ_{obs} (H_b) [ppm]	$\Delta\delta_{obs}$ (H_b) [ppm]	$\Delta\delta_{calc}$ (H_b) [ppm]
0.01137846	0.011525959	7.9562	1.0010	1.0013
0.00568923	0.005762979	8.0140	0.9432	0.9536
0.00284462	0.00288149	8.0658	0.8914	0.8901
0.00142231	0.001440745	8.1419	0.8153	0.8078
0.00094821	0.000960497	8.1877	0.7695	0.7502
0.0004741	0.000480248	8.3388	0.6184	0.6363

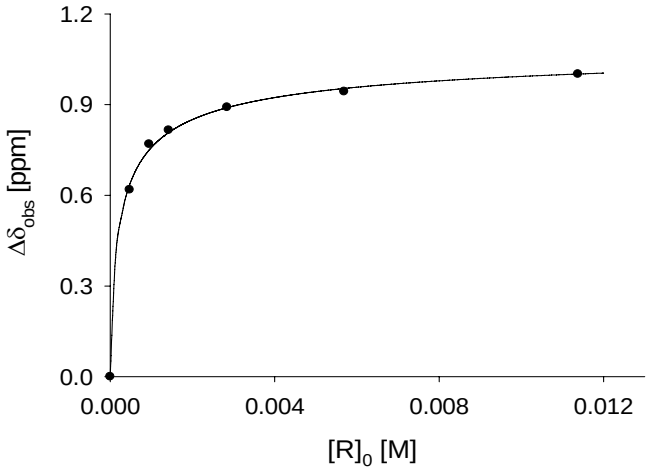

K_a [M^{-1}]	=	6240 ± 630
$\Delta\delta_{max}$ (H_a) [ppm]	=	0.60
$\Delta\delta_{max}$ (H_b) [ppm]	=	1.13
$\Delta\delta_{max}$ (H_c) [ppm]	=	2.04
$\Delta\delta_{max}$ (H_d) [ppm]	=	0.76
$\Delta\delta_{max}$ (H_e) [ppm]	=	0.32
$\Delta\delta_{max}$ (H_g) [ppm]	=	0.33
$\Delta\delta_{max}$ (H_h) [ppm]	=	0.30

37@**35** ^{1}H NMR (500MHz, D_2O) δ[ppm]: 2.51 (dd, 2H, H-19a+H-20a), 2.72 (d, 2H, H-19i+H-20i), 4.76 (s, 4H, H-6+H-8+H-15+H-17), 5.85 (d, 1H, NAD^+, H_h), 5.87 (d, 1H, NAD^+, H_g), 6.27 (t, 1H, NAD^+, H_c), 6.81 (dd, 4H, H-2+H-3+H-12+H-11), 7.07 (dd, 4H, H-1+H-4+H-10+H-13), 7.37 (s, 4H, H-5+H-9+H-14+H-18), 7.83 (d, 1H, NAD^+, H_b), 8.29 (s, 1H, NAD^+, H_e), 8.54 (d, 1H, NAD^+, H_d), 8.85 (s, 1H, NAD^+, H_a)

Receptor:	**37**	M_R [g/mol]	610.50
Solvent:	D_2O	M_G [g/mol]	663.43
T [°C]:	25	m_R [mg]:	12.53
Substrat:	NAD^+ (**35**)	m_G [mg]:	14.20
	δ_0 (H_a) [ppm] = 9.3407	V_0 [mL]:	1.50
	δ_0 (H_b) [ppm] = 8.8373	$[G]_0$ [mM]:	12.23
	δ_0 (H_d) [ppm] = 9.1583		
	δ_0 (H_e) [ppm] = 8.4289		
	δ_0 (H_f) [ppm] = 8.1539		
	δ_0 (H_g) [ppm] = 6.0872		
	δ_0 (H_h) [ppm] = 6.0366		

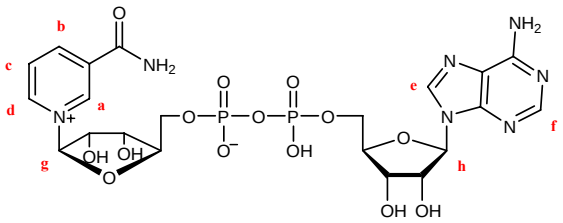

Neutralized with NaOD

$[R]_0$ [M]	**$[G]_0$ [M]**	**δ_{obs} (H_b) [ppm]**	**$\Delta\delta_{obs}$ (H_b) [ppm]**	**$\Delta\delta_{calc}$ (H_b) [ppm]**
0.01172793	0.012234742	7.237	1.601	1.587
0.005863965	0.006117371	7.403	1.435	1.404
0.002931983	0.003058686	7.659	1.179	1.184
0.001465991	0.001529343	7.905	0.933	0.937
0.000977328	0.001019562	8.081	0.757	0.788
0.000488664	0.000509781	8.347	0.491	0.547

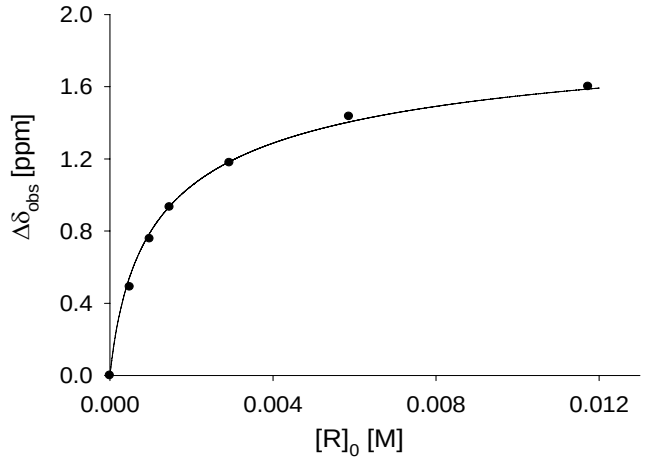

K_a [M^{-1}]	=	920 ± 90
$\Delta\delta_{max}$ (H_a) [ppm]	=	1.03
$\Delta\delta_{max}$ (H_b) [ppm]	=	2.19
$\Delta\delta_{max}$ (H_d) [ppm]	=	1.42
$\Delta\delta_{max}$ (H_e) [ppm]	=	0.21
$\Delta\delta_{max}$ (H_f) [ppm]	=	0.38
$\Delta\delta_{max}$ (H_g) [ppm]	=	0.19
$\Delta\delta_{max}$ (H_h) [ppm]	=	0.43

37@35 ^{1}H NMR (500MHz, D_2O/NaOD) δ[ppm]: 2.52 (dd, 2H, H-19a+H-20a), 2.73 (d, 2H, H-19i+H-20i), 4.74 (s, 4H, H-6+H-8+H-15+H-17), 5.61 (d, 1H, NAD^+, H_h), 5.89 (d, 1H, NAD^+, H_g), 6.65 (d, 1H, NAD^+, H_b), 6.89 (dd, 4H, H-2+H-3+H-12+H-11), 7.02 (dd, 4H, H-1+H-4+H-10+H-13), 7.28 (s, 4H, H-5+H-9+H-14+H-18), 7.74 (d, 1H, NAD^+, H_d), 7.78 (s, 1H, NAD^+, H_f), 8.22 (s, 1H, NAD^+, H_e), 8.32 (s, 1H, NAD^+, H_a)

Receptor:	**37**	M_R [g/mol]:	610.51
Solvent:	D_2O/Buffer (pH=7.2)	M_G [g/mol]:	267.24
T [°C]:	25	m_R [mg]:	11.13
Substrat:	Adenosine (**31**)	m_G [mg]:	4.95
	δ_0 (H_a) [ppm] = 8.1848	V_0 [mL]:	1.50
	δ_0 (H_b) [ppm] = 8.2932	$[G]_0$ [mM]:	12.35
	δ_0 (H_c) [ppm] = 6.0388		
	δ_0 (H_d) [ppm] = 4.2763		
	δ_0 (H_e) [ppm] = 4.4099		
	δ_0 (H_g) [ppm] = 3.8583		

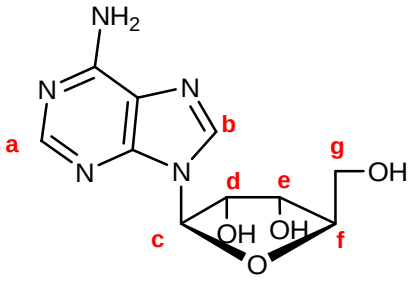

$[R]_0$ [M]	$[G]_0$ [M]	δ_{obs} (H_b) [ppm]	$\Delta\delta_{obs}$ (H_b) [ppm]	$\Delta\delta_{calc}$ (H_b) [ppm]
0.012153805	0.012348451	7.5022	0.6826	0.6941
0.006076902	0.006174225	7.6235	0.5613	0.5460
0.003038451	0.003087113	7.7761	0.4087	0.3964
0.001519226	0.001543556	7.9191	0.2657	0.2629
0.001012817	0.001029038	7.9999	0.1849	0.1983
0.000506409	0.000514519	8.0988	0.0860	0.1151

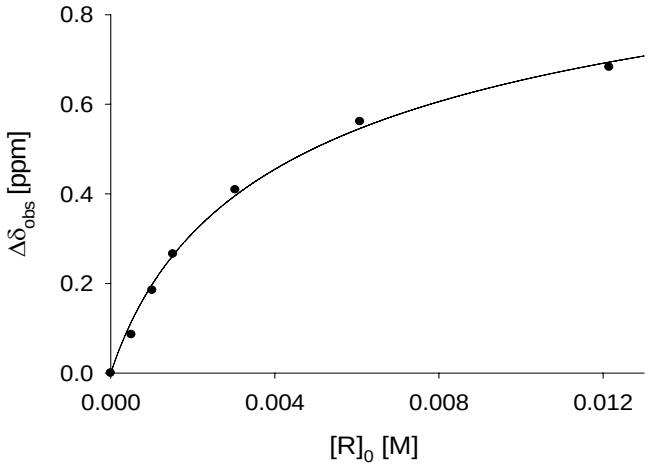

K_a [M^{-1}]	=	210 ± 20
$\Delta\delta_{max}$ (H_a) [ppm]	=	1.29
$\Delta\delta_{max}$ (H_b) [ppm]	=	1.06
$\Delta\delta_{max}$ (H_c) [ppm]	=	0.44
$\Delta\delta_{max}$ (H_d) [ppm]	=	0.11
$\Delta\delta_{max}$ (H_e) [ppm]	=	0.15
$\Delta\delta_{max}$ (H_g) [ppm]	=	0.06

37@31 ^{1}H NMR (500MHz, D_2O) δ[ppm]: 2.44 (dd, 2H, H-19a+H-20a), 2.66 (d, 2H, H-19i+H-20i), 3.80 (ddd, 2H, Adenosine, H_g), 4.17 (dd, 1H, Adenosine, H_d), 4.26 (dd, 1H, Adenosine, H_e), 4.69 (s, 4H, H-6+H-8+H-15+H-17), 5.60 (d, 1H, Adenosine, H_c), 6.67 (dd, 4H, H-2+H-3+H-12+H-11), 6.89 (s, 1H, Adenosine, H_a), 6.97 (dd, 4H, H-1+H-4+H-10+H-13), 7.24 (s, 1H, Adenosine, H_b), 7.28 (s, 4H, H-5+H-9+H-14+H-18)

Receptor:	**37**	M_R [g/mol]:	610.51
Solvent:	D_2O/Buffer (pH=7.2)	M_G [g/mol]:	334.23
T [°C]:	25	m_R [mg]:	10.23
Substrat:	Nicotinamide mononucleotide (**111**)	m_G [mg]:	5.42
		V_0 [mL]:	1.50
	δ_0 (H_a) [ppm] = 9.4635	$[G]_0$ [mM]:	10.77
	δ_0 (H_b) [ppm] = 8.9828		
	δ_0 (H_c) [ppm] = 8.2958		
	δ_0 (H_d) [ppm] = 9.2853		

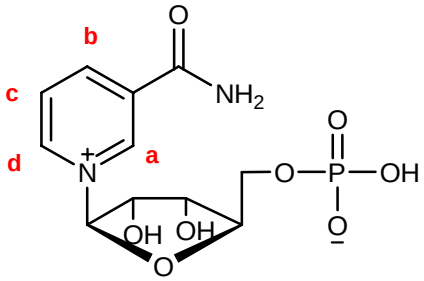

$[R]_0$ [M]	$[G]_0$ [M]	δ_{obs} (H_c) [ppm]	$\Delta\delta_{obs}$ (H_c) [ppm]	$\Delta\delta_{calc}$ (H_c) [ppm]
0.011138258	0.010771026	5.6694	2.6265	2.6376
0.005569129	0.005385513	5.9301	2.3658	2.3698
0.002784564	0.002692756	6.2155	2.0804	2.0403
0.001392282	0.001346378	6.6305	1.6654	1.6590
0.000928188	0.000897585	6.9293	1.3666	1.4222
0.000464094	0.000448793	7.2481	1.0478	1.0228

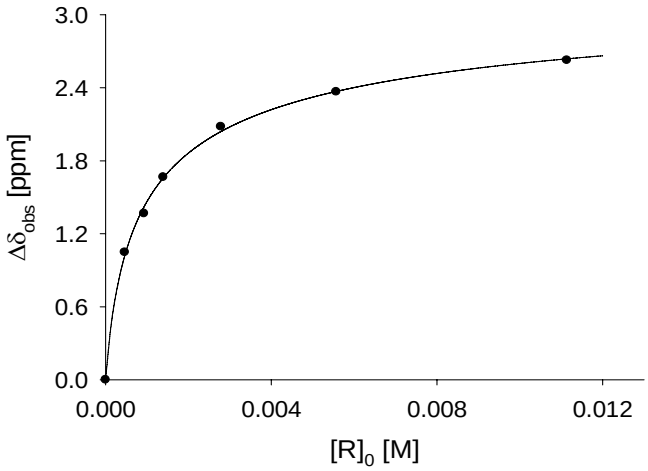

K_a [M^{-1}] = 1330 ± 130

$\Delta\delta_{max}$ (H_a) [ppm] = 1.20

$\Delta\delta_{max}$ (H_c) [ppm] = 3.43

$\Delta\delta_{max}$ (H_d) [ppm] = 1.64

37@111 ^{1}H NMR (500MHz, D_2O) δ[ppm]: 2.50 (dd, 2H, H-19a+H-20a), 2.71 (d, 2H, H-19i+H-20i), 4.74 (s, 4H, H-6+H-8+H-15+H-17), 4.87 (d, 1H, NMNAMN, H_c), 6.99 (dd, 4H, H-2+H-3+H-12+H-11), 7.12 (dd, 4H, H-1+H-4+H-10+H-13), 7.36 (s, 4H, H-5+H-9+H-14+H-18), 7.64 (d, 1H, NMNAMN, H_d), 8.26 (d, 1H, NMNAMN, H_a)

Receptor:	**38**	M_R [g/mol]:	742.72
Solvent:	D_2O	m_R [mg]:	3.69
T [°C]:	25	V_0 [mL]:	1.50
Substrat:	Itself (self-association)	$[R]_0$ [mM]:	3.31

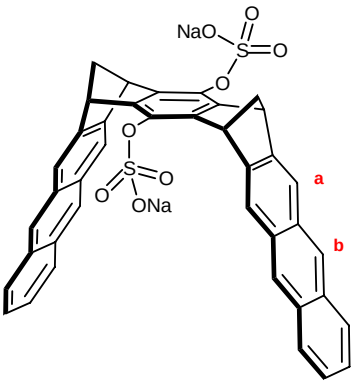

δ_0 (H_a) [ppm] = 7.7140

δ_0 (H_b) [ppm] = 8.0915

$[R]_0$ [M]	δ_{obs} (H_a) [ppm]	$\Delta\delta_{obs}$ (H_a) [ppm]	$\Delta\delta_{calc}$ (H_a) [ppm]
0.00331214	6.6431	1.0709	1.0729
0.00165607	6.6535	1.0605	1.0606
0.00082803	6.6669	1.0471	1.0434
0.00041402	6.6914	1.0226	1.0195
0.00027601	6.7189	0.9951	1.0016
0.00013801	6.7500	0.9640	0.9623

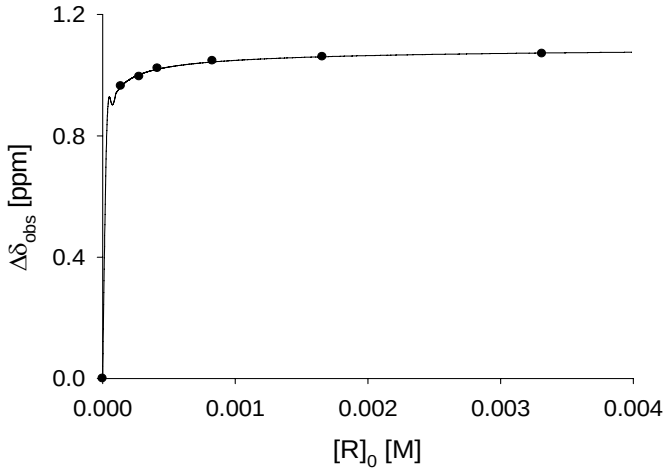

K_{dim} [M^{-1}] = $(1.94 \pm 0.2)\cdot 10^5$

$\Delta\delta_{max}$ (H_a) [ppm] = 1.10

$\Delta\delta_{max}$ (H_b) [ppm] = 2.26

Receptor:	**38**	M_R [g/mol]:	742.72
Solvent:	D_2O	m_R [mg]:	3.69
T [°C]:	45	V_0 [mL]:	1.50
Substrat:	Itself (self-association)	$[R]_0$ [mM]:	3.31

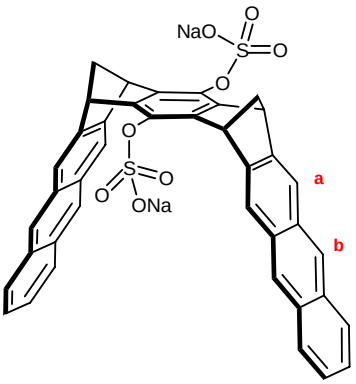

δ_0 (H_a) [ppm] = 7.7140

δ_0 (H_b) [ppm] = 8.0915

$[R]_0$ [M]	δ_{obs} (H_a) [ppm]	$\Delta\delta_{obs}$ (H_a) [ppm]	$\Delta\delta_{calc}$ (H_a) [ppm]
0.00331214	6.6756	1.0384	1.0437
0.00165607	6.6936	1.0204	1.0212
0.00082803	6.7197	0.9943	0.9902
0.00041402	6.7621	0.9519	0.9480
0.00027601	6.7936	0.9204	0.9168
0.00013801	6.8692	0.8448	0.8505

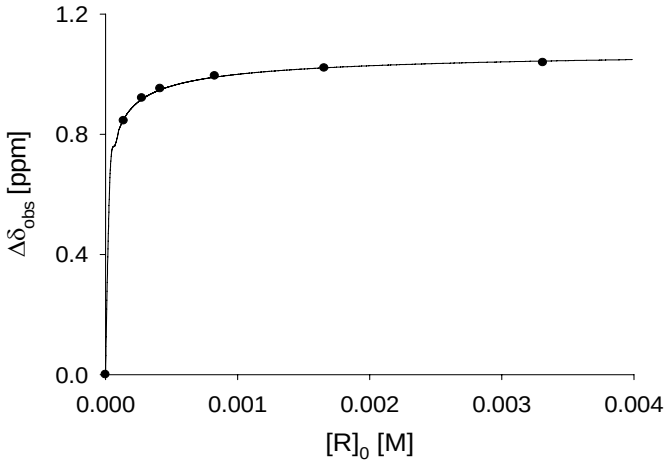

K_{dim} [M^{-1}] = $(5.44 \pm 0.5)\cdot 10^4$

$\Delta\delta_{max}$ (H_a) [ppm] = 1.10

$\Delta\delta_{max}$ (H_b) [ppm] = 2.33

Receptor:	**38**	M_R [g/mol]:	742.72
Solvent:	D_2O	m_R [mg]:	3.69
T [°C]:	65	V_0 [mL]:	1.50
Substrat:	Itself (self-association)	$[R]_0$ [mM]:	3.31

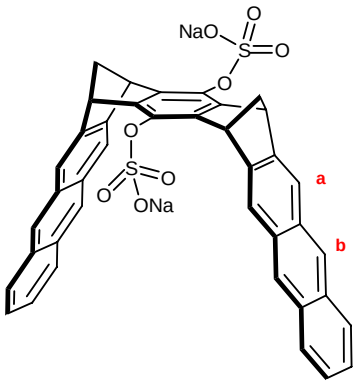

δ_0 (H_a) [ppm] = 7.7140

δ_0 (H_b) [ppm] = 8.0915

$[R]_0$ [M]	δ_{obs} (H_a) [ppm]	$\Delta\delta_{obs}$ (H_a) [ppm]	$\Delta\delta_{calc}$ (H_a) [ppm]
0.00331214	6.7289	0.9851	0.9864
0.00165607	6.7650	0.9490	0.9488
0.00082803	6.8125	0.9015	0.8982
0.00041402	6.8858	0.8282	0.8313
0.00027601	6.9295	0.7845	0.7836
0.00331214	6.7289	0.9851	0.9864

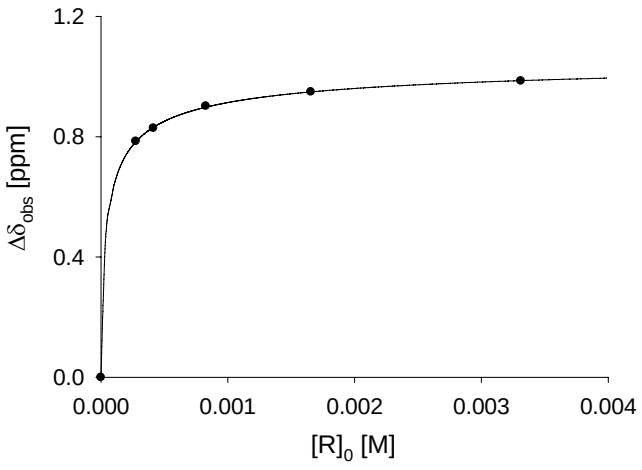

K_{dim} [M^{-1}] = $(1.71 \pm 0.2)\cdot 10^4$

$\Delta\delta_{max}$ (H_a) [ppm] = 1.08

$\Delta\delta_{max}$ (H_b) [ppm] = 2.34

Receptor:	**38**	M_R [g/mol]:	742.72
Solvent:	D_2O	m_R [mg]:	3.69
T [°C]:	85	V_0 [mL]:	1.50
Substrat:	Itself (self-association)	$[R]_0$ [mM]:	3.31

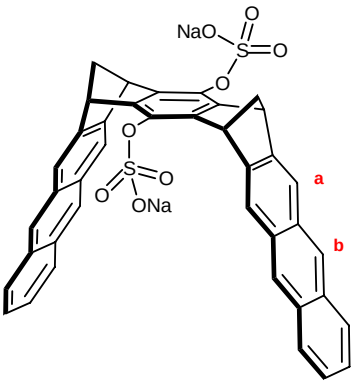

δ_0 (H_a) [ppm] = 7.7140

δ_0 (H_b) [ppm] = 8.0915

$[R]_0$ [M]	**δ_{obs} (H_a) [ppm]**	**$\Delta\delta_{obs}$ (H_a) [ppm]**	**$\Delta\delta_{calc}$ (H_a) [ppm]**
0.00331214	6.8072	0.9068	0.9066
0.00165607	6.8642	0.8498	0.8489
0.00082803	6.9406	0.7734	0.7737
0.00041402	7.0364	0.6776	0.6794
0.00027601	7.0986	0.6154	0.6157

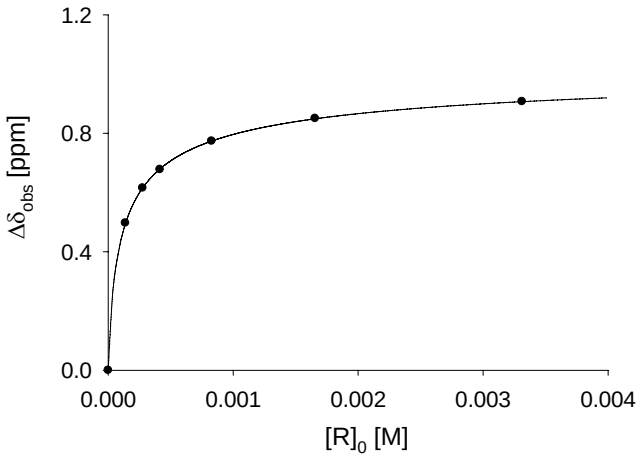

K_{dim} [M^{-1}] = $(5.91 \pm 0.6)\cdot 10^3$

$\Delta\delta_{max}$ (H_a) [ppm] = 1.06

$\Delta\delta_{max}$ (H_b) [ppm] = 2.32

Receptor:	**38**	M_R [g/mol]:	742.72
Solvent:	D_2O	m_R [mg]:	3.69
T [°C]:	95	V_0 [mL]:	1.50
Substrat:	Itself (self-association)	$[R]_0$ [mM]:	3.31

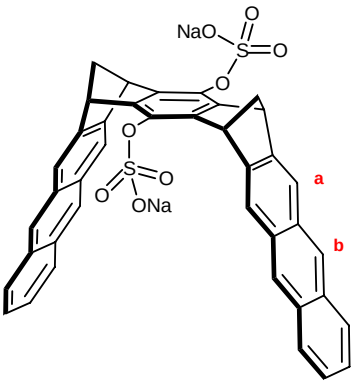

δ_0 (H_a) [ppm] = 7.7140

δ_0 (H_b) [ppm] = 8.0915

$[R]_0$ [M]	**δ_{obs} (H_a) [ppm]**	**$\Delta\delta_{obs}$ (H_a) [ppm]**	**$\Delta\delta_{calc}$ (H_a) [ppm]**
0.00331214	6.8588	0.8552	0.8565
0.00165607	6.9179	0.7961	0.7882
0.00082803	7.0147	0.6993	0.7014
0.00041402	7.1260	0.5880	0.5962
0.00027601	7.1915	0.5225	0.5275

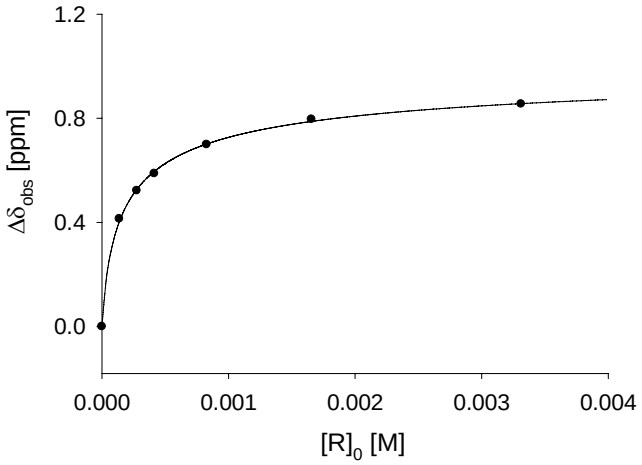

K_{dim} [M^{-1}] = $(3.70 \pm 0.4)\cdot 10^3$

$\Delta\delta_{max}$ (H_a) [ppm] = 1.05

$\Delta\delta_{max}$ (H_b) [ppm] = 2.31

Receptor:	**38**	M_R [g/mol]	742.72
Solvent:	D_2O/Buffer (pH=7.2)	M_G [g/mol]	663.43
T [°C]:	25	m_R [mg]:	6.65
Substrat:	NAD^+ (**35**)	m_G [mg]:	6.66
	δ_0 (H_a) [ppm] = 9.3351	V_0 [mL]:	1.50
	δ_0 (H_b) [ppm] = 8.8302	$[G]_0$ [mM]:	6.36
	δ_0 (H_d) [ppm] = 9.1468		
	δ_0 (H_e) [ppm] = 8.1527		
	δ_0 (H_f) [ppm] = 8.4211		

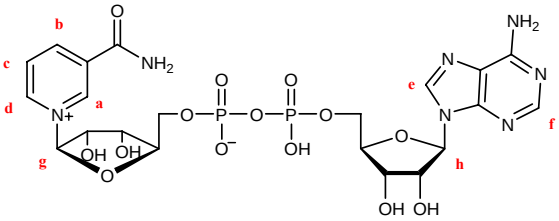

$[R]_0$ [M]	$[G]_0$ [M]	δ_{obs} (H_b) [ppm]	$\Delta\delta_{obs}$ (H_b) [ppm]	$\Delta\delta_{calc}$ (H_b) [ppm]
0.00298451	0.00317893	8.6856	0.1446	0.1405
0.00149226	0.00158947	8.7006	0.1296	0.1330
0.00074613	0.00079473	8.7091	0.1211	0.1229
0.00049742	0.00052982	8.7161	0.1141	0.1157
0.00024871	0.00026491	8.7264	0.1038	0.1010

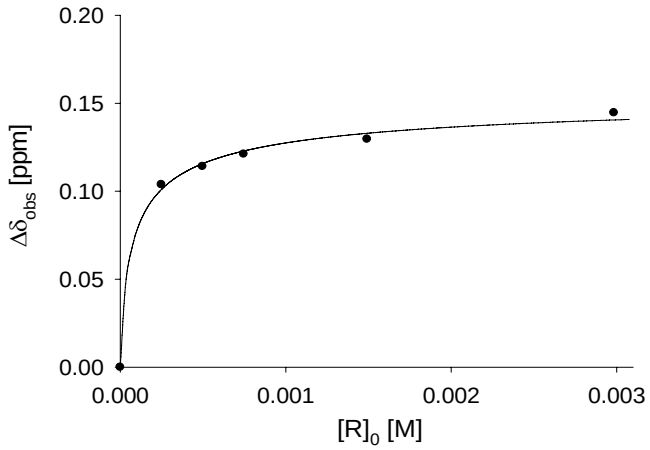

K_a [M^{-1}]	=	$(1.74 \pm 0.2)\cdot 10^4$
$\Delta\delta_{max}$ (H_a) [ppm]	=	0.79
$\Delta\delta_{max}$ (H_b) [ppm]	=	1.17
$\Delta\delta_{max}$ (H_d) [ppm]	=	1.08
$\Delta\delta_{max}$ (H_e) [ppm]	=	0.30
$\Delta\delta_{max}$ (H_f) [ppm]	=	0.17

Receptor:	**38**	M_R [g/mol]:	742.42
Solvent:	CD_3OD	M_G [g/mol]:	260.06
T [°C]:	25	m_R [mg]:	7.22
Substrat:	NMNA (**33**)	m_G [mg]:	2.52
		V_0 [mL]:	1.50
		$[G]_0$ [mM]:	7.36

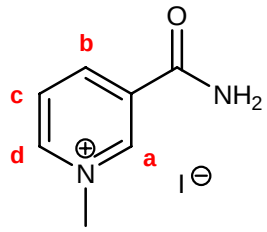

δ_0 (H_a) [ppm] = 9.3827
δ_0 (H_b) [ppm] = 8.9488
δ_0 (H_c) [ppm] = 8.1949
δ_0 (H_d) [ppm] = 9.0472

$[R]_0$ [M]	$[G]_0$ [M]	δ_{obs} (H_c) [ppm]	$\Delta\delta_{obs}$ (H_c) [ppm]	$\Delta\delta_{calc}$ (H_c) [ppm]
0.00648068	0.006362118	5.8490	2.3459	2.3447
0.00324034	0.003181059	5.9010	2.2939	2.2830
0.00162017	0.00159053	6.0029	2.1920	2.1982
0.00081009	0.000795265	6.1294	2.0655	2.0836
0.00054006	0.000530177	6.2009	1.9940	1.9999
0.00027003	0.000265088	6.3528	1.8421	1.8236

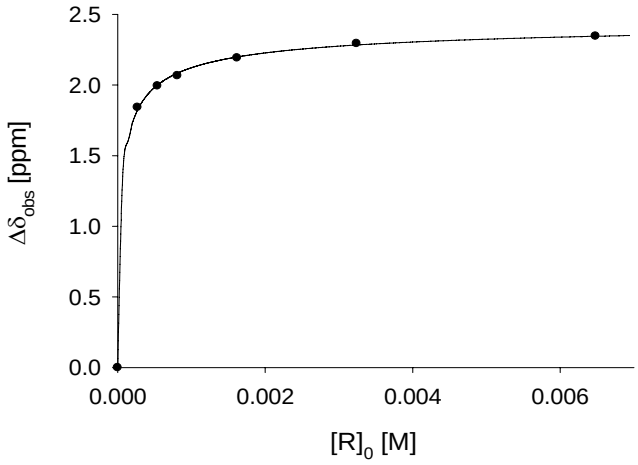

K_a [M^{-1}] = $(3.69 \pm 0.4)\cdot10^4$
$\Delta\delta_{max}$ (H_a) [ppm] = 2.09
$\Delta\delta_{max}$ (H_b) [ppm] = 1.41
$\Delta\delta_{max}$ (H_c) [ppm] = 2.48
$\Delta\delta_{max}$ (H_d) [ppm] = 0.30

38@**33** ^{1}H NMR (500MHz, CD_3OD) δ[ppm]: 2.39 (dt, 2H, H-23a+H-24a), 2.64 (dt, 2H, H-23i+H-24i), 4.82 (s, 4H, H-6+H-8+H-15+H-17), 5.71 (t, 1H, NMNA, H_c), 7.23 (dd, 4H, H-2+H-3+H-13+H-14), 7.29 (s, 1H, NMNA, H_a), 7.54 (d, 1H, NMNA, H_b), 7.68 (s, 4H, H-6+H-10+H-17+H-21), 7.69 (dd, 4H, H-1+H-4+H-12+H-15), 7.75 (d, 1H, NMNA, H_d), 7.90 (s, 4H, H-6+H-10+H-17+H-21)

Receptor:	**38**	M_R [g/mol]:	742.72
Solvent:	CD_3OD	M_G [g/mol]:	293.10
T [°C]:	25	m_R [mg]:	6.54
Substrat:	Kosower Salt (**84**)	m_G [mg]:	2.63
		V_0 [mL]:	1.50
	δ_0 (H_a) [ppm] = 9.2008	$[G]_0$ [mM]:	5.98
	δ_0 (H_b) [ppm] = 8.5459		
	δ_0 (H_c) [ppm] = 4.7677		
	δ_0 (H_d) [ppm] = 1.2246		

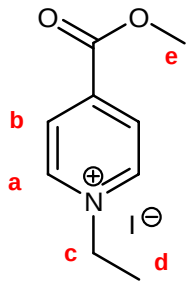

$[R]_0$ [M]	$[G]_0$ [M]	δ_{obs} (H_b) [ppm]	$\Delta\delta_{obs}$ (H_b) [ppm]	$\Delta\delta_{calc}$ (H_b) [ppm]
0.00587031	0.005981827	6.3967	2.1492	2.1342
0.00293516	0.002990914	6.4931	2.0528	2.0502
0.00146758	0.001495457	6.6039	1.9420	1.9370
0.00073379	0.000747728	6.7274	1.8185	1.7879
0.00048919	0.000498486	6.8338	1.7121	1.6817
0.0002446	0.000249243	7.0798	1.4661	1.4665

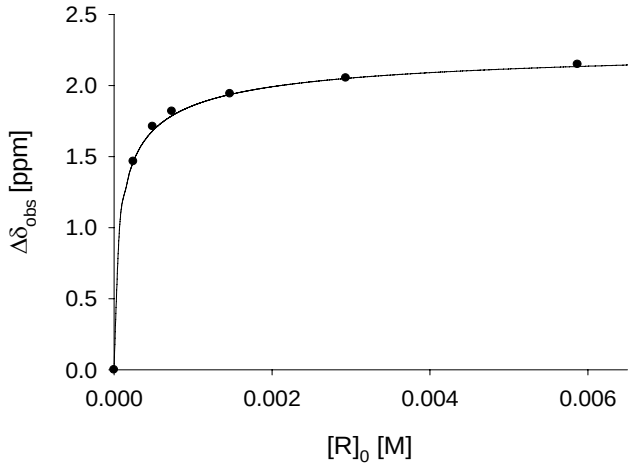

K_a [M^{-1}] = $(1.78 \pm 0.2)\cdot 10^4$

$\Delta\delta_{max}$ (H_a) [ppm] = 1.63

$\Delta\delta_{max}$ (H_b) [ppm] = 2.38

$\Delta\delta_{max}$ (H_c) [ppm] = 0.69

$\Delta\delta_{max}$ (H_d) [ppm] = 0.16

38@**84** ^{1}H NMR (500MHz, CD_3OD) δ[ppm]: 1.06 (t, 1H, KS, H_d), 2.39 (dt, 2H, H-23a+H-24a), 2.68 (dt, 2H, H-23i+H-24i), 3.78 (q, 1H, KS, H_c), 4.84 (s, 4H, H-6+H-8+H-15+H-17), 6.17 (d, 1H, KS, H_b), 7.23 (dd, 4H, H-2+H-3+H-13+H-14), 7.57 (d, 1H, KS, H_a), 7.57 (s, 4H, H-6+H-10+H-17+H-21), 7.66 (dd, 4H, H-1+H-4+H-12+H-15), 7.78 (s, 4H, H-6+H-10+H-17+H-21)

4.5.3 Fluorimetric titrations

Receptor:	**38**	M_R [g/mol]:	742.72
Solvent:	H_2O Buffer (pH= 7.2)	M_G [g/mol]:	663.43
T [°C]:	25	m_R [mg]:	0.120
Substrat:	NAD^+ (**35**)	m_G [mg]:	1.298
		V_{NAD^+} [mL]:	0.40
		V_R [mL]:	1.50
		$[R]_0$ [mM]:	0.10771
		λ_{exc} [nm]:	354

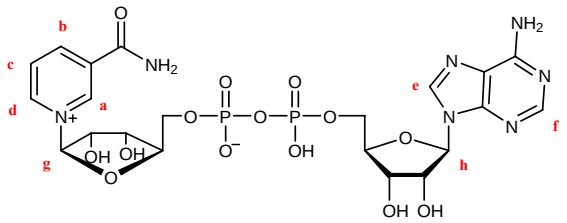

V_{NAD^+} [µL]	V_{TOTAL} [µL]	[R] [mM]	[NAD^+] [mM]	[NAD^+]/[R]	I_{504}	ΔI_{obs}	ΔI_{cal}
0	700	0.10771	0.0000	0.0000	998.0540	0.0000	0.0000
10	710	0.10771	0.06889	0.6396	840.1500	157.904	155.213
10	720	0.10771	0.13587	1.2614	707.0210	291.033	272.419
10	730	0.10771	0.20101	1.8662	617.0090	381.045	362.307
10	740	0.10771	0.26439	2.4546	558.0110	440.043	432.539
20	760	0.10771	0.38615	3.5850	482.7600	515.294	533.784
20	780	0.10771	0.50167	4.6575	409.7590	588.295	602.330
40	820	0.10771	0.71579	6.6454	326.9370	671.117	688.036
30	850	0.10771	0.86316	8.0136	277.5270	720.527	728.285
30	880	0.10771	1.0005	9.2885	243.3970	754.657	757.301
40	920	0.10771	1.1696	10.8590	206.4960	791.558	785.311
40	960	0.10771	1.3247	12.2986	185.1250	812.929	805.658
40	1000	0.10771	1.4674	13.6231	163.1590	834.895	821.097

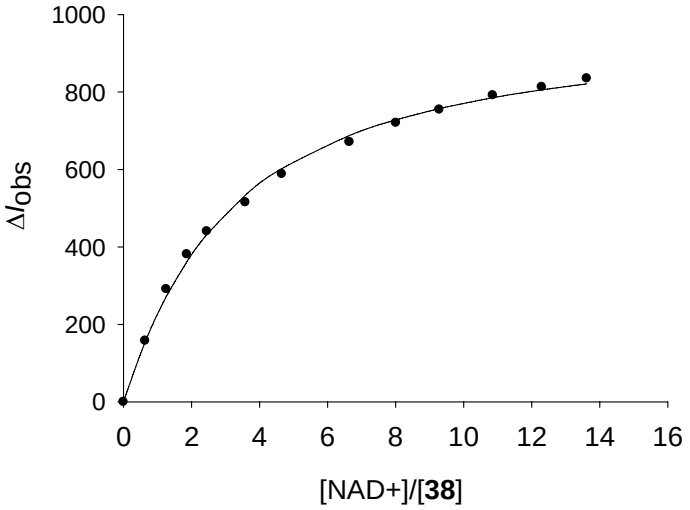

K_a [M^{-1}] = 3592 ± 196

Receptor:	**20g**	M_R [g/mol]:	706.51
Solvent:	H_2O Buffer (pH= 7.2)	M_G [g/mol]:	663.43
T [°C]:	25	m_R [mg]:	0.276
Substrat:	NAD^+ (**35**)	m_G [mg]:	3.793
		V_{NAD^+} [mL]:	1.20
		V_R [mL]:	3.65
		$[R]_0$ [mM]:	0.10703
		λ_{exc} [nm]:	354

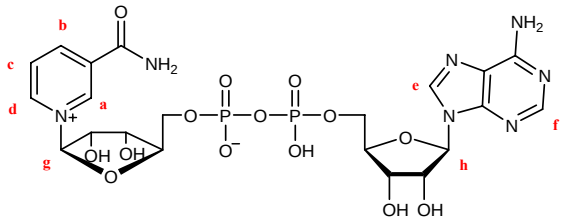

V_{NAD^+} [µL]	V_{TOTAL} [µL]	[R] [mM]	[NAD^+] [mM]	[NAD^+]/[R]	I_{508}	ΔI_{obs}	ΔI_{cal}
0	700	0.10703	0.00000	0.0000	928.549	0.000	0,00000
10	710	0.10703	0.06710	0.6270	712.034	216.515	244,07288
10	720	0.10703	0.13234	1.2365	523.243	405.306	408,08132
10	730	0.10703	0.19580	1.8294	405.468	523.081	517,53441
10	740	0.10703	0.25753	2.4062	329.76	598.789	592,49415
20	760	0.10703	0.37614	3.5144	246.432	682.117	685,07272
20	780	0.10703	0.48865	4.5657	178.266	750.283	738,50248
40	820	0.10703	0.69723	6.5145	123.659	804.890	796,46945
30	850	0.10703	0.84077	7.8557	103.797	824.752	820,78909
30	880	0.10703	0.97453	9.1054	90.7621	837.787	837,31535
40	920	0.10703	1.13931	10.6450	80.0792	848.470	852,53459
40	960	0.10703	1.29035	12.0563	71.3477	857.201	863,16980
40	1000	0.10703	1.42931	13.3546	65.7461	862.803	871,01589

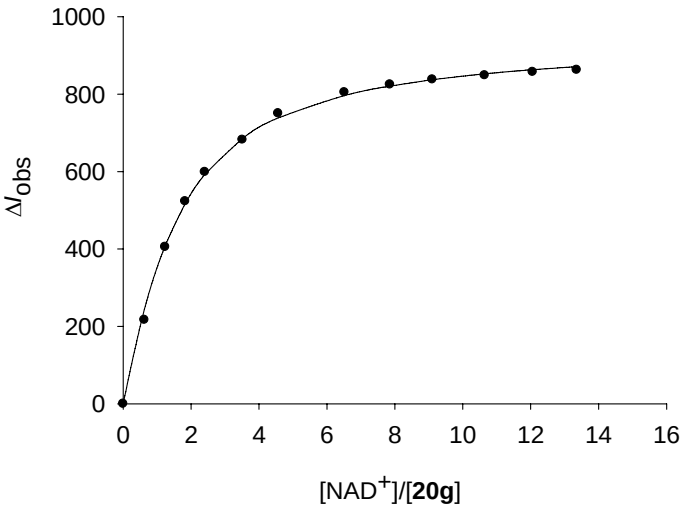

K_a [M^{-1}] = 8800 ± 370

4.6 Single-crystal structure analysis

4.6.1 Single-crystal structure analysis of the naphthalene clip 104

Preparation of the single crystal of the naphthalene clip **104**

15 mg of the anthracene clip **104** were dissolved with 15 mL of acetone in a 100 mL round-bottomed flask. The flask was closed with a glass cap to allow the acetone to evaporate slowly. After 36 hours at room temperature all the acetone was evaporated leading to white needle crystals.

Table 4.1: Data for the structure elucidation of **104**

- Identification code: vipinknc_0m
- Empirical formula: $C_{38}H_{30}O_2$
- Formula weight: 518.62 Da
- Crystal description: needle
- Crystal color: colorless
- Crystal size: 0.28x 0.08 x 0.05 mm

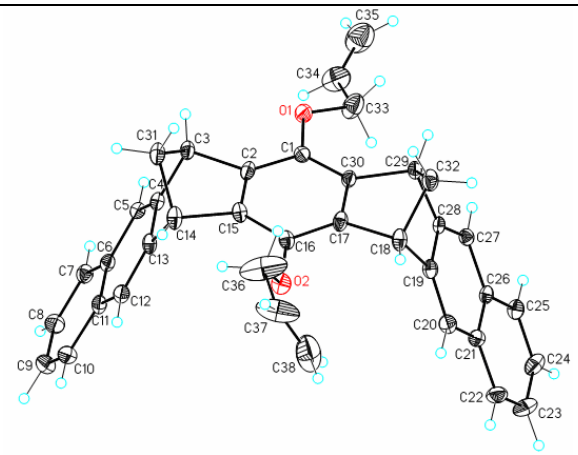

Measurement

- Diffractometer measurement device: Siemens SMART three axis goniometer with APEX II area detector system
- Diffractometer control software: Bruker AXS APEX 2 Vers. 1.0-27 2005
- Temperature: 203(2) K
- Wavelength: 0.71073 Å
- Theta range for data collection: 1.47° to 28.27°
- Completeness to theta = 28.27°: 99.3 %
- Index ranges: -9<=h<=9, -24<=k<=24, -27<=l<=27

Cell Data

- Crystal system: orthorhombic
- Space group: $P2_12_12_1$
- Z: 4
- Volume: 2720.0(9) $Å^3$
- Reflections: 4689
- θ (Cell): 2.69° to 22.34°
- Density: 1.266 $g \cdot cm^{-3}$
- F(000): 1096

- *a* [Å]: 7.0185(14)
- *b* [Å]: 18.602(4)
- *c* [Å]: 20.834(4)
- α: 90°
- β: 90°
- γ: 90°

Data reduction

- Data reduction: Bruker AXS APEX 2 Vers. 1.0-27 2005
- Empirical absorption correction: Bruker AXS APEX 2 Vers. 1.0-27 2005
- Absorption coefficient: 0.077 mm^{-1}
- $R_{(merg)}$ before/after correction: 0.0946 / 0.0694
- Max. / min. transmission: 1.00 / 0.83
- Reflections collected: 76250
- Independent reflections: 6685
- $R_{(int)}$: 0.1350

Data refinement

- Software: Bruker AXS SHELXTL Vers. 6.12
- Data / restraints / parameters: 4269 / 0 / 361
- Goodness-of-fit on F^2: 1.016
- Weighting details: w= 1 /[$\sigma^2(Fo^2)$ +(0.0723*P)^2 + 1.0437*P] where P = (Fo^2+2Fc^2)/3
- R_1 / wR_2: 0.0680 / 0.1427
- R_1 / wR_2 (all data): 0.1182 / 0.1677
- Flack parameter: 0(2); Flack H.D., *Acta Cryst*. **1983**, *A39*, 876-881
- *e* min/max [e $Å^{-3}$]: -0.242 / 0.388

Treatment of hydrogen atoms: Riding model on idealized geometries with the 1.2 fold isotropic displacement parameters of the equivalent Uij of the corresponding carbon atom.

Table 4.2: Atomic coordinates ($\cdot 10^4$) and equivalent isotropic displacement parameters ($\cdot 10^3$)[Å^2] for **104**. U(eq) is defined as 1/3 of the trace of the orthogonalized U_{ij} tensor.

	x	y	z	U(eq)
O(1)	10616(3)	5962(1)	1630(1)	35(1)
O(2)	4684(3)	3930(1)	1689(1)	33(1)
C(1)	9134(4)	5478(1)	1689(2)	24(1)
C(2)	8337(5)	5235(2)	1120(1)	27(1)
C(3)	8796(4)	5423(2)	415(1)	27(1)
C(4)	9561(4)	4740(2)	98(1)	25(1)
C(5)	11277(4)	4572(2)	-164(1)	25(1)
C(6)	11524(4)	3883(2)	-464(1)	26(1)
C(7)	13281(5)	3688(2)	-759(1)	29(1)
C(8)	13464(5)	3030(2)	-1058(2)	34(1)
C(9)	11938(6)	2547(2)	-1084(2)	39(1)
C(10)	10242(5)	2718(2)	-800(2)	35(1)
C(11)	9997(5)	3387(2)	-479(1)	28(1)
C(12)	8218(5)	3575(2)	-189(1)	28(1)
C(13)	8021(4)	4234(2)	90(1)	26(1)
C(14)	6340(5)	4615(2)	396(1)	32(1)
C(15)	6833(4)	4738(2)	1106(1)	25(1)
C(16)	6089(4)	4454(1)	1675(2)	26(1)
C(17)	6837(4)	4725(2)	2239(1)	27(1)
C(18)	6241(4)	4565(2)	2932(1)	29(1)
C(19)	7945(4)	4195(2)	3251(1)	26(1)
C(20)	8200(5)	3519(2)	3486(1)	30(1)
C(21)	9982(4)	3335(2)	3771(1)	25(1)
C(22)	10338(5)	2639(2)	4032(2)	36(1)
C(23)	12053(6)	2479(2)	4309(2)	43(1)
C(24)	13504(6)	2993(2)	4339(2)	40(1)
C(25)	13214(5)	3667(2)	4091(1)	29(1)
C(26)	11479(4)	3858(2)	3800(1)	24(1)
C(27)	11159(4)	4565(2)	3539(1)	24(1)
C(28)	9426(4)	4721(1)	3271(1)	24(1)
C(29)	8599(4)	5401(2)	2978(1)	27(1)
C(30)	8314(5)	5233(2)	2257(1)	25(1)
C(31)	6719(5)	5391(2)	141(1)	34(1)
C(32)	6526(4)	5333(2)	3218(1)	34(1)
C(33)	11924(6)	6074(2)	2139(2)	54(1)
C(34)	13743(6)	6357(2)	1879(2)	60(1)
C(35)	14683(8)	6876(3)	2080(3)	80(2)
C(36)	2871(5)	4142(2)	1531(3)	101(2)
C(37)	1404(6)	3656(2)	1767(3)	88(2)
C(38)	1630(9)	3148(3)	2140(2)	92(2)

Table 4.3: Bond lengths [Å] and angles [°] for **104**.

O(1)-C(1)	1.382(3)	C(34)-C(35)	1.242(6)
O(1)-C(33)	1.418(4)	C(36)-C(37)	1.456(6)
O(2)-C(36)	1.372(4)	C(37)-C(38)	1.233(7)
O(2)-C(16)	1.387(3)		
C(1)-C(2)	1.388(4)	C(1)-O(1)-C(33)	121.0(2)
C(1)-C(30)	1.392(4)	C(36)-O(2)-C(16)	116.9(3)
C(2)-C(15)	1.404(4)	O(1)-C(1)-C(2)	116.0(3)
C(2)-C(3)	1.543(4)	O(1)-C(1)-C(30)	126.9(3)
C(3)-C(4)	1.529(4)	C(2)-C(1)-C(30)	117.0(2)
C(3)-C(31)	1.567(4)	C(1)-C(2)-C(15)	122.3(3)
C(4)-C(5)	1.359(4)	C(1)-C(2)-C(3)	131.0(3)
C(4)-C(13)	1.434(4)	C(15)-C(2)-C(3)	106.7(3)
C(5)-C(6)	1.435(4)	C(4)-C(3)-C(2)	107.2(2)
C(6)-C(11)	1.415(4)	C(4)-C(3)-C(31)	97.9(2)
C(6)-C(7)	1.425(5)	C(2)-C(3)-C(31)	98.2(2)
C(7)-C(8)	1.379(4)	C(5)-C(4)-C(13)	120.8(3)
C(8)-C(9)	1.399(5)	C(5)-C(4)-C(3)	132.5(3)
C(9)-C(10)	1.366(5)	C(13)-C(4)-C(3)	106.7(2)
C(10)-C(11)	1.422(4)	C(4)-C(5)-C(6)	119.2(3)
C(11)-C(12)	1.431(4)	C(11)-C(6)-C(7)	118.6(3)
C(12)-C(13)	1.362(4)	C(11)-C(6)-C(5)	120.0(3)
C(13)-C(14)	1.518(4)	C(7)-C(6)-C(5)	121.3(3)
C(14)-C(15)	1.536(4)	C(8)-C(7)-C(6)	120.1(3)
C(14)-C(31)	1.560(5)	C(7)-C(8)-C(9)	121.1(3)
C(15)-C(16)	1.400(4)	C(10)-C(9)-C(8)	120.1(3)
C(16)-C(17)	1.381(4)	C(9)-C(10)-C(11)	120.8(3)
C(17)-C(30)	1.404(4)	C(6)-C(11)-C(10)	119.3(3)
C(17)-C(18)	1.533(4)	C(6)-C(11)-C(12)	119.4(3)
C(18)-C(19)	1.532(4)	C(10)-C(11)-C(12)	121.2(3)
C(18)-C(32)	1.561(4)	C(13)-C(12)-C(11)	119.2(3)
C(19)-C(20)	1.360(4)	C(12)-C(13)-C(4)	121.3(3)
C(19)-C(28)	1.429(4)	C(12)-C(13)-C(14)	132.7(3)
C(20)-C(21)	1.426(4)	C(4)-C(13)-C(14)	105.9(2)
C(21)-C(22)	1.427(4)	C(13)-C(14)-C(15)	107.4(2)
C(21)-C(26)	1.433(4)	C(13)-C(14)-C(31)	99.0(2)
C(22)-C(23)	1.367(5)	C(15)-C(14)-C(31)	98.7(2)
C(23)-C(24)	1.398(5)	C(16)-C(15)-C(2)	120.8(3)
C(24)-C(25)	1.371(4)	C(16)-C(15)-C(14)	132.6(3)
C(25)-C(26)	1.406(5)	C(2)-C(15)-C(14)	106.7(3)
C(26)-C(27)	1.439(4)	C(17)-C(16)-O(2)	120.6(3)
C(27)-C(28)	1.369(4)	C(17)-C(16)-C(15)	116.2(3)
C(28)-C(29)	1.520(4)	O(2)-C(16)-C(15)	123.2(3)
C(29)-C(32)	1.544(4)	C(16)-C(17)-C(30)	123.3(3)
C(29)-C(30)	1.547(4)	C(16)-C(17)-C(18)	128.8(3)
C(33)-C(34)	1.484(6)	C(30)-C(17)-C(18)	107.9(3)

C(19)-C(18)-C(17)	106.5(2)	C(28)-C(27)-C(26)	119.1(3)
C(19)-C(18)-C(32)	98.3(2)	C(27)-C(28)-C(19)	120.8(3)
C(17)-C(18)-C(32)	98.4(2)	C(27)-C(28)-C(29)	132.8(3)
C(20)-C(19)-C(28)	121.8(3)	C(19)-C(28)-C(29)	106.3(2)
C(20)-C(19)-C(18)	132.4(3)	C(28)-C(29)-C(32)	99.3(2)
C(28)-C(19)-C(18)	105.8(2)	C(28)-C(29)-C(30)	105.7(2)
C(19)-C(20)-C(21)	119.1(3)	C(32)-C(29)-C(30)	100.2(2)
C(20)-C(21)-C(22)	122.0(3)	C(1)-C(30)-C(17)	120.2(3)
C(20)-C(21)-C(26)	119.9(3)	C(1)-C(30)-C(29)	134.9(3)
C(22)-C(21)-C(26)	118.2(3)	C(17)-C(30)-C(29)	104.9(2)
C(23)-C(22)-C(21)	120.8(3)	C(14)-C(31)-C(3)	94.0(2)
C(22)-C(23)-C(24)	120.7(3)	C(29)-C(32)-C(18)	94.2(2)
C(25)-C(24)-C(23)	120.0(3)	O(1)-C(33)-C(34)	109.6(3)
C(24)-C(25)-C(26)	121.5(3)	C(35)-C(34)-C(33)	127.6(5)
C(25)-C(26)-C(21)	118.7(3)	O(2)-C(36)-C(37)	113.3(4)
C(25)-C(26)-C(27)	122.0(3)	C(38)-C(37)-C(36)	126.7(5)
C(21)-C(26)-C(27)	119.3(3)		

Table 4.4: Anisotropic displacement parameters ($\cdot 10^3$) [$Å^2$] for **104**. The anisotropic displacement factor exponent takes the form: $-2\pi^2 [h^2 a^{*2} U_{11} + ... + 2 h k a^* b^* U_{12}]$

	U_{11}	U_{22}	U_{33}	U_{23}	U_{13}	U_{12}
O(1)	41(1)	34(1)	29(1)	2(1)	-8(1)	-10(1)
O(2)	20(1)	42(1)	36(1)	1(1)	-3(1)	-2(1)
C(1)	23(1)	24(1)	25(1)	-1(1)	-4(1)	4(1)
C(2)	29(2)	33(2)	18(1)	4(1)	3(1)	11(2)
C(3)	28(2)	33(2)	19(1)	0(1)	-3(1)	6(1)
C(4)	26(2)	31(2)	18(1)	2(1)	-1(1)	1(1)
C(5)	29(2)	25(2)	21(1)	2(1)	0(1)	0(1)
C(6)	29(2)	28(2)	20(1)	3(1)	-4(1)	2(1)
C(7)	29(2)	33(2)	25(2)	1(1)	2(1)	5(2)
C(8)	32(2)	34(2)	36(2)	-2(1)	3(2)	6(2)
C(9)	50(2)	32(2)	37(2)	-7(1)	-1(2)	5(2)
C(10)	41(2)	28(2)	35(2)	-2(1)	-3(2)	-1(2)
C(11)	32(2)	34(2)	20(1)	1(1)	-1(1)	-2(1)
C(12)	27(2)	32(2)	23(2)	1(1)	-1(1)	-4(1)
C(13)	20(2)	38(2)	19(1)	-2(1)	-3(1)	1(1)
C(14)	24(2)	49(2)	22(2)	-2(1)	-1(1)	3(2)
C(15)	17(2)	36(2)	21(1)	-4(1)	0(1)	2(1)
C(16)	22(1)	33(2)	23(1)	-4(1)	0(1)	5(1)
C(17)	24(2)	37(2)	19(1)	1(1)	2(1)	10(2)
C(18)	21(2)	46(2)	21(1)	-1(1)	1(1)	3(2)
C(19)	23(2)	34(2)	22(2)	-2(1)	2(1)	1(1)
C(20)	27(2)	34(2)	28(2)	-2(1)	4(1)	-9(1)
C(21)	24(2)	26(2)	26(2)	0(1)	5(1)	-1(1)
C(22)	42(2)	26(2)	41(2)	5(1)	4(2)	-7(2)
C(23)	44(2)	32(2)	54(2)	16(2)	4(2)	8(2)
C(24)	40(2)	44(2)	36(2)	13(2)	2(2)	9(2)
C(25)	25(2)	37(2)	26(2)	1(1)	0(1)	0(2)
C(26)	25(2)	30(2)	17(1)	1(1)	4(1)	0(1)
C(27)	25(2)	27(2)	21(1)	-2(1)	3(1)	-2(1)
C(28)	30(2)	27(1)	13(1)	0(1)	1(1)	0(1)
C(29)	33(2)	29(2)	18(1)	-2(1)	-3(1)	3(1)
C(30)	29(2)	27(2)	19(1)	1(1)	-2(1)	5(1)
C(31)	35(2)	46(2)	20(2)	-1(1)	-1(1)	12(2)
C(32)	34(2)	44(2)	24(2)	-3(1)	2(1)	10(2)
C(33)	54(2)	64(3)	44(2)	17(2)	-15(2)	-19(2)
C(34)	42(2)	59(3)	78(3)	13(2)	-21(2)	-11(2)
C(35)	74(4)	89(4)	77(3)	20(3)	-7(3)	-23(3)
C(36)	25(2)	63(3)	216(7)	48(4)	-40(3)	-5(2)
C(37)	32(2)	47(3)	183(6)	-19(4)	4(4)	-3(2)
C(38)	87(4)	133(5)	57(3)	-14(3)	19(3)	-61(4)

Table 4.5: Hydrogen coordinates ($\cdot 10^4$) and *i* displacement parameters ($\cdot 10^3$) [Å^2] for **104**.

	x	y	z	U(eq)
H(3)	9498	5858	341	32
H(5)	12311	4909	-147	30
H(7)	14332	4018	-755	35
H(8)	14658	2900	-1250	41
H(9)	12077	2095	-1300	47
H(10)	9204	2383	-818	42
H(12)	7178	3240	-184	33
H(14)	5103	4418	307	38
H(18)	5018	4343	2992	35
H(20)	7193	3171	3461	36
H(22)	9364	2277	4010	44
H(23)	12264	2010	4489	52
H(24)	14708	2872	4529	48
H(25)	14210	4019	4118	35
H(27)	12151	4919	3547	29
H(29)	9253	5841	3076	32
H(31A)	6684	5420	-319	40
H(31B)	5887	5744	326	40
H(32A)	5672	5691	3028	41
H(32B)	6427	5343	3687	41
H(33A)	12138	5633	2368	65
H(33B)	11418	6422	2433	65
H(34)	14243	6113	1509	72
H(35A)	14214	7130	2449	96
H(35B)	15848	7025	1879	96
H(36A)	2788	4127	1071	122
H(36B)	2639	4627	1668	122
H(37)	100	3751	1657	105
H(38A)	2908	3029	2265	111
H(38B)	580	2868	2296	111

5 References

[1] J. M. Lehn, *Pure Appl. Chem.* **1978**, *50*, 871-892.
[2] J. M. Lehn, *Supramolecular Chemistry: Concepts and Perspectives*, VCH, Weinheim, New York, Basel, Cambridge, Tokio, **1995**.
[3] E. P. Kyba, R. C. Helgeson, K. Madan, G. W. Gokel, T. L. Tarnowski, S. S. Moore, D. J. Cram, *J. Am. Chem. Soc.* **1977**, *99*, 2564-2571.
[4] E. Fischer, *Chem.Ber.* **1894**, *27*, 2985-2993.
[5] J. M. Berg, J. L. Tymoczko, L. Stryer, *Biochemie*, 5. Auflage ed., Spektrum Akademischer Verlag, Heidelberg, Berlin, **2003**.
[6] J. D. Watson, F. H. C. Crick, *Nature* **1953**, *171*, 737-738.
[7] W. Saenger, *Principles of Nucleic Acid Structure*, 2nd corr. print. ed., Springer-Verlag, New York, Berlin, Heidelberg, London, Paris, Tokyo, **1988**.
[8] L. J. Prins, D. N. Reinhoudt, P. Timmerman, *Angew. Chem. Int. Edit.* **2001**, *40*, 2383-2426.
[9] G. A. Jeffrey, *An Introduction of Hydrogen Bonding*, Oxford University Press, New York, **1997**.
[10] M. M. Conn, G. Deslongchamps, J. Demendoza, J. Rebek, *J. Am. Chem. Soc.* **1993**, *115*, 3548-3557.
[11] Y. L. Cho, D. M. Rudkevich, A. Shivanyuk, K. Rissanen, J. Rebek, *Chem. Eur. J.* **2000**, *6*, 3788-3796.
[12] J. P. Gallivan, D. A. Dougherty, *J. Am. Chem. Soc.* **2000**, *122*, 870-874.
[13] P. J. Smith, E. I. Kim, C. S. Wilcox, *Angew. Chem. Int. Edit.* **1993**, *32*, 1648-1650.
[14] T. H. Chemical Society ReviewsWebb, C. S. Wilcox, *Chem. Soc. Rev.* **1993**, *22*, 383-395.
[15] C. Raposo, C. S. Wilcox, *Tetrahedron Lett.* **1999**, *40*, 1285-1288.
[16] C. A. Hunter, K. R. Lawson, J. Perkins, C. J. Urch, *J. Chem. Soc., Perkin Trans. 2* **2001**, 651-669.
[17] M. O. Sinnokrot, E. F. Valeev, C. D. Sherrill, *Journal of the American Chemical Society* **2002**, *124*, 10887-10893.
[18] E. Kim, S. Paliwal, C. S. Wilcox, *J. Am. Chem. Soc.* **1998**, *120*, 11192-11193.
[19] K. Nakamura, K. N. Houk, *Org. Lett.* **1999**, *1*, 2049-2051.
[20] E. A. Meyer, R. K. Castellano, F. Diedrich, *Angew. Chem. Int. Ed.* **2003**, *42*, 1210-1250.
[21] E. G. Cox, D. W. J. Cruickshank, J. A. S. Smith, *Proc. R. Soc. London A* **1958**, *247*, 1-21.
[22] K. C. Janda, J. C. Hemminger, J. S. Winn, S. E. Novick, H. S. J., W. Klemperer, *J. Chem. Phys.* **1975**, *63*, 1419-1421.
[23] J. M. Steed, T. A. Dixon, W. Klemperer, *J. Chem. Phys.* **1979**, *70*, 4940-4946.
[24] R. Laatikainen, J. Ratilainen, R. Sebastian, H. Santa, *J. Am. Chem. Soc.* **1995**, *117*, 11006-11010.
[25] S. K. Burley, G. A. Petsko, *Science* **1985**, *229*, 23-28.
[26] S. K. Burley, G. A. Petsko, *Adv. Protein Chem.* **1988**, *39*, 125-189.
[27] S. K. Burley, G. A. Petsko, *J. Am. Chem. Soc.* **1986**, *108*, 7995-8001.
[28] W. L. Jorgensen, D. L. Severance, *J. Am. Chem. Soc.* **1990**, *112*, 4768-4774.
[29] R. L. Jaffe, G. D. Smith, *J. Chem. Phys.* **1996**, *105*, 2780-2788.
[30] P. Hobza, H. L. Selzle, E. W. Schlag, *J. Chem. Phys.* **1996**, *100*, 18790-18794.
[31] F. Tran, J. Weber, T. A. Wesolowski, *Helv. Chim. Acta* **2001**, *84*, 1489-1503.
[32] S. Tsuzuki, K. Honda, T. Uchimaru, M. M., K. Tanabe, *J. Am. Chem. Soc.* **2002**, *124*, 104-112.
[33] C. A. Hunter, J. K. M. Sanders, *J. Am. Chem. Soc.* **1990**, *112*, 5525-5534.
[34] K. Müller-Dethlefs, P. Hobza, *Chem. Rev.* **2000**, *100*, 143-167.
[35] S. Paliwal, S. Geib, C. S. Wilcox, *J. Am. Chem. Soc.* **1994**, *116*, 4497-4498.
[36] F. G. Klärner, B. Kahlert, *Acc. Chem. Res.* **2003**, *36*, 919-932.

[37] F. Cozzi, M. Cinquini, R. Annuziata, J. S. Siegel, *Journal of the American Chemical Society* **1993**, *115*, 5330-5331.
[38] S. C. Zimmerman, *Frontiers in Bioorganic Chemsitry, Vol. Vol. 2* (Ed.: H. Dugas), Springer-Verlag, New York, Berlin, Heidelberg, London, Paris, Tokyo, **1991**.
[39] R. Foster, *Organic Charge Transfer Complexes*, Academic Press, London, New York, **1969**.
[40] J. C. Ma, D. A. Dougherty, *Chem. Rev.* **1997**, *97*, 1303-1324.
[41] J. Sunner, K. Nishizawa, P. Kebarle, *J. Phys. Chem.* **1981**, *85*, 1814-1820.
[42] R. Breslow, *Isr. J. Chem.* **1979**, *18*, 187-196.
[43] D. J. Cram, M. DeGrandpre, C. B. Knobler, K. N. Trueblood, *J. Am. Chem. Soc.* **1984**, *106*, 3286-3292.
[44] H. J. Schneider, *Angew. Chem. Int. Edit.* **1991**, *30*, 1417-1436.
[45] C. J. Pedersen, *J. Am. Chem. Soc.* **1967**, *89*, 7017-7036.
[46] C. J. Pedersen, Frensdor.Hk, *Angew. Chem. Int. Edit.* **1972**, *11*, 16-26.
[47] C. J. Pedersen, *Angew. Chem. Int. Edit.* **1988**, *27*, 1021-1027.
[48] J. M. Lehn, *Science* **1985**, *227*, 849-856.
[49] C. M. Starks, *J. Am. Chem. Soc.* **1971**, *93*, 195-199.
[50] C. M. Starks, C. Liotta, *Phase Transfer Catalisys, Principles and Techniques*, Academis Press, London-New Yok, **1978**.
[51] W. P. Weber, G. W. Gokel, *Phase Transfer Catalisys in Organic Chemistry*, Springer Verlag, Berlin-Heilderberg, **1977**.
[52] E. V. Dehmlow, S. S. Dehmlow, *Phase Transfer Catalisys, Vol. 3*, Vergal Chemie, **1993**.
[53] F. Diederich, *Cyclophanes*, Royal Society of Chemistry, Cambridge, **1991**.
[54] D. Philp, J. F. Stoddart, *Angew. Chem. Int. Edit.* **1996**, *35*, 1155-1196.
[55] S. M. Ngola, D. A. Dougherty, *J. Org. Chem.* **1996**, *61*, 4355-4360.
[56] M. V. Rekharsky, Y. Inoue, *Chem. Rev.* **1998**, *98*, 1875-1917.
[57] F. Venema, C. M. Baselier, M. C. Feiters, R. J. M. Nolte, *Tetrahedron Lett.* **1994**, *35*, 8661-8664.
[58] P. R. Ashton, V. Balzani, M. Clemente-Leon, B. Colonna, A. Credi, N. Jayaraman, F. M. Raymo, J. F. Stoddart, M. Venturi, *Chem.-Eur. J.* **2002**, *8*, 673-684.
[59] A. Collet, J. P. Dutasta, B. Lozach, J. Canceill, *Top. Curr. Chem.* **1993**, *165*, 103-129.
[60] Z. L. Zhong, A. Ikeda, S. Shinkai, S. Sakamoto, K. Yamaguchi, *Org. Lett.* **2001**, *3*, 1085-1087.
[61] D. J. Cram, *Container Molelcules and their Guests*, Royal Society of Chemistry, Cambridge, **1994**.
[62] R. Warmuth, J. Yoon, *Acc. Chem. Res.* **2001**, *34*, 95-105.
[63] C.-W. Chen, H. W. Whitlock, *J. Am. Chem. Soc.* **1978**, *100*, 4921-4922.
[64] S. C. Zimmerman, *Top. Curr. Chem.* **1993**, *165*, 71-102.
[65] S. C. Zimmerman, C. M. VanZyl, *J. Am. Chem. Soc.* **1987**, *109*, 7894-7896.
[66] S. C. Zimmerman, C. M. VanZyl, G. S. Hamilton, *J. Am. Chem. Soc.* **1989**, *111*, 1373-1381.
[67] A. E. Rowan, J. A. A. W. Elemans, R. J. M. Nolte, *Acc. Chem. Res.* **1999**, *32*, 995-1006.
[68] J. Benkhoff, Universität GH Essen (Essen), Dissertation **1994**.
[69] F.-G. Klärner, J. Benkhoff, R. Boese, U. Burkert, M. Kamieth, U. Naatz, *Angew. Chem. Int. Edit.* **1996**, *35*, 1130-1133.
[70] F. H. Kohnke, A. M. Z. Slawin, J. F. Stoddart, D. J. Williams, *Angew. Chem. Int. Edit.* **1987**, *26*, 892-894.
[71] F. H. Kohnke, J. F. Stoddart, *Pure Appl. Chem.* **1989**, *61*, 1581-1586.
[72] M. Kamieth, Universität GH Essen (Essen), **1998**.
[73] F.-G. Klärner, U. Burkert, M. Kamieth, R. Boese, J. Benet-Buchholz, *Chem. Eur. J.* **1999**, *5*, 1700-1707.
[74] U. Burkert, Universität GH Essen (Essen), Dissertation **1999**.

[75] F.-G. Klärner, J. Panitzky, D. Preda, L. T. Scott, *J. Mol. Model.* **2000**, *6*, 318-327.
[76] M. Kamieth, F.-G. Klärner, F. Diederich, *Angew. Chem. Int. Edit.* **1998**, *37*, 3303-3306.
[77] F.-G. Klärner, J. Panitzky, D. Bläser, R. Boese, *Tetrahedron* **2001**, *57*, 3673-3687.
[78] J. Panitzky, Frauenhofer IRB Verlag (Stuttgart), Dissertation **2002**.
[79] F.-G. Klärner, B. Kahlert, R. Boese, D. Bläser, A. Juris, F. Marchioni, *Chem. Eur. J.* **2005**, *11*, 3363-3374.
[80] C. Jasper, T. Schrader, J. Panitzky, F.-G. Klärner, *Angew. Chem. Int. Edit.* **2002**, *41*, 1355-1358.
[81] M. Fokkens, C. Jasper, T. Schrader, F. Koziol, C. Ochsenfeld, J. Polkowska, M. Lobert, B. Kahlert, F.-G. Klärner, *Chem. Eur. J.* **2005**, *11*, 477-494.
[82] M. Lobert, Universität Duisburg-Essen (Essen), Dissertation **2005**.
[83] F.-G. Klärner, M. Lobert, U. Naatz, H. Bandmann, R. Boese, *Chem. Eur. J.* **2003**, *9*, 5036-5047.
[84] F. Marchioni, A. Juris, M. Lobert, U. Seelbach, B. Kahlert, F.-G. Klärner, *N. J. Chem.* **2005**, *29*, 780-784.
[85] P. J. Dandliker, F. Diederich, M. Gross, C. B. Knobler, A. Louati, E. M. Sanford, *Angew. Chem. Int. Edit. Engl.* **1994**, *33*, 1739-1742.
[86] R. Murray, D. K. Granner, P. A. Mayer, V. W. Rodwell, *Harper's Illustrated Biochemistry*, 36 ed., McGraw-Hill, New York, **2003**.
[87] M. J. Hannon, P. C. Mayers, P. C. Taylor, *J. Chem. Soc.-Perkin Trans. 1* **2000**, 1881-1889.
[88] A. Sunder, R. Mülhaupt, R. Haag, H. Frey, *Advanced Materials* **2000**, *12*, 235-239.
[89] F. G. Klarner, B. Kahlert, A. Nellesen, J. Zienau, C. Ochsenfeld, T. Schrader, *J. Am. Chem. Soc.* **2006**, *128*, 4831-4841.
[90] J. Polkowska, K. Kowski, F.-G. Klärner, T. Schrader, *unpublished results*.
[91] P. W. Sorensen, J. M. Fine, V. Dvornikovs, C. S. Jeffrey, F. Shao, J. Z. Wang, L. A. Vrieze, K. R. Anderson, T. R. Hoye, *Nat. Chem. Biol.* **2005**, *1*, 324-328.
[92] J. M. Fine, P. W. Sorensen, *J. Chem. Ecol.* **2005**, *31*, 2205-2210.
[93] M. Foot, M. Mulholland, *J. Pharm. Biomed. Anal.* **2005**, *38*, 397-407.
[94] S. Iida, H. Tsuiji, Y. Nemoto, Y. Sano, M. A. Reddish, T. Irimura, *Oncol. Res.* **1998**, *10*, 407-414.
[95] H. Tsuiji, J. C. Hong, Y. S. Kim, Y. Ikehara, H. Narimatsu, T. Irimura, *Biochem. Biophys. Res. Commun.* **1998**, *253*, 374-381.
[96] J. R. Bundgaard, J. Vuust, J. F. Rehfeld, *J. Biol. Chem.* **1997**, *272*, 21700-21705.
[97] J. E. Rose, P. D. Leeson, D. Gani, *J. Chem. Soc. Perkin Trans. 1* **1994**, 3089-3094.
[98] F.-G. Klärner, U. Burkert, M. Kamieth, R. Boese, *J. Phys. Org. Chem.* **2000**, *13*, 604-611.
[99] L. Brunsveld, H. Zhang, M. Glasbeek, J. Vekemans, E. W. Meijer, *Journal Of The American Chemical Society* **2000**, *122*, 6175-6182.
[100] N. Hoffmann, J. P. Pete, *Synthesis* **2001**, 1236-1242.
[101] W. L. Caulfield, I. T. Collie, R. S. Dickins, O. Epemolu, R. McGuire, D. R. Hill, G. McVey, J. R. Morphy, Z. Rankovic, H. Sundaram, *J. Med. Chem.* **2001**, *44*, 2679-2682.
[102] I. Kato, M. Higashimoto, O. Tamura, H. Ishibashi, *J. Org. Chem.* **2003**, *68*, 7983-7989.
[103] F. G. Klärner, M. K. Diedrich, in *The Chemistry of Dienes and Polyenes, 1* (Ed.: Z. Rappoport), Wiley, New York, **1997**, pp. 547-617.
[104] p. table, **2002**.
[105] H. Friebolin, *Ein- und zweidimensionale NMR-Spektroskopie: eine Einführung*, VCH, Weinheim, **1992**.

[106] M. Kamieth, U. Burkert, P. S. Corbin, S. J. Dell, S. C. Zimmerman, F.-G. Klärner, *Eur. J. Org. Chem.* **1999**, 2741-2749.
[107] *TableCurve 2D* 5.01, TableCurve 2D 5.01, SYSTAT Software, Inc., Richmond, CA.
[108] U. P. Seelbach, Essen (Essen), Dissertation **2002**.
[109] H.-J. Schneider, A. Yatsimirsky, *Principles and Methods in Supramolecular Chemistry*, Wiley-VCH, Weinheim, **2000**.
[110] P. J. Garratt, A. J. Ibbett, J. E. Ladbury, R. O'Brien, M. B. Hursthouse, K. M. A. Malik, *Tetrahedron* **1998**, *54*, 949-968.
[111] J. L. Atwood, J. E. D. Davies, D. D. MacNicol, F. Vögtle, K. S. Suslick, *Comprehensive Supramolecular Chemistry*, Elsevier, Oxford, **1996**.
[112] A. Thibblin, *J. Phys. Org. Chem.* **2002**, *15*, 233-241.
[113] V. Mandiyan, R. Obrien, M. Zhou, B. Margolis, M. A. Lemmon, J. M. Sturtevant, J. Schlessinger, *J. Biol. Chem.* **1996**, *271*, 4770-4775.
[114] Y. L. Zhang, Z. Y. Zhang, *Annal. Biochem.* **1998**, *261*, 139-148.
[115] F. G. Klärner, J. Polkowska, J. Panitzky, U. P. Seelbach, U. Burkert, M. Kamieth, M. Baumann, A. E. Wigger, R. Boese, D. Bläser, *Eur. J. Org. Chem.* **2004**, 1405-1423.
[116] K. Wang, G. W. Gokel, *Pure Appl. Chem.* **1996**, *68*, 1267-1272.
[117] M. Suzuki, A. Ii, T. Saegusa, *Macromolecules* **1992**, *25*, 7071-7072.
[118] M. Suzuki, S. Yoshida, K. Shiraga, T. Saegusa, *Macromolecules* **1998**, *31*, 1716-1719.
[119] A. Kleemann, R. Wagner, *Glycidol: Properties; Reactions; Applications*, Hüthig, Heilderberg, **1981**.
[120] M. Hanriot, *Ann. Chim. Phys.* **1879**, *17*, 116-119.
[121] F. E. Bailey, J. V. Koleske, *Alkylene Oxides and Their Properties, Vol. 35*, Marcel Dekker, New york, **1990**.
[122] A. Sunder, R. Hanselmann, H. Frey, R. Mulhaupt, *Macromolecules* **1999**, *32*, 4240-4246.
[123] A. Sunder, H. Frey, R. Mülhaupt, *Polym. Mater. Sci. Eng.* **1999**, *80*, 203-208.
[124] H. Pasch, W. Schrepp, *MALDI-TOF mass spectrometry of synthetic polymers*, Springer, Berlin, **2003**.
[125] A. Garcia-Bernabe, M. Kramer, B. Olah, R. Haag, *Chem. Eur. J.* **2004**, *10*, 2822-2830.
[126] Z. M. Wang, M. Shen, *J. Org. Chem.* **1998**, *63*, 1414-1418.
[127] *Mercury* 1.4.1, Cambridge Crystallographic Data Centre
[128] A. Nellesen, Universität Duisburg-Essen (Essen), Dissertation, presumably **2007**.
[129] F. Bastkowski, Universität Duisburg-Essen (Essen), Dissertation, presumably **2007**.
[130] M. Bogenstatter, A. Limberg, L. E. Overman, A. L. Tomasi, *J. Am. Chem. Soc.* **1999**, *121*, 12206-12207.
[131] N. Kawai, Y. Fujibayashi, S. Kuwabara, K. Takao, Y. Ijuin, S. Kobayashi, *Tetrahedron* **2000**, *56*, 6467-6478.
[132] The D_2O Buffer is prepared with: 1.06 mmol NaOH and 1.33 mmol KH_2PO_4 in 20 mL D_2O
[133] *Macromodel* 9.0, MacroModel v9.0, Schrödinger, Inc., Portland, OR.
[134] D. F. Shriver, P. W. Atkins, C. H. Langford, *Química Inorgánica, Vol. 1*, Reverté, Barcelona, **1998**.
[135] W. Blokzijl, J. Engberts, *Angew. Chem. Int. Edit. Engl.* **1993**, *32*, 1545-1579.
[136] S. B. Ferguson, E. M. Sandford, E. M. Seward, F. Diederich, *J. Am. Chem. Soc.* **1991**, *113*, 5410-5419.
[137] D. B. Smithrud, T. B. Wyman, F. Diederich, *J. Am. Chem. Soc.* **1991**, *113*, 5420-5426.
[138] F. Diederich, D. B. Smithrud, E. M. Sandford, S. B. Ferguson, D. R. Carcanague, I. Chao, K. N. Houk, *Acta Chem. Scand.* **1992**, *46*, 205-215.

[139] S. B. Ferguson, E. M. Seward, F. Diederich, E. M. Sandford, P. Chou, P. Inocencio-Syweda, C. B. Knobler, *J. Org. Chem* **1988**, *53*, 5593-5595.
[140] B. Kahlert, Universität Duisbrug-Essen (Essen), Dissertation **2005**.
[141] *SPARTAN 04* 1.0.0, SPARTAN´04, Wavefunction, Inc., Irvine, CA.
[142] T. Schrader, M. Fokkens, F.-G. Klärner, J. Polkowska, F. Bastkowski, *J. Org. Chem* **2005**, *70*, 10227-10237.
[143] C. Breitkreuz, Universität Duisburg-Essen (Essen), Diplomarbeit **2006**.
[144] We thank Frau Dipl.-Chem. Caroline Breitkreuz for providing us with the necessary amount of clip **20g**
[145] F.-G. Klärner, M. Kirsch, J. Polkowska, F. Bastkowski, *Unpublished results*.
[146] D. A. Skoog, J. J. Leary, *Principles of Instrumental Analysis*, Fourth ed., McGraw-Hill, México D.F., **1994**.

Curriculum Vitae

Name	Marçal Casas Cartagena
Birthday	29.08.1976
Birth place	Badalona (Catalunya)
Nationality	Spanish
Marital status	Single
Address	Am Sonnenberg 75a, 44879 Bochum

September 1982 – July 1991	Artur Martorell primary school in Badalona
September 1991 – May 1996	IES Pompeu Fabra high school in Badalona
September 1996 – December 2001	Chemistry study at the University of Barcelona with the final title of "*Llicenciat en Química*"
January 2002 – February 2003	Post-graduate course at the University of Barcelona with the final title of "*Màster en Química Orgànica Experimental*"
April 2003 – May 2007	Execution of the present dissertation in the Institut für Organische Chemie at the University of Duisburg-Essen, campus Essen, under the supervision of Prof. Dr. F.-G. Klärner
April 2003 – May 2007	Research associate (Wissenschaftlicher Mitarbeiter) at the University of Duisburg-Essen

Compound index

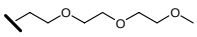

TEG (unit)

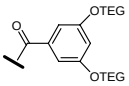

G_1-TEG (unit)

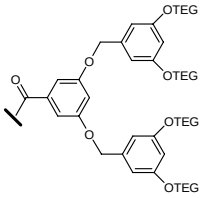

G_2-TEG (unit)

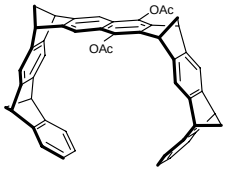

15

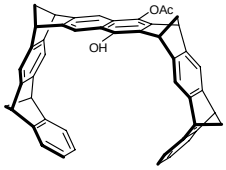

58

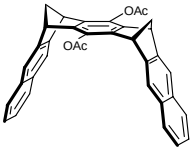

18b

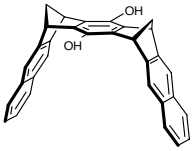

18c

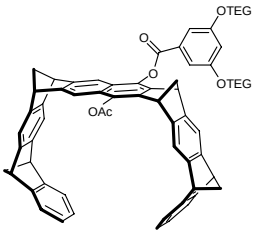

26

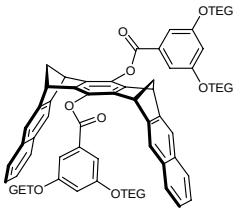

27

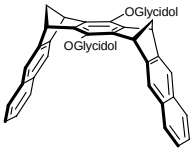

98 and **99**

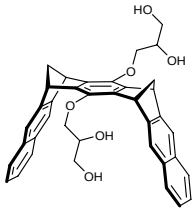

28

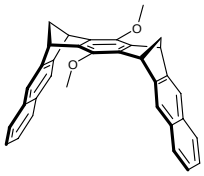

18d

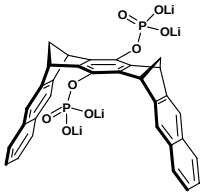

18h

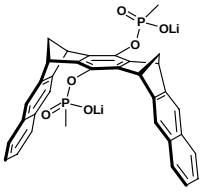

18g

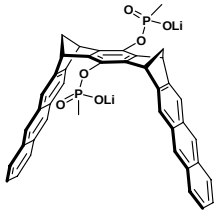

20g

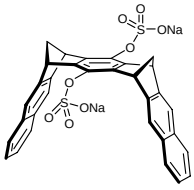

36

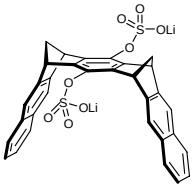

37

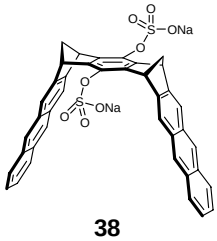

38

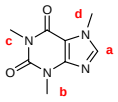

Caffeine

34

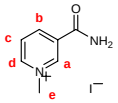

NMNA

33

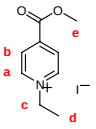

KS

84

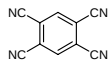

TCNB

85

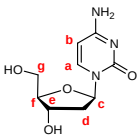

109

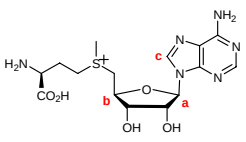

SAM

110

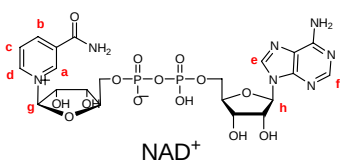

NAD^+

35